IMPACTION IN HIP ARTHROPLASTY

Ruben J. Doyle

Imperial College London

Mechanical Engineering

A thesis submitted to

Imperial College London

for the degree of

Doctor of Philosophy

September, 2019

Originality Declaration

The work presented in this thesis was produced by the author

unless otherwise stated in the acknowledgements section of each chapter

Copyright Declaration

Abstract

Surgical technique is a critical factor in the success of Total Hip Arthroplasty (THA). Cementless implants must be seated by the surgeon through the process of impaction – using a surgical mallet to generate enough force to push an oversized implant into an undersized bone cavity. A careful balance of adequate hoop strain in the bone to ensure implant fixation, but not so much that the bone is fractured, is required. The overarching aim of this PhD thesis was to better understand the process of impaction during THA. An *ex-vivo* cadaveric study of THA was used to design an *in-vitro* rig that can replicate impaction in the surgical environment. Patient compliance was identified as an important factor in impact dynamics. Using the *in-vitro* model, a range of traditional impaction techniques were tested in high and low density bone. It was found that large impaction energies (15J) showed little fixation advantage over strikes of half the energy, but could increase the risk of fracture of bone. In addition a mechanism of strain deterioration, and therefore fixation deterioration, was identified if too many high energy impaction strikes were used. Therefore a medium energy strike, using a heavy surgical mallet but low velocity, is recommended. As well as traditional mallet strikes, emerging oscillatory seating technologies were evaluated. A pneumatic oscillatory device was found to produce similar peak bone strain (and therefore fracture risk) as traditional methods, but less implant fixation. Therefore more research is required to prove the efficacy of these devices over traditional techniques.

Acknowledgements

The support of my supervisor, Dr. Jonathan Jeffers, has been invaluable during my PhD. Thank you for the freedom you have given me to pursue my own ideas; without it this experience wouldn't have been anywhere near as enjoyable.

To my co-authors, collaborators and supporting technicians: it has been a pleasure to work with such bright minds and driven individuals. Thank you for sharing your knowledge with me, I wish you all the best in your future research.

I would like to thank Desoutter Medical for their financial and technical support. In particular I would like to acknowledge the enthusiasm and friendliness of George Desoutter and his team. I hope we have achieved significant goals for your business together, however more importantly hope that our strong relationship between industry and academia continues to thrive.

I am also grateful for the financial support I have received from the Engineering and Physical Sciences Research Council, Wellcome Trust, Desoutter Medical and Imperial College.

Mum, Dad, Sarah, Honor and our canine friends: thank you for your unwavering support.

Table of Contents

List of figures

List of tables

Nomenclature

ASTM	American Society for Testing and Materials
BMI	Body Mass Index
CNC	Computer Numerical Control
CT	Computed Tomography
FBD	Free Body Diagram
MSD	Mass-Spring-Dashpot
OA	Osteoarthritis
PU	Polyurethane
RCT	Randomized Controlled Trial
RMANOVA	Repeated Measures Analysis of Variance
RMS	Root Mean Square
THA	Total Hip Arthroplasty
THR	Total Hip Replacement

Terminology

in-vivo	Performed in a whole, living organism
ex-vivo	Performed in or on tissue from an organism in an external environment with minimal alteration of natural conditions
in-vitro	Performed in a lab environment, outside the biological environment
in-silico	Performed on a computer or via computer simulation
bovine	From a cow
periprosthetic	A structure (bone) close to an implant

Chapter 1: Introduction

Modern hip replacements do not require any ‘glue’ to secure them to bone. Instead an implant is forced into a bone cavity that is slightly undersized; generating friction. By fixing the implant securely, bone ingrowth into the implant can occur, ensuring implant longevity. The process of forcing an implant into the bone, known as impaction, is not currently well understood. This thesis describes a number of studies intended to better understand and improve this surgical technique.

1.1 Background

Musculoskeletal conditions account for a third of all years lived with disability in the UK.[1] The most common musculoskeletal disease, osteoarthritis (OA), currently affects nearly 9 million people and around a third of people over the age of 45.[2] Age and obesity have been identified as two key risk factors for developing OA.[3] With these population groups growing year-on-year the burden of OA is only likely to increase.[4]

Symptoms of OA include joint stiffness, pain and loss of muscle strength. Although not fully understood, it is believed that OA is a disease of the entire synovial joint.[5] Characterized by a degenerative loss of cartilage and morphological changes to the bone and surrounding synovium, OA is most common in the fingers, spine, knees and hips (Figure 1.1.1). Due to its effect on mobility and symptom of chronic pain, OA is considered a leading cause of disability in the world.[6] In addition, the mental health impact of chronic arthritis is becoming clearer, with OA sufferers three times more likely to suffer poor mental health as a result of their condition.[7]

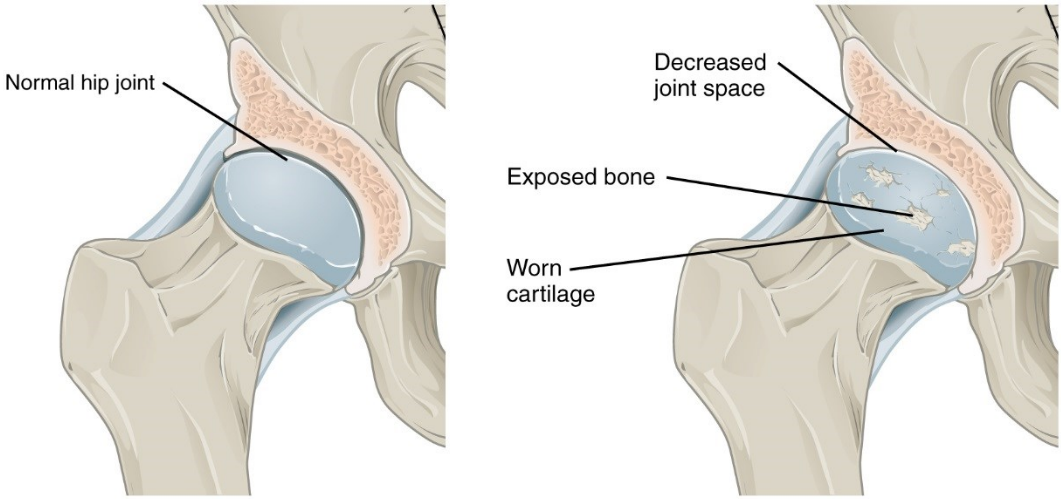

Figure 1.1.1: Artist illustration of osteoarthritis: the articulating surface of the hip (cartilage) is damaged and causes the patient pain during movement. The gold standard treatment is a complete replacement of the cartilage surface[1]

While there are a number of treatment options for the symptoms of OA, there remains no biological cure.[8–10] A total replacement of the joint with an artificial prosthesis remains the recommended gold standard treatment.[6] The two most common replacement procedures, knee and hip arthroplasty, were carried out over 200,000 times in the UK in 2017.[11] Total Hip Arthroplasty (THA) is a surgical procedure that has been shown to be hugely effective at reducing joint pain and restoring satisfactory range of motion.[12,13]

THA represents an engineering solution to a medical problem. Joint mobility is restored by replacing the articulating surfaces of the femoral head and acetabulum with artificial implants. Early attempts at THA, characterized by unsuitable materials such as glass or ivory, were plagued with implant failures.[14] However in the late 1950s, John Charnley paired a steel femoral stem with a polymer acetabular cup, and fixed both in place with cement. In doing so Charnley paved the way for what is considered by many to be the most successful surgical procedure to date. The survivorship of an early example of the Charnley hip replacement has been reported

[1] Credit: BruceBlaus, used under creative commons license: [CC BY-SA 4.0 (https://creativecommons.org/licenses/by-sa/4.0)]

as high as 84.7% at 15 years.[15] Such was the success of the Charnley hip replacement that much has remained the same for the past six decades.

It can be argued that there have been only two major deviations from Charnley's formula. The first; implant material. Although the pairing of steel and polyethylene as bearing surfaces has proven successful and is still hugely popular[11] there are concerns of the effects of polyethylene wear on surrounding tissues. As materials science and engineering has progressed, new materials for the articulating bearing surfaces have been developed.[16] Nearly half of procedures in 2017 used ceramic for at least one bearing surface.[11]

Secondly, the use of bone cement is on the decline.[11] There are several recognized issues with cemented implants. Firstly, during curing bone cement may reach temperatures as high as 86ºC, and may cause bone necrosis.[17] More rarely other untoward clinical events occur during cemented THA, namely hypoxia, hypotension or even cardiac arrest.[18] These events, sometimes classified as Bone Cement Implantation Syndrome, can have serious conqeuences.[19] Finally, bone cement does not offer true bone fixation. Instead the cement fills gaps between the bone cavity and hardens, acting as a 'grout' rather than a 'glue'. The body does not recognize the bone cement and may try to encapsulate the implant, sometimes leading to early revision.[20]

Early attempts to replace bone cement with bone ingrowth were plagued with issues.[14,15] However the development of modern manufacturing techniques facilitated porous coatings that mimic bone structure.[21] Material developments also saw the advent of bioactive coatings such as hydroxyapatite.[22] Such developments have been shown to produce strong ingrowth of bone into the implant coating. Known as 'cementless', 'press-fit' or 'uncemented', these procedures have excellent survival rates and reduced mortality risk compared to cemented implants.[23,24]

1.2 Motivation

Cementless implants are also not without their issues. Fixation, (or 'stability') is the strength of the bond between implant and bone. A disadvantage of cementless procedures is that secure biological fixation is not achieved for a number of weeks post-implantation.[25] During this time period the implant must be held securely against the bone surface. If the relative motion between the bone and implant (known as 'micromotion') is excessive, adequate ingrowth will not occur.[26] In the short-term cementless implants use a press-fit technique to obtain fixation. Press-fit involves preparing a bone cavity that is slightly smaller than the implant. When the implant is forced into this under-sized cavity stress is induced in the surrounding bone. This stress exerts a frictional force upon the implant surface – providing the fixation and stability required for bone in-growth.

Significant forces are required to force an oversized metal implant into bone. The technique used to generate these forces in a cramped surgical environment is known as 'impaction'. A surgeon will traditionally use a surgical mallet and an intermediate tool between the mallet and implant (known in this thesis as an 'introducer'). The introducer is struck with the surgical mallet in order to seat the implant (Figure 1.2.1). Impaction and press-fit techniques create a difficult balancing act for the operating surgeon. If the press-fit is too large the forces required to seat the implant may induce such stress in the bone that it fractures.[27] Even if fracture does not occur the implant may not be in proper contact with the bone, making it difficult for bone ingrowth to occur.[28] The component may also suffer large deformations which may affect implant performance.[29]

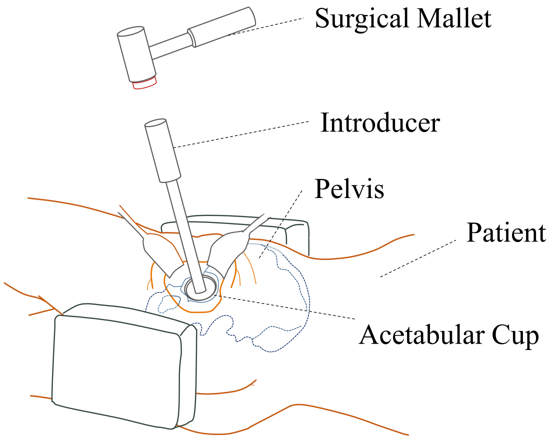

Figure 1.2.1: Impaction of an acetabular cup. A surgical mallet is used to strike an intermediate introducer, which pushes the implant further into the bone

Conversely, if the implant is not adequately impacted and the amount of press-fit is too little, the implant will not have the frictional support required for bone ingrowth. If adequate fixation and stability have not been achieved micromotion may occur, jeopardizing bone ingrowth and implant longevity.[26] This is particularly true of revision cases where a previous implant is replaced and the host bone is already damaged, meaning it is more difficult to generate appropriate fixation (in these cases the operating surgeon may choose to use a cemented implant, despite the longevity of cementless techniques).[30,31]

Impaction is a surgical technique that is used in around 60,000 cementless THA procedures every year in the UK. It is a process that requires a careful balance between fracture and fixation. Despite the importance of the impaction very little literature discusses how best to carry out the technique. There is also much variation in the findings currently reported which may be due to inconsistencies in experimental methods. In order to avoid the problems mentioned above, impaction technique deserves more thorough scientific exploration.

1.3 Aims and objectives

The aim of the work of this PhD is to develop a more thorough understanding of the process of surgical impaction when used to generate press-fit in cementless implants. Through an enhanced understanding, recommendations can be made regarding surgical technique (to benefit surgeons), *in-vitro* test methods (to benefit researchers) and implant design (to benefit engineers). These aims can be broken down into the following specific objectives:

i. Investigate the current methods used intraoperatively to seat implants
   - Determine the magnitude of the energies, forces and other impact parameters used to seat cups

ii. Replicate the clinical scenario with an *in-vitro* model that is both representative of surgery but also repeatable, allowing lab based exploration of parameters not possible within the surgical environment

iii. Investigate the effects of different impaction techniques and technologies upon the desirable and undesirable outcomes of press-fit fixation
   - Consider both traditional impaction technique and emerging impaction technologies

1.4 Thesis structure

The structure of this thesis will be based upon four experimental studies. Each chapter is presented with individual introduction, methods, results and discussion sections. Chapters 4 and 5 share their materials and methods. The thesis is concluded with a summary of the research conducted and a discussion of possible future work.

1.4.1 Chapter breakdown

Chapter 1: Introduction

Background to the research area and thesis aims.

Chapter 2: Literature review

A review of the prior literature relevant to the research presented in Chapters 3-6.

Chapter 3: An in-vitro model of impaction in hip arthroplasty

An *ex-vivo* measurement of intraoperative impaction as performed by an experienced orthopaedic surgeon. Subsequently an *in-vitro* model of impaction is developed, with the aims of closely replicating the clinical scenario in a highly repeatable setup.

Chapter 4: The effect of impaction technique

The first of two investigations into traditional impaction technique. The effect of impaction energy upon key press-fit factors, including bone and implant strains, implant fixation and seating, is investigated and discussed using the model presented in Chapter 3. Using an idealized model (assuming the surgeon has used the correct number of strikes) relationships are determined between these key factors.

Chapter 5: The effect of impaction technique: Number of strikes, mallet mass and strike velocity

The second of two investigations into traditional impaction technique. The effect of the number of impaction strikes, as well as mallet mass and mallet velocity during impact upon key press-fit factors as discussed in Chapter 4, is investigated and discussed. A mechanism of fixation loss with excessive strikes is discussed.

Chapter 6: An assessment of oscillatory seating

An investigation into the performance of a new method of impaction. A model impaction device (based upon emerging surgical tools) is tested against the same impaction factors as discussed in Chapters 4 & 5. This study represents a preliminary investigation which may inform both engineers and surgeons in the design and possible suitability of this device to seat implants.

Chapter 7: Conclusion and future work

A discussion of key findings of this thesis, key points of relevance to clinicians and to engineers and impact of research output. Possible avenues of future study are identified.

Appendix

Data that may not be essential to the understanding of Chapters 3-6, but may still be of interest to readers of this thesis. This includes raw data that can be used to construct further studies, validation data and ethical approvals.

Chapter 2: Literature review

2.1 Introduction

This chapter discusses the background relevant to the studies detailed in this thesis. In Section 2.1, an overview of the key elements of cementless hip arthroplasty are given, which may be referred to. Section 2.2 highlights the issues that are currently associated with cementless arthroplasty. Section 2.3 describes the key mechanisms which create initial fixation for press-fit implants which are vital for bone ingrowth, as well as the testing methods and models that are used during pre-clinical testing. Section 2.4 describes the current understanding of traditional impaction techniques with a surgical mallet, as well as some of the effects of measurement variables. In addition to the traditional impaction technique used by the vast majority of surgeons, there is a new trend of vibration assisted, or oscillatory impaction tools. Therefore Section 2.5 details the current understanding of these devices, and the claims made by manufacturers to support their use.

2.1.1 Total Hip Arthroplasty

The aim of Total Hip Arthroplasty (THA) is to replace the damaged articulating elements of the hip.[13] There are two main components used for a total hip replacement: one for the acetabulum (the concave hemispherical cavity in the pelvis) and one for the femur (thigh bone, Figure 2.1.1).

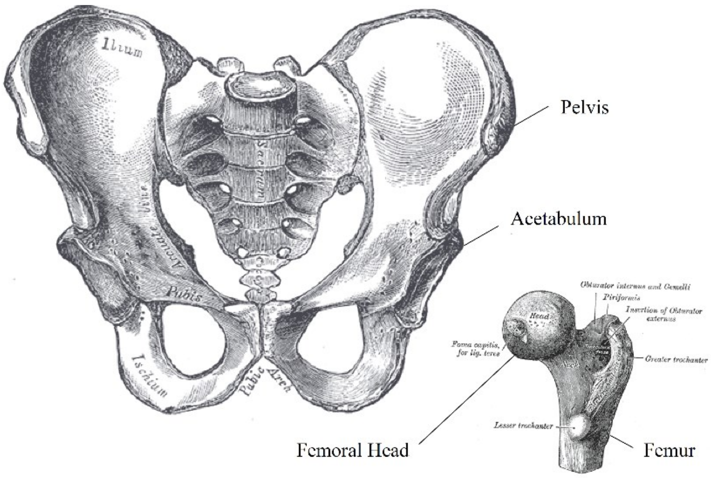

Figure 2.1.1: The pelvis and femur (Gray's Anatomy, 1918). The articulating surfaces of the femoral head and acetabulum (highlighted) are replaced during THA

The femoral component, known as the femoral stem, is characterized by a spherical head and a thin stem that sits in the femoral shaft (Figure 2.1.2). An offset and angle between the two is used to more closely represent the native femoral anatomy. The acetabular component is hemispherical with an inner bearing surface, known as the acetabular cup.

In order to implant the components the surrounding soft tissues must first be resected. There are a number of different surgical approaches to hip replacement surgery currently in use.[32] The most common, known as the posterior approach, enters the body via an incision to the gluteus.[11] Once the capsule surrounding the hip has been opened the hip joint is dislocated, exposing the femoral head and acetabulum. The femoral head is then removed exposing the femoral intramedullary canal. Subsequently the acetabulum is prepared for the impaction of the acetabular cup by reaming away the remaining cartilage using a rotating reamer and surgical drill, exposing the subchondral bone. The cup can then be impacted in place. For this process a surgical mallet is used to strike an introducer (also known as an impactor, or implanter) which is attached to the cup and gives the surgeon a handle to steady and position the cup with. When the acetabular cup is seated a femoral rasp is used to prepare the femoral cavity, and the femoral stem inserted, again using mallet strikes. The processes of seating the acetabular cup, rasping the femoral canal and seating the femoral seat are all critical to the stability, and therefore success, of the implants.[33] When complete, the entire joint has been replaced and all range of motion and function is provided by the prostheses.

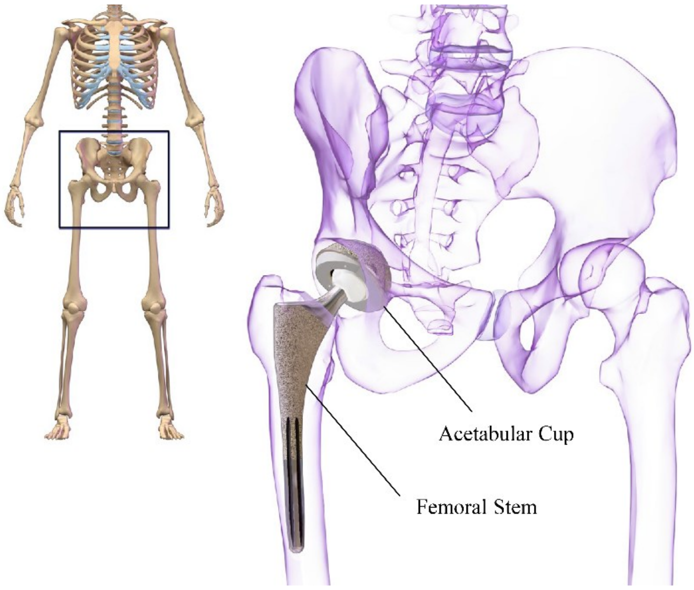

Figure 2.1.2: Completed Total Hip Arthroplasty. The acetabular cup and femoral stem replace the articulating surfaces of the hip.[2]

2.1.2 Hip resurfacing

Hip resurfacing is a far less common arthroplasty than THA, accounting for just 1% (960) of arthroplasty procedures in the UK in 2017.[11] Rather than resecting the femoral head completely only the articular cartilage is reamed away and resurfaced with a 'resurfacing head', preserving more bone.[34] Both the femoral and acetabular components may be cementless and rely upon impaction and press-fit fixation, although impaction is often used to seat the resurfacing head even when cement is used.[35]

[2] Credit to BruceBlaus, used under creative commons license: [CC BY-SA 4.0 (https://creativecommons.org/licenses/by-sa/4.0)]

2.1.3 Modular implants

Modular implants are used to allow surgeons to adapt key implant parameters, such as femoral neck offset or head size, without requiring a huge number of implants in the operating theatre.[36] In order to make assembly simple in the surgical environment a taper system is most often used. Components use male and female tapers which are assembled with impact strikes. Tapers are used for securing femoral heads to stems (Figure 2.1.3a) and fixing the bearing surface within an acetabular cup (Figure 2.1.3b). Small ridges are deliberately machined into the male surfaces (Figure 2.1.3c). The force of an impact strike slightly deforms the two mating surfaces which provides a strong connection.[37]

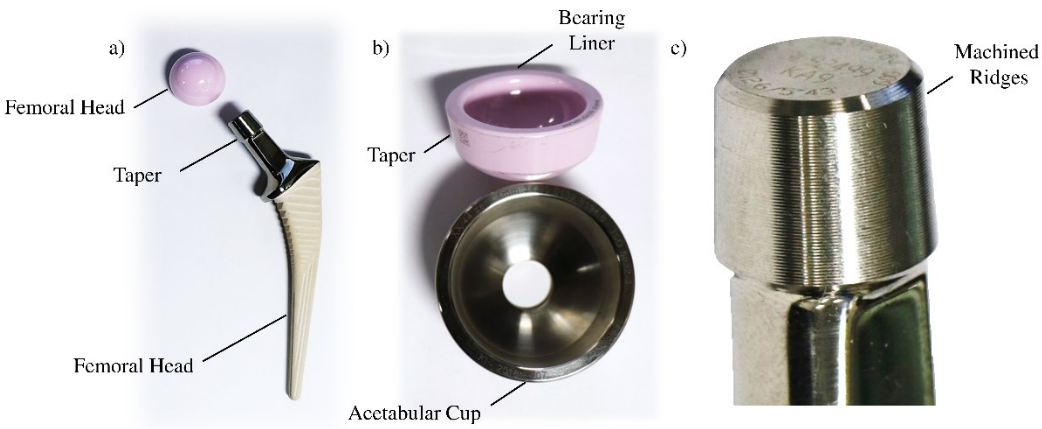

Figure 2.1.3: A total hip replacement prostheses: a) Femoral stem and head, assembled with a Morse taper; b) Modular acetabular cup with ceramic lines, assembled with a taper; c) Close up of the ridges on femoral taper that are deformed when assembled

The amount of force required to correctly seat the taper receives much attention in the literature, due to issues with corrosion at the taper junction if assembly isn't carried out correctly.[38–42]

2.1.4 Impaction allografting

In some cases, particularly during implant revision, bone stock is poor and fixation (cemented or otherwise) is difficult to achieve. A technique has been developed to improve implant stability by packing the bone cavity with bone chips before inserting the implant, promoting bone–regrowth.[43,44] The bone chips are often impacted to improve density and strength.[45] An appropriate level of impaction is required to ensure adequate graft stiffness,[46,47] without damage to bone structure or individual cells.[48,49]

2.1.5 Summary and thesis relevance

Impaction is used to seat cementless implants and generate press-fit fixation during Total Hip Arthroplasty. The impaction process is used heavily in orthopaedic surgery to seat both femoral and acetabular components. However other processes, such impaction allografting or the assembly of taper junctions, are useful to understand as testing methods may also be applicable to THA impaction. In addition data concerning the magnitudes of impact forces and energies that may be generated by a surgeon during these processes can be compared to THA literature (Section 2.4.2.1).

2.2 Challenges in cementless Total Hip Arthroplasty

Cementless Hip Arthroplasty is considered an extremely successful operation, with recent 10-year survivorships of >95% being reported.[50] However there remain a number of issues with cementless implants. Due to the large volume of procedures even small percentages of unfavourable outcomes is undesirable. Some issues occur intraoperatively (periprosthetic fractures,[51] implant deformation[29]), immediately post-operatively (instability or gross migration[52]) or after a long period of time *in-vivo* (implant loosening[53]).

If an implant is considered to be failing, or has failed, it may be revised. Revision THA is more dangerous and more costly than primary THA and has a shorter implant survivorship.[31] Therefore improving the longevity of primary THA is a key aim of surgeons and engineers.

This section reviews the main issues associated with cementless implants.

2.2.1 Periprosthetic fracture

During THA it is possible for either the acetabulum or femur to fracture. Risk factors include high Body Mass Index (BMI),[54] osteoporosis/osteolysis (poor bone quality),[55] impaction grafting[56] and minimally invasive surgery.[57] However the biggest risk factor is cementless implants[27,51,58–60] and excessively oversized cups. [61,62] 60% more fractures occurred in cementless procedures than cemented in 2017.[11] Cementless implants require strain, and therefore stress in the host bone.[63] These stresses are highest during impaction.[64] Clinically this is when intraoperative fracture is most often observed.[51]

Periprosthetic acetabular fracture was first described in 1972.[65] Fractures of the acetabulum are less common than of the femur, reported in between 0.7% and 3.5% of cases, depending upon implant design.[11,66,67] This is compared to just 0.2% fracture rate reported for cemented cups.[69] The complication rates for femoral fractures are higher than acetabular (between 20-60%),[68] however the outcomes of acetabular fracture are more severe than femoral (Figure 2.2.1).[27,70] The issue is compounded by the difficulty of recognizing the fracture intra-operatively.[51] No current study relates acetabular fracture risk to impaction technique. Work has already been carried out to quantify the risk of fracture of the femur with different impaction tehcniques.[71,72]

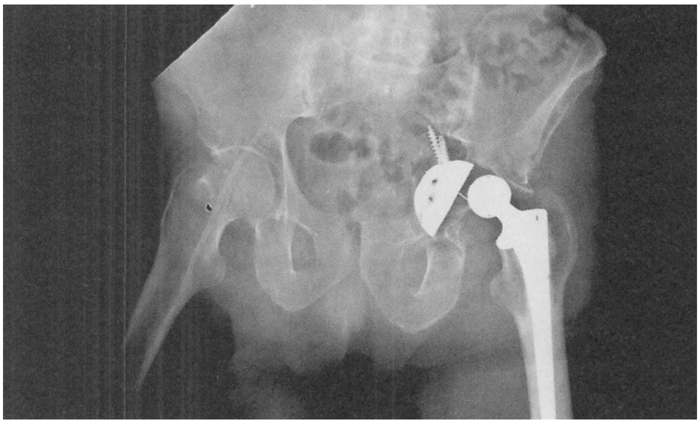

Figure 2.2.1: Catastrophic acetabular fracture following cementless THA. In this case the iliac artery was severed, leading to patient death[54]

2.2.2 Component deformation

Press-fit fixation relies upon friction generated by stresses in the bone and implant. Radial forces are applied to the implant.[20] For acetabular cups these forces may be large enough to generate appreciable deformations.[29] This is particularly true of thin walled or modular implants.[73] Such deformations have been shown to be detrimental to cup performance, causing excessive wear,[74] hindering liner seating[75] or even causing cup or liner damage.[76]

2.2.3 Mechanical instability

The initial stability of an implant is governed by the fixation it achieves in the bone immediately after press-fit.[62] It is widely acknowledged that initial stability is essential to implant longevity.[77–82] When a porous cementless implant is firmly fixed in place, bone in-growth can occur.[20] However if fixation is inadequate the bone/implant interface is subject to repeated, small, movements when loaded.[83] These displacements are known as micromotion.[26] The ability of the body to tolerate micromotion while still growing into the implant surface has been reported at between 40 -150 με.[84–86]

Clinical failures of hip replacements due to inadequate fixation are difficult to quantify. In 2017 in the USA 13.3 % of hip replacement revisions were due to implant instability codes and can be confidently linked to a lack of fixation.[87] However the UK registry does not use instability as a code, referring rather to 'loosening' as the reason for 41% of revisions.[11] Aseptic loosening (implant loosening without infection) is the most common cause of implant revision and is attributed to a range of factors. The exact reasons for implant loosening are not known, but a lack of bone ingrowth may be a key contributing factor.[53] Acetabular cups have been shown to be particularly susceptible to loosening and are revised more often than femoral stems for this reason.[67,88] A further outcome associated with a lack of initial fixation is early implant migration - when an implant displaces a large amount shortly after surgery.[89] Migration has been demonstrated as predictive of subsequent poor clinical outcome.[52]

2.2.4 Inadequate bone apposition (polar gap)

Good apposition (contact) between bone and implant is required for bone ingrowth.[28] While this is true of both femoral stems and acetabular cups, clinically acetabular cup apposition is more difficult to achieve.[28]

Press-fit requires a bone cavity that is smaller than that of the implant. If this mismatch (known as 'interference', 'oversizing', 'underream' or sometimes 'press-fit') is too large then the insertion force (impaction force) cannot overcome the frictional forces applied by the interfering cup and bone surfaces[90] and gaps are observed. Due to their occurrence at the pole of the implant, these are known as 'polar gaps'. Greater polar gaps are observed with increasing interference between cup and bone.[91] Due to the lack of accuracy and control of exact reaming size in a surgical environment, polar gaps are considered an unwanted but unavoidable consequence of press fitting.[92] In addition it has been shown that it is very difficult for a surgeon to accurately determine when an implant is fully seated.[93]

Clinically, polar gaps are tolerated to a certain degree. In a canine model, Spires et. al. found that bone ingrowth would occur with polar gaps of up to 2 mm, but gaps of < 0.5 mm produced optimum ingrowth[28] and gaps of 1mm or less have been observed to be filled without intervention.[94] In a retrospective study, polar gaps were identified in 47 of 151 hip resurfacings (Figure 2.2.2).[95] At two years all gaps were filled, although gaps of 2 mm or more had a higher risk of migration.[96]

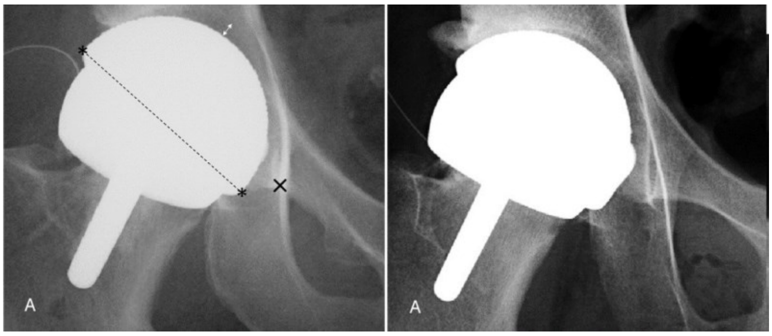

Figure 2.2.2: Polar gaps observed following hip resurfacing. In this study, gaps of up to 4.3 mm were observed. Gaps of less than 2 mm were tolerated and filling with trabecular bone after a year[95]

2.2.5 Revision surgery

Adequate press-fit fixation is more difficult to achieve in revision surgery due to reduced bone stock and quality.[30,31] The risk of bone fracture is also higher,[27] reported in up to 8% of cases.[97,98] Attempts to impact the graft in order to improve bone stock are also difficult as risk of fracture increases even further, with as many as 1 in 5 cases suffering fracture.[56] For this reason cemented fixation may be favoured in difficult cases.[99]

2.2.6 Summary and thesis relevance

In order to ensure the success of a cementless hip replacement, several factors must be ensured:

- Bone fracture must be avoided and risk minimized

- In more extreme cases acetabular cup deformation may contribute to excessive wear, improper liner seating and therefore fracture. Therefore this should be minimized where possible
- Secure implant fixation and subsequent bone ingrowth are essential to implant longevity therefore must be maximized
- Small polar gaps can be tolerated clinically, but more than 2 mm should be avoided. Ideally gaps of less than 0.5 mm should be obtained.

It is proposed that appropriate press-fit and impaction technique may improve these outcomes. Acetabular cups will be the focus of this thesis due to their relatively poorer fixation performance,[67] and more severe consequences if intraoperative fracture occurs.[27] However it is apparent that femoral implants have a higher risk of periprosthetic fracture and are also deserving of further research. Therefore Chapter 3 details the necessary models to conduct further studies. The need for better fixation during revision surgery is also a motivation.

2.3 Press-fit fixation

Cementless implants utilize two methods of fixation. The long term fixation method utilises the ingrowth of surrounding bone into the porous surface of the implant. Ingrowth of bone into an implant provides an extremely strong bond aiding long term implant survival.[26] However bone ingrowth is a complex biological process. In order to achieve a good level of bone ingrowth certain conditions must be met, including appropriate surface finish, pore size and implant micromotion that does not exceed a certain limit.[100]

In order to measure the effects of different impaction techniques, the quality of press-fit fixation must be measured against the factors in Section 2.2.6. This section examines the engineering mechanisms of press-fit mechanics, clinical observations of press-fit and influencing factors, as well as testing methods and models used to assess press-fit fixation in *in-vitro* and *ex-vivo* models.

2.3.1 Engineering analysis

2.3.1.1 Strain and stress

Engineering strain is defined as the ratio of change in gauge length of a material during application of a force (F) to the initial dimension of the material body before forces are applied. This is expressed by Equation 2.3.1 where L is the length of the body, δx is the extension of the body under load and ε is engineering strain, a dimensionless value (Figure 2.3.1).

$$\varepsilon = \frac{x}{L} \qquad \textit{Equation 2.3.1}$$

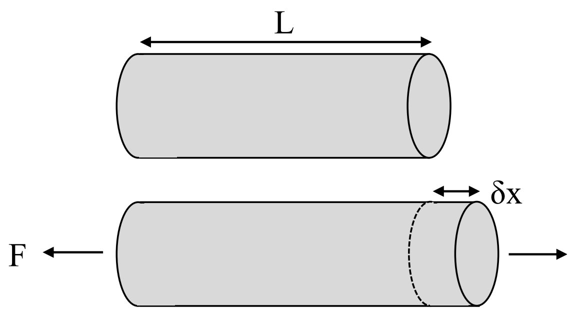

Figure 2.3.1: A force applied to a material body causes deformation, known as strain

Stress (σ) is defined as the force per unit area of material when tension, compression, or shear forces are applied (Equation 2.3.2), where A is the cross-sectional area across which a force (F) acts (Figure 2.3.2).

$$\sigma = \frac{F}{A} \qquad \textit{Equation 2.3.2}$$

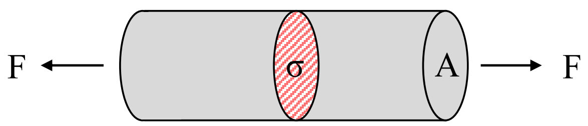

Figure 2.3.2: Force applied to a material causes stress over its cross section

In order to derive a relationship between strain and stress material properties must be known (constitutive equations). For elastic materials the relationship between stress and strain is linear and may be defined by a constant, known as Young's Modulus (E, Equation 2.3.3). Such materials do not exhibit time-dependent behaviour.

$$E = \frac{\Delta\sigma}{\Delta\varepsilon} \qquad \textit{Equation 2.3.3}$$

Real elastic materials also have an elastic limit: the point at which no further strain can be applied without permanent deformation of the material (Figure 2.3.3). This permanent deformation is known as plastic deformation and the material is considered to have exceeded its yield stress/strain. Upon unloading, plastic deformation is not recovered.

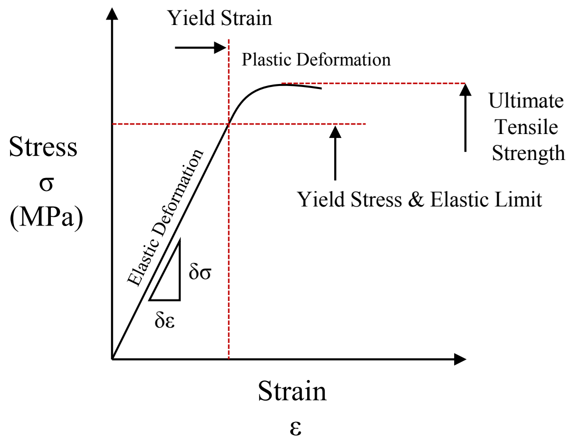

Figure 2.3.3: Typical stress-strain curve for an elastic-plastic material

Some materials also exhibit time dependent as well as elastic properties. These materials are known to be viscoelastic and the constitutive relationship between stress and strain has to be further defined as a function of time and material history. When loaded at increasing strain rates certain materials, such as polymers and some biological materials, exhibit increasing modulus (Figure 2.3.4).[181]

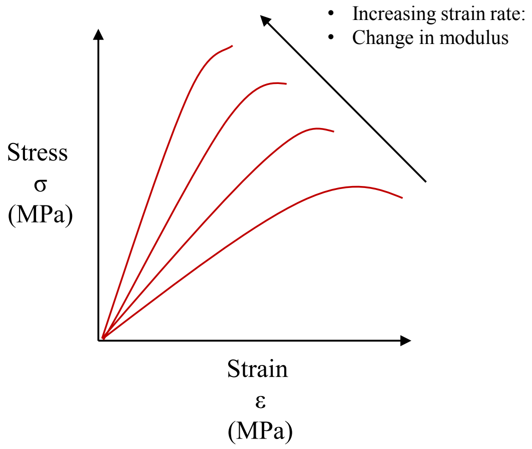

Figure 2.3.4: Example stress-strain curves for a viscoelastic materials loaded at increasing strain rates, resulting in increased apparent modulus

2.3.1.2 Contact mechanics

Materials in contact at one or more points exhibit deformation and stresses at the contact point, propagating through surrounding material. Largely, classical contact mechanics considers two contact distinctions: stresses in the direction normal to the applied force, and tangential forces (friction, Section 2.3.1.3).

Analytical calculation of contact mechanics relies on the following assumptions:[93]

- Strains are small and within the elastic limit
- Surfaces are continuous and non-conforming (area of contact is much smaller than the characteristic dimensions of the contacting bodies)
- Each body can be considered an elastic half-space (infinite lateral extent and depth)
- The surfaces are frictionless

If any of these conditions are violated, numerical methods are usually required. However the central concept of differentiating between normal and tangential loads is useful for subsequent analyses of press-fit mechanics (Section 2.3.1.4).

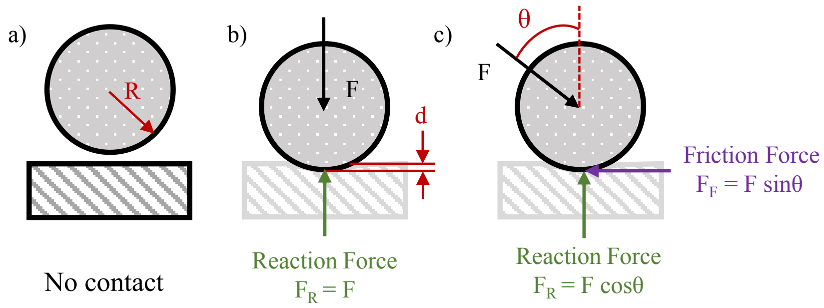

Figure 2.3.5: a) A spherical body and surface before contact b) A Free Body Diagram (FBD) for a sphere in contact with a surface: a force normal to the surface applied to the sphere results in a normal reaction force c) A force applied to the sphere at an angle (θ) to the normal direction can be resolved into normal and frictional forces

2.3.1.3 Friction

Frictional forces always oppose movement (or potential movement) between two bodies and act tangentially to the plane of contact at any given point. There are several types of frictional models. Those of interest to this thesis include 'dry' and 'lubricated'.

A commonly used model of dry friction is Coulomb friction, as given by Equation 2.3.4, where F_F is the frictional force exerted by each surface upon one another, μ is the coefficient of friction (an empirical property of contacting materials) and F_R is the normal force between the surfaces.

$$F_F \leq \mu \, F_R \qquad \textit{Equation 2.3.4}$$

F_F will resist a tangentially applied force (F_T) until that force exceeds μF_R. While $F_F \geq F_T$, no movement will occur (static friction, sometimes known as 'stiction'). A static coefficient of friction (μ_S) applies. If $F_T > F_F$ the resultant force will cause movement between the two bodies in contact. A kinetic coefficient of friction then applies (μ_k), usually smaller than its static counterpart.[93]

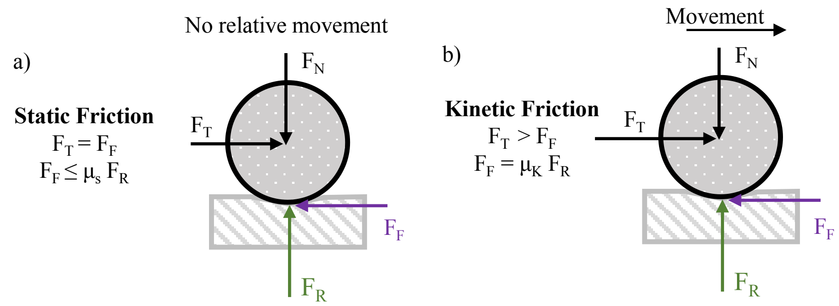

Figure 2.3.6: FBD for spheres: a) Static friction whereby $F_T = F_F$ and no movement occurs; b) Kinetic friction whereby F_T exceeds F_F and movement occurs

Coefficient of friction is determined experimentally and is a function of many aspects of the materials in contact, including material deformation characteristics and surface roughness.[111]

Lubrication may also significantly affect the friction coefficient, a key factor that is discussed but not often accounted for in either *in-silico* or *in-vitro* models, decreasing the friction coefficient when present.[112]

2.3.1.4 Press-fit

If a cylinder of outside diameter 2R+2δR is forced into another cylinder of inner diameter (bore) of 2R, the interference between the two diameters induces strain, and therefore stress, in each (Figure 2.3.7a,b,c). An interface pressure, *p*, results and is applied to the outer surface of the inner cylinder, and the inner surface of the outer cylinder (Figure 2.3.7d,e). Due to the pressure between these two surfaces, frictional forces will resist relative axial movement between each cylinder. This is the basis of a press-fit, commonly used in engineering applications, and also in cementless cups.[21]

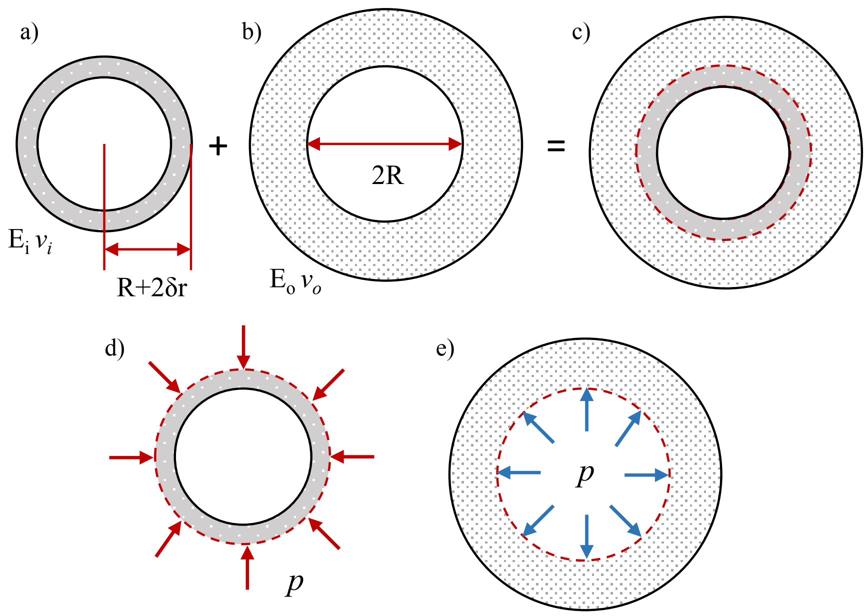

Figure 2.3.7: The basis of press fit: a) An oversized cylinder is inserted into b) a cylindrical bore in to create c) a press-fit between the two. The interference between cylinder and bore results in a pressure (p) between: d) the outer surface of the cylinder and e) the inner surface of the bore

The magnitude of the interfacial pressure p is dependent upon the values of interference δ, the material properties of each cylinder (E,v) and inner, interfacial and outer radius of the compound cylinder (r_i, R, r_o, Equation 2.3.5). Increasing interference or material modulus results in increased pressure, and therefore more friction between the two compound cylinders.

$$p = \frac{\delta_r}{\frac{R}{E_o}\left(\frac{r_o^2 + R^2}{r_o^2 - R^2} + v_o\right) + \frac{R}{E_i}\left(\frac{r_i^2 + R^2}{r_i^2 - R^2} + v_i\right)} \qquad \textit{Equation 2.3.5}$$

The stress in each of the cylinders can be divided into two components (when not considering axial stress). These stresses are known as radial stress, σ_r (acting in the direction normal to the cylinder surface), and hoop stress, σ_θ (acting tangentially to the cylinder surface). For the external cylinder σ_r at the interface is equal to $-p$ (compression) and reduces (in magnitude) to zero at r_o, where no radial forces are acting. Hoop stresses are tensile throughout the cylinder radius, and greatest at the interface (Equation 2.3.6).

$$\sigma_\theta(r) = \frac{pr_i}{r_o^2 - r_i^2}\left[1 - \frac{r_o^2}{r^2}\right] \qquad \textit{Equation 2.3.6}$$

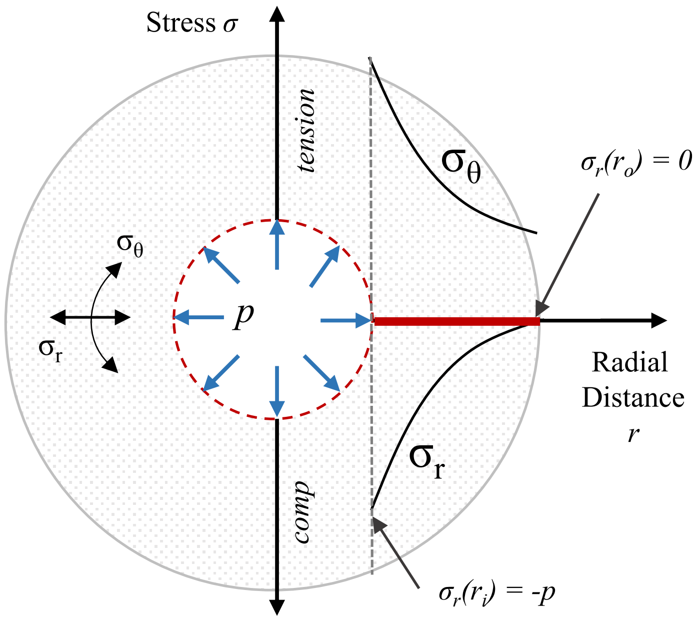

Figure 2.3.8: Radial and hoop stress induced in the outer cylinder due to press-fit. The greatest tensile strain is hoop strain at the surface of the bore

For the inner cylinder radial stress at r_i is equal to zero, due to the lack of radial forces acting on this surface. Radial stress increases to $-p$ at the interface. Similar to the outer cylinder hoop strains are larger in magnitude than radial stresses throughout, although these are compressive, not tensile. The stress distribution of hoop stress in the outer cylinder can be calculated (Equation 2.3.7).

$$\sigma_\theta(r) = \frac{-pr_o}{r_o^2 - r_i^2}\left[1 - \frac{r_i^2}{r^2}\right] \qquad \textit{Equation 2.3.7}$$

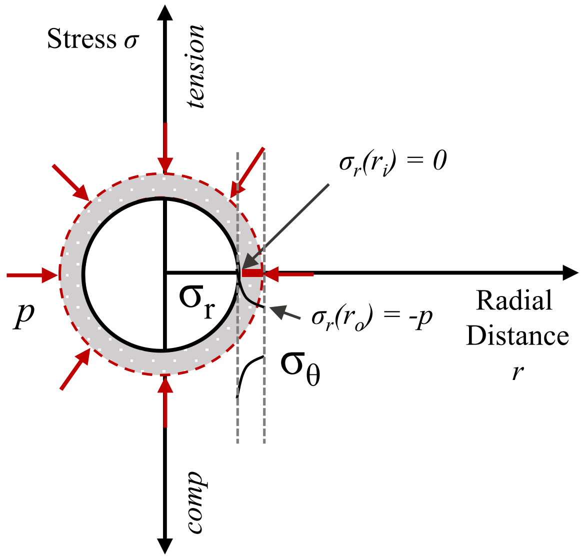

Figure 2.3.9: Radial and hoop stress induced in the inner cylinder due to press-fit

In orthopaedic applications the implant and bone cavity are not cylinders. However the concepts of radial and hoop strain (including their relative magnitudes), as well as the effects of interference and material properties upon interfacial pressure (and therefore friction) are relevant.

2.3.1.5 Force balance of acetabular cups

In order to understand the mechanics of a press-fit acetabular cup, the fundamentals of contact mechanics discussed in Section 2.3.1.2 can be combined with free body diagrams (FBD), to determine the balance of forces acting upon the cup at any point during insertion, unloading or removal. These loading scenarios can be considered quasi-statically in order to remove the need to consider inertial effects.

Figure 2.3.10 shows an engineering approximation of the acetabular cup in the acetabular cavity. Due to the difference in diameters between cup and bone, an area of interference is created, applying forces to the cups which can be resolved.

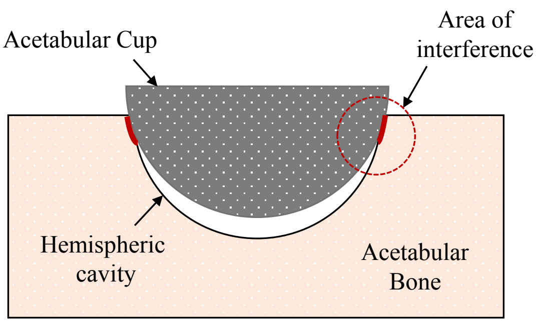

Figure 2.3.10: Approximation of acetabular cup and acetabulum for engineering analyses

As the acetabular cup is inserted into the undersized bone cavity, the area of interference can be expected to grow. From cup rim to cup pole the angle at which the reaction force between cup and bone acts will vary. In order to conduct force analysis a segment of bone/cup interference is considered (Figure 2.3.11). Total forces can be calculated by integrating all infinitesimally small segments within this area.

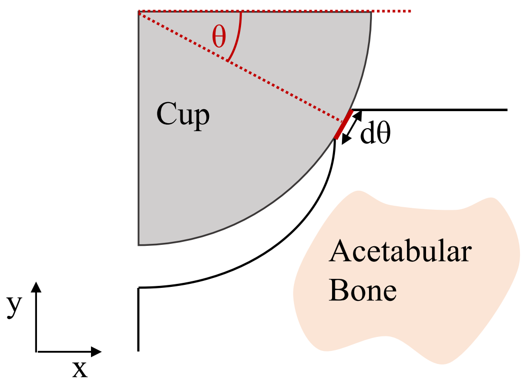

Figure 2.3.11: Contact area between acetabular cup and reference frames. The small area covered by dϑ can be solved analytically. Loading cases across a range of angles can then be summed for complete loading cases.

Cup insertion

During cup insertion a vertical force F_{in} is applied. As discussed in Section 2.3.1.2, two force components due to cup/bone contact can be considered as acting upon the cup: reaction force (F_R) acting perpendicular to the cup surface, and frictional force (F_F) acting tangentially to the cup surface (Figure 2.3.12). As the cup is axisymmetric the components of both F_R and F_F in the x-direction balance with the other half of the cup. In the y-direction the cup insertion force is balanced by y-components of both F_R and F_F (Equation 2.3.8). F_F is acting in the positive y-direction, resisting the movement of the cup into the cavity, and can act up to the value μF_R (where μ is the coefficient of friction between cup and bone). If F_{in} exceeds $F_R \sin\vartheta + F_F \cos\vartheta$ there will be a resultant force in the negative y-direction, accelerating the cup into the cavity.

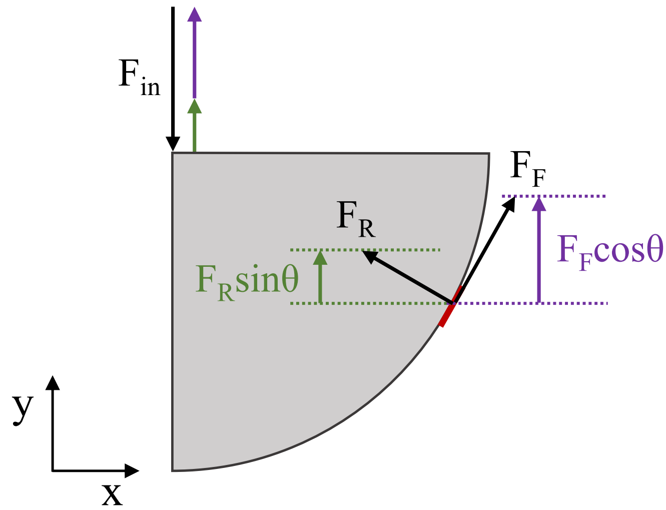

Figure 2.3.12: FBD of acetabular cup during insertion: y-components of friction and normal reaction force can be balanced in the y-direction for cup push-in

$$F_R \sin\theta + F_F \cos\theta - F_{in} = 0 \qquad \text{Equation 2.3.8}$$

Unloaded cup

When the insertion force F_{in} is removed the y-component of the reaction force, due to press fit, remains. This is now balanced by the y-component of frictional force, which has changed direction in order to resist the motion of the cup out of the cavity (Equation 2.3.9). Due to the reduced loading F_F is also reduced in magnitude (Figure 2.3.13).

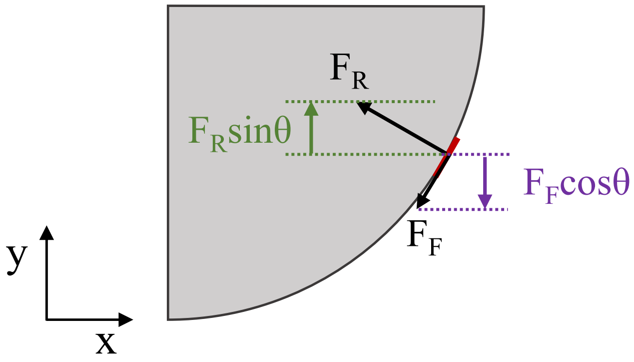

Figure 2.3.13: FBD of acetabular cup when insertion force is removed. The y-component of normal reaction force remains in the positive y-direction and are balanced by the y-component of frictional force, which has changed directions

$$F_R \sin\theta - F_F \cos\theta = 0 \qquad \text{Equation 2.3.9}$$

Cup removal

When the insertion force is reversed in order to remove the acetabular cup (F_{out}) the y-component of friction must now resist both the y-component of reaction force and this additional force (Figure 2.3.14, Equation 2.3.10). It is therefore easier to remove a cup than insert it, as the y-component of reaction force is positive in both scenarios.

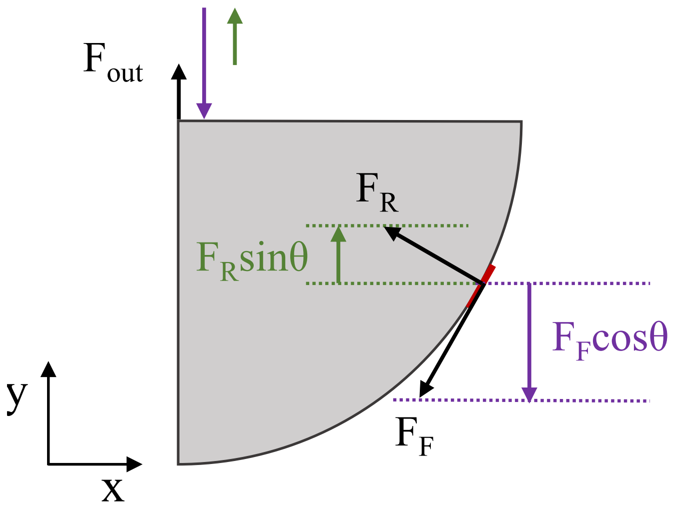

Figure 2.3.14: FBD of acetabular cup during removal. The y-component of friction now opposes both the y-component of F_R and F_{out}

$$F_{out} + F_R \sin\theta - F_F \cos\theta = 0 \qquad \textit{Equation 2.3.10}$$

2.3.2 Clinical press-fit application

2.3.2.1 Rim fixation

Press-fit induces strain, and therefore stress, in the bone. Radial stress pushes the bone into the surface of the cup.[63,101] Adler et. al. concluded that the most important mode of cup fixation was engagement around the periphery of the cup rim. If there are defects in the acetabular rim stability can be severely compromised.[77] In a finite element model, Zhang et. al. also measured the greatest strains in the periacetabular region.[102] Using pressure–sensitive film MacKenzie et. al. also noted that the acetabular rim was in strongest contact with the bone (Figure 2.3.15).

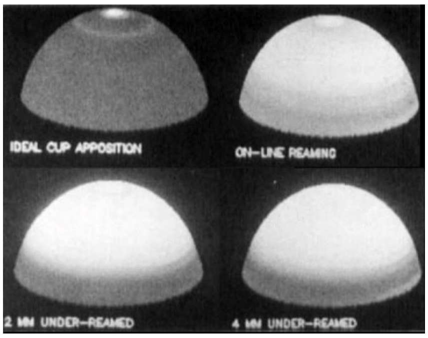

Figure 2.3.15: Using pressure-sensitive film MacKenzie et. al. observed the majority of cup-bone contact at the implant rim[103]

2.3.2.2 'Pinching' effect

While acetabular implants are axisymmetric and 'hoop strain' is often referred to as the key contributor to the radial forces acting upon the cup, in reality the acetabulum is nonaxisymetric. The most common approximation of the forces exerted by the acetabulum is a 'pinching' effect between the ischial and ilial columns (Figure 2.3.16). A number of studies have demonstrated this phenomenon by implanting cups into cadaveric tissues and observing the manner in which the cup is deformed.[74,104–106] In reality this pinching is not entirely symmetrical, with deviations in peak opposing forces of up to 11.5º [105] Examples of three point loading (including the pubic bone)[106] or one point loading[74] have also been described. However the simplicity and reasonably high accuracy of the two point loading approximation has subsequently lead to its general acceptance and adoption in many studies.[29,76,107–110]

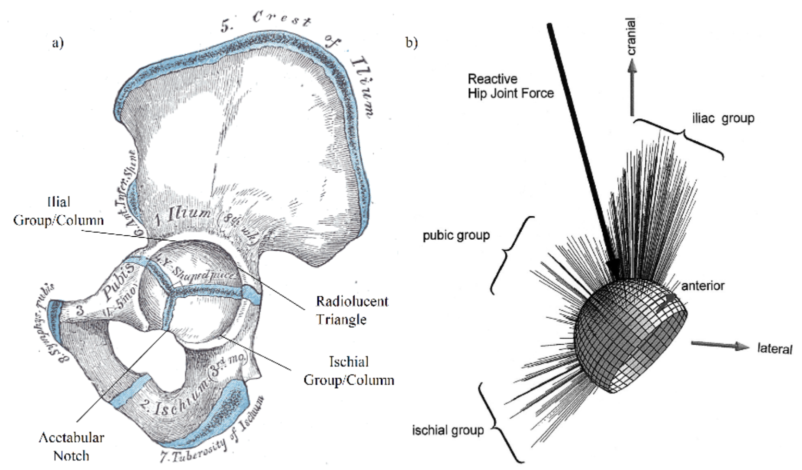

Figure 2.3.16: Press-fit mechanics are characterized by a 'pinching' of the acetabular cup: a) The ilial and ischial columns form two opposing supports; b) Reaction forces are mainly observed in these areas of denser bone[106]

2.3.3 Influencing factors upon fixation and stability

2.3.3.1 Coefficient of friction: Effect of cup surface finish

It has been reported that modifying the surface finish of a cup affects the fixation strength that can be achieved.[83,92,115,116] The two most common surface finishes applied to implants used clinically are plasma spraying and sintered bead (Figure 2.3.17). Weissman et. al. observed a difference between fixation strengths when surface finishes were additively manufactured to have different unit cell sizes.[116] Wetzel et. al. found that a plasma sprayed finish provided more fixation than a wire mesh or sintered bead finish.[117]

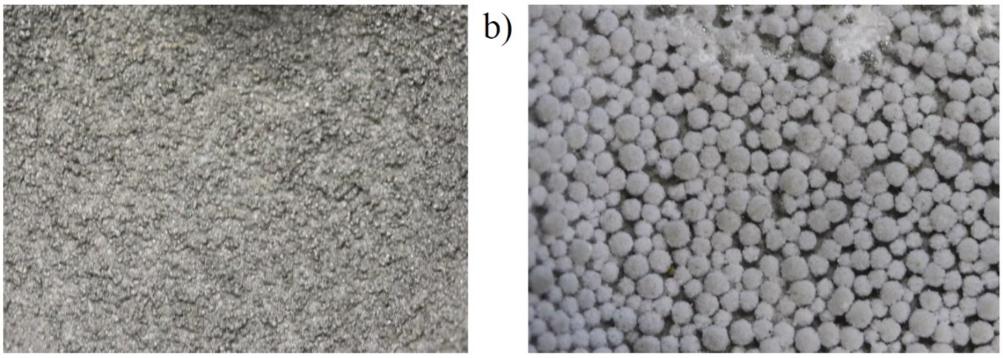

Figure 2.3.17: Examples of the topography of the two most common implant finishes: a) Plasma sprayed b) Sintered bead

While increasing friction increases implant stability, therefore reducing motion during the recovery period and aiding bone ingrowth[83], negative trade-offs are reported. For the same implantation force, increasing friction increases polar gap, and reduces area of contact between cup and bone.[92] Therefore to maintain the same level of seating of the cup more implantation force must be applied. In surgery this translates to higher strike forces and higher chance of fracture of the bone. In addition increasing surface roughness causes damage to bone during implantation. 'Macro' features on a cup increase bone damage.[115,116] Damm et. al. summarized that rougher surfaces can attain higher frictional forces, however are more likely to reduce levels of fixation if contact stresses are too high and cause excessive damage to the bone.[113]

Bone also undergoes plastic deformation and damage during seating.[113,114] Reaction force is dependent upon the amount of underream chosen by the surgeon & the stiffness of the surrounding bone.[91]

2.3.3.2 Reaction force: Effect of underream and cup geometry

Effect of underream

The terms *underream, interference, press-fit* and *oversizing* tend to be used synonymously in orthopaedic literature. All refer to the diametric interference between bone cavity and implant. For example a 2 mm underream when seating a 54 mm diameter cup will require a surgical reamer of 52 mm. Often a suggested underream amount is provided by the implant manufacturer.[118–120] However ultimately the choice of underream falls to the operating surgeon. Generally an underream of between 1-3 mm is used by clinicians, with the choice being made based upon factors such as bone strength, implant stiffness and implant geometry.[62,96,103,121]

Table 2.3.1: An increase in implant fixation is observed with increasing underream/oversizing[122]

Oversizing (mm)	Pull-out (kN)	Lever-out (N m)	Torque (N m)
2.00	2.009	37.94	56.2
1.50	4.482	33.4	31.6
1.00	1.313	23.15	Not Tested

Increasing underream increases interference and creates larger stresses in the bone and more fixation (Table 2.3.1).[122] A 'dramatic' increase in bone stress has been observed in cups of 2 mm or greater.[63,101] Due to increased stresses on the cup, cup deformation has also been shown to increase with increasing underream.[104] However if underream is too great the cup cannot properly seat.[77] Therefore peak stability may occur at different levels of underream in different qualities of bone. For example Curtis et. al. found the best fixation was achieved at 3 mm underream in cadaveric acetabula,[62] while MacKenzie et. al. found 2 mm underreaming to be the most stable.[103] 4 mm underream has both been reported as both producing a high risk of fracture[123] and clinically acceptable.[96] No clear best practice is given in the literature.

Effect of cup geometry

The design of an acetabular cup has a significant effect upon its stability when seated.[122] A focus of the literature has been the use of hemispheric cups versus those with an enlarged rim (Peripheral Self-Locking, PSL), and study conclusions are inconsistent. Some studies claim a hemispherical cup has a greater area of contact and is more stable,[77] while requiring a higher force to seat than a PSL cup.[123] Others find the opposite [81,117,124]. This uncertainty is reflected in the use of both hemispherical and PSL cups in clinic.[11]

2.3.3.3 Effect of cup size

A larger cup size with the same underream in the same quality bone has a larger engagement area and therefore exhibits greater fixation strength.[122] The risk of fracture increases with decreasing cup size.[125]

2.3.3.4 Effect of cup stiffness

A wide range of rim-to-rim acetabular cup stiffness's have been reported in the literature. A summary of this data can be found in Table 2.3.2. Cup stiffness is a function of cup size, thickness and material.[29]

Table 2.3.2: Summary of cup specifications available in the literature, including material and geometric properties

				Value Range			
				Low			
Study	**Cup Model**	**Manufacturer**	**Cup Material**	**Stiffness (N/mm)**	**Cup Size (mm)**	**Rim Thickness (mm)**	**Pole Thickness (mm)**
Dold 2016	~	~	~	3111	62	3	3
Springer 2012	Cormet	Stryker	~	16000	58	4.21	6.35
	Conserve Plus	Wright Medical	~	8000	62	3.87	4.89
	Magnum	Biomet	~	5000	66	3.05	5.83
	Birmingham	Smith & Nephew	~	10000	64	3.47	5.64
Squire 2006	Depuy	Pinnacle 100	~	2400	54	~	~
				High			
Dold 2016	~	~	~	14341	44	4	4
Springer 2012	Cormet	Stryker	~	36000	56	5.51	7.65
	Conserve Plus	Wright Medical	~	13000	42	3.8	4.07
	Magnum	Biomet	~	21000	44	3.33	5.8
	Birmingham	Smith & Nephew	~	39000	46	4.54	6.47
Small 2013	Biomet	M2a-Magnum	CoCr	5626	58	3.29	6.07
Squire 2006	Depuy	Pinnacle 100	~	5000	66	~	~
				Average			
Small 2013	Biomet	Regenerex Ringloc	Ti-6AL-4V	4598	58	5.04	
		Ranawat/Burstein	Ti-6AL-4V	2604	58	4.18	
		M2a-38	CoCr	47244	58	10.16	

Cup stiffness is important for a number of reasons. If a cup lack stiffness, the compressive forces applied by the 'pinch' of the acetabulum may result in excessive deformation. For large head metal-on-metal cups the condition of minimum clearance required for lubricated motion might be violated, resulting in excessive wear.[74] Deformation is also an issue for modular acetabular cups that require the insertion of a liner, particularly if the liner material is a stiff ceramic.[107] However stiffer implants are detrimental to the quality of surrounding bone[126] and so a compromise must be reached.

2.3.3.5 Effect of bone quality

Better quality bone generally results in a more secure fixation. However, if the bone is too dense the cup may not seat to the rim and stability may be compromised.[77,127]

2.3.4 Press-fit fixation testing methods

2.3.4.1 Physiological loading

In order to test for implant fixation strength it is important to understand the mechanisms and magnitudes of implant loading. This ensures that pre-clinical *in-vitro* testing is representative and an accurate indicator of the likelihood of implant failure.

Daily activities are known to apply appreciable force on the acetabulum[128] and may lead to interfacial micromotion.[83] Another source of implant loading is bearing friction. Resurfacing and arthroplasty procedures commonly use a combination of metal, ceramic and polymer bearing surfaces, all of which produce a frictional force resisting the movement of the hip when loaded.[129] This effect is more pronounced in large diameter heads, where torques have been reported at similar magnitudes as those that can be sustained by the fixation of cementless cups.[130] An acetabular implant may also experience ‘pulsing’ into the acetabular cavity as a force is applied parallel to the cup pole by the loaded femur.[83] Additionally the cup may impinge on the femoral neck, making contact with the anterior or antero-superior acetabular rim, causing edge loading.[131]

2.3.4.2 Destructive versus non-destructive testing methods

It is possible to test acetabular cup initial fixation using a number of different methods. These can broadly be split into two groups: destructive and non-destructive methods. Destructive methods apply displacement to the implant beyond the limits of fixation – the implant/bone interface is destroyed during testing and the implant is generally removed following the test. Such tests require virgin substrate for each test.

Non-destructive tests aim to apply loads or displacements that do not exceed the limits of fixation. Both types of test may be conducted *in-vitro* or *in-silico*, and may use synthetic or cadaveric samples.

2.3.4.3 Destructive testing methods

Push-out/pull-out

Often favoured for its simplicity, push-out (or pull-out) testing involves loading a cup axially, normal to the pole of the cup. Usually displacement controlled, a materials testing machine loads the cup from the pole, while the max force taken to fully remove the cup is recorded (Figure 2.3.18).

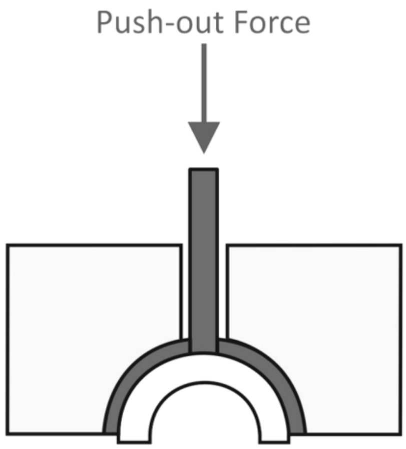

Figure 2.3.18: Fixation tested by pushout mechanism[132]

In some cases an axial torque is applied instead of an axial force.[77] It is acknowledged that push-out loading does not usually occur *in-vivo*,[122] a limitation of the method. However pushout testing compares well with other methods and is therefore often used as a metric of fixation. [80,115,132,133] A wide range of pushout values are reported as variables such as cup design, underream and substrate density are likely to have a significant effect upon results (Table 2.3.3).

Table 2.3.3: Summary of acetabular cup push-out forces measured in literature. A wide range of values are reported

Study	Substrate	Density	Cup Underream	Pushout Force (N)		
				Low	Average	High
Ries 1997	PU Foam	N/A	1-2mm	220	470	680
Macdonald 1999	PU Foam	0.2 g/cm^3	2mm	510	1300	2010
	Cadaveric Bone	N/A	2mm	~	560	~
Crosnier 2015	PU Foam	0.24 g/cm^3	1 mm	~	420	~
	PU Foam	0.48 g/cm^3	1 mm	~	1050	~
Le Cann 2014	0.32 sawbone	0.32 g/cm^3	1 mm	280	~	480
	Bovine Bone	N/A	1 mm	295	~	360

Lever-out

Lever out is a torque applied about a vector on the plane made by the rim of the cup. Tests are usually conducted using a lever arm attached to the cup to which a normal load is applied using a materials testing machine (Figure 2.3.19). Lever-out represents the bearing torques occurring *in-vivo* and therefore is representative, but at the expensive of complexity versus push-out methods.[80]

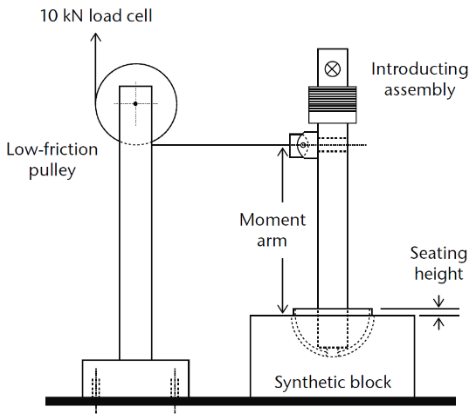

Figure 2.3.19: Fixation tested by lever mechanism[81]

Rim/edge loading

Rim loading is conducted by applying a force directly to the rim of the cup. This may be done with a materials testing machine, with failure load recorded at that when the cup rotates within the bone cavity.[78] Rim loading tests for what might be considered a worst case scenario, when the cup and femoral neck impinges.[131]

Contact force, contact area and photo-elastic stresses

Widmer et. al. and MacKenzie et. al. both used a pressure sensitive film to determine the area and force of contact between cup and bone.[103,106] Similarly, photo-elastic materials have been used to determine the regions of stress around the acetabular area (Figure 2.3.20).[124] Both methods give an estimation of acetabular stress and areas of contact for bone ingrowth, but less indication of absolute fixation.

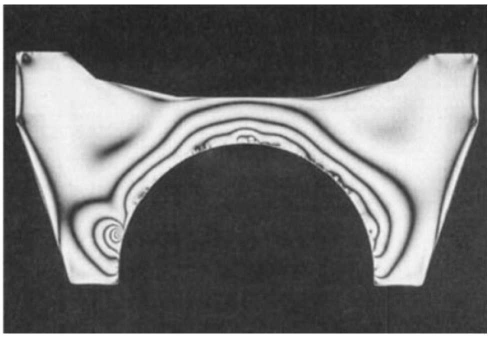

Figure 2.3.20: Photo-elastic analysis of the strains present in the acetabulum following press-fit seating.[103]

2.3.4.4 Non-destructive testing methods

Micromotion

In-vitro micromotion testing involves seating an implant in a cadaveric or synthetic cavity and applying an external load. The applied loads are usually of the same order of magnitude as those applied *in-vivo* and are based upon loads predicted by force plate and gait mechanic studies. Motion of the implant is then measured using Linear Variable Differential Transformers (LVDTs) or similar small range sensors. Some studies have also suggested the use of multiple LVDTs in order to determine both the movement of the implant and surrounding bone, in order to separate the movement due to deformation of the bone from that of the implant.[132] Micromotion measurements *in-vivo* provide a good indication of the chances of implant failure.

Bio-reactors can also be used to measure the effects of micromotion using *in-vivo* animal models. By isolating an area of the bone, bio-reactors allow a known load to be applied to an implant while still allowing bone ingrowth. From such work different values for the threshold at which bone ingrowth can occur are reported, varying between 40 – 150 µm.[26,85,86,100]

Impulse and acoustic measurement

A change in key indicators of force-time traces, or acoustic emissions produced by a surgical mallet during impaction have been identified (Figure 2.3.21).[134–137] These works show significant promise for identifying the point of ideal fixation.

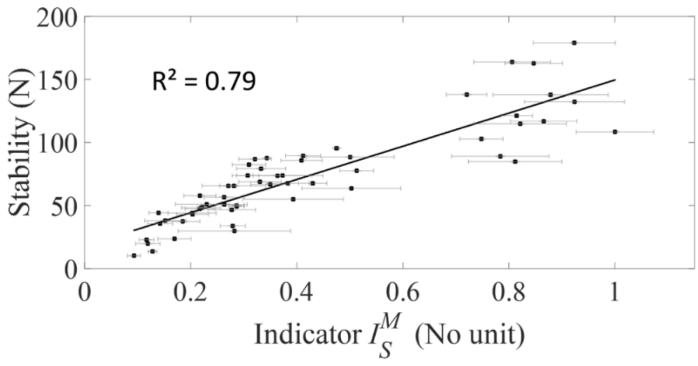

Figure 2.3.21: Indicators derived from the impulse shape of a surgical mallet has been found to correlate well with implant staiblity[135]

2.3.4.5 *In-silico* methods

As computing power and modelling techniques improve computational models are being increasingly used throughout the engineering field. Finite Element (FE) models can be used in situations where experimental modelling is not possible, or prohibitively expensive, and can be accurate predictors of *in-vivo* phenomena.[138] Many believe FE methods hold great promise, but still require further validation.[139]

During impaction the bone/implant interaction is extremely complex. A significant limitation of FE models is to simplify the cup/bone interaction, often with a single friction coefficient used[90], and with no lubrication considered. Material properties must also be simplified.[140] This is particularly important when measuring the stresses induced in bone during press-fit. If the damage (plastic deformation) that occurs during implantation[114] is not modelled appropriately the predicted stresses will far exceed those predictive of frature,[113] and cup deformation may be overestimated,[108] even if fracture does not occur experimentally.

2.3.5 Press-fit fixation bone models

2.3.5.1 Cadaveric bone models

Cadaveric specimens are often used for biomechanical testing as they best represent anatomy and bone material properties of humans. In addition, and of particular importance to this thesis, intact soft tissues surrounding the bone ensure the boundary conditions of the specimen are appropriate, (although soft tissues are often stripped from bone, Figure 2.3.22).[33] Despite excellent representation of the in-situ environment for implants, cadaveric tissues also create testing difficulties.

Figure 2.3.22: A typical cadaveric specimen following preparation: soft tissues are removed and therefore any compliance provided in surgery is removed[33]

A key issue with cadaveric specimens is inter-specimen variability. Biological specimens show variations in properties that often eclipse the effects of experimental variables.[80,141] For example, Dold et. al. did not find an expected correlation between cup stiffness and component deformation.[105] Similarly Small et. al. expected to measure increased periacetabular strains when a stiffer cup was implanted, but no trend was observed.[142] It is likely these findings were dominated by inter-specimen variability. Variability is also an issue with specimen preparation. For example the preparation of the cadaveric acetabular cavity is difficult to standardize and replicate.[143] In addition tissue must be preserved, either through freezing or by replacing blood with a chemical fixant. Different preservation techniques have been shown to affect the mechanical properties of soft and hard tissues.[144]

There are many other factors to consider when using cadaveric tissue. Ethical approval must be obtained, transport, storage and testing location must all be approved by the appropriate legal bodies. For these reasons many researchers opt to use synthetic bone models rather than cadaveric.

2.3.5.2 Synthetic bone models

In order to mitigate the challenges posed by cadaveric testing, synthetic bone models have been developed. A prominent and widely used substitute for bone is expanded Polyurethane (PU) foam.[145] The products available for testing in orthopaedics fall into two categories: anatomical and biomechanical. Anatomical models simulate the anatomy and variation in strength of human bone. The most advanced at the time of writing, the Sawbones 4th generation composite model (Figure 2.3.23),[146] uses different materials to simulate variation between cortical and cancellous bone.[147,148] More commonly used are homogenous biomechanical blocks. These can be CNC machined to fit mimic bone cavities to a high level of repeatability.[143] The use of PU foams is acknowledged as a viable alternative to cadaveric tissues by ASTM, with a standard to control the mechanical properties of the material,[145] and certain common orthopaedic tests, such as screw pull-out.[149]

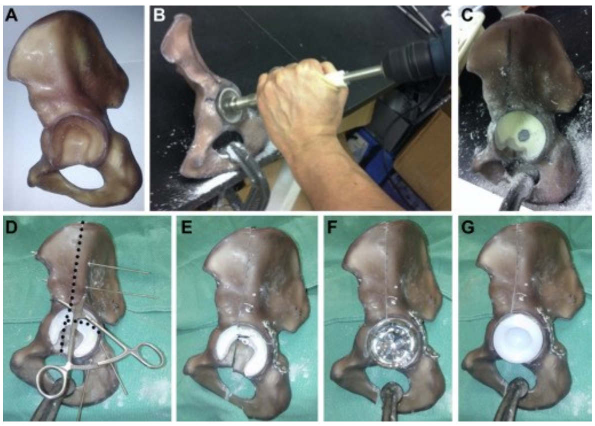

Figure 2.3.23: 4th generation Sawbones model representing both cortical and cancellous bone being used for biomechanical implant testing[150]

A number of studies have compared the properties of sawbones to animal and cadaveric tissues. Adler et. al. reported similar trends in fixation between different geometry cups in PU foams when compared to bovine acetabulum.[77] Macdonald et. al. reported comparable strength of cup fixation for PU foams and cadaveric bone, although PU foams were found to over-estimate stability when compared to bone. The differences in fixation between the two were found to be less than those of the fixation test mode.[122] A later study found no significant difference in impact energy measured during impaction of a femoral stem into PU substitute and embalmed cadaver.[151] Characterization of the mechanical properties of expanded PU foams also reported adequate similarity with biological tissues for orthopaedic testing.[122,152,153] More recently it has been reported that morcelised PU foams are an acceptable substitute for cadaveric bone.[154]

A key limitation of testing with PU foams is that the fluids found *in-vivo* (blood, saline) are not represented. Baleani et. al. found that as the friction between PU foam and implant was lower than that between bone and implant, the lubrication effect could be accounted for.[80] In addition PU foams do not accurately represent bone geometry or variations in stiffness. Different 'anatomical' milled cavities have been explored to address this issue. Early models used a purely hemispherical cavity.[122] Following reports of the 'pinching' applied to cups by the acetabulum, the model was updated with diametrically opposite cut-outs (Figure 2.3.24).[104] The model has subsequently been shown to produce similar cup deformations[108] and fixation strength[80,106] as cadaveric models, and has been used in a large body of work.[76,82,132,155,156]

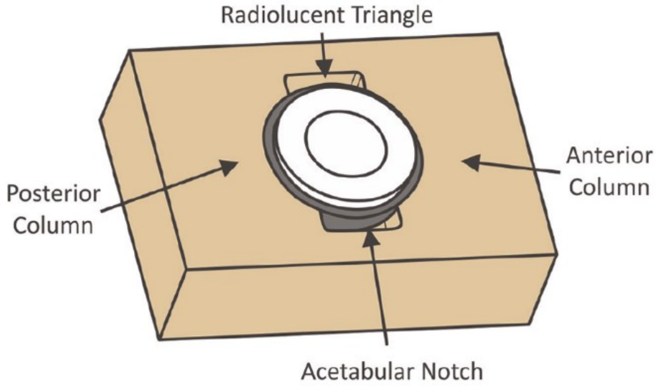

Figure 2.3.24: Bone model using PU foam: the 'pinching' of the ilial and ischial columns are presented with cutouts[132]

In order to develop an *in-vitro* model with properties closely matching the *in-vivo* scenario it is important to match density (Table 2.3.4). The range of densities shown (0.2 – 0.5 g/cm^3) have been validated to match the range of material properties measured in cadavers, from poor to good quality bone.[140,141]

Table 2.3.4: Densities of PU foam and the bone quality it has been used to replicates in different studies

Study	Density (g/cm^3)	Density (PCF)	Bone Quality Aiming to Replicate
Crosnier 2015	0.48	30	High
	0.24	15	Low
Baleani 2001	0.5	31.3	High
	0.2	12.5	Low
Adler 1992	0.5	31.3	High
	0.2	12.5	Low
Fritsche 2008	0.5	31.3	High
	0.3	18.8	Low
Small 2013	0.3	18.8	High
	0.2	12.5	Low

2.3.6 Summary and thesis relevance

The most representative model of implant fixation would be *in-vivo*, in live patients' bone exhibiting the complex mechanical and biological properties of the body. However testing post-implantation would not be ethical. Any non-destructive setup to measure micromotion during surgery would be too complex and delay surgery – compromising patient safety. All destructive methods to measure fixation post-implantation rely on finding load-to-failure, which would damage the bone & prevent further fixation. Impulse based techniques do show some promise for *in-vivo* fixation assessment.[157] However even if such a tool were available clinically, it still would not permit the kind of experimental studies used to optimize implant and surgical technique. In order to determine secure fixation intra-operatively, the surgeon must still rely on the humble 'wiggle' test.[93]

In order to test outside of the clinic researchers must rely on *in-vitro* testing techniques. Test methods to measure implant fixation are varied and ultimately each is best suited to testing a certain mode of loading.[81,122] As rim fixation is dominant in press-fit cups,[77] the push-out test has been shown to correlate well with other testing methods, while offering ease of use.[80,115,132,133] While cadaveric bone models are superior to synthetic in their representation of the *in-vivo* environment, they pose significant hurdles in terms of repeatability. Synthetic models are superior in consistency and ease of use.

2.4 Traditional seating techniques: Impaction

Traditional impaction uses a surgical mallet that gains kinetic energy when swung by a surgeon and generates large forces when decelerated by an impact with an introducer. The magnitude of this energy, the amount of force generated and other impact parameters are of interest to surgeons and engineers.

By understanding the impact mechanics of an impaction strike in theatre, *in-vitro* work can be more representative, and recommendations for force levels can be made to optimize seating and implant fixation. Therefore there has been work to develop methods of measuring impact in the surgical theatre and in the laboratory. Collectively these works build a picture of the impact magnitude that are typically used during surgery and the effect of impaction technique upon implant fixation and seating.

This section examines the engineering mechanisms of impaction, and details the literature that describes the measurement of impaction in surgery and in the lab. In addition to the surgical recommendations made from this testing, the techniques used to measure impaction are discussed.

2.4.1 Engineering analysis

2.4.1.1 Key terms

Force

When an unopposed force (F) is applied to an object with mass it acts to change its momentum (P, Equation 2.4.1).

$$F = \frac{dP}{dt}$$ *Equation 2.4.1*

Momentum is defined as the product of an object's mass (m) and velocity (v, Equation 2.4.2).

$$P = mv$$ *Equation 2.4.2*

By substituting Equation 2.4.2 into Equation 2.4.1 an expression for force, in terms of mass and velocity, is obtained (Equation 2.4.3). Mass is considered constant.

$$F = \frac{d(mv)}{dt} = m\frac{dv}{dt}$$ *Equation 2.4.3*

Using the definition of acceleration (a) as rate of change of velocity, Equation 2.4.4 is obtained. This expression, known as Newton's Second Law, is fundamental to dynamic analyses.

$$F = ma$$ *Equation 2.4.4*

Energy

Energy is the capacity, or potential, of a system to do work. Energy can be stored in many forms, including chemical, gravitational potential, kinetic, nuclear, among others.

A type of energy relevant to this thesis is kinetic, whereby a mass (m) has a velocity (v) relative to a reference frame. The energy (W) of this system is that required to decelerate the system to zero velocity, with respect to the given reference frame. An expression for the kinetic energy of an object can be obtained from the Work-Energy theorem (Equation 2.4.5).

$$dW = Fdx$$ *Equation 2.4.5*

By integrating with respect to distance (x) an expression for total energy (or work) is obtained (Equation 2.4.6).

$$W = \int_{x_1}^{x_2} F(x)dx$$ *Equation 2.4.6*

The force term can be substituted for Equation 2.4.3 (Equation 2.4.7).

$$W = \int_{x_1}^{x_2} m\frac{dv}{dt}dx$$ *Equation 2.4.7*

In order to integrate the expression, the chain rule must be applied (Equation 2.4.8).

$$\frac{dv}{dt} = \frac{dx}{dt}\frac{dv}{dx} = v\frac{dv}{dx}$$ *Equation 2.4.8*

By combining Equation 2.4.7 and Equation 2.4.8, an expression that can be integrated is obtained (Equation 2.4.9).

$$W = \int_{x_1}^{x_2} mv\frac{dv}{dx}dx = m\int_{v_1}^{v_2} vdv$$ *Equation 2.4.9*

When integrated between two velocities, v_2 (final velocity) and v_1 (initial velocity) an expression for the kinetic energy of an object is obtained (Equation 2.4.10).

$$W = m\left[\frac{v^2}{2}\right]_{v_1}^{v_2} = \frac{1}{2}m(v_2^{\,2} - v_1^{\,2})$$ *Equation 2.4.10*

Impulse

Impulse is the integral of a force (F) applied to an object with respect to the time for which it is applied (Equation 2.4.11). Impulse applied to an object is equivalent to its vector change in momentum.

$$I = \Delta P = \int_{t_1}^{t_2} F(t)dt \qquad \textit{Equation 2.4.11}$$

2.4.1.2 Force/energy relationship

During impact it is possible to derive an expression for the energy transferred as a function of impaction force. To do so we assume an object with unknown mass impacts another object, imparting a known force trace during collision. The velocity before the impact v_i is known but no velocity remains post-strike. Beginning with Equation 2.4.10 an expression is derived for the impacting object just before strike (Equation 2.4.12).

$$W = \frac{1}{2} m v_i^2 \qquad \textit{Equation 2.4.12}$$

This expression can be rearranged to isolate m and v_i (Equation 2.4.13).

$$m v_i = \frac{2W}{v_i} \qquad \textit{Equation 2.4.13}$$

The change in momentum of the object as a function of velocity can be obtained (Equation 2.4.14). Again v_f is considered to be zero and is removed.

$$dP = d(mv) = m(v_i - v_f) = m v_i \qquad \textit{Equation 2.4.14}$$

Expressions for impulse (Equation 2.4.11), kinetic energy (Equation 2.4.13) and change in momentum (Equation 2.4.14) can be combined (Equation 2.4.15).

$$\frac{2W}{v_i} = \int_{t_1}^{t_2} F(t)dt \qquad \textit{Equation 2.4.15}$$

By rearranging for W an expression that allows us to calculate energy from a known force trace and velocity prior to impact is obtained (Equation 2.4.16). Mass is not required, allowing use in situations where the impacting mass is not known (for example the combination of hand and surgical mallet during impaction).

$$W = \frac{1}{2} v_i \int_{t_1}^{t_2} F(t)dt \qquad \textit{Equation 2.4.16}$$

2.4.1.3 Mass-Spring-Dashpot (MSD) systems

Mechanical models can be used to represent different elements of dynamic processes, and link the key concepts of Section 2.4.1.1. Three common elements are mass, springs and dashpots. The resistance of each to displacement with applied force is given in Figure 2.4.1. Mass is represented as a small, rigid body obeying Newton's Second Law. Spring components apply a resisting force directly proportional to displacement from original length. Dashpot components apply a resisting force directly proportional to the velocity of deformation. In these idealised models the components that make up the spring and dashpot are considered to have zero mass.

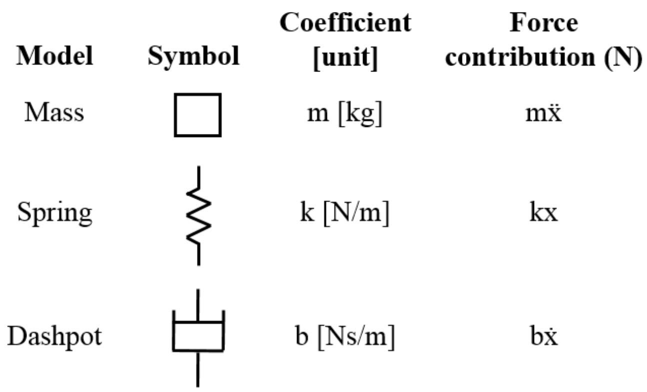

Figure 2.4.1: Elements of spring/dashpot models and their contributions of force

Four commonly used models are the mass-spring, Maxwell, Voigt and Kelvin models (Figure 2.4.2).[182]

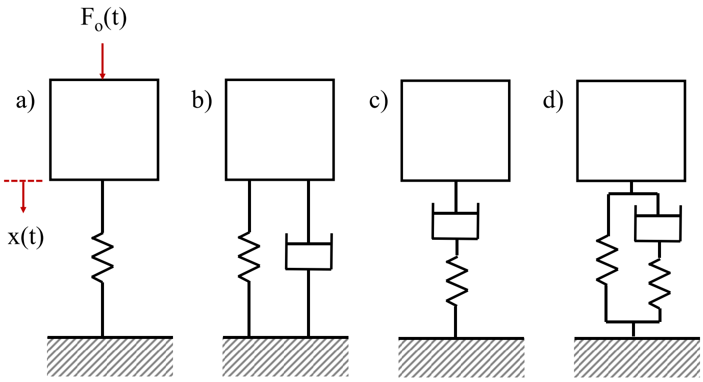

Figure 2.4.2: Model configurations for: a) Mass-spring b) Voigt c) Maxwell d) Kelvin

The simplest model, the mass-spring, is useful for materials or systems with very little hysteric energy loss during motion (for example metals in the elastic region). Using the definitions of Figure 2.4.1, a force balance can be applied to the system when a force (F_o) is applied over time (Equation 2.4.17).

$$F_0(t) = m\ddot{x} + kx \qquad \textit{Equation 2.4.17}$$

Impulse excitation

One of the key applications of MSD systems in this thesis is the behaviour of systems (impactor, implant, patient) during impact. Therefore simulations to quantify the effects of varying MSD parameters were performed.[a] The effect of varying mass can be seen in Figure 2.4.3. It can be seen that with increasing mass, natural frequency is reduced, as well as amplitude.

[a]Initially a mass-spring then mass-spring-dashpot (Voigt) model was simulated in MATLAB. Unit mass, spring and dashpot values were imposed upon the system unless otherwise defined. An impulse of unit force and occurring for a unit time was used to excite the systems. Subsequently displacement of the systems is reported. The MATLAB code used is reported (Appendix 9.1)

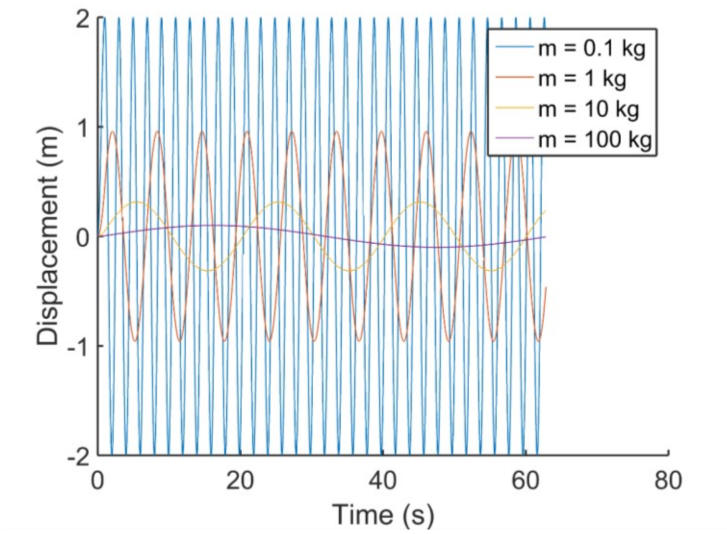

Figure 2.4.3: Simulation of mass-spring model excited using a unit impulse excitation. Increasing mass reduces peak amplitude and natural frequency of the system

The natural frequency of a mass-spring system is given by Equation 2.4.18. It can be seen that an increase in system mass will result in a lower natural frequency.

$$\omega_n = \sqrt{\frac{k}{m}}$$ *Equation 2.4.18*

An expression for the peak amplitude of a mass-spring system in terms of the input impulse can be derived, starting with the definition of impulse (Equation 2.4.2). By considering impulse in terms of the change in velocity of an object, Equation 2.4.19 is obtained.

$$I = \Delta P = mdv = m(v_2 - v_1)$$ *Equation 2.4.19*

As the system is initially at rest, $v_1 = 0$. Subsequently the expression can be rearranged (Equation 2.4.20).

$$\frac{I}{m} = v_2$$ *Equation 2.4.20*

This expression can be substituted into Equation 2.4.14 in order to derive an expression for energy input to the system in terms of impulse (Equation 2.4.21).

$$W = \frac{I}{2m} \cdot \int_{t_1}^{t_2} F(t)dt$$ *Equation 2.4.21*

The definition of impulse (Equation 2.4.11) can be further utilized in to remove the force term (Equation 2.4.22).

$$W = \frac{I^2}{2m}$$ *Equation 2.4.22*

This expression quantifies the work done on the system during the impact. At peak displacement the system has no kinetic energy but maximum potential stored in the spring system. Therefore Equation 2.4.22 can be equated Equation 2.4.31 (derived in the following section).

$$\frac{1}{2} k x_{max}{}^2 = \frac{I^2}{2m}$$ *Equation 2.4.23*

Rearranging for maximum displacement amplitude of the system (x_{max}) obtains an expression with respect to input impulse and mass/spring properties (Equation 2.4.24).

$$x_{max} = \frac{I^2}{\sqrt{km}}$$ *Equation 2.4.24*

As shown in Figure 2.4.3, Equation 2.4.24 demonstrates that an increase in system mass reduces peak displacement.

Varying spring constant instead of system mass also causes variations in system natural frequency and peak amplitude (Figure 2.4.4). Similar to increasing mass, peak amplitude is decreased with increasing spring stiffness. However increasing spring stiffness increases natural frequency of the system.

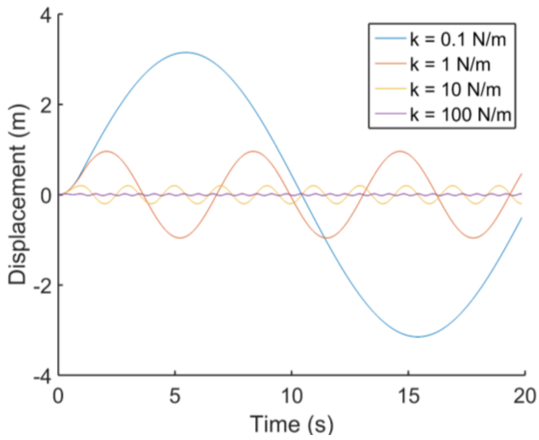

Figure 2.4.4: Simulation of mass-spring model excited using a unit impulse excitation. Increasing spring stiffness reduces peak amplitude but increases natural frequency of the system

The manner in which impulse is applied to MSD systems also has an effect upon the displacement output. A unit impulse can be applied over a very short period of time with a high force, or over a longer period of time with a smaller force. The resultant maximum deflection of the system after impulse loading can be converted to total energy transferred using Equation 2.4.23.

The energy transferred to a mass spring system is reduced with an increasing impulse period (Figure 2.4.5, Appendix 9.2). An appreciable difference in energy transfer is seen when the impulse duration is a fifth or more of the length of the total duration of the systems natural period.

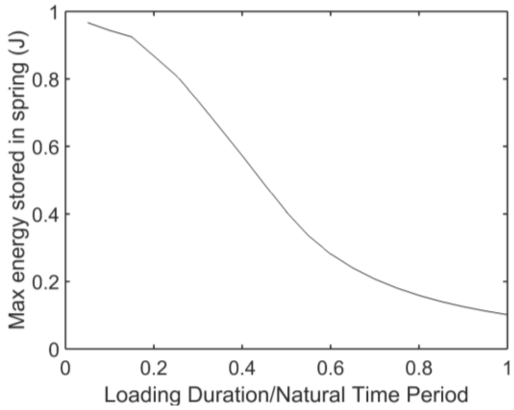

Figure 2.4.5: Energy transfer for a mass-spring system excited by a unit impulse. The x-axis is the ratio of the length of the pulse over the natural time period of the system

If a dashpot element is added in parallel with the spring, a Voigt model is created (Figure 2.4.2). A new force balance can be produced (Equation 2.4.25).

$$F_0(t) = m\ddot{x} + b\dot{x} + kx \qquad \textit{Equation 2.4.25}$$

The effect of a damping element is a reduction in displacement amplitude with time (Figure 2.4.6).

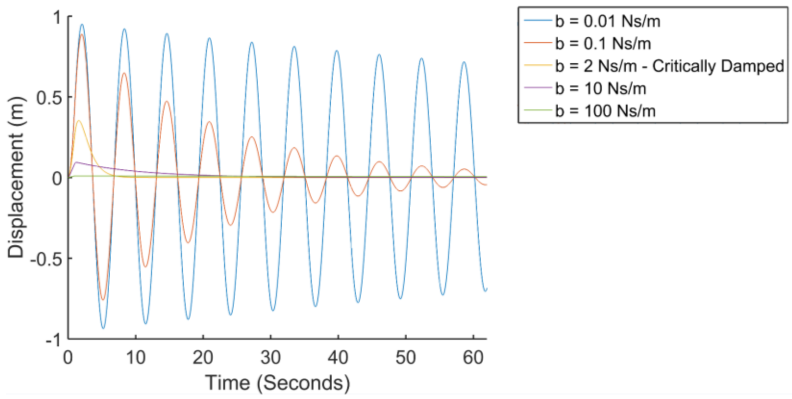

Figure 2.4.6: Simulation of Voigt model excited using a unit impulse excitation. Increasing dashpot coefficient increases the rate at which peak amplitude is attenuated. Only one oscillation is achieved for critically, or overdamped, systems.

It can be seen that for certain conditions oscillations are attenuated peak-by-peak, but still occur more than once. These systems are under-damped. For damping exceeding a critical value, only one positive peak is observed. The critical dashpot coefficient for which this condition is achieved can be given as a function of system mass and spring constant (Equation 2.3.1).

$$b_{critical} = 2\sqrt{km} \qquad \textit{Equation 2.4.26}$$

Harmonic excitation

When a mass-spring-damper system, of natural frequency ω_n is forcibly oscillated at a frequency ω_f, the solution to Equation 2.4.25 can be complex, as many transient responses may be created. However given a suitably long time, the steady state solution can be found, where A is peak system amplitude and φ is a phase shift between excitation and response frequency (Equation 2.4.27).[182]

$$x(t) = A\cos(\omega_f t + \varphi) \qquad \textit{Equation 2.4.27}$$

By differentiating this expression to obtain $\dot{x}$ and $\ddot{x}$ and then substituting into Equation 2.4.25 an expression relating maximum displacement amplitude (A) and input force F_o is found for steady state conditions.

$$A = \frac{F_0}{\sqrt{m(\omega_f^{\,2} - \omega_o^{\,2})^2 + b\omega_f^{\,2}}} \qquad \textit{Equation 2.4.28}$$

When $\omega_f = \omega_n$ the resultant amplitude of displacement is at a maximum, a condition known as resonance. This amplitude increases with decreasing damping, tending to infinity for zero damping (Figure 2.4.7).

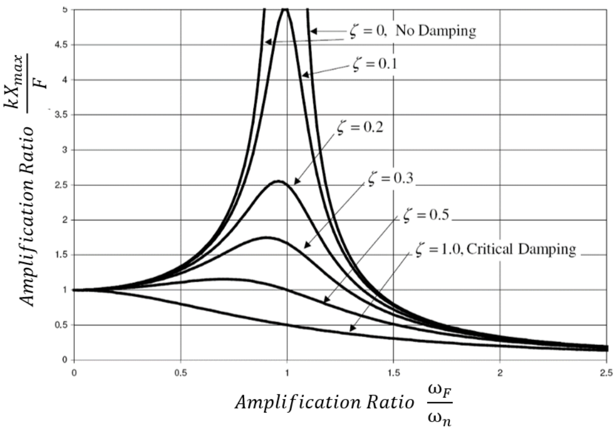

Figure 2.4.7: Amplification of sinusoidal input force to an MSD system: a maximum is reached when forcing frequency is equal to the natural frequency of the system, a condition known as resonance

2.4.1.4 Impaction elements

The impaction process can be described as involving 4 main elements. These are the surgical mallet, the introducer, the implant and the bone (supported by the surrounding soft tissues of the hip, Figure 2.4.8). As the introducer and implant are rigidly connected these can be considered one mass. Three main interactions occur; between surgical mallet and introducer, between cup and bone and between bone and soft tissues. This section examines the analytical relationships that can be used to describe these interactions.

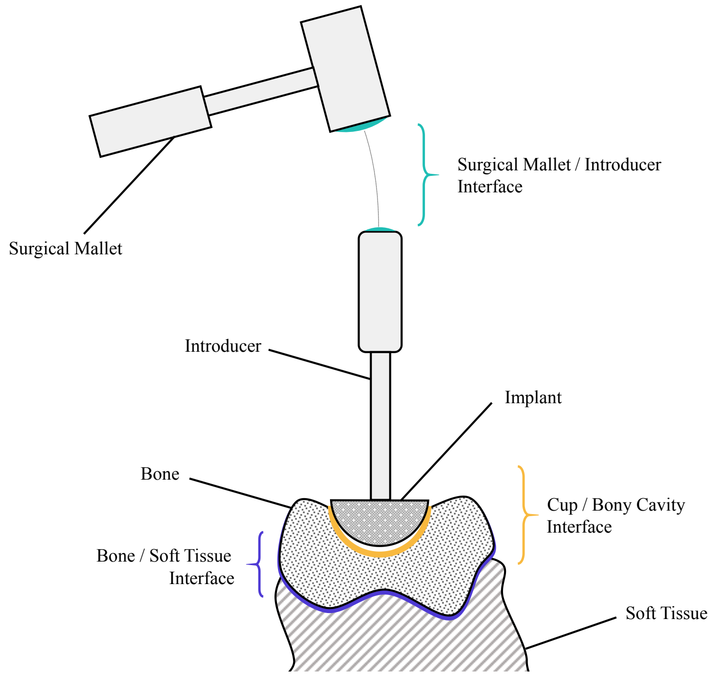

Figure 2.4.8: Various elements and interfaces to consider during orthopaedic impaction

Surgical mallet/introducer interface

During the mallet strike, momentum is transferred to the introducer/implant body. Two elements of this interaction may be of interest to engineers and surgeons: peak force and impact duration.

Both mallet and introducer tend to be metal and so can be approximated with mass-spring systems (Figure 2.4.9). As the mallet of the hammer contacts the introducer its energy is converted from kinetic to potential energy stored in the spring. At peak spring deformation the peak force exerted by the spring can be calculated.

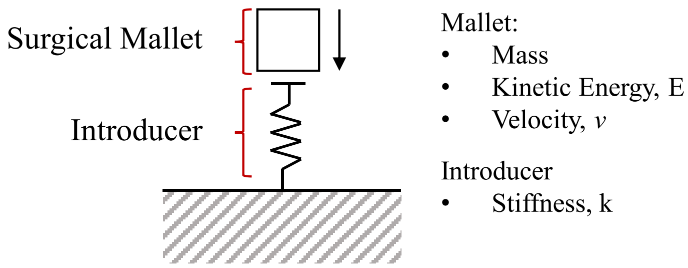

Figure 2.4.9: Approximation of mallet/introducer interaction. The mallet has a mass, m, and the introducer a stiffness, k.

In order to calculate peak force the force/displacement response of the spring is first required (Equation 2.4.29).

$$F = kx$$ *Equation 2.4.29*

Using the integral of the Work-Energy theorem (Equation 2.4.6).an expression for the energy required to deform the spring from an initial displacement (x_1) to final displacement (x_2) can be derived (Equation 2.4.30, Equation 2.4.31).

$$W = \int_{x_1}^{x_2} (kx)dx$$ *Equation 2.4.30*

$$W = \frac{1}{2}k({x_2}^2 - {x_1}^2)$$ *Equation 2.4.31*

If initial displacement is assumed to be zero, the expression can be rearranged for any displacement x (Equation 2.4.32).

$$x = \sqrt{\frac{2W}{k}}$$ *Equation 2.4.32*

Equation 2.4.29 and Equation 2.4.32 can be combined in order to define an expression relating peak impact force and impact energy.

$$F_{peak} = \sqrt{W}\sqrt{2k}$$ *Equation 2.4.33*

Using the same model the duration of impact can be approximated. The time period of the mass-spring system (in seconds) can be calculated from the natural frequency of the system (Equation 2.4.34).

$$T = \frac{2\pi}{\omega_n} \qquad \textit{Equation 2.4.34}$$

By combining Equation 2.3.1 (engineering strain), Equation 2.3.2 (engineering stress) and Equation 2.3.3 (Young's modulus for an elastic material) an expression for the stiffness of the introducer is obtained. Here the introducer is assumed to be of a constant cross section and modulus.

$$\frac{EA}{L} = \frac{F}{x} = k \qquad \textit{Equation 2.4.35}$$

By combining this expression with that defining the natural frequency (Equation 2.4.18) and the time period of a mass-spring system an expression for the time period of impact is derived.

$$T = \pi\sqrt{\frac{mL}{EA}} \qquad \textit{Equation 2.4.36}$$

Cup/bony cavity interface

Section 2.3.1.5 details the reaction between cup and bony cavity during cup insertion. This mass is accelerated into the bone cavity, but is resisted by the friction induced at the implant/bone interface. It is known that the dynamic interaction of implant and bone is difficult to accurately predict due to the mechanisms of kinetic friction, lubrication and bone damage.[113,114] Attempts have been made to recreate the seating process numerically using time dependent 'slip-stick' models.[83,92]

Bone/soft tissue interface

A number of analytical models have been suggested to represent soft tissue compliance.[181]

A simple spring-mass model has been used to replicate the stiffness of the femur during primary impact and was found to satisfactorily predict peak force.[172] However such a model does not predict the viscoelasticity properties measured in soft tissues.[181] Viscosity can be represented with a dashpot in either Maxwell or Voigt models, both shown to produce a similarly accurate prediction of peak forces in the femur,[172] with the Voigt model published as a suitable biomechanical model in several studies.[165,167,183] The Kelvin model was shown to have only a small improvement over Maxwell and Voigt models.[184] In the field of orthopaedic impaction, Voigt models have been used to model impaction during seating of hip resurfacings.[185]

2.4.2 Clinical impaction

2.4.2.1 Impaction magnitudes

Impaction magnitudes have been measured for a number of different arthroplasty procedures. These include: seating the acetabular cup or femoral stem, rasping the cavity for the femoral stem, seating a femoral head on the femoral stem and seating an acetabular liner in the acetabular cup. Different metrics are reported in the literature, including impact force, impact energy or mallet velocity. Peak impact force is most commonly quoted (Figure 2.4.10).

Figure 2.4.10: Peak Impaction forces measured for a variety of arthroplasty procedures. A wide spread of values for each is reported

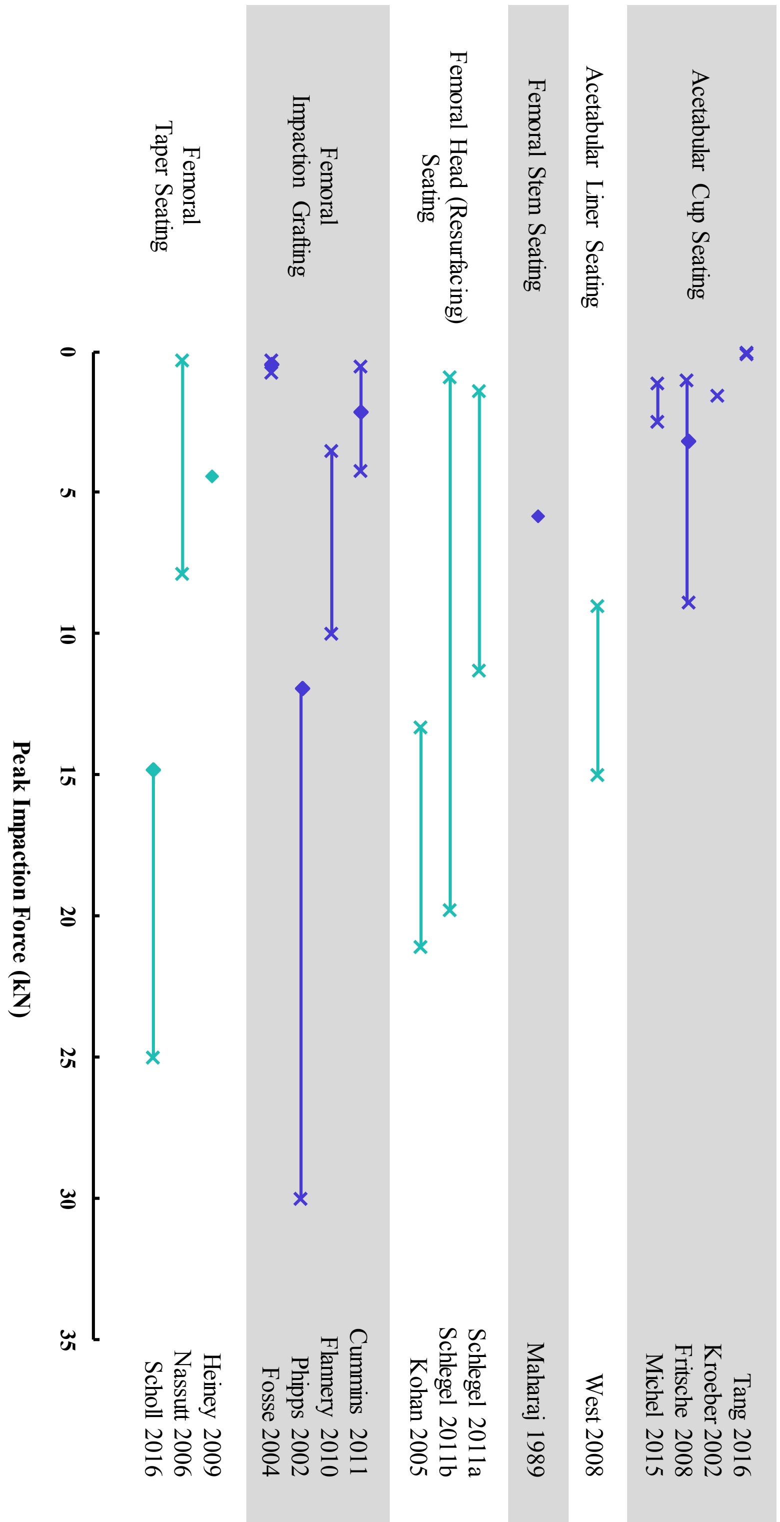

The values reported for each procedure are useful for a variety of reasons. They can be used to replicate impaction conditions *in-vitro*, or *in-silico*. They can be used to inform surgeons of the effects of different impaction techniques. They can also be used to test surgical devices.

It is clear from the very large spread of values that there isn't much consensus on the magnitudes of strike that actually occur during arthroplasty. This could be for two reasons. It is likely that *in-vivo* values vary a large amount. In addition values measured might vary due to discrepancies in measurements techniques. The reality is likely a combination of both.

2.4.2.2 Effects of impaction magnitude

There is little literature explicitly examining the effects of different levels of impaction upon the seating of implants. For the femoral stem the existence of a threshold force, below which impaction is unlikely to fracture the bone, has been investigated. It was found that the majority of femurs fractured when an impaction force of above 0.5 kN was applied.[72] This is considerably lower than the impaction forces previously measured during femoral seating in other studies.[151,158] One evaluation of the effects of seating load upon fixation are reported using a quasi-static test. Increased seating loads increased fixation strength (Figure 2.4.11).[115] Using computational techniques Michel et. al. found that higher strike velocity reduced final polar gap, and reduced the number of strikes required to reach steady polar gap.[138] Similar findings are reported for femoral head tapers.[159] An increase in impaction force also increased likelihood of fracture during the seating of hip resurfacing femoral heads.[35]

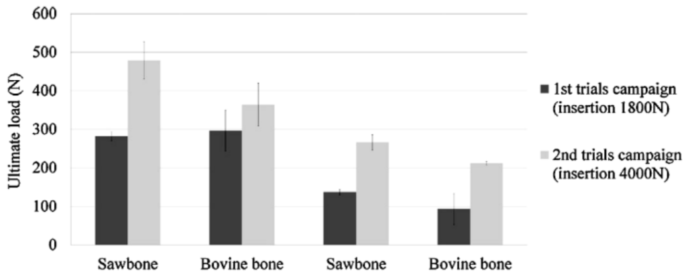

Figure 2.4.11: Fixation strength for different seating loads: higher insertion force increases fixation (ultimate load)

2.4.2.3 Effect of frequency of impaction

West et. al. measured the average frequency of any impaction procedure (including cup/liner insertion and femoral rasping) to be 2.3 hz.[158] No statistical difference between surgeons was found, and no comment on the effect of impaction frequency was made. Cummins et. al. looked to define the difference between 1 hz and 10 hz impaction frequency to determine how this affects threshold impaction force.[72] It was reported that impaction frequency had no effect upon threshold impaction force.

2.4.2.4 Effect of number of strikes

No manufacturer recommendations exist to guide the number of strikes used by surgeons to seat implants. It has been reported that the number of strikes used to seat an implant varies between surgeons[158] and by a range of 7 to 46 strikes.[127] It is also reported that it is not possible for the surgeon to accurately determine when an acetabular cup is seated.[93]

The effect of number of impaction strikes is assessed by a number of studies, but none recommend an absolute number or technique. When seating an acetabular cup an increase in periacetabular strains for each impact strike cups has been reported,[33,93] suggesting that both fixation, and fracture risk, increase with post-seating strikes. During impaction, it has been found that the majority of the implant displacement occurs in the early phases of seating, with progression slowing after excessive seating (Figure 2.4.12).[93,108,160]

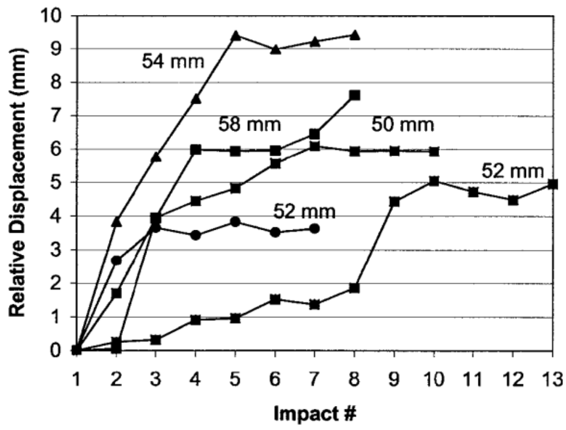

Figure 2.4.12: Progression of cups into a cadaveric acetabulum. Initial progression is large, but slows after a number of strikes

2.4.3 Variability in measurement methods

Measuring and characterizing impaction technique requires sensors and acquisition systems that can deal with highly dynamic events, with impact durations of less than 5 ms.[160] Many of the issues associated with instruments impact tests have been highlighted,[161] but are not always addressed in orthopaedic literature. Many different methodologies are used to measure orthopaedic impaction, as summarized in Table 2.4.1.

2.4.3.1 Boundary conditions/support compliance

A key factor in the measurement of any impaction event is the compliance of the medium supporting the test piece.[161,162] Force is applied to the object during impact. If the object is being supported by a compliant medium it will accelerate in the direction of the force. It is this acceleration that increases the overall collision time of the impact and therefore reduces peak force transferred to the object (Figure 2.4.5). In the scenario of interest to this thesis (impaction of cementless implants into bony cavities) the support of the bone is soft tissues. Most often, the soft tissue compliance of the hip isn't replicated during impaction testing, and when it is compliance values are unknown (Figure 2.4.13).[93]

Table 2.4.1: A summary of the different methods used to measure orthopaedic impaction. Varied methodology may go some way to explaining a wide spread of values quoted

Procedure Type	Study	Sample	Soft tissues/boundary conditions	Method	Load Cell			Aquistion Rate (kHz)	Strike Surface
					Limit (kN)	Type	Location		
Acetabular Cup Seating	Tang 2016	Anatomical Sawbone	Rigid	Load Cell	0.20	Strain	Base of introducer	~	Steel
	Kroeber 2002	Cadaveric	Rigid	Load Cell	~	Piezo	Hammer tip	~	~
	Frische 2008	Cadaveric & Sawbone	Rigid	Load Cell	~	Strain	Hammer tip	~	~
	Michel 2015	Bovine acetabular	Rigid	Load Cell	4.40	Piezo	Hammer tip	51.2	Steel
Acetabular Liner Seating	West 2008	Cadaveric	Soft tisse	Load Cell	~	~	Hammer tip	~	~
Femoral Stem Seating	Maharaj 1993	Cadaveric & Sawbone	Both rigid & soft tisse	Load Cell	22.00	Piezo	Top of introducer	33.3	Delrin
	Scholl 2012	Cadaveric	Rigid	Load Cell	~	~	Hammer tip	~	~
Femoral Head (Resurfacing) Seating	Schlegel 2011	Cadaveric	Rigid	Load Cell	22.40	Piezo	Under introducer	60.0	~
	Schlegel 2011	Cadaveric	Rigid	Load Cell	22.40	Piezo	Under introducer	~	~
	Kohan 2005	Patient	Soft tissue	Load Cell	100.00	Piezo	Hammer tip	200.0	Steel
Femoral Impaction Grafting	Cummins 2011	Cadaveric	Rigid	Load Cell	~	Strain	Under femur	~	~
	Flannery 2010	Sow femur	Rigid	Load Cell	~	Strain	Under femur	~	~
	Phipps 2002	Patient	Soft Tissue	~	~	~	~	~	~
	Fosse 2004	Rubber	Rubber	Load Cell	~	Strain	Under rubber	~	~
Femoral Taper Seating	Heiney 2009	Fuji film	Rigid	Fuji Film	~	Fuji Film	~	~	~
	Nassutt 2006	None	~	~	~	~	~	~	~
	Scholl 2016	Anatomical Sawbone	Rubber	Load Cell	50.00	Piezo	Hammer tip	100.0	Steel

a) b)

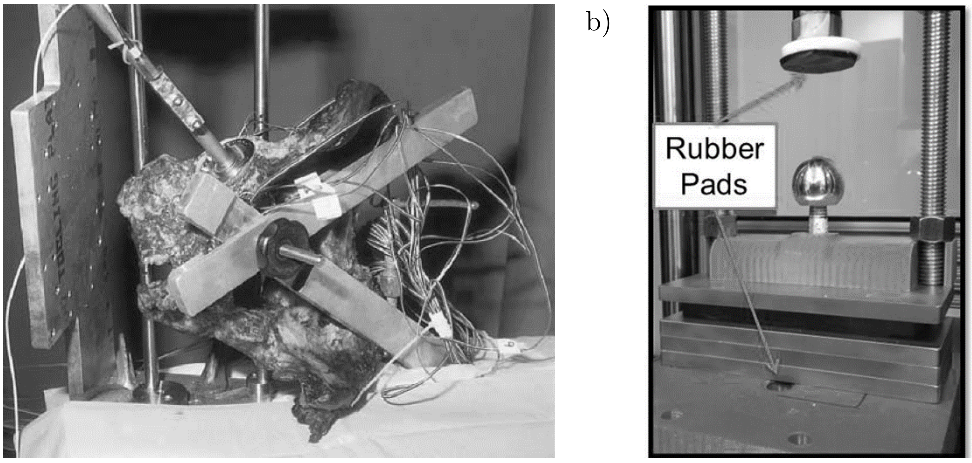

Figure 2.4.13: Impaction testing setups using with: a) A very stiff support structure; b) Rubber used to estimate patient compliance

In the biomechanical field there is a large body of work exploring the effect of soft tissues surrounding the hip upon the peak force experienced by the femur during sideways falls.[163–166] It has been reported that compliance of soft tissues and the non-infinite stiffness of the femur contributes significantly to the reduction of peak force that the femur experiences during impact.[165,167] Studies have determined how BMI, bone density, sex, and age all affect the compliance of the hip.[166,168,169] Subsequently test setups have been developed to accurately replicate the effects of hip compliance during testing of sideways hip falls.[170–172] These methods are now frequently used to pre-clinically test devices intended to shield the hip during falls and reduce the peak force experienced by the femur.[170,173,174] These studies are an example of a field that has developed a sophisticated understanding of the effects of compliance during impact and has implemented these ideas into pre-clinical testing.

The work in this thesis is also based upon dynamic impaction work that is applied to specimens (the femur and acetabulum) encased within a compliant structure (soft tissues surrounding the hip). There has been a number of studies that have suggested that the compliance of the hip and surrounding tissues may have an effect upon the risk of fracture or other impact behaviours of bone. When examining the effects of impaction technique upon femoral taper locking strength, Nambu et. al. used ballistic gel as a surrogate of soft tissue.[175] In similar setups, Scholl et. al. used two sheets of neoprene, Kold et. al. used a ‘dense foam’ and Krull et. al. used springs for the same purpose.[37,159,176] Cummins et. al. and Flannery et. al. both cite lack of representative compliant support for embalmed cadaveric specimens as a limitation of their studies to measure fracture forces in the femur.[71,72] It has been reported that patient BMI has an effect upon the amount of force transferred between segments of the acetabulum during impaction.[177] Similarly a difference was shown between compliant and rigid boundary conditions when seating femoral stems; with a rigid boundary condition stems were seated in less strikes but had a higher chance of fracture.[178] Studies reporting the importance of boundary conditions upon seating of femoral tapers are conflicting reporting both a different of stem seating with patient boundary conditions,[179] and no difference.[180]

Clearly the idea of compliance of soft tissues affecting the hip has been explored, but no current model accurately replicates the compliance of the hip.

2.4.3.2 Load cell variables

The two most common choices of load cell are based upon either strain gauges or piezo crystals. Strain gauges measure the strain of a material for which the relationship between stress and strain is known. Therefore stress (and subsequently load) can be calculated. Piezo crystals produce an electrical charge when strained. This is measured and load can be derived directly. The signal from a piezoelectric load cells decays very quickly and therefore cannot be used for quasistatic loading. However piezo load cells are inherently stiffer, and displace less during impact and therefore effect the measured force less that strain gauge based equivalents.[186] Strain gauge load cells also have lower resonate frequency and are therefore more likely to be in range of high frequency resonance produced by metal–on–metal impacts.[161] It has been reported that the effects of load cell resonance during impact loading can produce misleading results (the amplitude of resonance reported rather than the actual loading).[187] This issue is not often discussed, and is acknowledged to be omitted from various standards defining impact testing.[188]

2.4.3.3 Acquisition rate

Impact loading, particularly for hard-on-hard cases, requires very high acquisition rates.[187] The stiffness of the introducer and impactor lead to an extremely short impact duration which must be adequately described by sampling points.[160] If an impact load trace is under-sampled peak values may be underestimated.[189] A possible option is to filter impact data, however this has a similar effect to under-sampling.[190] Ideally acquisition rate must be high enough to capture all data points during testing.[191] The acquisition rate of load measurement apparatus and impact duration is rarely given in the literature and is therefore another possible factor in variability (Table 2.3.1).

2.4.3.4 Strike surface

Impact force is affected by the material of the two colliding materials.[192] Reducing stiffness and increasing plasticity reduces resultant impact force as the impact duration is increased.[162,193] Many studies do not state the materials used in the strike surfaces, making it difficult to compare results like-for-like.

2.4.3.5 Load cell location

The location of the load cell on impaction tools may have an influence upon the force measured.[159] For acetabular seating the average reported force with papers using hammer tip measurement[33,93,157] are indeed higher than the studies measuring at the base of introducer.[194] The same trend is observed for measurement of hip resurfacing values.[35,185,195] It is important for the location of the load cell to be stated and elements in the load path described.

2.4.3.6 Inertial effects

When an object with low damping (such as a metal introducer or load cell) is impacted it will resonate. This resonation is a high frequency alternating acceleration, generating force.[188] Inertial forces may be significant and mistaken for actual impact loads.[187] Therefore if there is undamped mass in an impaction load path care should be taken to minimize inertial loads.

2.4.3.7 Impaction versus quasi-static testing

As setup complexity is minimized by using a quasi-static setup many studies choose to seat implants using a displacement controlled materials testing machine.[81,115,132,196] However it is acknowledged that bone is strain-rate dependent.[81,115,147,181] Similarly dynamic and static friction value measured at the bone/implant interface have been found to be different and therefore vary when seating implants at high displacement rates.[197] Yew et. al. found that using displacement controlled seating (similar to quasi-static) and load controlled seating (similar to impact testing) produced different peak loads.[108] No current study validates quasi-static seating as a method of representing dynamic impaction.

2.4.4 Summary and thesis relevance

The mechanics during impaction are complex and are usually measured in physical models. The magnitudes of orthopaedic impaction processes have been reported, but the spread of values is very large. In addition little evaluation of the influence of impaction technique upon seating mechanics exists. Highly dynamic testing involves many challenges and sources of variability that may account for some of the variation in the literature

2.5 Novel seating techniques: Oscillatory seating

Although impaction is traditionally carried out with a mallet and introducer, new devices offer an alternative. Instead of large, single strikes oscillations are used to create many, smaller impulses. Two such devices currently exist in the surgical marketplace: the Depuy Kincise, and the IMT Woodpecker.

The Kincise (previously known at the ME-1000), a device only recently revealed following acquisition of Medical Enterprises Distribution LLC (Norcross, Georgia, USA) by Depuy Synthesis (Warsaw, Indianapolis, USA),[198] is an electric hand tool intended for both femoral cavity reaming and femoral/acetabular implant seating. Many claims are made by Depuy as to the benefits of the device over traditional impaction. It is suggested that the Kincise delivers a more accurate femoral cavity following rasping, while reducing stresses in the bone during the process,[199] a more constant energy delivery,[200,201] and reduced fatigue and injury to surgeon.[202] There are no peer reviewed studies discussing the Kincise at time of writing.

The Woodpecker, developed by Intergral Medizintechnik (IMT, Luzern, Switzerland), is marketed as an alternative to hammer strikes during femoral rasping (Figure 2.5.1). The Woodpecker is pneumatically driven. The impactor is driven at 70 Hz with a stroke length of 10mm. Similar to the Kincise, IMT's literature claims lots of advantages of the system over traditional hammer strikes. Accurate reaming, minimizing of damage to cortical bone, minimizing chance of fracture, reduction in operation time, reduced change of marrow emboli and more consistent results are all cited.[203] It is also claimed that use of the Woodpecker reduces axial force of implantation to just 1 N and minimizes radial hoop stresses.[204]

Figure 2.5.1: Pneumatic oscillatory impaction tool: The 'Woodpecker' by IMT[204]

Several studies have examined the use of the Woodpecker. Bolland et. al. reported a reduction in stem subsidence and a reduction of strain in the femoral bone when using the Woodpecker to compact bone graft during THA (Figure 2.5.2).[205] Eroglu et. al. reported a reduction in operation time, femoral fracture and amount of blood transfusion required when using the Woodpecker.[206] Branovacki et al. reported a 'low learning curve' with residents 'unfamiliar with the technique' of pneumatic broaching[207] but did not compare to a control group. Hourlier et. al. reported that use of the Woodpecker reduced stem subsidence from an average of 7mm to just 1mm when the results of one surgeon using the Woodpecker to several other surgeons using traditional methods.[208] This was attributed to 'intimate contact' between implant and cortical bone. None of the aforementioned studies use an appropriate control group or well defined outcome measures. Goosens et. al. have reviewed the feasibility of using the Woodpecker as a method of seating femoral implants using an *in-vitro* study.[209] It was reported that peak stresses in the bone were lower when seating were lower with the Woodpecker when compared to traditional mallet strikes. However the overall amount of strain that could be generated (and therefore the implied level of fixation) was lower for the Woodpecker than traditional strikes.

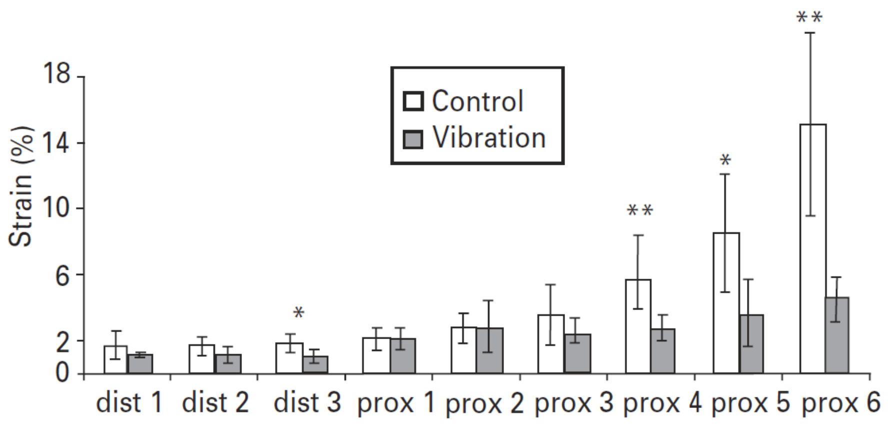

Figure 2.5.2: Bolland et. al. show a reduction in proximal femur strain when rasping using the Woodpecker versus traditional strikes

2.5.1 Summary and thesis relevance

There appears to be increasing interest in vibration assisted, oscillatory seating of implants as a method of reducing fracture risk and increasing the control a surgeon has over the impaction process, with some evidence of the superiority of such devices over traditional methods. However the current literature is sparse and manufacturer claims are often unsupported. Further work is required to assess the performance of these devices.

2.6 Chapter summary

- Many orthopaedic surgeries use a form of impaction to prepare bone cavities, seat implants or assemble tapers.
- While modern cementless implants have proven to be very effective, possible issues are identified as:
  - Bone fracture during seating
  - Excessive component deformation
  - Lack of initial fixation
  - Lack of bone/implant apposition
- Acetabular cups are more like to loosen than femoral stems and are chosen as the focus for this thesis.
- Rim fixation dominates acetabular cup fixation. Many methods of testing implant fixation are available, but push-out testing is simple and results are comparable to other methods.
- Cadaveric bone is more representative than synthetic bone but is not as repeatable. Synthetic bone models have been validated in many studies.
- Impaction data for many surgical procedures has been reported but vary a large amount, due to surgeon technique, and possibly the effects of measurement variables. A key variable might be the compliance of the testing rig.
- The effects of impaction technique are not well understood.
- Novel implant seating techniques show some promise but are mostly unproven.

Chapter 3: An *in-vitro* model of impaction in hip arthroplasty

3.1 Introduction

Cementless implants require precise implantation through impact strikes, usually delivered with a mallet, and an appropriate interference fit with the prepared bone. The impaction and interference fit need to be sufficient to provide primary fixation, but not so much that they cause deformation of the components or generate high strains in the bone. Issues due to improper impaction are widely reported. Acetabular cup deformation of over 0.5 mm has been recorded under worst case conditions[110] which is clinically important as deformations can lead to excessive wear[210] or improper component assembly.[40,211] High impact forces can also lead to fracture of both the acetabular and femoral bone.[51,58–60,212–214]

Therefore it is important to understand the impaction forces and fixation mechanisms that occur when a femoral or acetabular component is press-fit in the bone. A wide range of values exist for impaction force in THA surgery - between 1.5kN and 27kN have been measured for implant seating in the acetabulum[33,93,158] or between 5.8kN and 22kN for the femoral stem.[151,158] Further to these data, femoral bone has been reported to fracture at between 0.5kN and 4kN stem impaction.[71,72]

The wide range of values reported may be at least partly explained by the test setups used to measure impact. Few studies measure impact *in-vivo*[185,215] due to the cost, complexity and ethics of testing in surgery. More common is to study impaction *in-vitro* using cadaveric specimens stripped of soft tissue[33,35,72,93,104,158,159,195] or expanded polyurethane (PU) foams as an analogue for cadaveric bone.[33,108,216] These types of experiment are usually performed with specimens rigidly potted in the test frame of laboratory equipment, or fixed to laboratory benches of unknown stiffness, and ignore the compliance of the body segments and soft tissues that support the acetabulum and femur during the implant impaction strikes.

These rigid test setups may not be an adequate representation of the intraoperative conditions because any movement of the bone during impaction could cushion the impact and attenuate peak forces. For example, the cushioning effect of the trochanteric tissues influence risk of hip fracture during a fall, because they attenuate the impact force experienced by the bone.[164,165] The relative movement between body segments also influences the peak force – recent studies have found the force transmission during acetabular impact is different for patients of varying body weights.[177] Indeed boundary conditions have been found to directly influence the stress in the femur and the number of strikes to seat a femoral stem.[178]

There is no current bespoke testing platform for testing orthopaedic implants during impaction. The aim of this chapter is to create an *in-vitro* method for assessing implant impaction in THA that considers the support of the acetabulum and femur by body segments and soft tissues. To achieve this, mechanical compliance of the femur and acetabulum are measured in cadaver specimens and a testing rig is created to replicate these conditions. The *in-vitro* test rig that is developed and validated in this chapter is used for the following studies in Chapters 4, 5 & 6.

3.2 Materials and methods

3.2.1 Cadaveric experiment

Following approval from the local Research Ethics Committee (Appendix 9.5) four recently deceased intact phenol soft fixed cadavers (mean age 90 [81-94], mean weight 60kg [50-65], 2 male, 2 female) were prepared for THA by an experienced orthopaedic consultant (JC) using the posterior approach. Bolsters were used to position cadavers mimicking operating theatre conditions. Prior to testing each cadaver was imaged using computed tomography (CT) and each acetabular diameter measured. Press-fit and cemented (Simplex ACR308, Kemdent, Swindon UK) fixtures were used to couple a custom introducer to the acetabulum and pelvis respectively. Both couplings of introducer to bone were chosen to be highly rigid and to minimise relative motion, which could produce an inaccurate estimation of boundary condition values. The custom introducer closely matched the properties of a commercially used straight introducer, with bespoke fittings for the bone fixtures and mounting points for motion tracking markers (Figure 3.2.1).

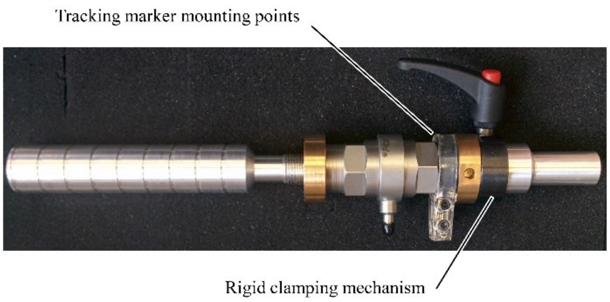

Figure 3.2.1: Custom surgical introducer with rigid clamping mechanism

A custom surgical mallet (700g, Figure 3.2.2) was fitted with a 100kN impact load cell (200C20, PCB Piezotronics, New York USA, Appendix 9.2) using the manufacturer supplied titanium strike surface. Force data were acquired using a high speed USB Acquisition unit (NI-9234, National Instruments, Newbury UK), sampling at 51.2kHz (Figure 3.2.3).

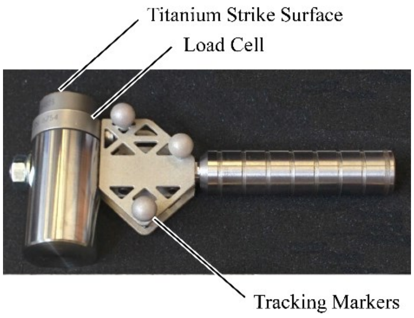

Figure 3.2.2: Custom surgical mallet fitted with a load cell and tracking markers

Both surgical mallet and introducer were fitted with passive infrared motion tracking markers. Displacement data were acquired at 355 Hz, with a Root Mean Square (RMS) error of 90µm (fusionTrack 500, Atracsys, Switzerland). Such acquisition rate resulted in around 70-80 data points per impact event.

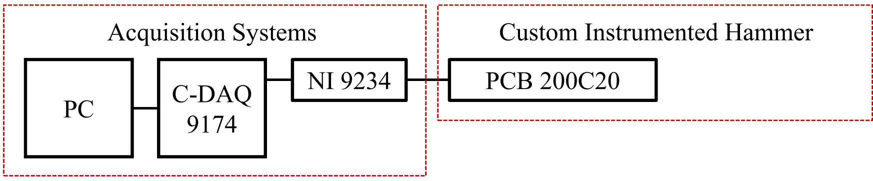

Figure 3.2.3: Mallet acquisition schematic

24 impact strikes were applied to the acetabulum and femur. Acetabular impacts were applied at approximately 45º inclination and 20º anteversion with respect to the bolstered pelvis, as current literature recommends.[217] The femur was internally rotated and held at approximately 30º inclination with the knee held into the surgical assistant's pelvis, representing typical surgery. Impact was directed along the long axis of the femur. Impacts were split into categories, with the surgeon asked to represent 3 levels of impact for each type of implant. A 'Low' level strike would represent a light strike used to broach/seat implants in fragile bone. 'Medium' would simulate strikes used on the most common patient type. 'High' represents the largest impact the surgeon would apply in strong bone.

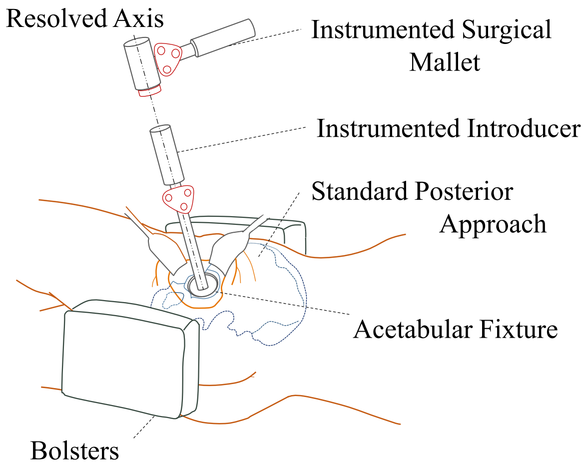

Figure 3.2.4: Experimental setup and axis of resolution for instruments

Each acquired force trace [$P(t)$] was analysed to find peak force for each strike. A numerical integration scheme with respect to time from zero value prior to strike (t_0) to the point at which load transients had fallen away (t_1) was used to determine impulse. Displacement data were transformed to the appropriate axis for each instrument (Figure 3.2.4). Introducer displacement was processed using a low pass, 3rd order Butterworth filter, 800 Hz cut-off, to remove random tracking error. Mallet displacement was numerically differentiated with respect to time to derive velocity, with the velocity immediately prior to impact (v_i) recorded for each strike (Figure 3.2.5).

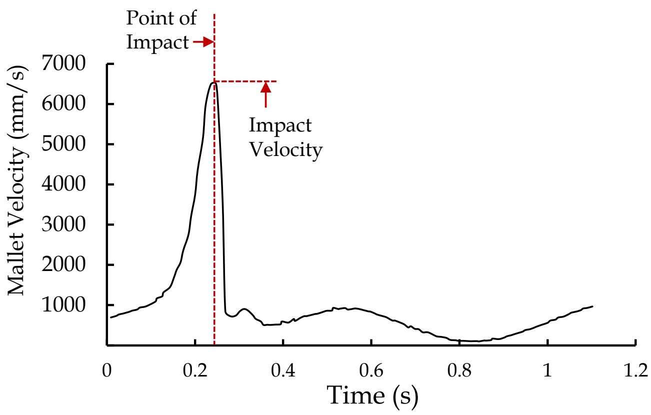

Figure 3.2.5: Example surgical mallet velocity trace. The mallet is accelerated to peak velocity shortly before impact occurs

Energy of the strike (E_{strike}) was derived from both impulse and velocity measurements (Equation 3.2.1, as demonstrated by Maharaj and Jamison[151])

$$E = {}^{V_i}/_2 \int P(t)\, dt \qquad \textit{Equation 3.2.1}$$

3.2.2 Soft tissue compliance simulation

In order to simulate the soft tissue compliance of the body a numerical mass-spring-damper (MSD) model was required to extract the impaction boundary conditions of the femur and acetabulum from the cadaver test. The measured impulse from the cadaver testing was applied to this model and the MSD variables iterated until the displacement response matched the cadaver test displacement data. The model approximates the rigidly coupled introducer, bone, musculature and upper body (in the case of the acetabulum) or leg (in the case of the femur) as an effective mass, supported by spring and dashpot elements to represent both the stiffness and viscoelasticity of the system (Figure 3.2.6).

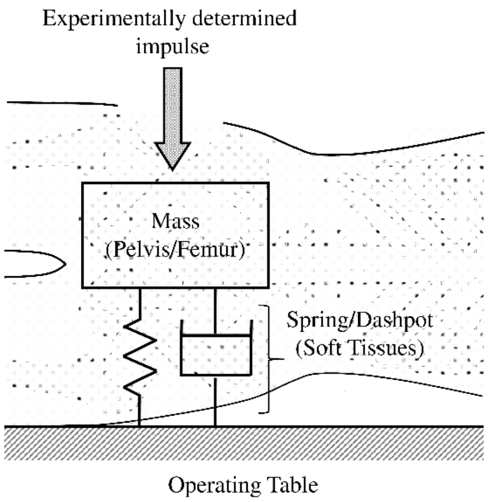

Figure 3.2.6: Approximation of acetabular/femoral soft tissue compliance using a Voigt model

The MSD model chosen to approximate the system was an effective mass (m, kg) coupled with parallel spring (k, N/m) and dashpot supports (b, Ns/m), known as a Voigt model. Preliminary analysis showed a significant level of damping post impact and a poor representation of the system if using mass-spring alone. Voigt models have also previously been used to model tissue response to impulse or step displacement.[181]

A Matlab (2015a, Mathworks, MA USA) script using the 'Control Systems Toolbox' was created, producing a displacement trace of a Voigt model in response to a force-time [P(t)] input (Figure 3.2.7). Impulses were defined as a half sine wave with a peak equal to that of average peak forces recorded, and area under curve (impulse) equal to those recorded experimentally.

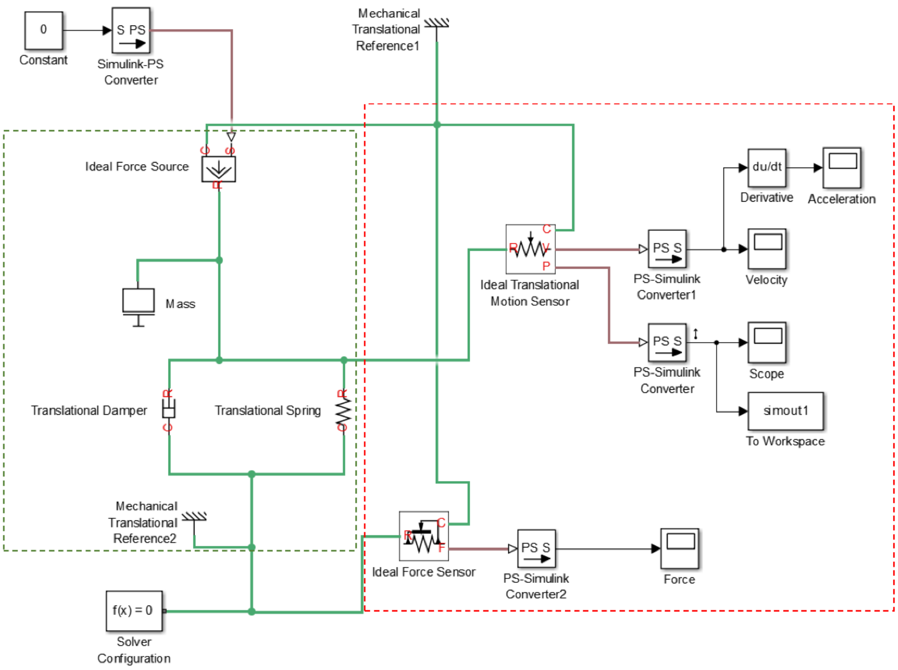

Figure 3.2.7: Simulink Voigt model. Mass, spring and damping coefficient inputs are used to calculate a displacement output

Each Voigt model parameter was varied using numerical iteration. Each simulated displacement trace was subtracted from the corresponding experimental trace and the resulting array used to calculate RMS error. The lowest average error simulated strike for each Voigt setup was recorded. Mass, stiffness and damping increments of 0.001 kg, 1 N/m and 0.01 NS/m were evaluated respectively. These data were then used to define the boundary conditions of the in vitro impact rig. An overview of this process is given (Figure 3.2.8).

A sensitivity analysis investigated the influence of the MSD parameters on the output displacement trace. A One-At-a-Time (OAT) approach was used. With the other two parameters held at their final calculated values, each of Mass, Stiffness and Damping were changed to 0.5 and 1.5 times their calculated value, and the peak displacement and rise time recalculated. The subsequent gradient was used to define sensitivity of peak displacement and rise time to miscalculations of MSD parameters.

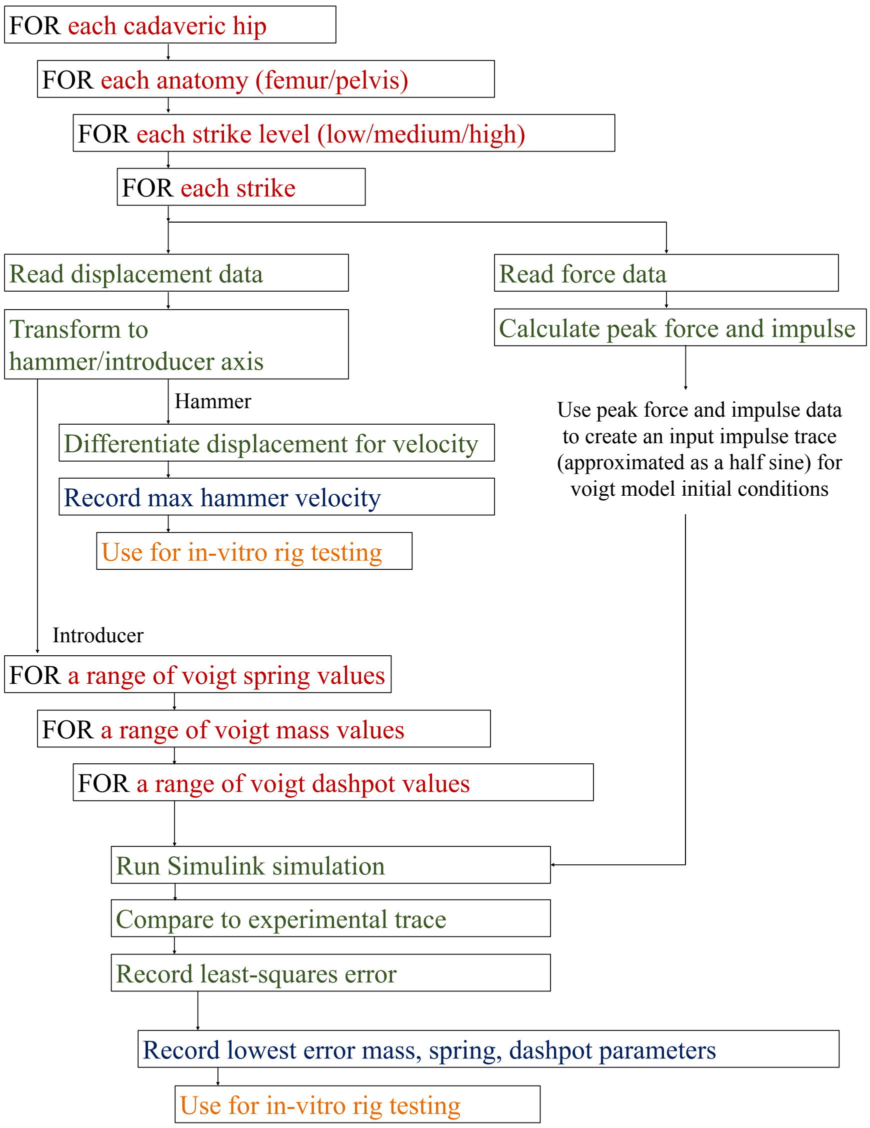

Figure 3.2.8: Simplified flow chart of simulation process. Raw force data are used to run a Simulink Voigt model. Resultant displacement traces are compared to experimental values. A least squares error method is used to determine the best fit.

3.2.3 *In-vitro* impact testing rig

An impact rig was built to simulate the impact boundary conditions of the cadaver test. The base of this rig, upon which the impact occurs, was a translatable platen supported by a parallel spring and dashpot to replicate a Voigt model. The mass of the platen, spring stiffness and dashpot coefficient were defined by the output of the Voigt model described in Section 3.2.2.

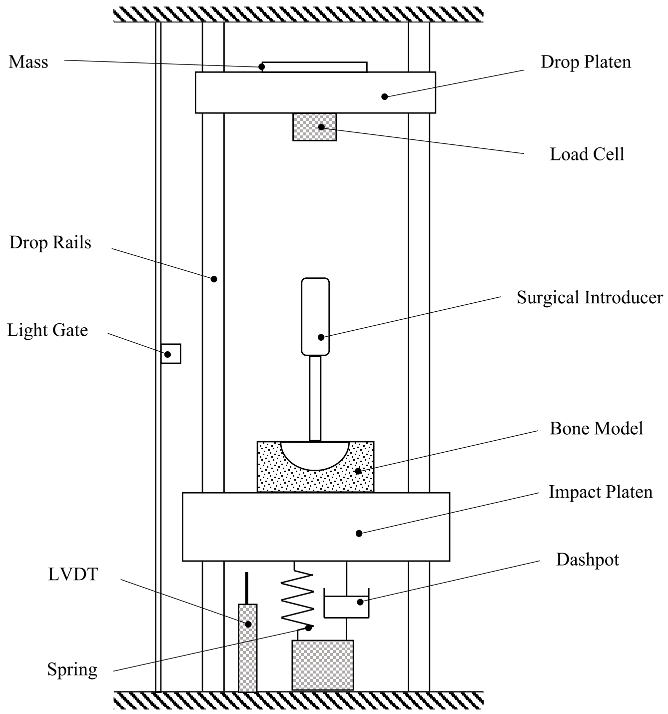

Figure 3.2.9: In-vitro drop rig setup. A spring and damper setup are used to mimic the soft tissue compliance of the hip

A drop weight, fitted with the same load cell used in Section 3.2.1, provided impact with adjustable velocity and mass (*Figure 3.2.9*). Due to errors in approximating impact velocity from a height alone, a light gate was used to determine the velocity of the drop weight immediately before impact. A 50mm stroke LVDT (S025.0, Solartron Metrology, Bognor Regis UK) was used to measure the displacement of the platen (Figure 3.2.10). A surgical introducer of the same mass and impact surface as the custom introducer in Section 3.2.1 was rigidly coupled to a 30 PCF Sawbones block (Sawbones Europe AB, Malmo Sweden).

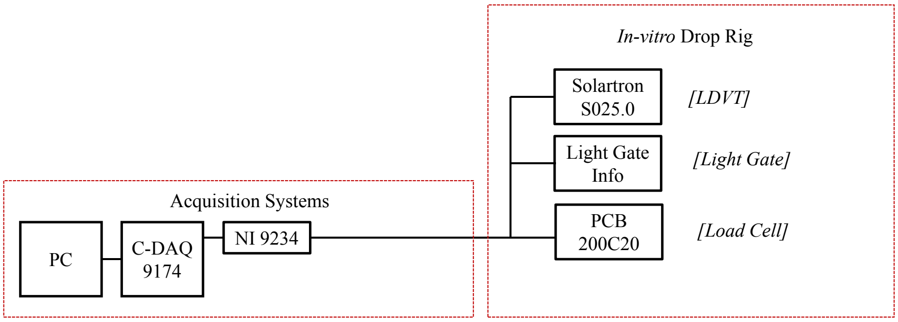

Figure 3.2.10: In-vitro Drop Rig Acquisition Systems

The mass of the drop weight was set to match that of the custom mallet used in Section 3.2.1 (700g). Velocity was set to values obtained during cadaveric testing (Section 3.3.1.2). Six strikes were carried out for each of the following six categories, to match the cadaver data: Low, Medium and High strikes for both acetabulum and femur. For each of the strikes, impact force, impulse, velocity and energy were measured. From the recorded impact platen displacement both peak displacement and rise time were recorded (defined in Figure 3.2.11). These metrics were chosen as they have previously been identified as appropriate to characterize impact.[165,169,171] They also define the two key parameters analysed in Section 2.4.1.3, quantifying the natural frequency of the system and max displacement amplitude, both of which are dependent upon system mass, spring stiffness and dashpot coefficient.

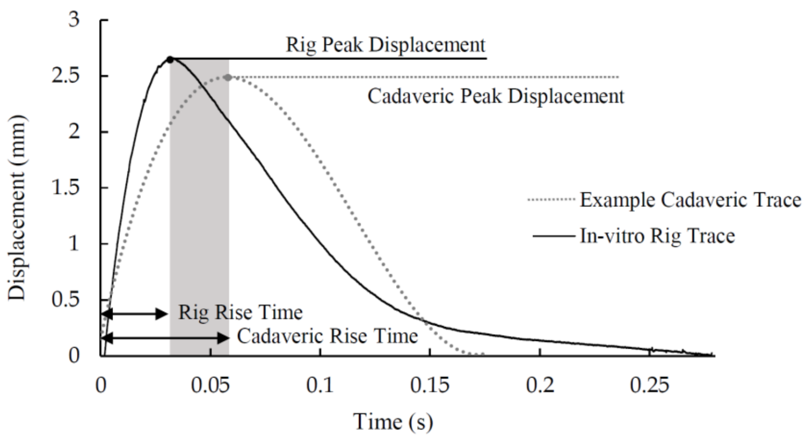

Figure 3.2.11: Comparison between peak displacement and rise time for cadaveric and in-vitro rig measurements

3.2.4 Statistical analysis

In order to determine whether the data from the acetabulum and femur should be averaged or analysed separately before being used as inputs to the Matlab Voigt model, statistical analyses were performed. The influence of anatomical site at each strike level upon peak force and impulse was analysed. First, peak force and impulse data were tested for normality with Shapiro-Wilk test in SPSS (v24, IBM, NY). Data were then analysed with two-way repeated measures analyses of variance with first the measured peak force, and then with impulse data as the dependent variable. For each dependent variable a RMANOVA was performed with independent variables of anatomy (femur/acetabulum) and intended strike force (low, med, high).

Additional analyses were carried out to determine whether it was appropriate to average or keep compliance values separate for each strike level. Two-way RMANOVAs were used, with Mass, Spring Stiffness and Damping Coefficient as the dependent variables. Anatomy and strike level were set as the independent variables. Main effects were considered if no two-way dependency was found.

The significance level was set to $p < 0.05$. Post-hoc paired t-test with Bonferroni correction were applied when differences across tests were found. Adjusted p-values, multiplied by the appropriate Bonferroni correction factor in SPSS, have been reported rather than reducing the significance level. Post-hoc power analyses were conducted in G*Power (v3.1.9.2, Universität Kiel, Germany) for strike force and mass, spring and dashpot values when comparing anatomy. A minimum power value of 0.63 was achieved, with an average of 0.76.

3.3 Results

3.3.1 Cadaveric experiment

3.3.1.1 Force and impulse

Force traces were characterized by an initial peak, followed by one or two secondary peaks which are attributed to multiple mallet strikes as the introducer accelerates (Figure 3.3.1). Oscillations post-strike are attributed to minor inertial effects which are appreciably smaller than the main peak. In order to ensure this acquisition rate was sufficient a series of 20 hard-on-hard strikes were conducted, measuring peak force for each. Deviation of the results was found to be just 1.22% of the mean value. Between 125 and 500 data points were captured per impact, with a duration of between 2 and 5 ms. The first half-sine force trace averaged 0.52 ± 0.36 ms in duration.

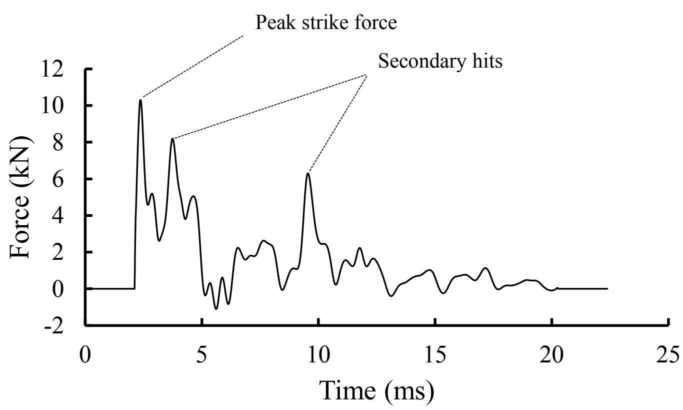

Figure 3.3.1: Example force trace characterized by an initial peak force and several secondary strikes. Inertial effects are also observed

The effect of intended strike level (low, medium, high) was dependent on the anatomical site (femur/acetabulum) ($p<0.0005$). For all strikes, lower forces were measured for the femur than the acetabulum, however the difference increased with increasing strike force (Figure 3.3.2): At a low strike level a 23% difference in mean was observed (1930 ± 502 N, $p=0.031$), 15% at medium strike level (2570 ± 490 N, $p<0.0005$), and 29% at high strike level (8630 ± 414 N, $p<0.0005$). The same was observed for impulse data, with the effect of anatomical site dependent on the intended strike level, and the femur always lower than the acetabulum (p<0.0005, *Table 3.3.1*). Due to the differences, femoral and acetabular data were separated in subsequent analyses.

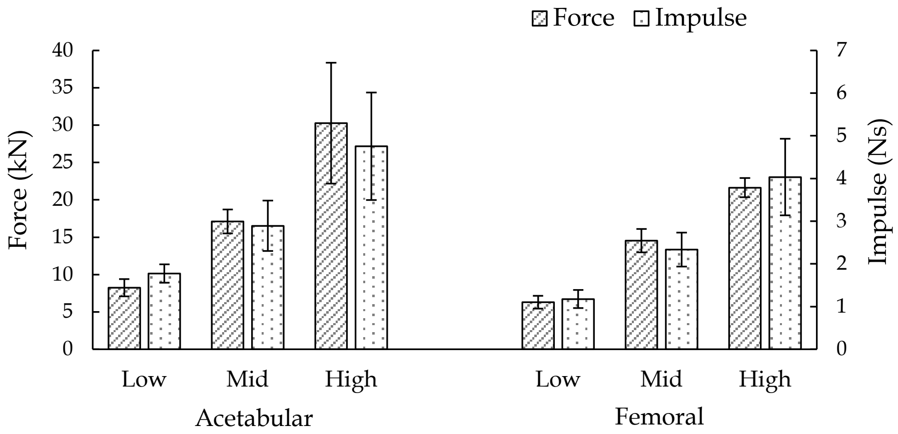

Figure 3.3.2: Peak force (mean with standard deviation) and impulse of mallet strikes during cadaveric testing. Both force and impulse increase with strike level. Acetabular values are consistently higher than femoral values

Table 3.3.1: The difference between peak force and impulse measured for the femur and acetabulum during cadaveric testing

Strike Level	**Force (kN)**								
	Acetabular			**Femoral**			**Difference**		
	Mean	SD	N	Mean	SD	N	%	Abs	P
Low	8.24	1.15	18	6.31	0.86	25	23.4	1.92	0.031
Medium	17.10	1.60	15	14.53	1.57	24	15.0	2.57	<0.005
High	30.26	8.08	12	21.63	1.29	21	28.5	8.64	<0.005

	Impulse (Ns)								
	Acetabular			Femoral			**Difference**		
	Mean	SD	N	Mean	SD	N	%	Abs	P
Low	1.775	0.217	19	1.176	0.211	24	33.7	0.60	<0.005
Medium	2.892	0.590	14	2.335	0.399	24	19.3	0.56	<0.005
High	4.757	1.260	12	4.033	0.896	22	15.2	0.72	<0.005

3.3.1.2 Velocity and energy

Figure 3.3.3, Table 3.3.2 presents the mean measured velocity for each intended strike level for both femoral and acetabular anatomical sites, and the resultant energy of the impact. Velocity values were used as input velocities for the *in vitro* rig described in Section 3.3.3.

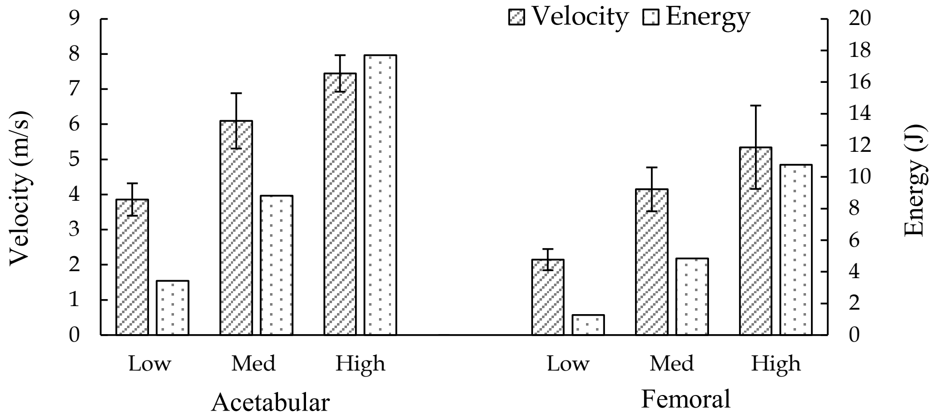

Figure 3.3.3: Velocity (mean with standard deviation) and energy of mallet strikes during cadaveric testing. Both velocity and energy increase with strike level. Acetabular values are consistently higher than femoral values

Table 3.3.2: The difference between mallet velocity and energy measured for the femur and acetabulum during cadaveric testing

Strike Level	Peak Mallet Velocity (m/s)							
	Acetabular			Femoral			Difference	
	Mean	SD	N	Mean	SD	N	%	Abs
Low	3.86	0.46	59	2.14	0.30	44	1.7	44.4
Med	6.10	0.79	41	4.15	0.62	13	1.9	32.0
High	7.45	0.52	54	5.34	1.18	19	2.1	28.2

Strike Level	Calculated Energy (J)					
	Acetabular		Femoral		Difference	
	Mean	SD	Mean	SD	%	Abs
Low	3.42	0.58	1.26	0.29	2.2	63.2
Med	8.81	2.13	4.84	1.10	4.0	45.1
High	17.71	4.85	10.78	3.38	6.9	39.1

3.3.2 Soft tissue compliance simulation

Data for one hip could not be collected due to the cadaver already having had a unilateral THA prior to death. Traces were split into individual strikes and time, and initial displacement was zeroed for each. A total of 174 strikes were analysed, with an average of 24 usable data sets for each hip. Each was analysed using the Matlab script described in Section 3.2.2.

A typical displacement trace of the acetabulum or femur was characterized by an initial acceleration as momentum transferred from the surgical mallet, followed by a damped return to the initial zero position (Figure 3.2.11). The model indicated the main effect of anatomical site (i.e. acetabulum or femur) showed a statistical difference in output for both mass (p=0.02) and damping coefficient (p=0.009), but not spring stiffness (p=1.0). As both mass and damping showed differences at each anatomical site, setups for femoral and acetabular testing are separate.

The model spring stiffness showed no difference between low and medium, medium and high and low and high strike levels (p=1.00, p=0.3, p=0.7). The model did detect differences in effective mass between low and high ($p < 0.0005$) and medium and high ($p = 0.03$) but not low and medium strike levels ($p = 1.00$). The main effect for intended strike level upon damping coefficient was only significant for low and high strikes ($p = 0.03$). Due to differences only being found between certain strike levels it was decided that mass, spring stiffness and damping coefficient would be averaged over the three strike levels for each anatomical site (see 'average' strike level in Table 3.3.3). This decision was compounded by the desire for a testing setup that was as simple as possible, negating the need for constant compliance adjustment for different strike levels.

A summary of Effective Mass, Spring Stiffness and Damping Coefficient outputs can be found in Table 3.3.3.

Table 3.3.3: Mass, spring, damper values calculated with Matlab model

Strike Level	Mass (m, kg)			Spring Stiffness (k, kN/m)			Dashpot Coefficient (b, Ns/m)		
	Mean	SD	N	Mean	SD	N	Mean	SD	N
Acetabular									
Low	18.4	5.4	41	7.4	2.5	41	547	88	42
Med	17.0	4.6	29	8.4	2.8	28	585	116	28
High	23.7	5.1	30	8.3	3.6	29	664	143	30
Mean	19.7	5.1	100	8.0	3.0	98	595	114	100
Femoral									
Low	11.7	3.6	34	3.1	1.3	34	289	71	34
Med	10.6	1.0	21	3.5	0.6	21	290	28	21
High	15.9	2.6	19	5.6	1.5	19	389	61	19
Mean	12.7	2.8	74	4.1	1.2	74	322	59	74

3.3.3 *In-vitro* rig

For the acetabulum no differences between the test rig and cadaver traces were detected for peak displacement and rise time (Figure 3.3.4). The peak displacement increased from 2.5 mm for the surgeon's low strike force to 6 mm for the high strike force, but the rise time remained constant, at around 30 ms, for all three applied strike forces.

For the femur, no differences were detected between the test rig and cadaver traces for peak displacement. The peak displacement increased from 3 mm for the surgeon's low strike force to 5.6 mm for the high strike force. The test rig also matched the rise time for the surgeon's low and high impact strikes, but a 0.6 ms difference was detected for the surgeon's medium strike force. As with the acetabular data, the rise time did not vary with the surgeon's strike level.

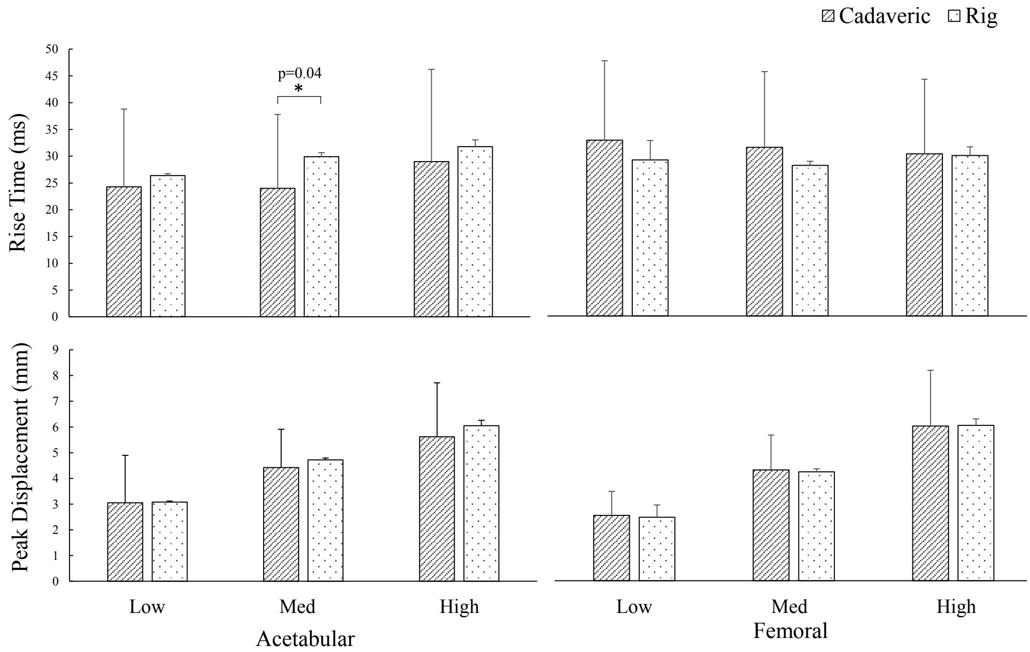

Figure 3.3.4: Comparison between peak displacement (mean with standard deviation) and rise time for cadaveric and in-vitro rig measurements

The sensitivity study indicated the peak displacement was more sensitive to MSD parameters at higher strike levels for the femur and acetabulum, and the femoral peak displacement was more sensitive to MSD parameters than the acetabular (Table 3.3.4). The rise time sensitivity was not affected by strike level, but was more sensitive to MSD parameters for the femur than acetabulum. The only detected difference between the cadaver and test rig displacement traces was the rise time for the medium strike level in the acetabulum. The sensitivity analysis indicated an error of 2.2 kg mass, or 0.37 kN/m spring constant, or 149 Ns/m damping could cause this difference.

Table 3.3.4: Displacement parameter statistics and sensitivity study

		Peak Displacement								
		Cadaveric vs Rig			Simulation Sensitivity			Possible error due to difference		
Strike Level		Absolute (mm)	%	p=	Mass (mm/kg)	Spring (mm/[kN/m])	Damping (mm/[Ns/m])	Mass (kg)	Spring (kN/m)	Damping (Ns/m)
Ace	**Low**	0.03	0.85	0.93	0.035	0.086	0.003	0.74	0.3	8.71
	Med	0.3	6.89	0.3	0.056	0.139	0.0048	5.39	2.19	63.4
	High	0.43	7.6	0.39	0.091	0.222	0.0077	4.71	1.91	55.4
Fem	**Low**	0.07	2.78	0.97	0.068	0.213	0.0061	1.05	0.34	11.8
	Med	0.07	1.65	0.79	0.13	0.4	0.0116	0.55	0.18	6.18
	High	0.03	0.51	0.95	0.233	0.714	0.0208	0.13	0.04	1.5
		Rise Time								
		Absolute (ms)	%	p=	Mass (ms/kg)	Spring (ms/[kN/m])	Damping (ms/[Ns/m)	Mass (kg)	Spring (kN/m)	Damping (Ns/m)
Ace	**Low**	2.02	8.3	0.39	2.7	15.9	0.04	0.75	0.13	51
	Med	5.91	24.7	0.04*	2.7	15.9	0.04	2.2	0.37	149
	High	2.77	9.53	0.43	2.7	15.9	0.04	1.03	0.17	69.7
Fem	**Low**	3.59	11.2	0.47	4.8	37	0.079	0.76	0.1	45.4
	Med	3.37	10.9	0.22	4.8	37	0.079	0.71	0.09	42.6
	High	0.3	1.02	0.92	4.8	37	0.079	0.06	0.01	3.82

As a further validation the impulse produced by the strikes of the *in-vitro* drop rig were compared to the cadaveric testing (Figure 3.3.5). No difference was measured in all cases but high level femoral strikes (Difference = 1.03 Ns, $p < 0.005$).

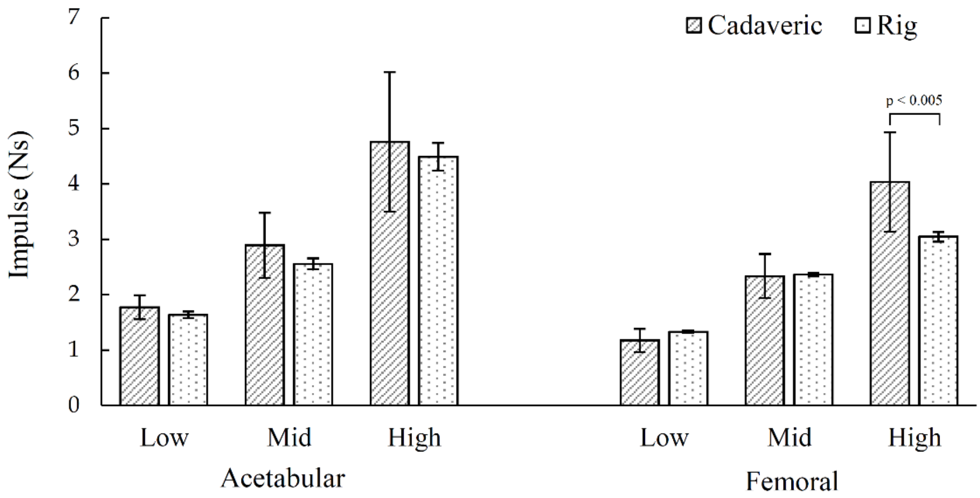

Figure 3.3.5: Comparison between impulse values (mean with standard deviation) measured cadaveric testing and when using the in-vitro drop rig. A difference was only detected in high level femoral strikes

3.4 Discussion

3.4.1 Key findings

The most important finding of this study is that the mechanical compliance of the acetabulum and femur can be measured *in-vivo* and replicated with a physical representation of a Voigt model. When a mallet impact is applied to the acetabulum or femur, the bone is displaced by between 2.5 and 6 mm over a duration of around 30 ms (between 80 and 200 µm/ms). This displacement is caused by the bone being supported by the non-rigid soft tissues and body segments of the musculoskeletal system. This boundary condition may influence the force experienced by the acetabulum during implant seating, or change the number of strikes to seat.[151,177] This chapter presents a method to replicate these boundary conditions using a spring and dashpot system that has been described as a limitation in many studies.[71,72,175,176,179]

The impact magnitudes measured and replicated in this study fall within the range of existing literature.[151,158,185,215] Maharaj. et. al. found similar femoral impaction energy (4.5J) but a peak force that was lower (6.2kN) than measured here.[151] The discrepancy in peak force could be explained by the polyacetal (Delrin™) tipped mallet used by Maharaj, attenuating peak force but transferring similar energy as the titanium tipped mallet used in this study. Our mallet velocities were also found to be within 20% of Maharaj's values. Peak force values measured intraoperatively for acetabular cup insertion and femoral rasping by West et. al.[158], Phipps et. al.[215] and Kohan et. al.[185] also fall within the values measured during this study. Additionally, variation of measurements are also of similar magnitude to the difference between 'low' and 'high' strike force measured for our consultant surgeon. Importantly, in these three studies, at these peak forces measured, few fractures of the bone were encountered. All three studies measured forces in cadavers or live patients, and thus had appropriate compliance boundary conditions to the acetabulum/femur. In contrast, a study by Cummins et. al report bone fracture at loads of 1.6kN.[72] This study used a rigid potting of the bone in a solid fixture with no compliant boundary condition. Thus, more of the energy in the impact may have been transmitted into the bone and not the surrounding tissue, and this could explain such a large reduction in peak force to fracture in these two studies.

The duration of impaction measured during this study are comparable to values measured during a similar study.[151] Using Equation 2.4.36 a predicted impact duration of 0.37 ms is obtained (Table 3.4.1). Therefore the approximation of the introducer as a spring gives a reasonable prediction of impact duration.

Table 3.4.1: Predicted impact duration by approximating the introducer as a spring of constant cross section and modulus

Parameter	**Value**	**Unit**
Impact mass	0.7	kg
Introducer length	0.3	m
Introducer material modulus	190	Gpa
Introducer cross sectional area	7.9E-05	m^2
Predicted impact duration	0.37	ms

While no direct comparison of Voigt model parameters for the hip can be made to other studies for intraoperative impact there is significant work determining model values for the hip during falls. Robinovich et al. have found both effective mass of the hip and dashpot coefficients in a similar range and sensitivity to the results of this study.[183] This study found that it was appropriate to represent the femur and acetabulum with separate setups *in-vitro.* While this increases setup complexity it highlights that boundary condition differences, even within the body, are important. The sensitivity study conducted found that the errors between cadaveric and *in-vitro* rise time were still an average of 12 % of total values, indicating the accuracy of this method.

Table 3.4.2: Key system parameters for experimental Voigt model of patient compliance. The system is overdamped

	Symbol	Unit	Acetabular	Femoral
Mass	m	kg	19.7	12.7
Spring	k	kN/m	8.00	4.10
Dashpot	b	Ns/m	595	322
Undamped natural frequency	ω_n	Hz	3.21	2.86
Critical damping coefficient	b_{crit}	Ns/m	794	456
Damping Ratio	ς	-	1.33	1.42
Damped natural frequency	ω_d	Hz	2.83	2.87

Both femoral and acetabular systems are overdamped, with the acetabulum having a higher undamped natural frequency that the femur, but a lower damped frequency (Table 2.3.4). These properties can be used to understand the differences between the driving frequency of cup into bone, and to determine whether modifications to introducer or cup could be made to increase the efficiency of seating by avoiding force transmission to soft tissues when close to resonance.

3.4.2 Limitations

A limitation of the Voigt model is that it predicts an instantaneous spike in force during impact that may not occur in tissue.[172] However, previous studies have found adaptation of the Voigt to a Standard Linear Solid arrangement (with series spring and dashpot in place of the dashpot of a Voigt) offers only a small improvement in response prediction.[172] A further improvement to this study would be to include a measurement of force within the hip cadaver system. Force data could provide further validation of the impact mechanics of the system. However such measurement would require a highly complex setup. An advantage of the methodology used in this study is that the methods described could be used to gather data in the operating room; an even more representative scenario.

A further limitation of this study is the use cadavers of similar weight and age. Patients of these BMIs and ages may not be selected for cementless arthroplasty. If possible the same methodology should be used with higher body mass index (BMI) cadavers of a lower age, where different Voight model parameters might be expected, such as slightly higher effective mass, as found by Levine et. al.[166] With further research it would be useful to characterize the effects of BMI, soft tissue thickness, sex, age and other factors. In addition, it is known that cadaveric tissue may not behave the same as living tissue. This was mitigated as much as possible by using phenol embalmed specimens rather than formaldehyde or formalin fixed, both known to alter tissue properties.[144] Furthermore, only one surgeon performed the cadaver work, whereas a larger number of surgeons would be useful to determine the average magnitude of impact in THA. However, the surgeon's three different strike values provide some information on the strike range that may exist, and these data agreed well with prior work.

3.4.3 Conclusion and clinical relevance

For very short duration events such as hard on hard contact between a mallet and introducer, or modular femoral head seating, replicating the compliance of the body segments may not be necessary. This is because the impact event is very short and the seating event is over before the implant/body segment has had time to accelerate.[180] However for a softer impact event, such as the introduction of an acetabular cup or femoral stem into a bony cavity, impact events are longer. Several studies have shown event durations of a similar magnitude to the rise time found in this study.[90,157,160,194] Therefore compliance during implant seating is a much more relevant consideration as the body segments are accelerated by the implant/introducer in a similar timescale as impact duration. Compliance has already been shown to be important when seating a femoral stem.[178] This may have an effect on experimental results and significance during pre-clinical testing.

Hip compliance has been recognized as a possible factor in implant seating and several groups have attempted to include this boundary condition in their testing[159,175,218] but have not been able to validate the compliance properties of their supports with *in-vivo* data. This paper provides a method to recreate the *in-vivo* compliance of the femur and acetabulum in a laboratory drop rig or computational model. Including this boundary condition in preclinical testing may provide an improved representation of the clinical conditions necessary to investigate implant seating.

3.5 Chapter summary

- The force, impulse, velocity and energy of low, medium and high level impaction strikes have been measured and reported.

- The compliance of the femur and acetabulum has been measured

- A computational Voigt model was successfully used to model hip compliance

- An *in-vitro* impaction rig mimicking the compliance of the hip with a physical mass, spring and damper system was built and subsequently validated against the ex-vivo measurements

- Both impaction magnitudes and *in-vitro* model are useful for researchers looking to test pre-clinically

3.6 Acknowledgements

All work, unless explicitly stated below, was conducted by myself.

I thank Justin Cobb, Kartik Logishetty, Sam Vargas, Oliver Boughton, Rachael Waddington and Lesley Honeyfield for their invaluable assistance during cadaveric testing. RW prepared the cadaveric lab and provided the cadaveric specimens. OB, KL and JC assisted in cadaver preparation and conducted THA surgery. SV assisted surgery and instrument preparation during testing. OB and LH assisted cadaver CT scanning.

I would also like to thank Ably Rosevere and Daniel Plant for their assistance in selecting the appropriate hardware for high speed acquisition when building the in vitro drop tower.

Chapter 4: The effect of impaction energy

4.1 Introduction

To implant cementless devices large forces must be generated by the surgeon, typically with a surgical mallet; a process known as impaction. Impaction technique is critical to implant longevity as enough energy must be used in order to seat the implant properly,[33,62,77,122] but not so much that the bone is fractured[51,62,72,138,212] or the implant excessively deformed.[29,74,110] Despite impaction being used in the majority of approximately 60,000 THAs performed per year in the UK, very little literature exists to guide surgeons to use appropriate energies. A surgeon can use his or her mallet to strike very softly (low energy), very hard (high energy) or somewhere in between. The forces and energies generated when a senior surgeon was asked to replicate the lowest and highest energy strikes that would be used in surgery are reported in Chapter 3.

Acetabular fracture is very often not detected during surgery[70] and while less common than femoral fracture, is more likely to have adverse outcomes.[27] Fractures of the acetabulum are commonly attributed to the impaction process,[62,66,212,219] but dynamic bone strains during the impaction event are yet to be characterised. In addition, excessive strain in the acetabulum, even when not causing fracture, may cause large deformation of the acetabular cup[29,110], hinder liner seating[211], cause excessive wear,[74] or even cup damage.[33]

Biomechanics of acetabular cup fixation has been investigated previously in the literature. As an implant is forced into the bone cavity elastic strain is created by deforming the acetabulum wall through a ‘pinching’ action of the ischial and ilial columns.[76,90,104,155,220] Sufficient energy must be used to seat the implant and prevent micromotion which, if more than 150 μm, may prevent bone ingrowth.[83,84,100] With good cup fixation, micromotion is reduced and bony ingrowth can occur.[85] Good apposition between bone and implant is also required for bone to fill any gaps and anchor the implant securely.[28] Gaps of more than 2mm have been shown to contribute to early implant migration,[95] a possible contributor to aseptic loosening,[52,221] the most common cause of THA implant revision.[222]

Therefore, to maximise chances of success, a surgeon should seek to maximise fixation and implant seating whilst minimising the risk of fracture. This study seeks to determine how the impaction energy used by surgeons may affect these parameters. 'How hard should I hit for the best outcomes?' is a commonly asked question by surgeons, which we can translate into the research engineering questions:

(1) How does impaction energy affect:

- Risk of fracture, quantified by measuring dynamic bone strains?
- Cup deformation, quantified by measuring cup strains?
- Cup fixation, quantified by pushout tests?
- Cup seating, quantified by measuring polar gap?

(2) How are the above factors changed in different qualities of bone?

4.2 Materials & methods

4.2.1 Common experimental setup

This section details setup that is common to Chapters 4, 5 & 6. 'Study Setup' (Section 4.2.2) refers to setup, testing procedures, data analyses and statistical analyses that are unique to individual Chapters.

An in-vitro drop rig (Section 4.2.1.1), described in Chapter 3, was used to impact custom acetabular cups (Section 4.2.1.2) into a synthetic bone model (Section 4.2.1.3) in a controllable and repeatable manner. During seating several parameters were monitored (impact load, bone & cup strain and polar gap, Sections 4.2.1.3, 4.2.1.4 and 4.2.1.6 respectively). Following seating fixation was assessed using a pushout test (Section 4.2.1.7).

4.2.1.1 *In-vitro* drop rig

A drop weight, representing the surgical mallet, could be adjusted for both height and mass to vary energy of the impact (Figure 4.2.1). The synthetic bone was attached to an impaction platen which was supported by a spring/dashpot/mass tuned to provide the same response as the human acetabulum during intraoperative impaction, ensuring the same damping of soft tissue seen *in-vivo* is represented *in-vitro* (Chapter 3).[223] A 700 g straight introducer guided by a support and linear bearing was used to further simulate intraoperative impact.

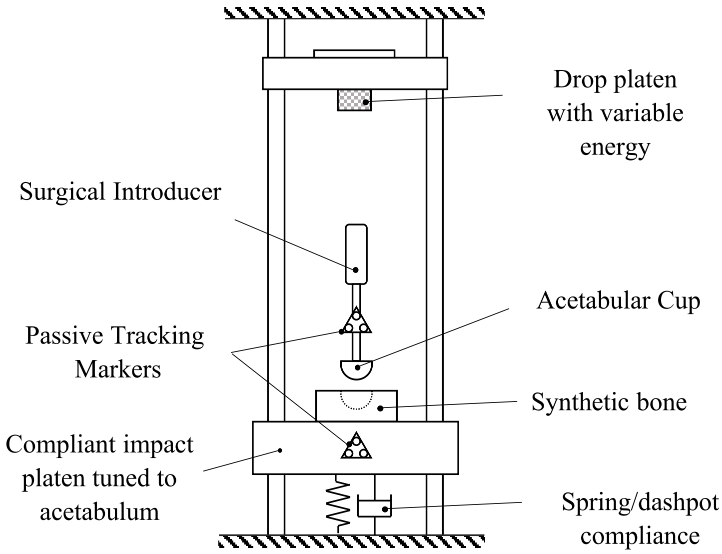

Figure 4.2.1: The experimental setup: the drop platen enabled repeatable hammer strikes to be applied with a known energy. The spring and dashpot were previously tuned to replicate intraoperative movement of the pelvis following impaction.[36]

4.2.1.2 Custom acetabular cups

The acetabular cups were manufactured from Ti-6Al-4V in 54 mm and 55 mm sizes with a 3 mm wall thickness. The 54mm cups were impacted into the high density foam forming a 1mm interference, while the 55 mm cups were impacted into the low density foam producing a 2 mm interference. These were chosen to represent clinical practice.[62,96,103,121] The cups were manufactured with a surface roughness to represent that of plasma spraying (Rz > 500 µm,[224] Figure 4.2.2) and a rim-to-rim stiffness similar to commercially available models.[110] As such, this model represents around 20,000 (30%) of the cementless acetabular cups implanted in the UK every year.[11] Each cup was manufactured with an extruded spigot, projected into the cup from the pole, allowing cups to be attached to a straight introducer for impaction.

Figure 4.2.2: Custom acetabular cup with surface finish resembling that of typical plasma-spraying

4.2.1.3 Synthetic bone model

Expanded polyurethane foam (Model #1522-02 and #1522-04, Sawbones, Pacific Laboratories, Malmoe Sweden) was used as a repeatable synthetic bone substitute for the acetabulum: the high density (30 PCF) foam replicated good quality bone with a strong cortical rim while the low density (15 PCF) foam replicated lower density bone, such as the exposed sub-chondral bone seen in revision cases.[77,80,132,142,225] The bones were CNC milled to create a ⌀53 mm acetabular cavity, with a previously validated anatomically representative geometry, including two ‘notches’; used to simulate the pinching effect of the ischial and ilial columns.[76,80,82,104,106,108,132,155,156] The center of the cavity hemisphere was centered 1mm below the surface of the block (Figure 4.2.3).

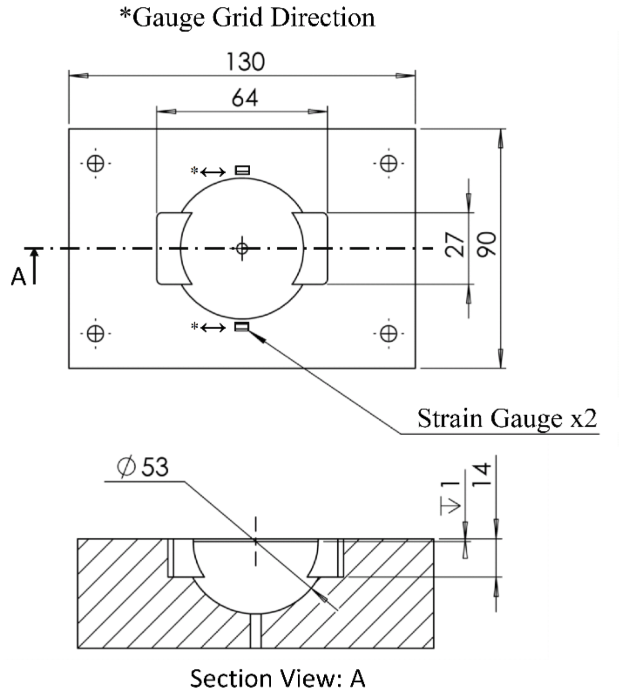

Figure 4.2.3: Synthetic bone model directions and strain gauge locations

4.2.1.4 Load acquisition

A load cell (PCB 200C20, New York, USA) was attached to the lower surface of the drop platen to measure peak impact load during strike (Figure 4.2.4). Load data was acquired at 51.2 kHz using a high speed USB data acquisition unit (NI9327, National Instruments, Hungary, Figure 4.2.5). The strike surface used was the manufacturer supplied titanium cap (PCB 084B23, New York, USA). Details of strike surface geometry and load cell characteristics can be found in the Appendix (Appendix 9.2).

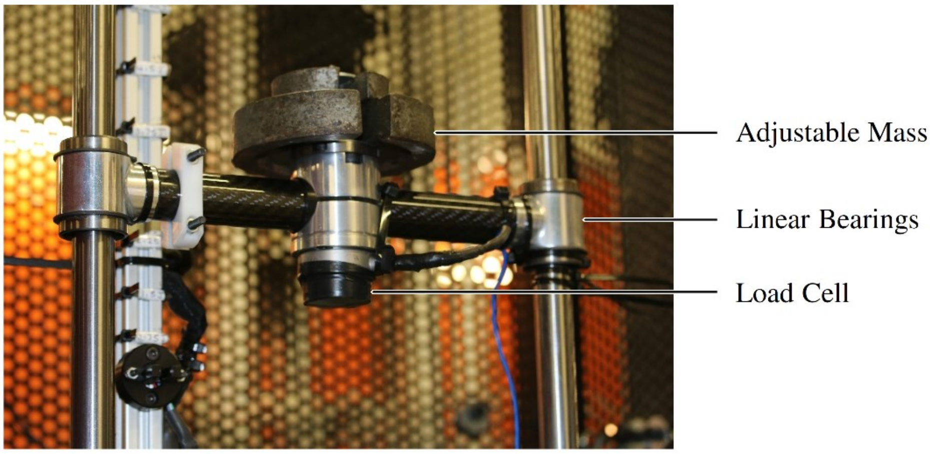

Figure 4.2.4: Drop platen for in-vitro rig

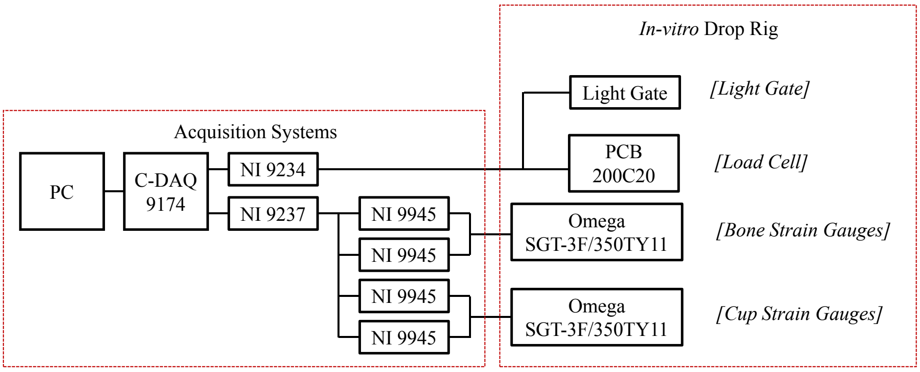

Figure 4.2.5: In-vitro rig data acquisition setup

4.2.1.5 Strain acquisition

DIC strain gauge location testing

The location of the strain gauges on the synthetic bone model was based on a pilot Digital Image Correlation (DIC) study. Four specifications were tested, using all combinations of low and high density synthetic bone and 1 & 2 mm cup underream. Cups (N = 4) were seated quasi-statically using a materials testing machine (Instron model 5565, High Wycombe, UK). Seating was conducted at 0.5 mm/min and stopped when load reached a limit of 2 kN (Figure 4.2.1). The surface of the synthetic bone was coated with a 'speckle' pattern that could be monitored by two calibrated cameras (Aramis SRX, GOM, Coventry, UK). The resulting data was analysed to measure strain fields (GOM Correlate, Build 11-15-2017, GOM).

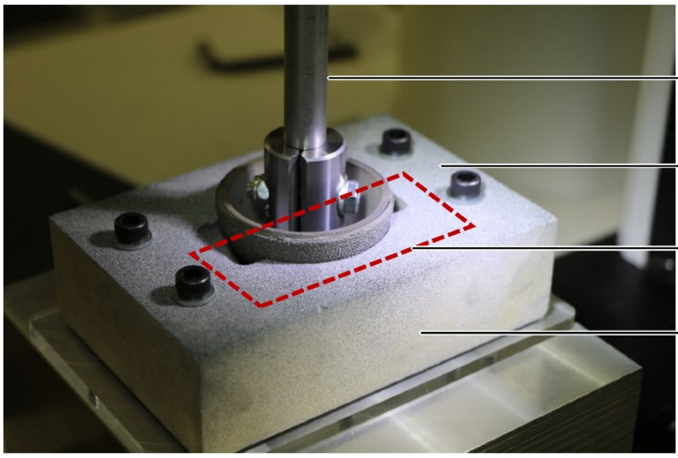

Figure 4.2.6: DIC setup. A speckle pattern was applied to the top face of the experimental model and strains measured during quasi-static seating

In all of the different specifications a trend of an increase in principal hoop compressive strain was observed nearer to the cup rim. Strain was greatest closest to the cup rim and was axisymmetric and reduced at distances further from the cup rim (Figure 4.2.7). Magnitudes of hoop exceed those measured radially, in line with the magnitudes measured in engineering press-fit applications (Figure 2.3.8). Strain maps for all specifications can be found in Appendix 9.6. It was decided that this tensile strain would be measured circumferentially, to isolate hoop strain, with a strain gauge mounted tangentially to the cup rim. A 2 mm gap was left between the cup rim and strain gauges to allow for plastic deformation that may take place during seating.[226]

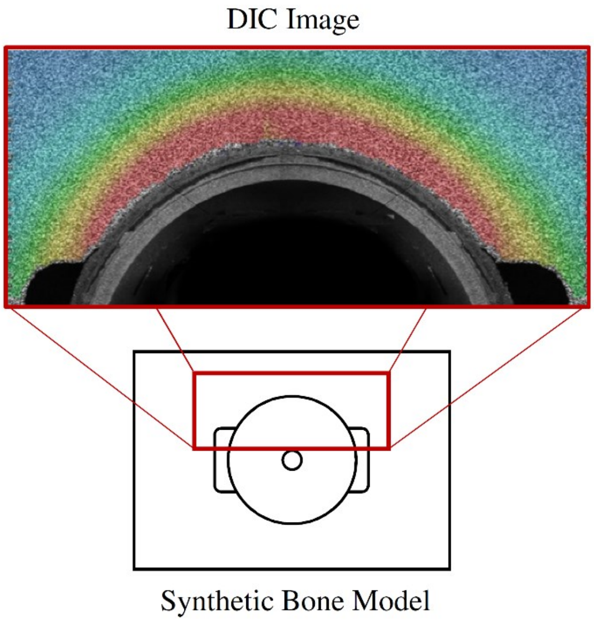

Figure 4.2.7: DIC image of strain in synthetic bone during seating, used to validate strain gage placement. An axisymmetric pattern is observed, with principal strain greatest near the cup rim and decreasing radially

High-rate in-vitro rig strain measurement

Strain was measured using linear strain gauges (350 ohm, SGT-3F/350TY11, Omega, Manchester, UK). Two per synthetic bone block were glued to opposing sides of the foam block, 2 mm from the edge of the cavity using superglue (Figure 4.2.8). 0.5 mm recesses were milled, the same dimensions as the strain gauge body, were milled into the synthetic bone model. This ensured accurate placement of the gauges for each sample. A further two gauges were glued to opposing sides of the internal acetabular cup rim. Cups were positioned so that the cup gauges were at a 90º offset circumferentially to the synthetic bone gauges to measure the main 'pinching' effect of the acetabulum. Strain data were acquired at 51.2 kHz using a high speed USB data acquisition unit (NI9327, National Instruments, Hungary). Strain was measured in a quarter bridge arrangement, with bridge completion completed using four resistor units (NI9945, National Instruments, Hungary, Figure 4.2.5). Raw data was captured using Labview (National Instruments, 2014) and analysed using MatLab (Mathworks, 2015b).

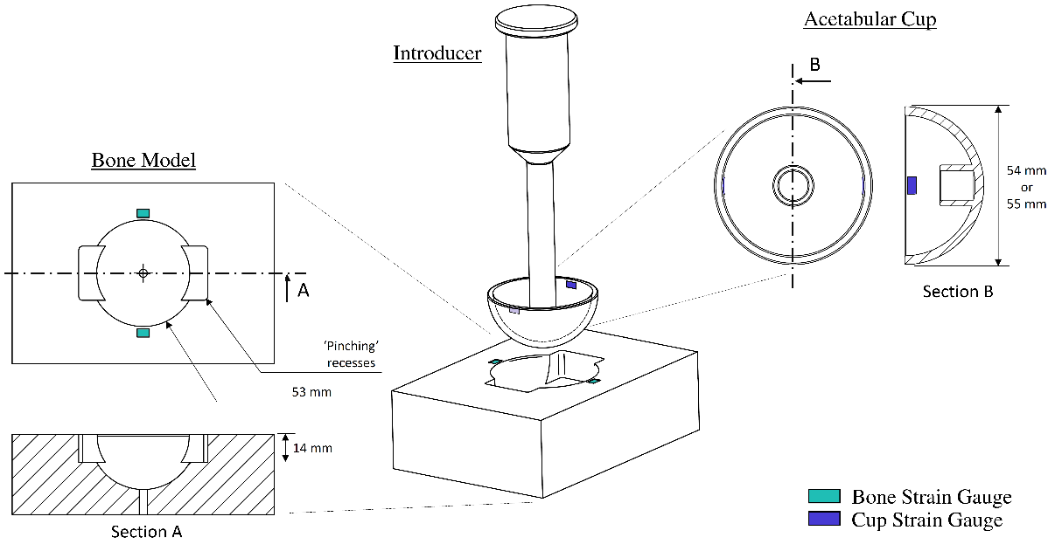

Figure 4.2.8: *Strain gauge placement: bone gauges were positioned to measure peak hoop strains whilst cup gauges were positioned a 90 degree offset to these gauges to measure the cup pinching effect.*

4.2.1.6 Displacement acquisition

A set of Infra-red reflective markers were attached to the cup introducer and impact platen (Figure 4.2.9) allowing their relative positions to be tracked by an optical tracker (fusionTrack 500, Atracsys, Switzerland). Following 10 strikes the final polar gap of each specimen was measured using a depth gauge micrometer. Superposition of final polar gap and relative cup movement during seating was used to calculate polar gap following each strike.

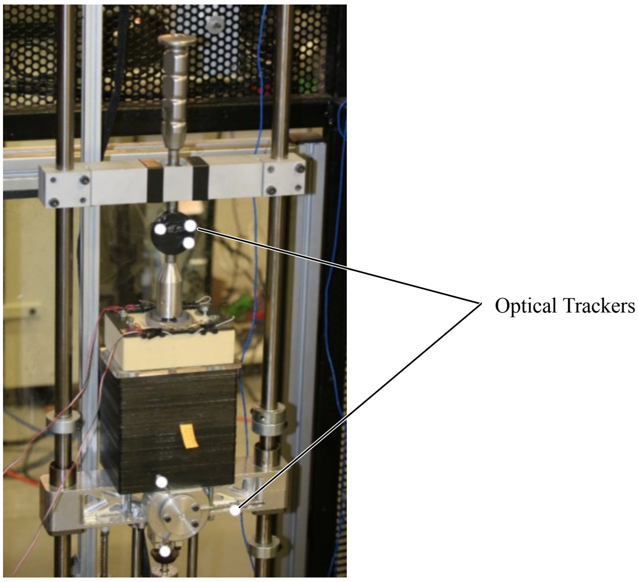

Figure 4.2.9: Optical trackers used to monitor relative displacement between bone substitute (rigidly fixed to the impaction platen) and acetabular cup (rigidly attached to introducer)

Using this data the 'optimum number of strikes' for each impaction setup could be recorded to be pushout tested. No current guidelines exist for 'optimally seated' acetabular cups. It was decided with the senior surgeons of our team that if the cup did not progress by 0.1 mm during a strike it was appropriately seated.

4.2.1.7 Pushout fixation

Bone and synthetic bone is known to be viscoelastic and undergo creep, or stress relaxtion.[181] A preliminary relaxation test was conducted to determine if this relaxation could have an effect upon cup fixation over time. A 6 mm pin was placed upon a 30 x 30 x 30 mm sawbones segment by a materials testing machine (Instron model 5565, High Wycombe, UK). A 0.2 kN force was initially applied and then this displacement held for 12 hours (simulating the fixed strain applied during cup seating). The force applied decreased by 50% (99 N) over 24 hours (Figure 4.2.10). Therefore the stress in the bone also decreases by this factor with time. This identifies the bone model material as viscoelastic, important for two reasons. Firstly, high strain rates will lead to higher stress in the material than low strain rates.

Secondly, fixation of cups will be reduced with time during to bone around the cup relaxing. Therefore it was decided that all pushout tests would be conducted 2 hours (± 5 minutes) following implantation to ensure the effects of relaxation were uniform.

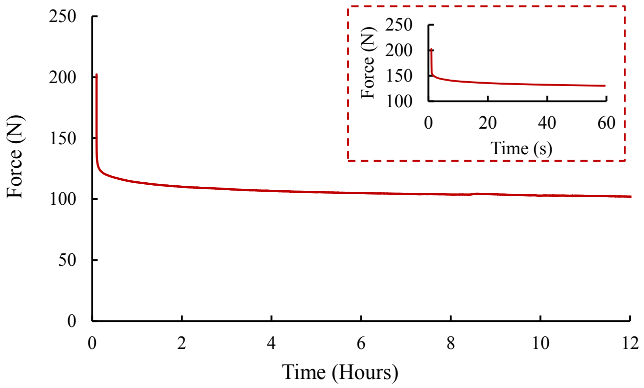

Figure 4.2.10: Relaxation curve for bone substitute over 12 hours and (inset) 60 seconds. At 2 hours the relaxation rate has slowed.

Pushout tests were conducted using a uniaxial load testing machine (Instron model 5565, High Wycombe, UK). Cups were pushed out using a 6 mm diameter steel pin through a 7 mm entry hole milled into the rear of the synthetic bone (Figure 4.2.11). Pushout was conducted at 0.5 mm/min.[227] Peak force of pushout was recorded. Push-out was chosen as a simple measure of fixation that well represents the same trends as a more sophisticated micromotion test.[132]

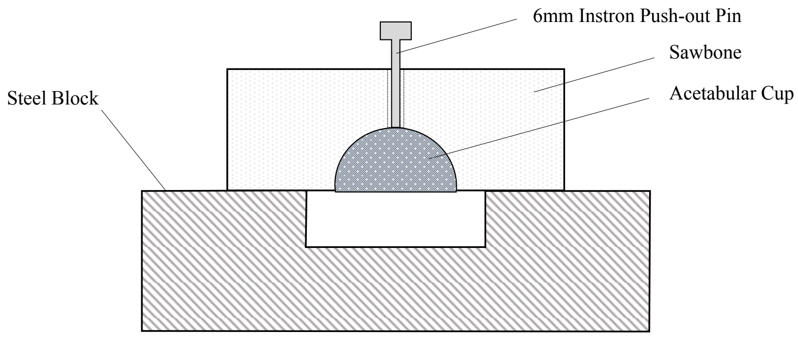

Figure 4.2.11: Pushout setup

4.2.2 Study setup

4.2.2.1 Experimental procedure

Cups (N = 5) were impacted into the low and high density synthetic bone using the drop rig, with strain, displacement and impact load data recorded for 10 strikes. This was repeated for 7 impact energies, representing a spread of impact energies that have previously been measured in cadaver trials (Table 1).[223] Following implantation with 10 strikes, the displacement data was analysed to determine after which strike each cup could be considered seated. Each cup was considered seated with the cup progressed by no more than 0.1 mm for the following strike: referred to as the optimum number of impacts. Subsequently, for each of the 7 energy levels, cups (N = 5) were impacted into virgin synthetic bones using the optimum number of impacts and pushout tests conducted.

In total 140 tests were performed: 70 to established the optimum number of strikes for each testing condition, and then 70 to test pushout fixation following impaction with the optimum number of strikes. Virgin synthetic bone samples were used for each of the 140 tests.

Table 4.2.1: The impaction variables studied: both increases in drop mass and velocity were used to increase the impaction energy

Energy Level	1	2	3	4	5	6	7
Drop Mass (kg)	0.6	1.2	0.6	0.6	1.8	1.2	1.8
Drop Velocity (m/s)	1.5	1.5	2.75	4	2.75	4	4
Energy per strike (J)	0.7	1.4	2.0	4.5	6.8	9.6	14.4

4.2.2.2 Data analysis

Risk of fracture was quantified by correlating the dependent variables of peak bones strain and implantation force with the independent variable of energy per strike. Cup deformation was quantified by correlating the dependent variable of post-strike cup strain with pushout fixation. The strength of fixation was quantified by correlating the dependent variables of pushout fixation with the independent variable of energy per strike. Cup seating was analysed by correlating the final polar gap with the independent variable of energy per strike.

For each dependent variable, two types of least-squares trend line fits were evaluated to characterize the relationship and to identify any limits of the dependent variable (for example is there a maximum strength of fixation that can be achieved?). Both were chosen based upon their application to real world problems and previous use.[228] The first was a linear trend line, Equation 4.2.1.

$$y=\alpha x+\beta \qquad \textit{Equation 4.2.1}$$

Where y is the dependent variable, x the independent variable, with a and β constants. As x becomes large, y scales directly, either linearly increasing or decreasing depending on whether a is found to be positive or negative, respectively (Figure 4.2.12a, Figure 4.2.12b). A linear fit has no upper/lower limit, and therefore cannot account for phenomena that tend to a maximum or minimum value.

The second trend line fit was a hyperbolic asymptotic test, to determine if the data tended toward a maximum/minimum value and to calculate these limits (Equation 4.2.2), (Figure 4.2.12c, Figure 4.2.12d).

$$y={}^{\alpha x}/_{x+\beta} \qquad \textit{Equation 4.2.2}$$

Where y is the dependent variable, x the independent variable and a and β are constants determined during the fitting process. For Equation 4.2.2, as x becomes large, y tends towards the maximum α.

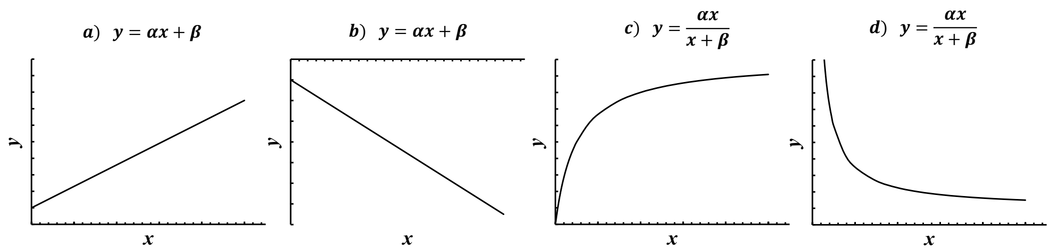

Figure 4.2.12: Graphical representation of different fits: a) Increasing linear (positive alpha) b) decreasing linear (negative alpha) c) Direct asymptotic d) Inverse asymptotic

A least squares method was used to fit both Equation 4.2.1 and Equation 4.2.2 to each relationship using the curve fitting toolbox in Matlab (2015a, Mathworks, MA USA) with a zero y-intercept for all dependent variables apart from polar gap. To assess the quality of fit for asymptotic fits the data was transformed to be linear, by inverting x and y data.

4.2.2.3 Statistical analyses

Regression analysis, conducted in Matlab, was used to assess the quality of data fitting for each relationship reported. Significance level was set to $\alpha = 0.05$. Differences between impact force data for low and high density synthetic bone were analysed using paired t-tests, conducted in SPSS (v24, IBM, NY).

4.3 Results

4.3.1 Bone and cup strain

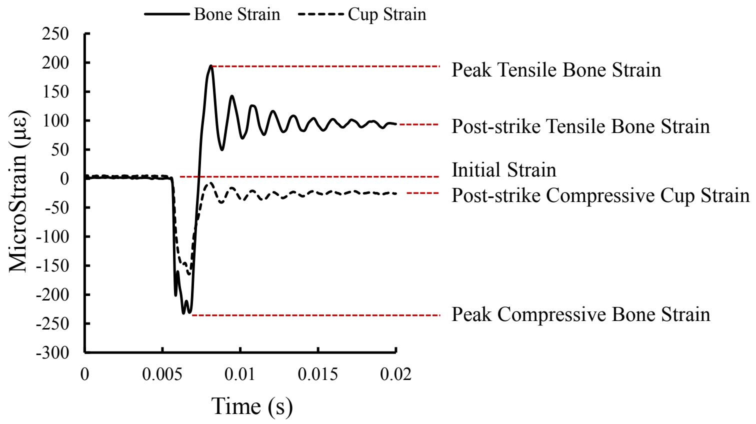

Figure 4.3.1: Strain behaviour during impaction in cup (solid line) and acetabular cup (dashed line). Peak tensile, peak compressive and post-strike strain are identified in bone. Post-strike strain is recorded in the acetabular cups

Two distinct patterns were observed for the behaviour of dynamic strain in the bone and acetabular cups (Figure 4.3.1). In the bone a compressive peak was immediately followed by a tensile peak, followed by a period of oscillation decaying to a final post-strike tensile strain. Both peak tensile and peak compressive peaks in the synthetic bone are of interest as they are both possible contributors to bone fracture. The strain in the cup also exhibited a compressive peak, but no distinct tensile peak. Similarly a period of oscillation preceded the final, post-strike strain. Peak compressive strain in the cup is not analysed as peak stress was estimated at less than 20% of the UTS of titanium, and fracture of titanium cups is not an issue raised in the literature. Duration of the impaction event varied from 5-10 ms depending upon strike energy.

An inverse linear relationship was observed between strike energy and optimum number of strikes to seat in both bone densities (the higher the impaction energy, the less strikes required to seat, $R^2 = 0.67$ and $R^2 = 0.82$, $p < 0.005$, *Table 4.3.1*). The cups only required two strikes to seat at the highest impaction energy, while the full ten strikes were required in the lowest energy group.

Table 4.3.1: Impact force and strikes required to seat for each energy level

Energy per strike (J)	Bone Density	0.7	1.4	2.0	4.5	6.8	9.6	14.4
Force (kN) (± SD)	Low	3.9 (± 0.4)	5.1 (± 0.4)	7.2 (± 0.6)	10.8 (± 0.6)	12.6 (± 1.4)	14.2 (± 1.9)	19.5 (± 1.4)
	High	4.2 (± 0.4)	5.5 (± 0.8)	7.7 (± 0.2)	11.7 (± 0.3)	15.2 (± 1.3)	15.0 (± 1.2)	20.6 (± 1.3)
Difference (kN) (± SD) [*p<0.005]		0.32* (± 0.032)	0.42* (± 0.08)	0.59* (± 0.04)	0.9* (± 0.045)	2.6* (± 0.365)	0.82* (± 0.505)	1.03* (± 0.365)
Strikes required to seat	Low	10	10	7	3	2	2	2
	High	7	7	8	7	3	3	2

Peak strike force versus strikes energy fit the half power law that has been derived analytically (Equation 2.4.33, Figure 4.3.2, $R^2 = 0.89$). However using Equation 2.4.33 the value of spring stiffness attained is far higher than that estimated analytically using Equation 2.4.35 ($k_{experimental} = 120 \times 10^3$ kN/m, $k_{analytical} = 49$ kN/m). Predicted force is much lower than those measured (maximum 1.12 kN predicted versus 20.5 ± 1.2 kN measured).

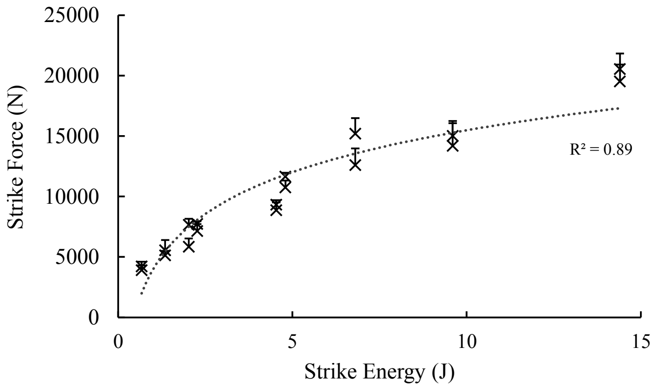

Figure 4.3.2: Relationship between strike energy and strike force. F is proportional to the square root of energy as derived analytically, although magnitude of force is poorly predicted.

Relationships between the features of each strain profile and different strike energies were identified (Figure 4.3.3). Peak tensile bone strains, post-strike bone strains, and post-strike compressive cup strain were all best described by a direct asymptotic function, tending to a finite limit value as energy tended to large magnitudes (Figure 4.3.3a, Figure 4.3.3c, Table 4.3.2). The exception was maximum compressive strain strike energy which was best described by a direct linear relationship (Figure 4.3.3b, Table 4.3.3).

Peak tensile bone strain was on average 2.1x larger than post-strike bone strain in the low density synthetic bone and 1.4x larger in the high. In the most extreme case, a 15 J strike in low density bone produced a peak tensile bone strain 3.4x larger than post-strike bone strain. The bone therefore experienced much higher strain during the impaction event than the steady state conditions post-strike.

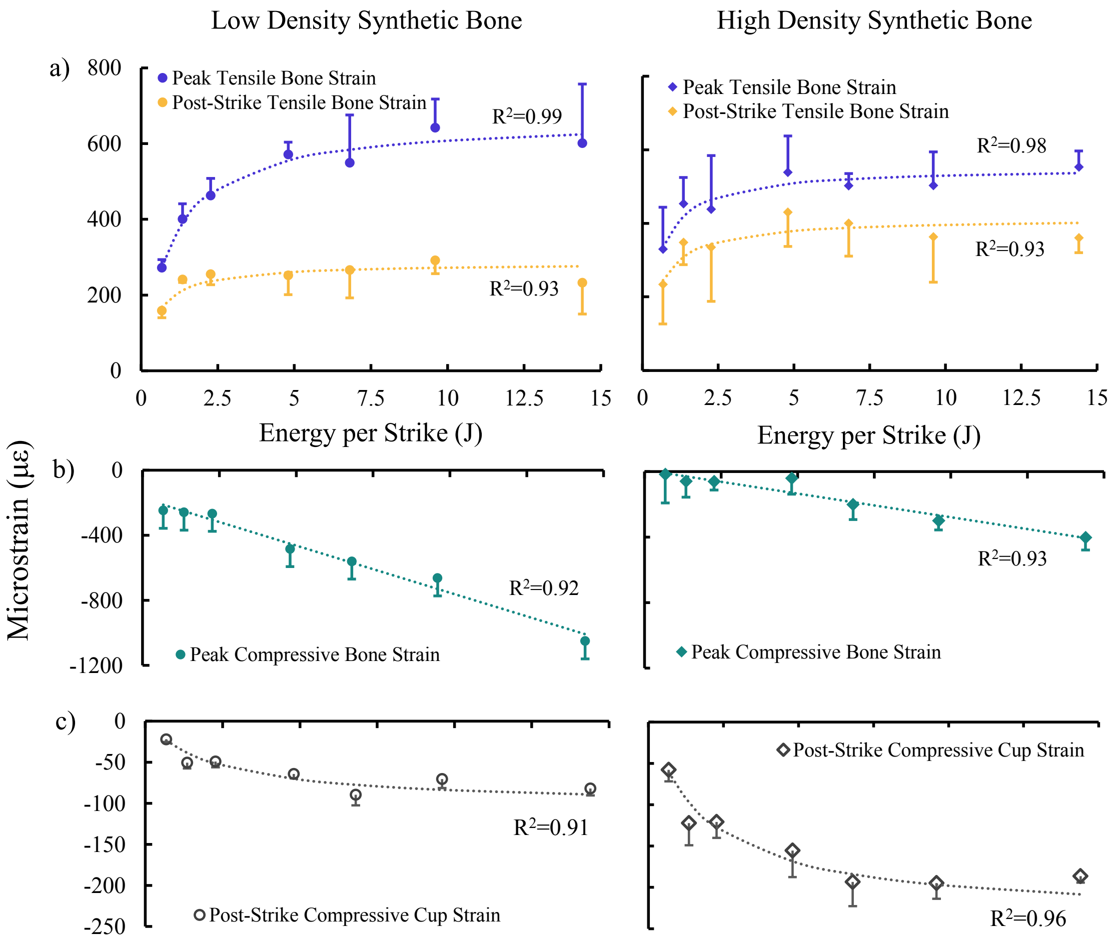

Figure 4.3.3: Relationships between energy per strike and a) peak bone strain, post-strike bone strain b) peak compressive bone strain and c) cup strain (mean with standard deviations). Peak bone strain, post-strike bone strain and cup strain all closely fit an asymptotic trend, suggesting a limit to these strains even at very high energies. Peak compressive strain closely fit a linear trend, suggesting very high strain at very high energies

*Table 4.3.2: Summary of results of asymptotic fits for each relationship. Fit coefficients, R^2 values, p-values and limits when x tends to infinity are given. Peak and post-strike tensile strain, post-strike compressive strain, polar gap and the pushout fixation were all best described by an asymptotic relationship (higher R^2), indicating that there was an upper limit to the*se variables during impaction. *Chosen fits are highlighted.*

Bone Density	**Variable** Independent	Dependant	**Aysmptotic** α	β	R^2	p*	Limit
Low	Energy per Strike	Peak Tensile Bone Strain	662	0.93	0.99	0.004	662
	Energy per Strike	Post-strike Tensile Bone Strain	277	0.35	0.93	0.015	277
	Energy per Strike	Peak Compressive Bone Strain	2000	15.4	0.90	0.004	2000
	Energy per Strike	Post-strike Compressive Cup Strain	91.7	1.57	0.91	0.000	91.7
	Energy per Strike	Pushout Fixation	692	3.22	0.93	0.000	692
	Energy per Strike	Polar Gap	1.10	-0.42	0.81	0.000	1.10
	Post-strike Compressive Cup Strain	Pushout Fixation	>10^5†	1553	0.94‡	0.000	>10^5
	Post-strike Tensile Bone Strain	Pushout Fixation	>10^5†	6220	0.66‡	0.001	>10^5
	Polar Gap	Post-strike Compressive Cup Strain	4.81	-14.6	0.77‡	0.080	4.81
High	Energy per Strike	Peak Tensile Bone Strain	550	0.41	0.98	0.016	550
		Post-strike Tensile Bone Strain	405	0.37	0.93	0.015	405
		Peak Compressive Bone Strain	>10^5†	348	0.91	0.000	>10^5
		Post-strike Compressive Cup Strain	217	1.46	0.96	0.001	216.6
	Energy per Strike	Pushout Fixation	1441	2.80	0.96	0.000	1440
	Energy per Strike	Polar Gap	0.45	-0.56	0.92	0.000	0.45
	Post-strike Compressive Cup Strain	Pushout Fixation	>10^5†	1620	0.96‡	0.000	>10^5
	Post-strike Tensile Bone Strain	Pushout Fixation	>10^5†	3920	0.73‡	0.001	>10^5
	Polar Gap	Post-strike Compressive Cup Strain	4.12	-47.2	0.89‡	0.260	4.12

‡ Dependant-dependant, not independent variable. R not R^2 reported

+ Zero intercept

*0.000 indicates <0.0005

†A high α coefficent tends to a linear-type fit

Chosen fit based upon lower R^2

Table 4.3.3: Summary of results of linear fits for each relationship. Fit coefficients, R^2 values, p-values and limits when x tends to infinity are given. Peak compressive strain was better described by a linear fit: compressive strain fracture risk increased linearly with impaction energy. Chosen fits are highlighted.

Bone Density	**Variable** Independent	Dependant	**Linear** α	β	R^2	p*	Limit
Low	Energy per Strike	Peak Tensile Bone Strain	61.4	0^{+}	0.65	0.002	∞
	Energy per Strike	Post-strike Tensile Bone Strain	27.1	0^{+}	0.55	0.008	∞
	Energy per Strike	Peak Compressive Bone Strain	76.3	0^{+}	0.92	0.000	∞
	Energy per Strike	Post-strike Compressive Cup Strain	7.89	0^{+}	0.68	0.001	∞
	Energy per Strike	Pushout Fixation	51.9	0^{+}	0.81	0.000	∞
	Energy per Strike	Polar Gap	-0.11	2.41	0.34	0.265	∞
	Post-strike Compressive Cup Strain	Pushout Fixation	6.16	0^{+}	0.95‡	0.000	∞
	Post-strike Tensile Bone Strain	Pushout Fixation	1.55	0^{+}	0.74‡	0.000	∞
	Polar Gap	Post-strike Compressive Cup Strain	-0.03	3.60	0.95‡	0.000	3.60
High	Energy per Strike	Peak Tensile Bone Strain	54.8	0^{+}	0.59	0.005	∞
	Energy per Strike	Post-strike Tensile Bone Strain	39.4	0^{+}	0.55	0.008	∞
	Energy per Strike	Peak Compressive Bone Strain	27.8	0^{+}	0.93	0.000	∞
	Energy per Strike	Post-strike Compressive Cup Strain	18.86	0^{+}	0.69	0.001	∞
	Energy per Strike	Pushout Fixation	111.0	0^{+}	0.78	0.000	∞
	Energy per Strike	Polar Gap	-0.04	1.81	0.28	0.600	∞
	Post-strike Compressive Cup Strain	Pushout Fixation	5.61	0^{+}	0.97‡	0.000	∞
	Post-strike Tensile Bone Strain	Pushout Fixation	2.33	0^{+}	0.78‡	0.000	∞
	Polar Gap	Post-strike Compressive Cup Strain	-0.02	3.20	0.92‡	0.000	3.20

‡ Dependant-Dependant, not independent variable. R not R^2 reported + Zero intercept

*0.000 indicates <0.0005

†A high α coefficent tends to a linear-type fit

Chosen fit based upon lower R^2

4.3.2 Pushout fixation

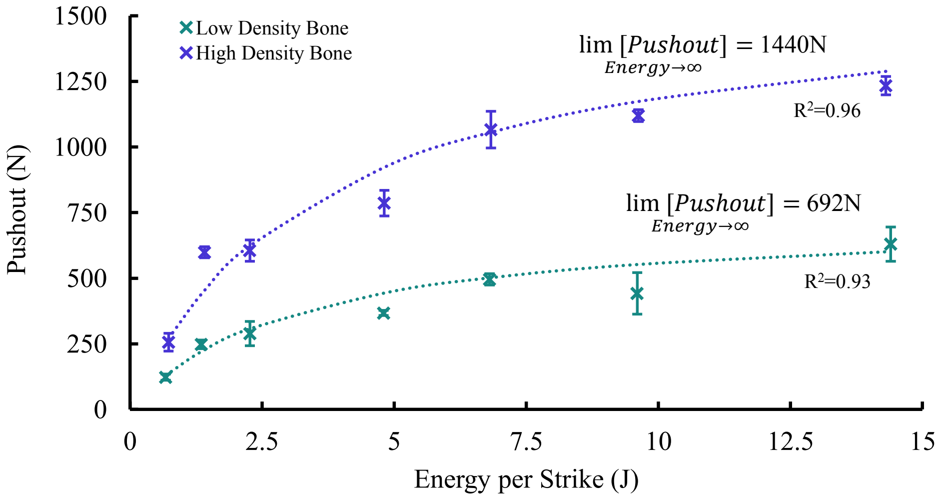

Figure 4.3.4: Pushout fixation for cups impacted with different energy levels (mean with standard deviations). An asymptotic relationship is fitted implying a limit to the amount of fixation that can be achieved even with extremely high impaction energy

The relationship between energy (per seating strike) and pushout fixation (measured after the optimum number of impacts) was best described by a direct asymptotic relationship in both low and high density synthetic bone ($R^2 = 0.93$ and $R^2 = 0.96$ respectively, Figure 4.3.4, Table 4.3.2). These relationships imply that even at higher strike energies there is a limit to how much pushout fixation that can be achieved. These limits were found to be 692 N and 1440 N.

4.3.3 Cup seating

A common trend was observed for the polar gap during seating at different energies. For each different energy, implant progression (movement of the cup into the cavity and reduction of polar gap for each strike) was greatest during early strikes, and reduced strike by strike (Figure 4.3.5a). The higher energy strikes reached a seated condition after fewer strikes. ($p < 0.023$, Table 4.3.1). The relationship between final polar gap and energy was best described by an inverse asymptotic relationship (Figure 4.3.5b, Table 4.3.2), indicating the polar gap reduces to a limit value and increasing the strike energy further may not progress the cup any further. The minimum polar gap achieved in the low and high density bone qualities were 0.60 mm and 0.17 mm respectively.

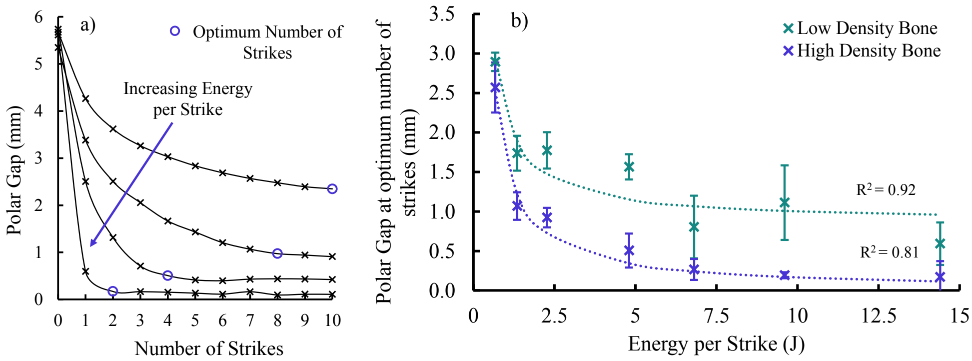

Figure 4.3.5: a) Polar gap at each of the 10 strikes, given for an illustrative range of energies. As energy per strike increases number of strikes taken to seat is reduced b) Final polar gap for each cup when impacted at different energies (mean with standard deviations). The fitted asymptotic relationship suggests that there is a limit to the minimum final polar gap that can be achieved

When each acetabular cup was extracted from the bone substitute debris were observed where contact had been made between the two (Figure 4.3.6). At lower energies, where final polar gap was larger, contact was only observed at the very rim of the cup. As impaction energy increased (and therefore final polar gap decreased) cup coverage also increased, progressing towards the cup pole.

Figure 4.3.6: Residue synthetic bone debris following implantation at: a) 1.4 J b) 6.8 J c) 14.4 J. An increase in energy corresponds with an increase in debris coverage, from the rim (at low energy) to the pole (at high energy)

4.3.4 Dependent – dependent correlations

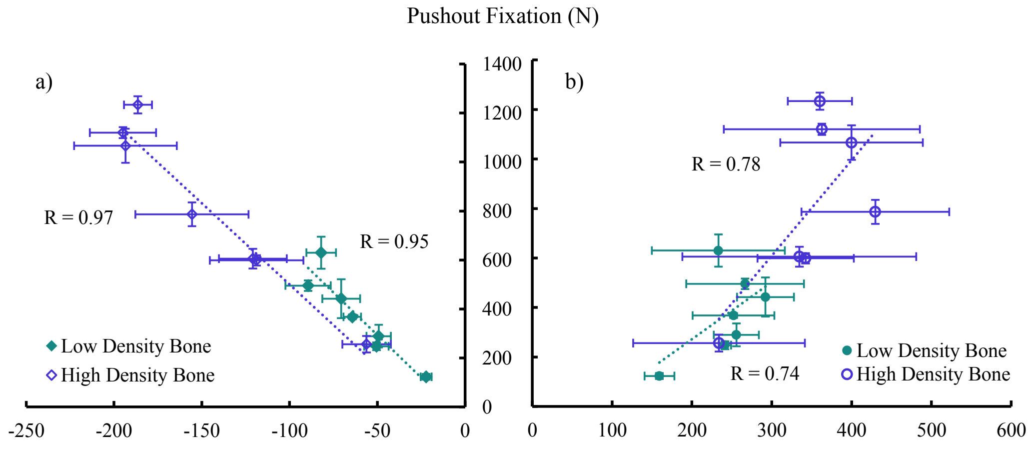

Figure 4.3.7: Relationship between pushout fixation and a) post-strike compressive cup strain and b) post-strike tensile bone strain (mean with standard deviations). Here cup strain is a better indicator of cup fixation than bone strain

A strong correlation was observed between post-strike compressive cup strain and pushout force in both bone densities (R > 0.95, Figure 4.3.7a). A weaker correlation was observed between the post-strike bone strains and pushout force for both bone densities (R > 0.74, Figure 4.3.7b).

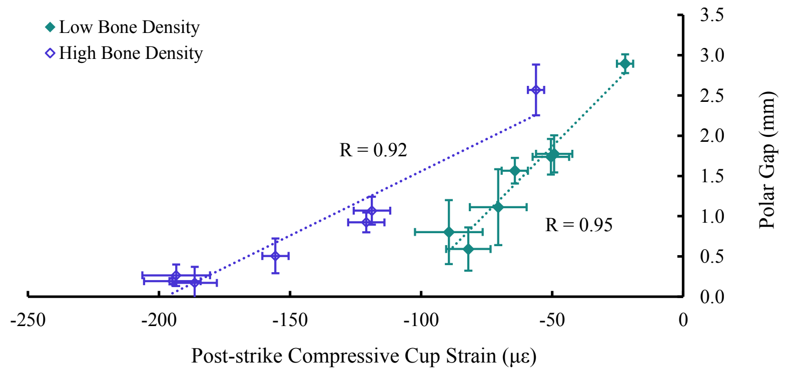

Figure 4.3.8: Relationship between polar gap post-seating and acetabular cup strain (mean with standard deviation). A strong linear relationship is observed in both cases.

A linear relationship was observed between post-strike compressive cup strain and polar gap, with increasing polar gap with reducing strain. Max cup strains of 109 με and 198 με are predicted for ideal (0 mm) polar gap (in low and high density bone respectively). For zero post-strike compressive cup strain polar gaps of 3.2 mm and 3.6 mm are predicted, roughly equivalent to the polar gap that occurs before a cup is impacted into the cavity.

4.4 Discussion

4.4.1 Key findings

This study demonstrated for the first time that peak strain in the bone during the impaction event can be several times higher than the post-impaction steady state strain. Our 2 mm diametrical interference in low density bone is in line with many manufacturers' recommended surgical techniques but generates a higher peak bone strain during impaction than a 1mm press fit in higher density bone. Higher peak strains in bone increase risk of bone fracture, and should be considered by manufacturers and surgeons when deciding impaction technique. This is compounded by the viscoelasticity of bone,[181] increasing the stress for any given strain when the strain rate is very high. At around between 5 - 10 ms for each strain event (compressive peak through to tensile peak) and a change of strain value of up to 2000 $\mu\varepsilon$ strain rates of up to 500 $\mu\varepsilon/s$ are observed. Dynamic strains are particularly important as compressive peak bone strain appears to scale linearly with impaction energy, a feature not apparent in post-strike strains. When assessing fracture risk dynamic stresses and strains should be considered. The resultant stresses at the strain gauge locations can be calculated by using values of elastic modulus measured for the bone substitute and constitutive relations (Equation 2.3.3).[135] It is seen that the stresses calculated are an order of magnitude lower than yield (Table 4.4.1).

Table 4.4.1: Bone model properties and resultant stress predicted from strain gauge measurements

		Bone Model Density	
		Low	**High**
Compressive	Peak strain ($\mu\varepsilon$)	1049	402
	Modulus (GPa)	0.123	0.592
	Calculated Stress (MPa)	0.129	0.238
	Yield Stress (Mpa)	4.9	12
Tensile	Peak strain ($\mu\varepsilon$)	601	552
	Modulus (GPa)	0.173	0.445
	Calculated Stress (MPa)	0.104	0.246
	Yield Stress (Mpa)	3.7	18

Yielding may still take place at the bone-cup interface. Stress increases up the bone according to a square power law (Figure 2.3.8). The average distance of the strain gauges from the cup rim was 4 mm (including strain gauge width). Therefore the stresses may increase significantly nearer to the interface. In addition the effect of strain rate is not considered – important when considering viscoelastic materials (Figure 4.2.10).

A second finding from this study was the law of diminishing returns applies to the amount of fixation strength and implant seating that can be achieved by increasing impaction energy. For example, at just 7.5 J, 85% and 84% of the total pushout available at 15 J (for low and high density synthetic bone respectively) was achieved. Similarly, the same doubling of impaction energy only reduced polar gap when seating by around 0.1 mm with the majority of the displacement occurring during earlier strikes, as previously reported.[93,108,160] The necessary gaps of < 2mm (which have been shown to be tolerable clinically[95,110]) were achieved in both bone densities at 7.5 J. However peak compressive bone strain would double with this change in energy. As it is difficult for surgeons to accurately deliver set impaction energies, impact-limiting instrumentation may be a useful addition in surgery to gain the maximum fixation and implant seating, but with the lowest delivery of energy and risk of damage to the bone.

The limit to the amount of implant fixation that can be achieved may be explained by the phenomenon of bone damage and compression that occurs during implantation that has previously been observed.[114] It has been shown that plastic deformation occurs locally around the cup surface. The stress distribution within the bone is at a maximum at the cup/bone interface, and is both hoop and radial (Figure 2.3.8). If the yield of the bone is exceeded at the interface, especially at the cup interface where the interference is greatest, implant reaction forces may be limited. The higher the impact forces used, the more deformation that may occur and therefore less elastic energy is stored The asymptotic behaviour of tensile bone strains do imply that stresses are self-limiting. However compressive peak strains appeared to scale linearly with energy, without a predicted upper limit. This may explain why fractures are observed in the acetabulum during impaction.[27,51]

Another important finding of this study was the identification of a strong linear relationship between pushout fixation and the deformation of the cup itself. During seating of an implant it would be beneficial to maximise fixation as much as possible. However it would also be beneficial to minimise cup strains in order to reduce component deformation (to lessen the chances of excessive component wear, or improper liner seating). However this study shows that these factors are inextricably linked – to generate fixation, you must generate bone stress, and therefore strain. The force of the 'pinch' of bone on cup relates to the amount of fixation and stability the cup receives.[29,105,110,229] Cup deformation might be reduced by increasing implant wall stiffness. However it is well documented that excessive implant stiffness leads to strain shielding, an undesirable function of bone.[126] This appears to be a trade-off: a balance between component deformation and stress shielding must be determined. A linear relationship between cup seating and polar gap predicts a max component deformation. This information could be used to predict whether component deformation may or may not be an issue during assembly or operation.

Implant fixations levels achieved during this study are of a similar magnitude to those measured in other studies. Crosnier et. al. measured pushout values of 0.42 kN and 1.05 kN in the same low and high density PU foam as used for our study.[132] Macdonald et. al. measured significantly higher pushout forces in similar foam (2.0 kN) indicating that other cup designs may produce more fixation than the design tested here. The only measurements of acetabular strain are from cadaveric measurements, and of a similar magnitude to those measured here, but are of such variability that direct comparison is difficult.[93] A number of other studies also find that cup deformation correlates with fixation.[110,124,156,230] Higher levels of fixation were measured in 30 PCF bone model when compared to 15 PCF model. This is due to an increase in material modulus (Table 4.4.1) outweighing the effects of interference decrease (Equation 2.3.5). Peak pushout forces were measured as several orders of frequency lower than those of the impact strikes. This is partly due to the requirement of the impulse to accelerate the introducer. As noted in Section 2.3.1.5, more force is required on insertion to seat an acetabular cup due to the additional vertical resistance of the bone reaction force (Figure 2.3.12).

At up to 10 ms, the duration of the strain event demonstrates that the compliance discussed in Chapter 3 may have a significant effect on the energy transmission to the bone. 10 ms equates to roughly a third of the 25 – 30 ms rise time of the system. The initial simulations of Section 2.4.1.3 show that impulse applied over such a proportion of the system natural time period may lead to a significant change in impact dynamics.

Peak strike forces derived analytically were an order of magnitude lower than those measured experimentally. Stiffness of the introducer, derived from experimental data using Equation 2.4.33, was calculated as several orders of magnitude higher than that estimated from material properties and geometry (Table 3.4.1). This is likely due to the limitations of approximating the introducer as an ideal spring (assuming zero mass). In reality the introducer is a continuous mass. At the introducer tip, in addition to the compression of the steel, the mass of the continuous body must also be accelerated.

4.4.2 Limitations

4.4.2.1 Common *in-vitro* model limitations

This section details limitations that are common to Chapters 4, 5 & 6. 'Study Limitations' refer to limitations that are unique to individual Chapters.

Use of synthetic bone may have influenced our results as the representative geometry and material properties only provides an approximation of the complex anatomy of the pelvis and the intraoperative environment. However, it allowed for experimentation that would not be ethical in patients. A cadaveric tissue model would be more representative of the *in-vivo* scenario but the variation between specimens is too great. Variables such as acetabular cup size & positioning, bony morphology & properties, BMI and hammer strike direction may interact with each other and thus necessitate prohibitively large sample sizes to detect differences in impaction technique. A repeated measures analysis would help mitigate this variation but is not possible for the present study as the bone is damaged by seating a cup, so the same cadaver could not have been used for multiple energies. Our impaction rig with synthetic bone model allowed us to control all these variables and thus isolate the effects of impaction energy. Every effort has been made to best represent the clinical scenario. The rig has been previously been validated through direct comparison to cadaveric THA in 8 hips; an important aspect of this validation was replicating the intraoperative boundary conditions to replicate the physiological movement of the acetabulum away from the surgeon following a hammer strike.[223] To account for variation in bone properties, we modelled two bone densities based upon previous literature.[77,80,132,142,225] Synthetic bone densities were carefully chosen using existing literature in order to most closely represent high density (mostly cortical in primary THA) and low density (more sub-chondral/defected) bone.[33,77,80,132,142] The anatomic model has also been rigorously validated against cadaveric tissue in literature, providing mechanical properties,[152] cup deformation,[104] cup frictional resistance[33] and stability within the variability of mechanical samples,[82] even when damaged.[154] Sawbones have been shown to model the mechanical properties of biological tissues[80,152,153] and result in cup fixation stability within the range measured in cadavers.[82] Previous literature demonstrates the value of these models to draw important conclusions.[155,224,231] The milled bone cavity has also been previously demonstrated to be a surrogate for the anatomy of the acetabular socket.[104]

Many brands of cementless shell are used clinically,[11] and thus we elected to use a representative acetabular cup rather than tailor the results to a specific device manufacturer. It is likely that different devices/coatings will alter the numeric values for the limits for minimum polar gap and pushout fixation strength. However, these changes are unlikely to influence the main findings (peak impaction strains exceeding post-strike strains and diminishing returns at high strike energies) as these are a result of the mechanics of press-fit impaction and the properties of bone. An advantage of our method is it provides a controlled model for measuring differences between devices and could provide a useful means to compare a new device/coating against a clinical gold-standard.

One method of fixation measurement was used, while many are available and may represent different failure modes. However the push-out test for fixation has shown to correlate well with other testing methods. [80,115,132,133] It should also be consiered that the slow pushout of cups in this study may result in higher values of friction than at higher distraction rates which may occur in-vivo.

Although carefully designed and validated, this study does represent only one set of conditions. There are other variables occur during THA surgery that may influence the results presented. These include:

- Introducer mass, stiffness and strike surface
- Implant stiffness, coating, underream and size
- Off axis or misaligned impaction

By choosing a representative model for the most common of each scenario the testing best represents the majority of surgery. However these variables might be suggested for future work.

4.4.2.2 Study limitations

The relationships presented in this study are valid only for the energy range that is presented. Such relationships may not hold at extremes of impaction energies; for example a very large energy strike might completely destroy surrounding bone and provide no fixation at all. However the energy of the strikes tested represent the region measured operatively (1-15 J), as previously reported,[33,223] and are therefore of most relevance. A factor not considered here is the ability of the surgeon to change impaction energy during seating (for example high initial energy strikes, decreasing as the cup is seated).

Additionally this study only considers the effects of energy when the number of impaction strikes are appropriate. In reality the surgeon may under, or over-impact the cup. These issues are assessed in Chapter 5.

4.4.3 Conclusion and clinical Relevance

In orthopaedic surgery, press-fit implant fixation is a proven technique, but achieving primary fixation is critical for long term success. The intraoperative impaction that creates the primary fixation is highly uncontrolled compared to the manufactured precision of the implant and bone preparing instruments. This chapter has highlighted important features of the strain that occurs in bone during the impaction event demonstrating the diminishing returns of fixation and seating with increasing energy. A twofold increase in impaction energy may double the risk of fracture, but only slightly increase fixation. The relationships presented in this study may be of use to engineers looking to validate *in-silico* models, or when developing surgical tools that deliver more precise amounts of energy or force.

The clinical message of this paper is that caution should be exercised with high energy impaction: moderate energy strikes may prove just as beneficial and reduce the chance of fracture.

4.5 Chapter summary

- Peak bone strains, measured at high acquisition rates during the impaction process, are several times larger than strain measured post-strike. These should be considered when assessing fracture risk

- Peak and post-stike tensile strains are limited at high impaction energies. However peak compressive strains (and possibly fracture risk) increase linearly

- Pushout fixation and polar gap is also limited, with diminishing gains for higher impaction energies

- Pushout fixation correlates with bone strain, and very well with cup strain

- Higher energy strikes should be avoided as they offer little fixation benefit and increase fracture risk

4.6 Acknowledgements

I thank Richard van Arkel and Shaaz Ghouse for designing and manufacturing the custom acetabular cups in this chapter.

I would also like to the Mechanical Engineering research workshop staff for CNC milling the synthetic bone models.

Chapter 5: The effect of impaction technique: Number of strikes, mallet mass and strike velocity

5.1 Introduction

Press-fit fixation is achieved by impacting an implant into an undersized cavity in the bone and generating hoop strain, creating friction at the implant/bone interface, and promoting long-term bone ingrowth.[21,121] However, if too little friction is achieved and the implant is unstable, small movements occur during physiological loading which may prevent bony ingrowth.[53,84] Implant stability is particularly important during revision cases, where bone stock and quality may be poorer, and secure fixation is more difficult to achieve.[30,31] Early instability and loosening has been reported as the main cause of cementless implant failure following revision.[66,232,233] In order to maximize the benefits of using cementless implants, particularly in more difficult cases, stable fixation must be achieved.[33]

Much previous research has focused on how initial fixation is influenced by implant/bony factors: cup design,[220,234] implant surface,[78] cup stiffness,[105] bone density[79] and bone/cup interference.[61,62,229] However there is a paucity of literature discussing surgical technique in seating cementless implants. Chapter 4 discusses the effects of different impaction energies and finds that high energy strikes do not offer substantial benefits versus medium energy in terms of fixation and implant seating, but do increase the risk of bone fracture. These conclusions were made under the assumption of optimum seating, when impaction was ceased if cups no longer progressed into the bony cavity. It has been demonstrated that it is very difficult for surgeons to determine exactly when this point of seating is.[93] This suggests that under, or over, impaction occurs in theatre (when too many or too few impaction strikes are used).

No current study discusses the effect of the number of strikes upon important press-fit parameters. In addition Chapter 4 discusses impaction in terms of energy. This is useful as an engineering quantity for use pre-clinically, and useful for surgeons as a gauge between 'light' strikes (low energy) and 'vigorous' strikes (high energy). This study discusses impaction in terms of strike velocity and mallet mass, two factors that aim to be more readily understood by a surgical audience.[3] In this study 'impaction technique' is defined as the combination of:

- Number of impaction strikes used to seat implant
- Mallet mass used to seat implant
- Velocity of hammer strike used to seat implant (how 'hard' the surgeon strikes)

The aim of this study is to maximize implant fixation, and reduce chance of implant loosening, particularly in low bone quality (i.e. revision) cases. This study uses an *in-vitro* model to answer two questions:

(1) How does impaction technique affect:

- Cup Fixation, quantified by measuring post-strike bone strains, post-strike cup strains and pushout fixation?
- Cup seating, quantified by measuring polar gap?

(2) Can an impaction technique be recommended to minimize risk of implant loosening while ensuring seating of the acetabular cup?

[3] This study is submitted to a journal with a mostly clinical readership

5.2 Materials and methods

5.2.1 Common experimental setup

Please refer to Chapter 4 for details of the following aspects of the setup of this study:

- *In-vitro drop rig*
- *Custom acetabular cups*
- *Synthetic bone model.*
- *Load, strain and displacement acquisition*
- *Pushout fixation testing*

5.2.2 Study experimental setup

5.2.2.1 Experimental procedure

Data were acquired for 3 strike velocities and 3 strike masses. Low, medium and high velocities of 1.5 m/s, 2.75 m/s and 4.0 m/s respectively were chosen based upon existing literature and previous testing.[90,151,159,223] A video demonstration intended to aid surgeon replication of these velocities is available.[235] Low, medium and high strike masses of 0.6 kg, 1.2 kg and 1.8 kg were implemented by changing the mass of the drop platen and chosen to cover a range of surgical mallet masses available (Table 5.2.1). Five repeats were completed for each of the nine mass/velocity combinations, in each of the two densities of synthetic bone. Strain and displacement data were recorded for 10 strikes for each setup. Pushout fixation was measured for two conditions, optimally seated and over-impacted (10 strikes). In total 180 tests were completed in virgin synthetic bone.

Table 5.2.1: Nine combinations of strike velocity and strike mass used to impact cups into each density of bone substitute

Strike Energy (J)	Strike Energy (J)		
	Strike Mass (kg)		
	Low [0.6]	Medium [1.2]	High [1.8]
Low [1.5]	0.7	1.4	2.0
Medium [2.75]	2.3	4.5	6.8
High [4]	4.8	9.6	14.4

5.2.2.2 Data analysis

Strain deterioration

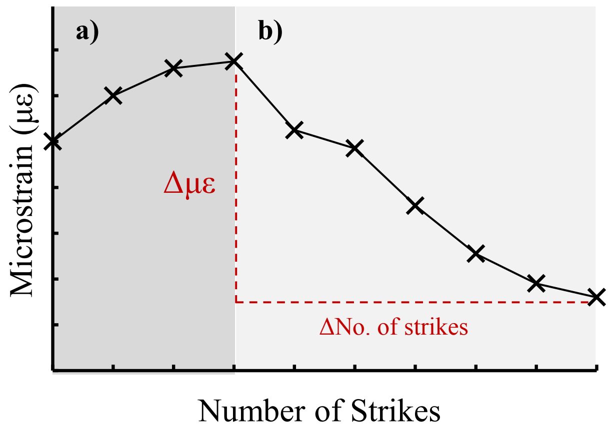

Figure 5.2.1: Representative bone/cup microstrain measurements during seating. (a) An increase of strain is observed, followed by an inflexion point and (b) subsequent deterioration.

Pilot testing indicated a characteristic pattern to the strain with increasing number of strikes (Figure 5.2.1): initially strain increased strike-by-strike (Figure 5.2.1a), which represents an increase in the press-fit fixation of the implant. This was followed by an inflexion point (peak strain) and a subsequent deterioration of strain with each strike (Figure 5.2.1b). This deterioration in strain with subsequent strikes was quantified and analysed as it poses a clinical risk: over impacting the cup may reduce fiction. A metric of strain reduction, hereby known as *strain deterioration* is defined by Equation 5.2.1, with terms defined graphically in Figure 5.2.1.

$$\text{Strain Deterioration} = \frac{\text{Max Strain} - \text{Min Strain } (\mu\varepsilon)}{\text{No. of strikes between max and min}} \qquad \textit{Equation 5.2.1}$$

A strain deterioration of zero would represent conditions where an excessive number of strikes beyond some optimum does not reduce bone strain at all. A larger strain deterioration magnitude represents conditions where excessive strikes cause a larger reduction in bone strain, and therefore reduction in cup fixation strength.

Pushout deterioration

Pushout fixation was measured for two conditions. The first was after ten strikes for all mass, velocity and bone density setups. The second was for optimum number of strikes, when the implant could be considered 'seated'. This was when the implant had progressed by no more than 0.1mm during the previous strike (Section 4.2.1.6, Chapter 4). The pushout after 10 strikes was always less than the 'seated' number of strikes, due to the strain deterioration illustrated in Figure 5.2.1. A metric of pushout reduction, hereby known as *pushout deterioration* is defined by Equation 5.2.2.

$$\text{Pushout deterioration} = \text{Pushout}_{10\ \text{strikes}} - \text{Pushout}_{\text{seated}} \qquad \textit{Equation 5.2.2}$$

5.2.2.3 Statistical analysis

Low density bone data were tested for normality with Shapiro-Wilk test in SPSS (v24, IBM, NY). Data were then analysed with a two-way repeated measures analysis of variance with strain deterioration as the dependent variable and mallet mass (low, medium, high) and strike velocity (low, medium, high) as independent variables. The significance level was set to $p < 0.05$. Post-hoc paired *t*-test with Bonferroni correction were applied when differences across tests were found. Adjusted *p*-values, multiplied by the appropriate Bonferroni correction factor in SPSS, have been reported rather than reducing the significance level. A linear regression analysis was also performed to compare determine if a relationship exists between strain and pushout deterioration. Polar gap data were analysed with paired t-tests. These analyses were then repeated for the high density bone data.

5.3 Results

5.3.1 Fixation: Strain deterioration

For both bone densities, at all velocities and all mass strikes, implant impaction was characterized by a period of increasing bone strain, followed by an inflection point, followed by strain deterioration (Figure 5.3.1). This severity of the peak and strain deterioration is observed to varying degrees depending upon the mass/velocity strike combination. In the most extreme case with low density bone, high strike mass and high strike velocity, the peak strain was generated after one strike, the second strike then halved the strain and the third strike reduces the strain to zero (Figure 5.3.1c). Peak strain took more strikes to achieve and some bone strain was maintained at 10 strikes in all cases in higher density bone (Figure 5.3.1d-f).

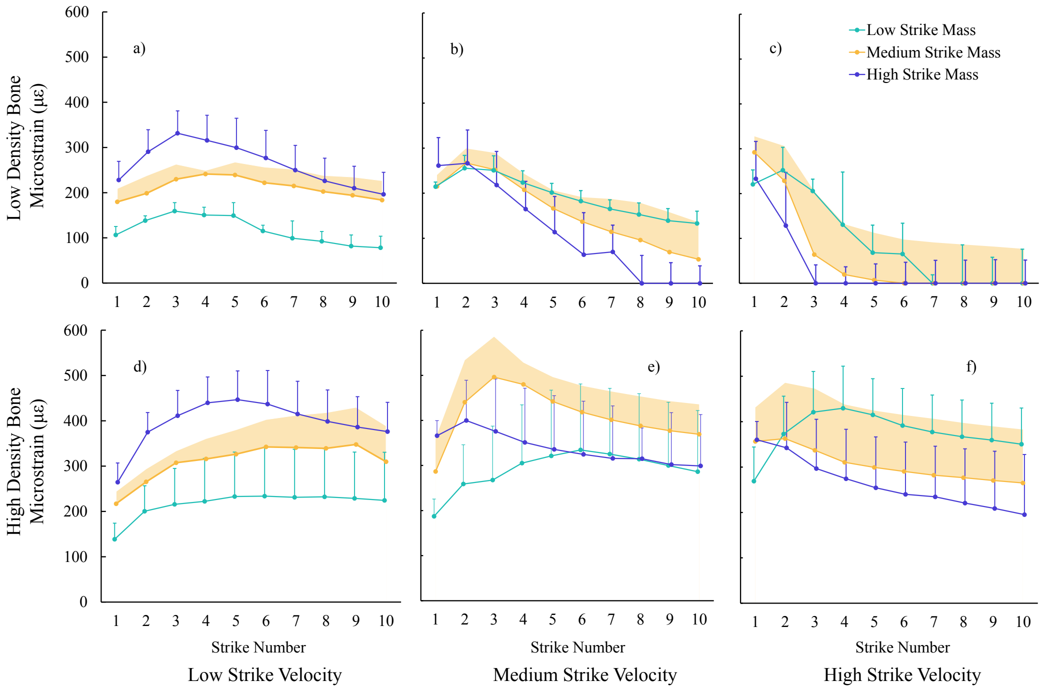

Figure 5.3.1: Mean post-strike bone microstrain measured (with standard deviation) post-strike for low density bone at (a) low, (b) medium and (c) high velocities and high density bone at (d) low, (e) medium and (f) high velocities. Strains are characterized by increasing strain, an inflexion point and strain reduction

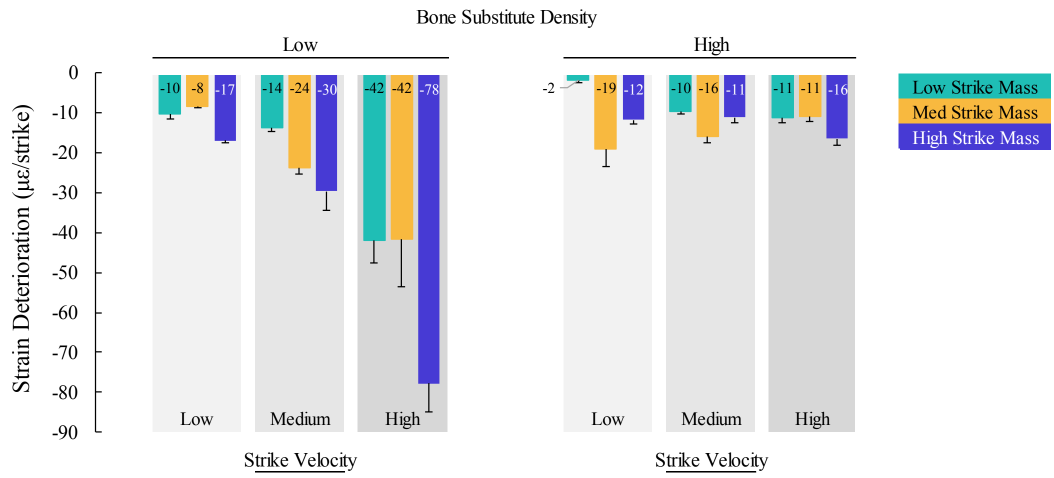

Figure 5.3.2: Strain deterioration (mean with standard deviation) for each impaction technique. Strain deterioration is greatest for lower density bone, and for medium or high velocity strikes

For low density bone, the effects of mallet mass upon strain deterioration depended upon the strike velocity (interaction $p = 0.007$) (Figure 5.3.2). At low velocity, all the strain deterioration values were low (range -8 to -17) and the effect of strike mass was low (max difference -9, p=0.07). Conversely, at high strike velocities, the strain deterioration was much higher (range -42 to -78) and the effects of strike mass were much greater (max difference -36, $p < 0.005$). This indicates that low velocities were less sensitive to over impaction and that increasing strike mass at low velocity in low density bone does not increase the strain deterioration if too many strikes are used. For high bone density strain deterioration magnitudes were low (range -2 to -19) for all velocities indicating that strain deterioration poses a greater clinical risk in low density bone.

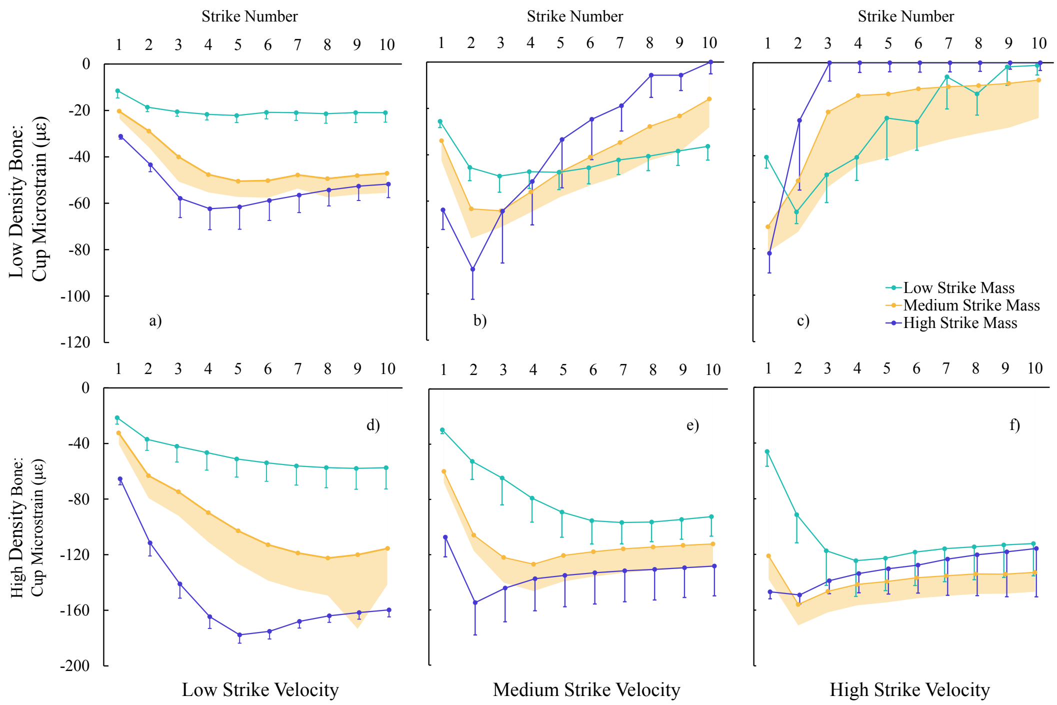

Figure 5.3.3: Mean post-strike cup microstrain measured (with standard deviation) post-strike for low density bone at (a) low, (b) medium and (c) high velocities and high density bone at (d) low, (e) medium and (f) high velocities. In a similar manner to bone strain, curves are characterized by an increase in strain magnitude, an inflexion point and subsequent reduction

Similar trends of increasing strain, an inflexion point and then strain deterioration were also observed for post-strike cup microstrain (Figure 5.3.3). Peak strains are reached with fewer strikes when higher velocity and higher mass strikes are used, in general agreement with the number of strikes to peak strain in bone (Table 5.3.1). Again high velocity strikes in low density bone appear to carry the highest risk of deterioration.

Table 5.3.1: Number of strikes required to reach peak post-strike strain in bone and cup. A general agreement between bone and cup is observed, with more strikes required in lower velocity and mass strikes

	Strike Velocity	Low			Medium			High		
Low Bone Density	**Strike Mass**	**Low**	**Medium**	**High**	**Low**	**Medium**	**High**	**Low**	**Medium**	**High**
	Post-strike bone strain	2	3	2	3	2	2	2	1	1
	Post-strike Cup Strain	5	6	4	3	3	2	2	1	1
High Bone Density	**Strike Velocity**	**Low**			**Medium**			**High**		
	Strike Mass	**Low**	**Medium**	**High**	**Low**	**Medium**	**High**	**Low**	**Medium**	**High**
	Post-strike bone strain	6	9	5	6	3	2	4	2	1
	Post-strike Cup Strain	9	8	5	7	4	2	4	2	2

During high velocity impaction, particularly high velocity high mass impaction in low bone density, debris gathered at the cup rim (Figure 5.3.4). This debris appears to be extracted from the implant cavity during impact. After 10 strikes this wear was significant and a gap between cup and bone could be clearly observed. In this condition the bone exhibited very poor pushout fixation (Figure 5.3.5).

Figure 5.3.4: An acetabular cup in seated in low density bone with 10 strikes of high velocity and high mass. A large amount of bone substitute debris has gathered around the cup rim. In addition a clear gap is visible between the cup and bone.

5.3.2 Fixation: Pushout

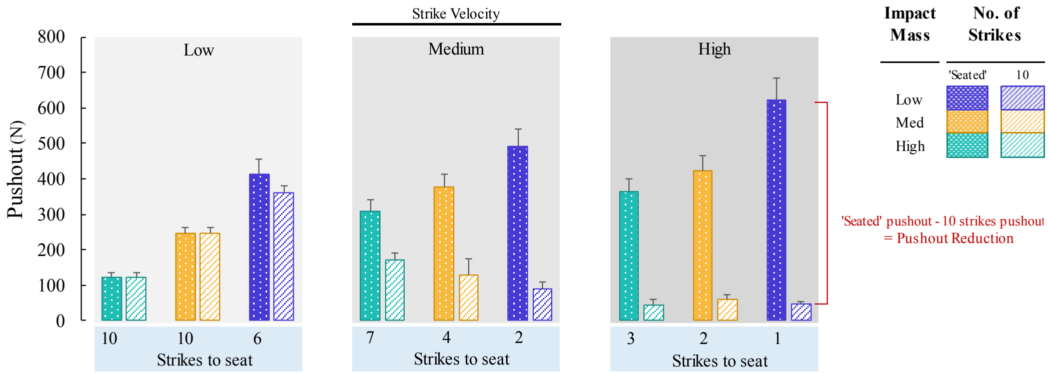

Figure 5.3.5: Bargraph demonstrating loss of pushout fixation (mean with standard deviation) between 10 strikes (over-impacted) and optimum number of strikes to seat. Less loss of fixation is observed for low velocity strikes. Loss of fixation increases with both increasing strike velocity and mallet mass

The number of strikes until the 'optimally seated' condition and pushout values are provided in Figure 5.3.5. For the group that were pushout tested when 'optimally seated', fixation increased with both strike mass and velocity. However, in the 10 strike group an increase in fixation with increasing mallet mass was only observed in the low velocity group. In the medium and high velocity group no increase in fixation was observed with mallet mass. If pushout deterioration is plotted as a function of strain deterioration it is confirmed that strain deterioration was an appropriate measure for risk of cup loosening as fixation strength reduced linearly with strain deterioration (Figure 5.3.6, $R^2 = 0.84$, $p < 0.05$).

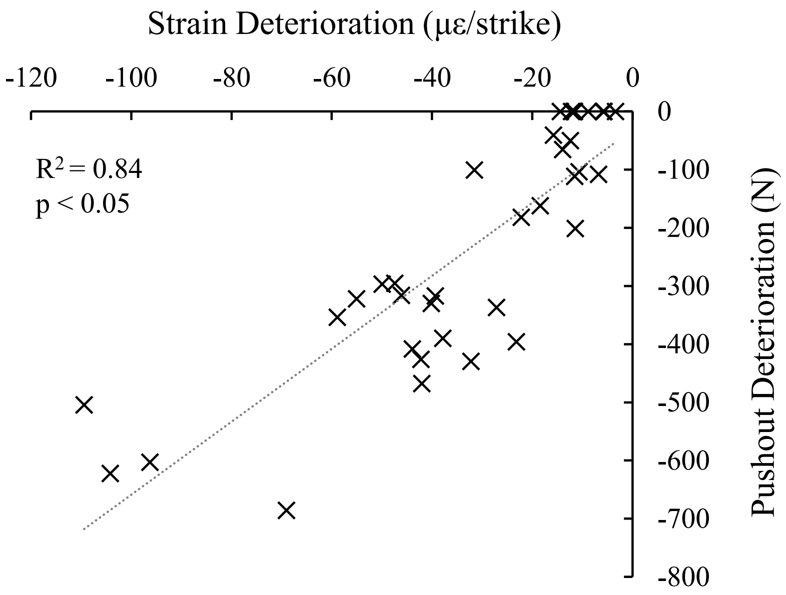

Figure 5.3.6: Relationship between strain and pushout deterioration. Larger magnitude strain deterioration correlates with a reduction in pushout. Strain deterioration should be avoided to ensure optimum fixation

5.3.3 Seating: Polar gap

Polar gap reduced with both increasing mallet mass and velocity in both low and high density bone in all but the high velocity, high density group (Figure 5.3.7). A difference in polar gap between low and high mallet mass was detected (0.335 mm, $p = 0.014$) but not between low/medium and medium/high masses. Combining the findings of Figure 5.3.2 & Figure 5.3.7, across the low and high density bone materials, the only mass/velocity combination that provided a low strain deterioration and full implant seating (polar gap <=1 mm) was the high mallet mass at low velocity.

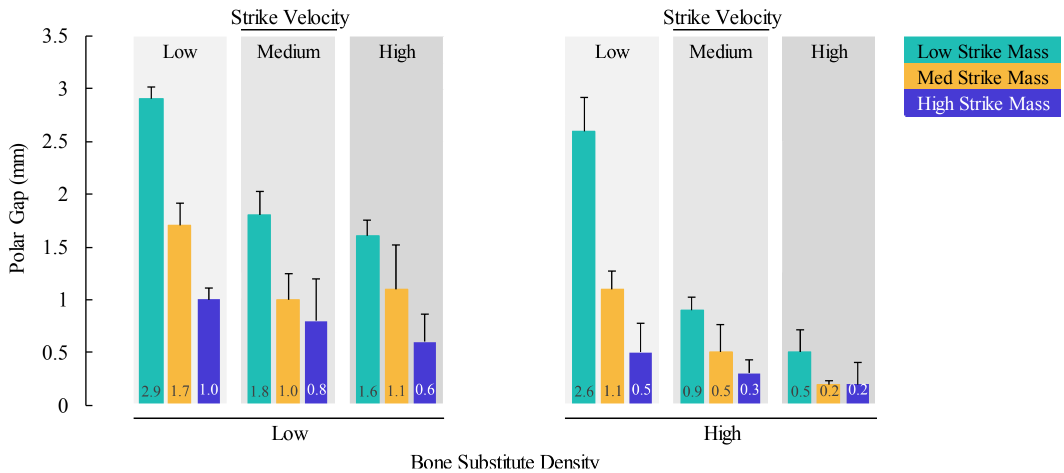

Figure 5.3.7: Mean polar gaps at seating (with standard deviation) for each impaction technique. Polar gap is reduced with both increasing impact mass and velocity

By plotting bone and tensile strains as a function of polar gap the point of strain deterioration following optimum seating is clear. At this point little to no displacement is made by the cup as it no longer progresses into the bone cavity. Instead strain in both bone (Figure 5.3.8a) and implant (Figure 5.3.8b) decrease strike by strike. As post-strike strain (and therefore fixation) is decreasing but no improvement in cup seating is being made strike-by-strike, it is again clear that over-impaction is detrimental to implant performance.

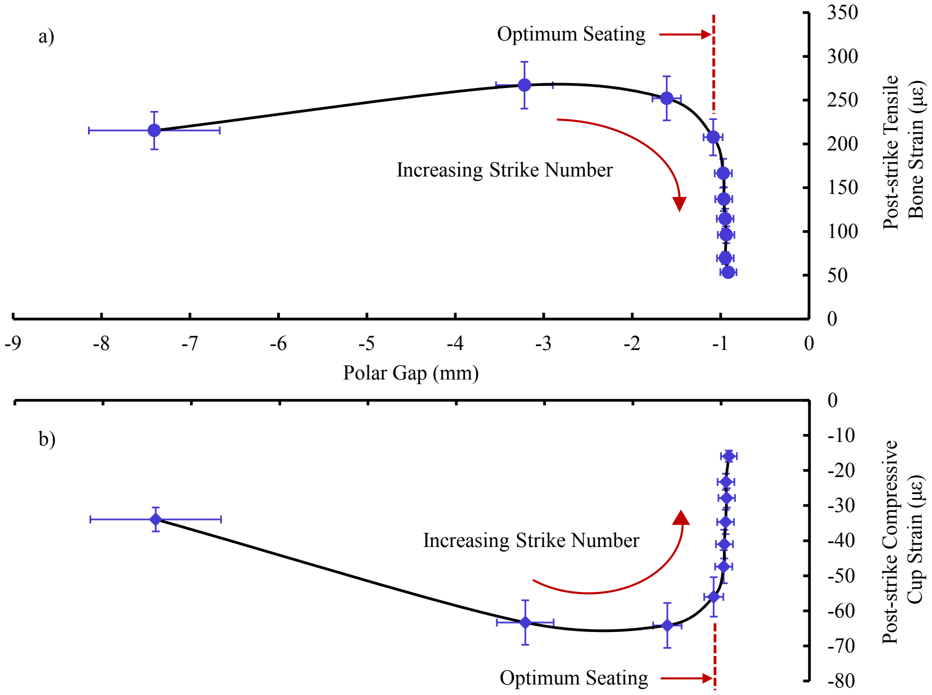

Figure 5.3.8: Representative trace of polar gap against: a) Post-strike tensile bone strain b) Post-strike compressive cup strain. Following optimum seating the cup stops progressing into the bony cavity while strain (and therefore implant fixation) decreases

5.4 Discussion

5.4.1 Key findings

The most important finding of this study was the strain in bone and cup deteriorated after a certain number of impaction strikes, and that impaction technique had a large effect on this deterioration. A deterioration in strain was measured in all cases but was most severe in the case of lower density bone (representing revision or poor quality bone cases). This deterioration correlated well with a reduction in fixation strength and so must be avoided. The strike velocity (which can be interpreted as how hard the surgeon hits the introducer) was a key risk factor for this deterioration – at high velocity even the lightest 0.6 kg mallet caused a severe deterioration in strain with excessive impaction strikes. At low velocity, for all mallet masses, the deterioration in strain still occurred, but was far less severe than at medium or high velocity. Therefore a lower strike velocity may be preferable. It should be considered that polar gaps of more than 2 mm have been linked to an increase in early cup migration[95] while gaps of less than 2 mm have been deemed clinically acceptable[96] and the gaps of 1mm or less have been observed to be filled without intervention.[94] A high mallet mass, coupled with a low strike velocity minimizes strain deterioration whilst achieving <1mm polar gap.

This study also demonstrated that high velocity mallet strikes achieve good fixation, but only if they use the correct number of strikes are used. However it has previously been shown that it is difficult for surgeons to accurately pinpoint when an implant is most effectively seated (i.e. the inflection points in Figure 5.2.1).[93] Therefore if high velocity strikes are used to seat cups in low density bone, extreme care should be taken to avoid an excessive number of strikes. Chapter 4 demonstrates that at these higher impaction energies, gains in fixation are more incremental and fracture risk is increased.

In addition it was demonstrated that a loss of fixation coincides with the point at which a cup stops progressing. If a cup is no longer progressing during impaction, even if a polar gap is still present, it should receive no additional strikes. This advice is at odds with previous literature, which states that several 'post-seating strikes' may be beneficial to maximize press-fit stability.[93]

It is proposed that two previously reported phenomena contribute to the loss of fixation measured when using too many high velocity strikes. The first is damage to the bone during each strike.[114] As the cup is seated the bone surface layer is overly compacted/abraded by the cup surface. Therefore the effective interference fit between cup and bone is reduced. In addition a 'bounce-back' of an acetabular cup out of the bone cavity has been identified in previous studies that employ dynamic testing techniques.[104] Mid-strike, elastic energy is stored in the acetabular cavity and surrounding soft tissues. As the force of the hammer strike is released the cup is subject to an 'extraction' force and can displace out of the bone cavity.

Using free body diagrams based upon those in Section 2.3.1.5 it is possible to identify the forces that may lead to the 'bounce-back' observed. As the cup progresses into the cavity the area of contact increases and the y-component of reaction force dominates over friction at due to high θ angle (Figure 5.4.1). The forces resisting the insertion of the cup grow and elastic strain energy may be stored in the surrounding bone.

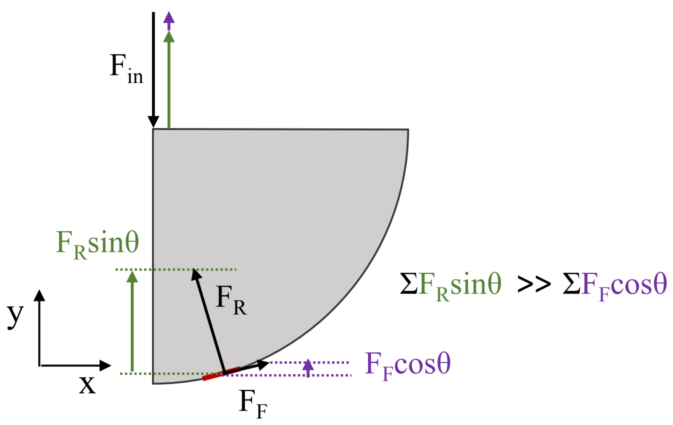

Figure 5.4.1: FBD during cup insertion when the cup is nearing the base of the bone cavity. Due to large θ angle, the y-component of reaction force is much larger than the y-component of frictional resistance

Upon release of the insertion load the energy stored in the bone will be released, pushing the cup in the positive y-direction. As the y-component of friction in this position is very small, it may not be able to resist the reaction force until θ is large enough to allow sufficient frictional resistance. The movement of the cup from loaded to unloaded position may be enough to cause the abrasion noted at the cup rim, and reduce the effective interference between cup and bone, reducing fixation.

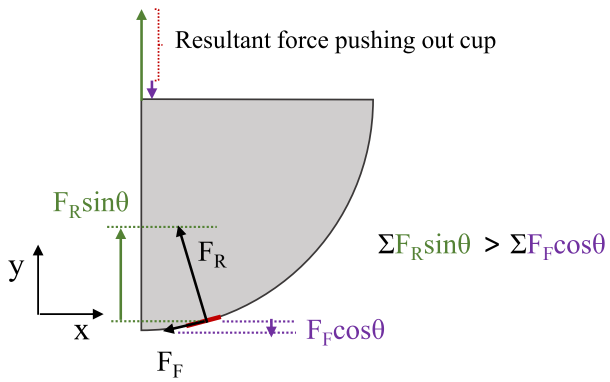

Figure 5.4.2: FBD during cup insertion when the cup is nearing the base of the bone cavity. When the insertion load is released, leading to a possible 'spring-back' on removal of insertion load.

Hothi et. al. observed this phenomenon during higher velocity strikes, but only in dynamic models.[90] It has been previously shown that the acetabulum undergoes significant acceleration during impact,[223] which could produce an extraction force when experienced by introducer/cup couplings with appreciable mass. Such mechanisms of elastic strain and acetabulum acceleration are known to occur in the *in-vivo* environment, and therefore the mechanism of strain and fixation deterioration demonstrated in this study warrants further investigation.

5.4.2 Limitations

5.4.2.1 Common limitations

Please refer to Chapter 4 for details of the following limitations of aspects of the setup of this study:

- *In-vitro drop rig*

- *Custom acetabular cups*
- *Synthetic bone model.*
- *Load, strain and displacement acquisition*
- *Pushout fixation testing*

5.4.2.2 Study limitations

It is important to consider that the key finding of this study – that implant fixation suffers deterioration if excessive impact strikes are used – is observed in an *in-vitro* model rather than the surgical scenario. The mechanism of this finding is likely due to the elastic nature of bone and the compliance of the hip during impact – two properties represented and validated for our model.[223] However as the mechanisms of deterioration are not fully understood or investigated here it would be pertinent to conduct further testing to both understand the exact nature of the phenomenon, and to test for it in cadaveric tissue.

Another limitation of this study is the use of a 0.1 mm threshold to categorize the implant at 'optimally seated'. Peak post-strike strain in either the bone or cup may be considered a better metric of seating as this is more likely to correspond with peak fixation which is arguably more important than polar gap. A displacement metric was chosen as it is difficult or impossible for a surgeon to infer bone or cup strain during surgery, with most using visual cues from the acetabular rim, or holes in the cup. 0.1 mm as a value could also be modified, and this may change number of strikes considered 'optimum', and the pushout may be different at the new strike value. However by examining strain data it is clear to see that under or over-impaction presents a risk in any of these cases, and the difficulty of a surgeon ascertaining the optimum seating point further compounds this risk.

5.4.3 Conclusions and clinical relevance

Inadequate fixation in revision THA or primary cases with poor bone stock remains challenging for orthopaedic surgeons, with second revisions often required if adequate stability is not achieved. The *in-vitro* model presented has indicated that surgeons should take great care if high velocity strikes are used (even with a low mallet mass) to seat cups in low density bone, in order to ensure stability isn't compromised with excessive strikes. If the cup no longer appears to be progressing it should not receive any additional strikes. The use of low strike velocity (1.5m/s) and high mallet mass (1.8kg) may mitigate a risk of loss of fixation when impacting cups into low density bone, while ensuring the implant is seated well enough to promote effective bone ingrowth. In order to aid understanding of a 'low velocity' strike, a supplementary video has been included.[235]

The strain deterioration mechanism discussed in this study requires further investigation as, if also present in the surgical scenario, it could significantly contribute to implant instability or loosening.

5.5 Chapter summary

- A mechanism of 'strain deterioration' was identified when too many impaction strikes were used
- Strain deterioration correlated with a deterioration of pushout fixation. Over-impaction leads to a loss of fixation
- Strain deterioration occurred most severely when using high-velocity impaction strikes. A combination of high mallet mass, but low strike velocity, minimized the effects of strain deterioration while ensuring a good level of seating and clinically acceptable polar gap.
- Supporting the conclusions of Chapter 4: High energy strikes should be avoided due to the possibility of un-detected strain deterioration and subsequent poor fixation

5.6 Acknowledgements

I thank Richard van Arkel and Shaaz Ghouse for designing and manufacturing the custom acetabular cups in this chapter.

I would also like to the Mechanical Engineering research workshop staff for CNC milling the synthetic bone models.

Chapter 6: An assessment of oscillatory seating

6.1 Introduction

Chapters 3 - 5 utilize an *in-vitro* model to evaluate the 'traditional' method of seating cementless implants; using a mallet with kinetic energy transferred to an implant introducer in a very short space of time – generating the large forces required to gain press-fit fixation. Traditional impaction is used in the vast majority of cementless procedures worldwide, and generally has favorable outcomes. For this reason the usage of a surgical mallet has not changed since the development of cementless implants in the 1960s.

More recently an alternative to traditional impaction has emerged. Oscillating power tools are being developed which aim to use a larger number of short impact pulses to perform the tasks usually performed by a mallet (including femoral rasping and femoral/acetabular component seating). This is achieved using an oscillating end effector.

Two such devices are currently available to orthopaedic surgeons. The first, the 'Woodpecker', is a pneumatic device is sold by IMT.[204] The Woodpecker uses an end effector oscillating at 70 Hz to drive a rasp into the femoral canal. More recently the 'Kincise' system was released by Depuy Synthes.[201] Similar to the Woodpecker, the Kincise uses an oscillating end-effector, although driven electrically. Fewer technical details for the Kincise are available.

Both suppliers claim significant advantages of their devices over traditional impaction methods. IMT documentation claims many benefits of the tool when rasping the femoral canal. These include no more than 1N of axial force on the femoral bone,[204] reduced operating time, accurate shaping of femoral canal and reduced chance of femoral fracture.[236] Depuy also claim advantages of their devices in promotional material. They suggest that more accurate femoral cavity rasping, reduced bone stress,[199] more consistent energy delivery[200,201] and reduced surgeon fatigue[202] are achievable with the Kincise versus traditional impaction.

The aim of this study is to assess the ability of oscillatory impaction devices to seat cementless acetabular cups. The same model developed and presented in Chapters 5 & 6 is used to test a device that mimics the Woodpecker and Kincise systems. These tests are then compared to the data obtained for traditional impaction strikes.

The research questions posed in this study are:

(1) How does an oscillatory device compare to traditional impaction techniques for:

- Risk of fracture, quantified by measuring dynamic bone strains?
- Strain deterioration, quantified by loss of post-strike strain?
- Cup deformation, quantified by measuring cup strains?
- Cup fixation, quantified by pushout tests?
- Cup seating, quantified by measuring polar gap?

(2) Are there indications that oscillatory seating is superior to traditional impaction and suitable for widespread adoption?

(3) Is more research required to further understand these devices and prove superiority over traditional methods?

6.2 Materials and methods

6.2.1 Common experimental setup

Please refer to Chapter 4 for details of the following aspects of the setup of this study:

- *In-vitro drop rig*
- *Custom acetabular cups*
- *Synthetic bone model.*
- *Strain and displacement acquisition*
- *Pushout fixation testing*

6.2.2 Study experimental setup

The impact drop weight from Chapters 4 & 5 (used to simulate the 'strike' of a surgical mallet) was replaced with an oscillating impaction device. Oscillations of the end effector of the device were driven pneumatically using compressed air at 6 bar. A slide valve produced movement of the end effector. The device used had a stroke length of ± 5 mm and oscillation frequency of 70 Hz. The acetabular cups were rigidly fixed to the end effector via clamp mechanism.

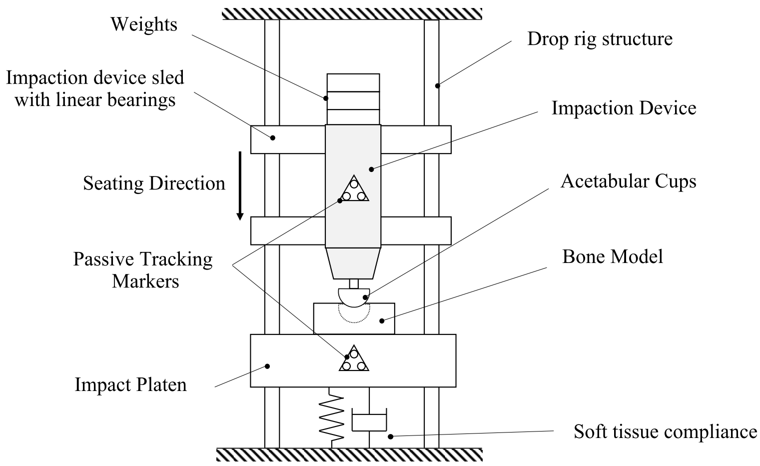

Figure 6.2.1: Experimental setup. An oscillating impaction device is mounted to the impaction rig. The impact platen is replaced with a sled supporting a pneumatic impaction device.

Table 6.2.1: Impaction parameters for oscillatory and traditional seating methods

Impaction Method		Impaction Level		
		Low	**Medium**	**High**
Oscillatory	**Axial Force (N)**	40	60	80
Traditional	**Impact Mass (kg)**	0.6	1.2	1.8
	Impct Velocity (m/s)	1.5	2.75	4
	Impact Energy (J)	0.68	4.55	14.4

A custom machined sled was used to hold the impaction device so the axis of impactor motion was held in line with the vertical rails of the drop tower (Figure 6.2.1). Linear bearings were used to allow movement of the device during seating. To simulate the pressure that a surgeon would exert on the device (in the direction of seating) different masses were added to the sled. 3 different masses were added to the sled and device to simulate a surgeon's applied force of 40 N, 60 N & 80N, forces estimated by a surgeon during preliminary testing (Table 6.2.1).

The oscillation period of the impaction device was controlled by means of an electronic solenoid, fed current in pre-defined pulses by a microcontroller (Arduino Uno, Boston, USA). In order to provide sufficient current to overcome the pressure of the compressed air in a suitably short rise time a mosfet amplifying circuit was designed (Figure 6.2.2).

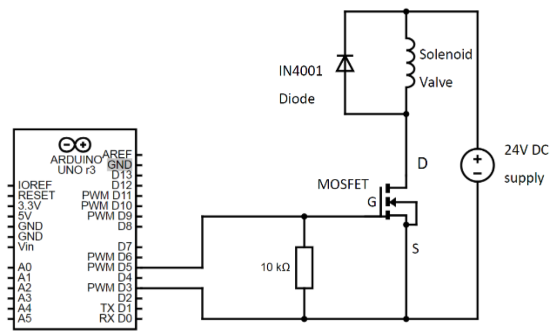

Figure 6.2.2: Circuit diagram used to amplify signal current to power solenoid valve

While some elements of the acquisition system remained the same as previous chapters, an additional microcontroller was used to send a trigger pulse to the DAQ system to trigger recording at the same time as air was delivered to the impaction device via solenoid valve (Figure 6.2.3).

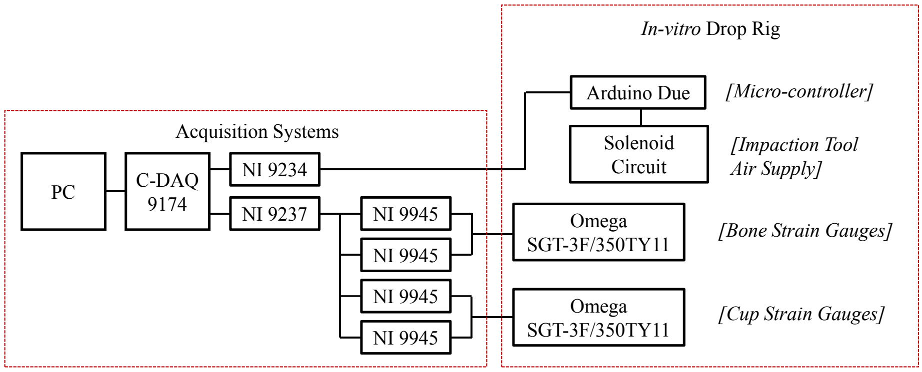

Figure 6.2.3: Acquisition setup.

6.2.2.1 Experimental procedure

54 mm diameter cups (N = 5) were impacted in high density (30 PCF) synthetic bones using 8 x 0.5 second pulses of oscillation, resulting in a total seating time of 4 seconds. Displacement data was recorded following each pulse. This was repeated for each of the 3 axial force conditions (40 N, 60 N, 80 N). Following implantation displacement data were analyzed to determine when each cup could be considered seated. Preliminary analysis showed a clear trend of the majority of seating occurring within the first 0.5 s (Figure 6.2.4). Therefore for all 3 of the axial force conditions, implants were considered optimally seated after 0.5 s. Subsequently, for each of the axial force conditions, cups (N = 5) were impacted into virgin synthetic bones using a 0.5 s pulse and pushout tests conducted.

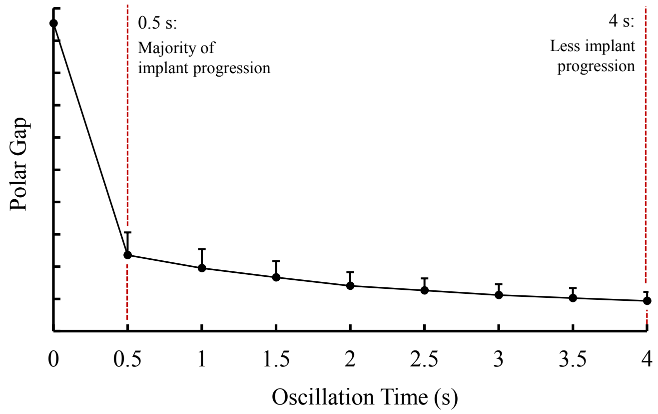

Figure 6.2.4: Typical displacement pattern during oscillating seating. The majority of displacement occurs in the first 0.5 s of oscillation, with less progression between 0.5 s and 4 s.

In total 30 tests were conducted: 15 to establish the optimum number of strikes for each testing condition, and then 15 to test pushout fixation following impaction with 0.5 s of oscillation. Virgin synthetic bone samples were used for each of the 30 tests.

6.2.2.2 Data analysis

In order to compare oscillatory data with traditional impaction data 3 energy levels from the data discussed in Chapters 4 & 5 were chosen. To represent the spread of results that are seen for traditional methods the lowest, highest and a middle energy were chosen (0.68 J, 4.55 J and 14.4 J respectively, Table 6.2.1)

Risk of fracture was quantified by correlating the dependent variables of peak bones strain with the independent variable of impaction level. Strain deterioration was quantified in the same manner as in Chapter 5, Section 5.2.2.2. Cup deformation was quantified by correlating the dependent variable of post-strike cup strain with independent variable of impaction level. The strength of fixation was quantified by correlating the dependent variables of pushout fixation with the independent variable of impaction level. Cup seating was analyzed by correlating the final polar gap with the independent variable of energy per strike.

Each set of strain, pushout and seating values were examined against oscillation time. In addition the maximum (or minimum in the case of compressive) strains that occur during 0.5 s and 4 s are assessed. This is to determine the risk of fracture at for the entire period. For example, if the highest peak strains occur in the first 0.5 s, the risk of fracture using 4 seconds of oscillation will be the same as the risk for 0.5 s.

6.2.2.3 Statistical analysis

In order to determine if there are differences between the impaction outcomes of oscillatory and traditional methods paired T-tests were used, conducted in SPSS (v24, IBM, NY).

6.3 Results

6.3.1 Bone and cup Strain

6.3.1.1 Strain behaviour

For each oscillation of the impaction device peaks were observed in strain traces for both bone and cup (Figure 6.3.1a, Figure 6.3.1b). During the initial phase of seating these peaks increased in magnitude; after around 200 ms the magnitude of these peaks stabilized. Closer inspection of strain behavior for one oscillation presented a very similar pattern to a single traditional impaction strike. Bone strain was characterized by an initial compressive peak, followed by a tensile peak, then a post-strike tensile strain (Figure 6.3.1c). Cup strain was characterized by a large compressive peak, followed by a post-strike compressive strain (Figure 6.3.1d).

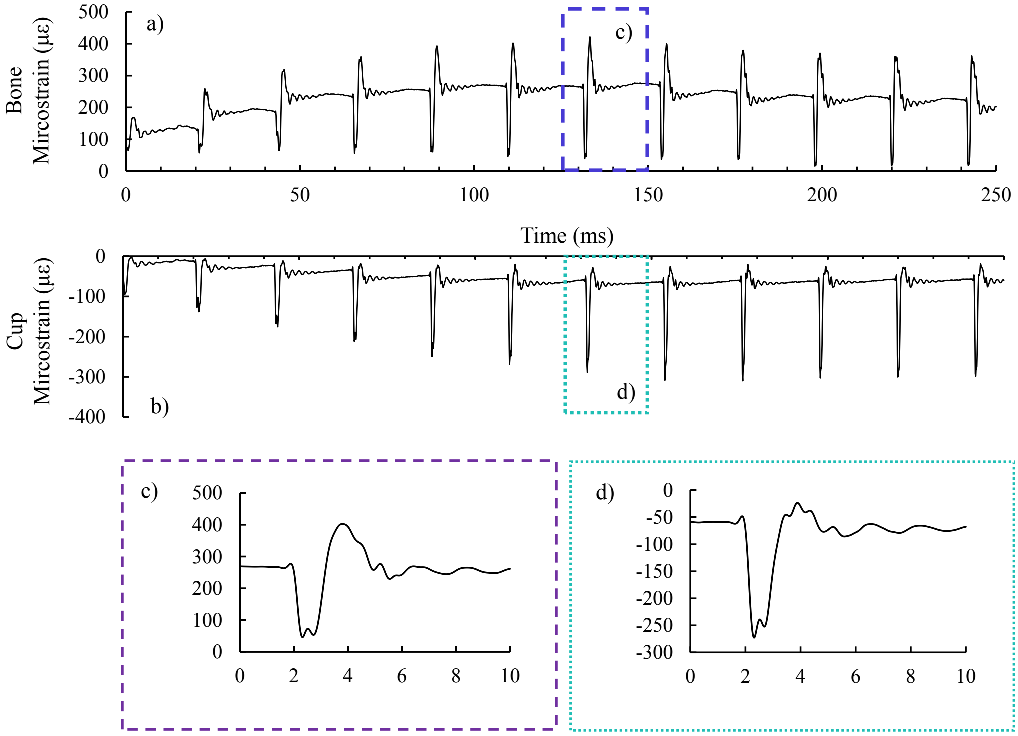

Figure 6.3.1: Example dynamic strain behavior of bone and cup during oscillatory seating: a) Bone microstrain over 250 ms b) cup microstrain over 250 ms c) bone microstrain over one oscillation d) cup microstrain over one oscillation. The behavior of both bone and cup strains both closely mimic that of traditional impaction over one oscillation. The same peak and post-strike characteristics can be identified

6.3.1.2 Fracture risk: Peak strains

Peak tensile bone strain exhibited two distinct behaviours over the 4 second oscillation period (Figure 6.3.2a). For the low axial force condition peak strains remained largely the same throughout. For the medium and high axial force conditions the highest peak tensile strain was recorded in the first 0.5 s of oscillation – subsequently decreasing at each 0.5s interval. No difference between peak values at any time interval was detected between medium and high axial force conditions during the first 2 seconds of oscillation ($p > 0.12$), however both were higher than low axial force (difference 253 με, $p < 0.005$).

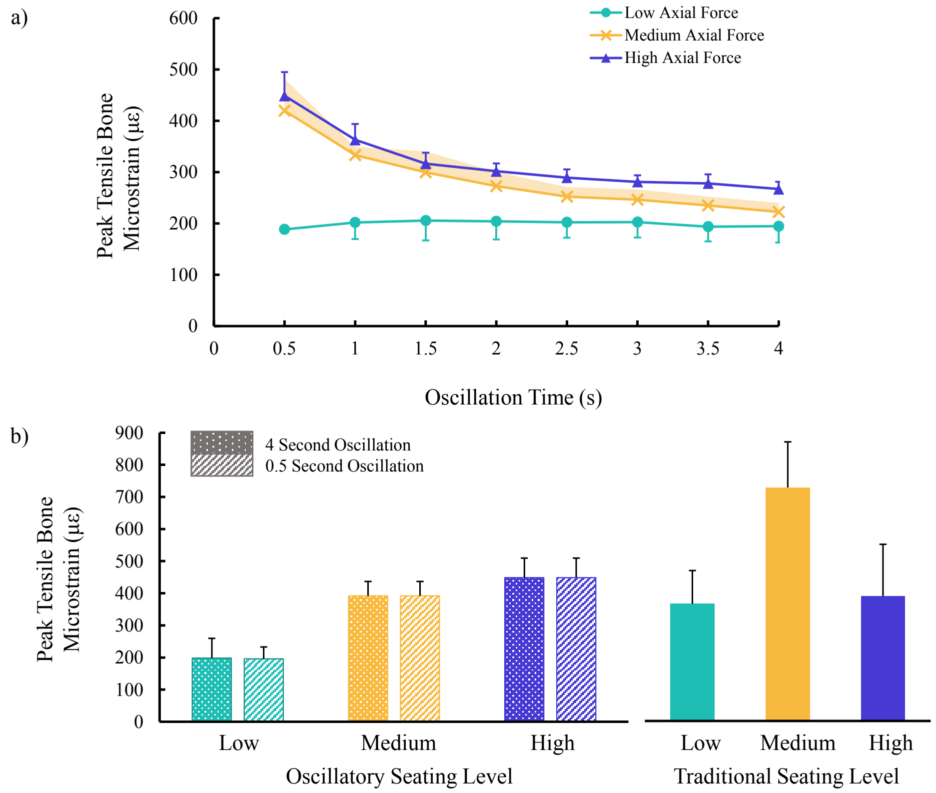

Figure 6.3.2: Peak Tensile Bone Strain (mean with standard deviation): a) vs oscillation time. A decrease in peak strain with time is observed for medium and high axial force; b) Comparison to traditional impaction values. An increase of strain is observed with increasing axial force

Due to peak strain occurring within the first 0.5 s for both medium and high axial force the peak tensile strain experienced during 0.5 s and 4 s were the same (Figure 6.3.2b). When comparing peak strains between oscillatory and traditional impaction types, values were very similar apart from medium traditional impaction, where peak strains were higher (334 με, p < 0.005,).

Peak compressive bone strains were found to increase at each 0.5 s time interval, with the highest strains being recorded for the 4 s interval for all axial force conditions (Figure 6.3.3a). Peak compressive strains increased with axial force, with high axial force providing the highest strains at both 0.5 s and 4 s oscillation time (-115 ± 41 με , -244 ± 51 με).

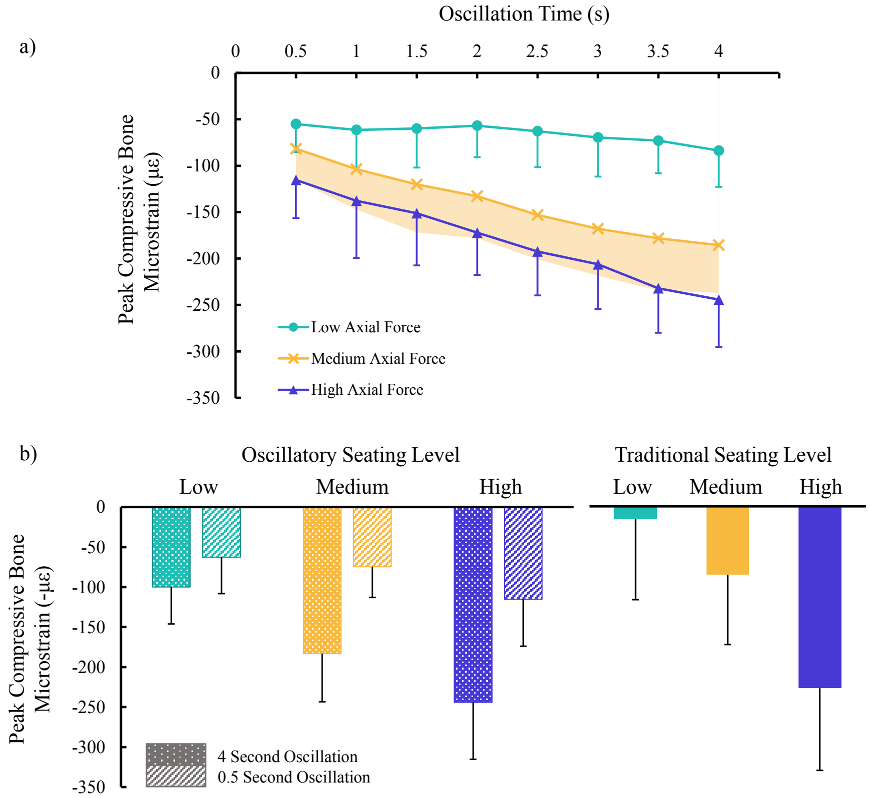

Figure 6.3.3: Peak Compressive Bone Strain (mean with standard deviation): a) vs oscillation time. Compressive strains increased in magnitude at each time interval; b) Comparison to traditional impaction values. Compressive strains increased in magnitude through low, medium and high seating conditions in both traditional and oscillatory seating

Similar peak compressive strain levels were obtained for both oscillatory and traditional seating methods when a 0.5 s pulse was considered. However peak oscillatory strains were higher than traditional if a 4 s time interval was considered

(Figure 6.3.3b). An exception was high axial force conditions, where no difference was detected (p = 0.727).

6.3.1.3 Fixation: Strain deterioration

An increase in post-strike tensile bone strain with oscillation time was only observed for the low axial force condition (Figure 6.3.4). At 0.5 s oscillation time no difference in post-strike tensile strain was detected between medium and high axial force conditions (p = 0.94), but strain was considerably lower for the low axial condition group (p < 0.005, 78.1 με). At 4 s, no difference could be found between any of the three groups (p = 0.096). Post-strike tensile strains were higher for traditional seating in all cases (implying more secure fixation).

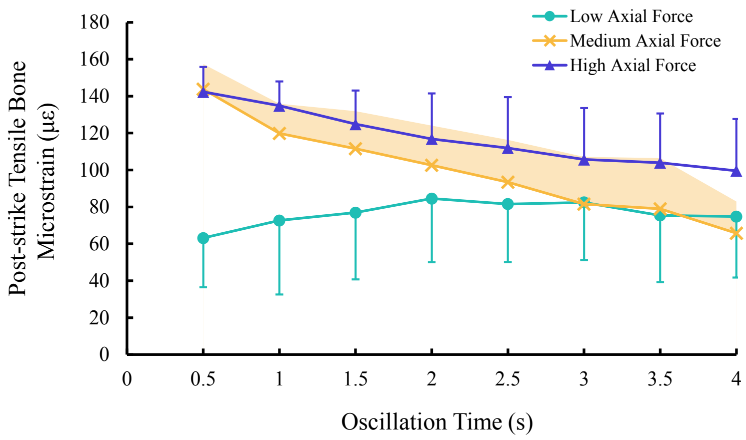

Figure 6.3.4: Post-strike Tensile Bone Strain (mean with standard deviation): a) vs oscillation time. An increase in strain is observed in the low axial force group, but not medium or high; b) Comparison to traditional impaction values. Oscillatory seating produces lower strains in all three groups

It is difficult to compare post-strike strain deterioration as different over-striking metrics (oscillation time versus number of strikes) and different impaction levels (axial force vs energy) are used in each. However if one strike is considered roughly one second of oscillation, strain deterioration in oscillatory seating is larger for low and medium impaction conditions, but smaller for high impaction conditions (Table 6.3.1).

Table 6.3.1: Strain deterioration comparison between oscillatory and traditional methods

Impaction Method		Strain Deterioration		
		Low	Medium	High
Oscillatory (µε/s)	Avg	8.5	19	11
	Std	13	3.9	2.5
Traditional (µε/strike)	Avg	2.0	16	16
	Std	0.5	1.8	1.4

6.3.1.4 Cup deformation: Post-strike strains

Post-strike compressive cup strain increased with oscillation time for the low axial force condition only, with medium and high force conditions remaining the same over 4 s Greater cup deformations were observed for medium and high traditional seating than any oscillatory condition (Figure 6.3.5), again implying more secure fixation is achieved by higher energy traditional seating. The largest cup deformation for traditional seating was 105 µε greater in magnitude than oscillatory seating.

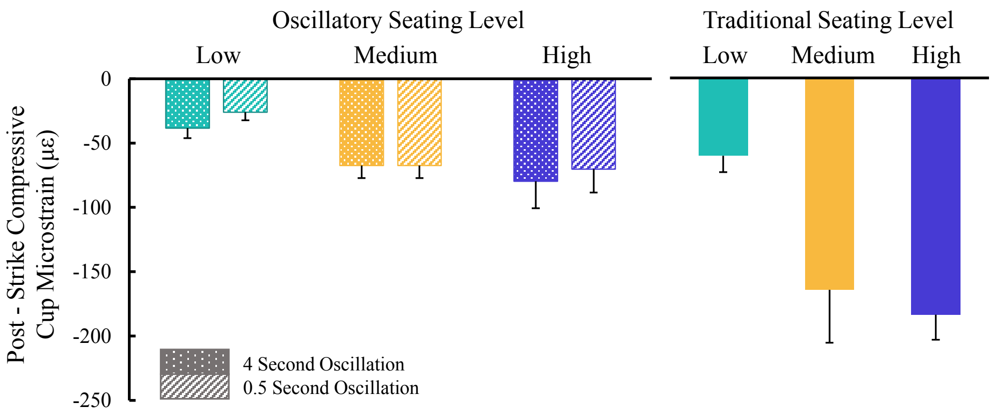

Figure 6.3.5: Post-strike compressive cup strain (mean with standard deviation) achieved with oscillatory and traditional impaction. Greater deformation was observed for medium and high traditional seating energies

6.3.2 Fixation: pushout

In all axial force groups, the fixation achieved after 0.5 s was larger than the fixation achieved after 4 s (an average 1.6x increase). An increase in fixation was also obtained with an increase in axial force in both groups (Figure 6.3.6). However, even the best fixation achieved (507 N, high axial force, 0.5 s) was 475 N less than for traditional impaction with a medium energy, and 720 N less than for traditional high energy impaction.

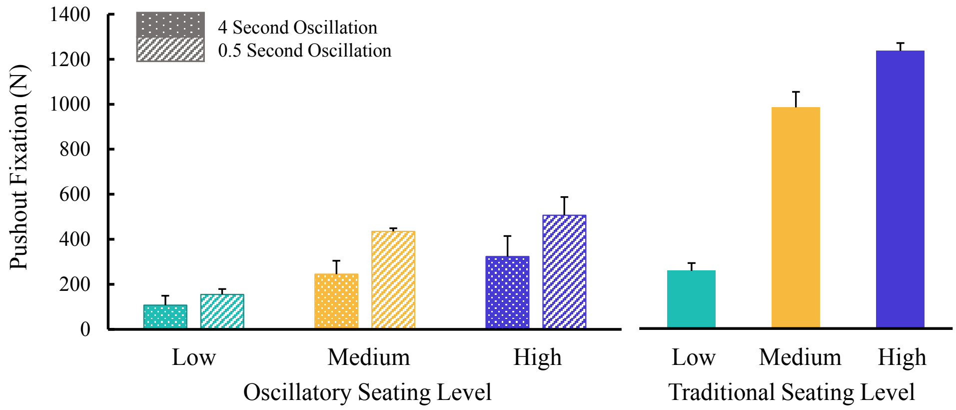

Figure 6.3.6: Pushout values (mean with standard deviation) compared to traditional impaction values. Far higher fixation is observed for the traditional seating methods

6.3.3 Seating: Polar gap

Final polar gaps of > 2 mm remained with both the low oscillatory seating (after 0.5 s) and the low energy traditional seating method. Polar gaps of < 1 mm were not achieved in any of the 0.5 s oscillatory groups. Smaller polar gaps were achieved with 4 s pulses in all cases.

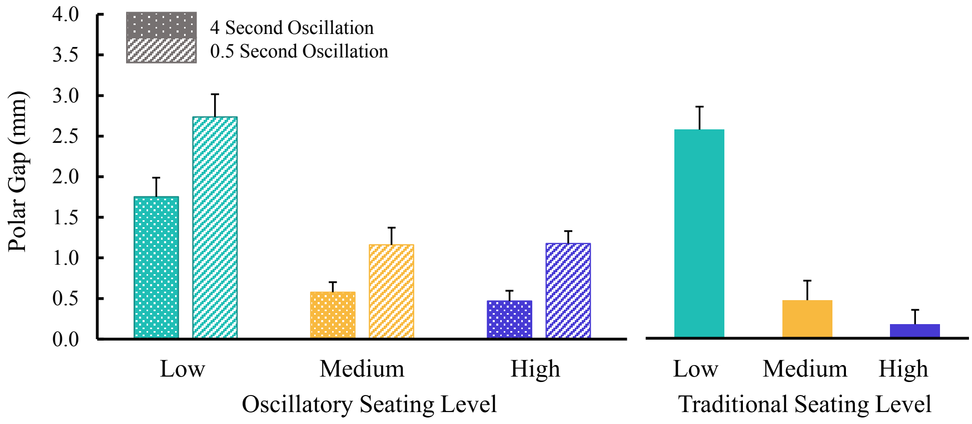

Figure 6.3.7: Polar gap (mean with standard deviation) for oscillatory seating compared to traditional impaction values

6.4 Discussion

6.4.1 Key findings

A key finding of this study is the similarity of the strain behavior in bone when using oscillatory seating versus traditional seating methods. When bone and cup strain is measured for one oscillation the same tensile and compressive peaks are observed. Therefore these characteristics can be directly compared to the strains during a single, traditional, impaction strike.

As with traditional impaction, it would be desirable if oscillatory impaction produces lower peak strains (in order to minimize fracture risk) but attains good fixation and seating levels. Both peak tensile and peak compressive bone strains were of a similar magnitude to those measured during traditional impaction. This would imply that fracture risk is largely the same between the two. However levels of fixation were poorer when oscillatory impaction was used, with twice the fixation attained using traditional strikes. The minimum polar gap achieved was also larger for oscillatory seating.

It is not clear why the performance of the oscillatory seating was inferior. It is possible that the peak forces generated by the tool are not sufficient to overcome the frictional forces are the walls of the cup. A more powerful oscillation may be required. A longer oscillatory period may also improve performance and reduce the polar gap measured. However another important finding of this study is an overall is decrease in pushout when a longer oscillation time is used. This decrease again correlated with a loss of both bone and cup post-strike strains. It is possible that a similar mechanism of fixation deterioration is occurring in oscillatory impaction as was identified in Chapter 5 for traditional impaction. As the impaction device oscillates shear forces are applied to the edge of the acetabular cavity by the acetabular cup, abrading the bone. This abrasion leads to a reduction in interference and therefore fixation. Another concern with oscillatory seating is the linear increase in peak compressive bone strain with time, suggesting extended periods of seating may also increase fracture risk (a trait shared with traditional seating). Cup deformations (an undesirable consequence of press-fit fixation) were less for oscillatory than traditional seating. However as demonstrated in Chapter 4, this only indicates poorer fixation.

Currently no peer-reviewed articles are available that measure the ability of the Kincsie to deliver the key desirable impaction outcomes discussed in Chapters 1, 4 & 5 of this thesis (minimized chance of fracture, maximized fixation and stability, reduced polar gap). Some literature exists analyzing the effectiveness of the Woodpecker. It has been suggested that the woodpecker may reduce fracture risk for femoral broaching[207] and during bone graft compaction.[205] The findings of this study do not indicate a reduction in fracture risk for the acetabulum. However the findings of Goossens et. al. also indicate poorer seating of a femoral implant when using the Woodpecker versus hammer blows.[237] Similar to this study they find post-strike bone strains to be around a factor of two lower in oscillatory seating than traditional.

It was found from analysis of the compliance model in Chapter 3 that the natural frequency of the acetabulum and femur is around 3 Hz. The impaction tool used in this study oscillated at 70 Hz, more than an order of magnitude higher. Therefore force transmission from bone to soft tissue should be low as the system is not at resonance. However it is important to note that force transmission to soft tissues may be reduced by increasing the frequency of impaction further from resonance, increasing the efficiency of seating. Such changes in setup should be examined in future works.

6.4.2 Limitations

6.4.2.1 Common limitations

Please refer to Chapter 4 for details of the following limitations of aspects of the setup of this study:

- *In-vitro drop rig*
- *Custom acetabular cups*
- *Synthetic bone model.*
- *Strain and displacement acquisition*

- *Pushout fixation testing*

6.4.2.2 Study limitations

Firstly our impaction device only had one setting (one set oscillatory speed, end effector travel and pneumatic air pressure). Clearly these parameters could also be varied and could have a large effect on the parameters reported. The parameters were chosen to best represent the current devices available to orthopaedic surgeons and so support the study's conclusions concerning current clinical practice. Further work is required in order to understand the effects of changing these parameters.

Secondly this study only presents data for a 4 second oscillation period. It is possible that more time would be used to seat implants intraoperatively. 4 seconds was chosen based upon preliminary data which suggested that a continuing trend of loss of bone strains, as well as fixation, occurs. Beyond 4 seconds fixation strength was reduced to such a point that the cup would have too little stability to be considered clinically. Additionally a range of axial forces (40 – 80 N) was investigated and lower, or higher forces ($<$ 40 N, 100 N +) were not reported. Forces $<$ 40 N were not reported as this was the weight of the impaction device and so was the force applied by gravity itself. Forces of 100 N or more were not considered as preliminary testing in a mock surgical environment (where the impaction tool was used free hand) showed that the user unlikely exceeded 80 N due to fear of fracture.

Finally only data for higher density (30 PCF) bone was recorded. Further work is required to understand the efficacy of oscillatory impaction devices in poorer quality bone.

6.4.3 Conclusion and clinical relevance

The aim of this study was to compare novel, oscillatory, impaction devices and traditional methods, and to understand whether the current evidence for the suitability of these devices to seating acetabular cups is sufficient. It is clear from the data presented that our impaction device model struggled to attain the same levels of implant fixation, or implant seating, as traditional methods. Despite the best fixation achieved using oscillatory impaction being less than half than that resulting from mallet impaction, peak tensile and compressive bone strains were of a very similar magnitude. This implies the same level of fracture risk but with far less fixation. Polar gaps for the most effective fixation (using a 0.5 s oscillation time) were 6x larger than those achieved with traditional impaction.

Although each impaction device is likely to vary from the model tested, our results do present some cause for concern. There is some published evidence that oscillatory impaction devices are beneficial for rasping or impaction grafting within the femoral canal.[205,207] However only one study presents evidence for such devices seating femoral implants, and draw conclusions largely similar to those presented here.[209] Further work and discussion is required before such devices are declared superior to traditional methods.

Clinically this work informs surgical practitioners and other healthcare professionals of the performance of oscillatory impaction devices for seating acetabular cups. Such end users may decide that further research is required before widespread adoption occurs.

6.5 Chapter summary

- Similar behavior of dynamic strains during implant seating are observed for oscillatory seating as traditional seating. Peak tensile bone strain, peak compressive bone strain, post-strike tensile bone strain and post-strike compressive bone strain are observed

- Peak tensile and compressive bone strains, and therefore fracture risk, are similar for oscillatory and traditional impaction methods. Peak compressive bone strains increase with time

- Strain deterioration, although difficult to compare to traditional impaction methods, appears to be similar for oscillatory methods

- Peak pushout fixation achieved through oscillatory impaction is much poorer than for traditional methods

- Polar gaps are also larger for oscillatory methods than traditional

- Further study is required to determine the advantages of new oscillatory technologies over traditional impaction

6.6 Acknowledgements

I thank Wei Ong for his able assistance during this study. Wei was responsible for manufacturing the impaction device sled and solenoid circuit. Wei also conducted a portion of the testing and assisted with data analysis.

I also thank Desoutter Medical for providing the impaction device.

Chapter 7: Conclusions and future works

7.1 Key findings

Despite the daily dependence of thousands of surgeons worldwide upon impaction techniques, previous research is less thorough than might be expected. The most important findings of this thesis are an improved understanding of how impaction technique affects key elements of the press-fit technique: risk of fracture, cup deformation, implant fixation and implant/bone apposition.

7.1.1 An *in-vitro* model of impaction in hip arthroplasty

In order to test impaction variables, a representative model of orthopedic impaction was required in the lab. Cadaveric samples provide a representative method of testing but are hindered by large inter-sample variation. Full torso cadaveric THA was used to measure impaction forces used to seat femoral stems and acetabular cups (6.31 kN – 21.6 kN and 8.24 – 30.2 kN respectively). These values are largely in-line with previous literature.[158,185,215] Importantly, an acceleration of the femoral or pelvic bone during impact was measured. Such compliance during impaction, provided by surrounding soft tissues, has been shown to affect the force experienced by bones,[177] the number of strikes required to seat implants and risk of bone fracture.[72,178] Therefore a computational model was used to estimate soft-tissue compliance which was subsequently replicated *in-vitro*. It was found that the *in-vivo* scenario could be replicated with a simple laboratory rig in a highly representative and repeatable manner.

7.1.2 Traditional impaction technique

Chapters 4 & 5 both examine the effect of impaction technique, and arrive at similar conclusions: high energy impaction strikes are difficult to justify. Chapter 4 examines the effect of impaction energy (assuming the ideal number of strikes are used) and finds that the beneficial factors of press-fit (implant fixation, bone apposition) are achieved with a mid-energy strike, with only very marginal gains being made by using a strike of twice the energy. Yet the negative associations of press-fit (component deformation, fracture risk) still increase linearly with impaction energy. Chapter 5 examines the effect of using the incorrect number of strikes. The most important finding of this study is a deterioration of strain in bone and implant if the cup is impacted past the point where it is optimally seated. This strain deterioration is particularly severe in low density bone, exactly the situation when instability and loosening is most likely to occur. High strike velocity and mallet mass (and therefore higher energy) exacerbate the problem. A combination of low strike velocity and high mallet mass provided the best fixation and bone apposition while minimizing strain deterioration.

7.1.3 Novel impaction techniques

Oscillatory impaction tools are now available to surgeons as an alternative method of seating cementless implants. Little published work exists to compare these technologies to traditional methods. Chapter 6 describes a model of these new technologies versus traditional methods. Importantly, the strain behavior of bone and cup appear to be very similar and can be compared to traditional methods. Overall the oscillatory device produced a similar fracture risk to traditional methods but resulted in poorer fixation and a larger polar gap. Modification of the impaction parameters, such as oscillation speed, stroke or power, may improve seating (although they may also increase fracture risk). In addition strain deterioration was also apparent in bone during testing, with an extended period of oscillation causing a reduction in implant fixation. It is difficult to conclusively state that these devices are superior to traditional methods and further testing and optimization is certainly required.

7.2 Clinical and engineering relevance

Orthopaedic research often requires both medical and engineering input. This thesis covers topics that may be of interest to both surgeons and engineers, reflected in the journals in which its studies are published or submitted.

From an engineering perspective the model presented in Chapter 1 is of use when conducting investigations into the effects of impaction technique (such as in Chapters 4 & 5) or for pre-clinical testing. New implants may now be tested in a more representative manner without the need to account for the variability that are inherent in cadaveric models. In addition the Voigt model values given are of use to researchers who may want to model impaction *in-silico* and ensure boundary conditions are representative. Furthermore the impaction dataset presented in Chapters 4 & 5 and in Appendix 9.7 can be used to derive additional impaction parameter relationships (that may not have already been presented) or validate the results of computational models. It is also demonstrated that researchers should consider the effects of dynamic strain when examining impaction.

From a surgeons perspective Chapters 4 & 5 clearly indicate the importance of impaction technique, particularly when using high impaction energies. While further work is required to better understand the effects of over-impaction Chapter 5 demonstrates a loosening mechanism that may be present in surgery. Finally, Chapter 6 provides surgeons with an assessment of the effectiveness of oscillatory seating devices.

7.3 Research output and impact

The work presented in this thesis consists of a published research article, two articles under review and a further article in preparation. Further collaborative studies inspired by this research are also underway, in both industrial and academic settings. In addition this work has been presented at 7 conferences attended by an international audience. The work has been well received by both engineering and clinical audiences, a highlight of which is the work presented in Chapter 5 being awarded a Young Investigator's Award at the 31st Annual Congress of the International Society for Technology in Arthroplasty. Finally, translational aspects of this work has led to the filing of two UK patents which are currently being developed in partnership with industry.

7.3.1 Research output

Doyle R, Boughton O, Plant D, Desoutter G, Cobb JP, Jeffers JRT. An in vitro model of impaction during hip arthroplasty. J Biomech 2019;82:220–7. doi:10.1016/j.jbiomech.2018.10.030.

Doyle R, van Arkel RJ, Jeffers JRT. The effect of impaction energy on dynamic bone strains, fixation strength and seating of cementless acetabular cups. *In Press* J Orthop Res, 2019

Doyle R, van Arkel RJ, Jeffers JR. Impaction technique may influence fixation quality in low density bone. *Under review*, J Arthroplasty

Doyle R, Boughton O, Desoutter G, Plant D, Cobb J, Jeffers J. Pre-clinical Impaction Testing in Hip Arthoplasty May Not Represent the Clinical Scenario Presented at International Society for Technology in Arthroplasy, Boston 2016: Published in *Orthopaedic Proceedings, ISSN (online): 2049-4416, A supplement to The Bone & Joint Journal*, Volume 99-B, Issue SUPP_301 Feb 2017

Doyle R, Jeffers J. The Importance of Considering Dynamic Strain in Bone During Seating of Cementless Components. Presented at International Society for Technology in Arthroplasy, London: 2018. Published, *Orthopaedic Proceedings, ISSN (online): 2049-4416, A supplement to The Bone & Joint Journal*

Doyle R, Jeffers J. Minimizing bone strain while maximising fixation during impaction of the acetabular cup. Presented at International Society for Technology in Arthroplasy, London: 2018. Published, *Orthopaedic Proceedings, ISSN (online): 2049-4416, A supplement to The Bone & Joint Journal*

Doyle R, Jeffers J. Over-impaction of acetabular cups can reduce fixation strength. Presented at British Orthopaedic Research Society, Cardiff: 2019. In-press, *Orthopaedic Proceedings, ISSN (online): 2049-4416, A supplement to The Bone & Joint Journal*

Doyle R, Ong WW, Desoutter G, Jeffers J. Using the Woodpecker to seat acetbabular cups during hip arthroplasty. BioMedEng, London: 2018. *Published ISBN 978-1-9996465-0-9 (Print)*

Doyle R, Boughton O, Desoutter G, Plant D, Cobb J, Jeffers J. An *In-vitro* Model of Impaction in Hip Arthroplasty. Presented at Orthopaedic Research Society, New Orleans: 2018.

Doyle R, Boughton O, Plant D, Desoutter G, Cobb J, Jeffers J. The importance of compliance during pre-clinical testing. Eng. Knee, London: Institute of Mechanical Engineers; 2018.

Doyle R, Boughton O, Desoutter G, Plant D, Cobb J, Jeffers J. Measurement and Replication of Mechanical Boundary Conditions of the Acetabulum and Femur during Arthroplastic Impacton. Presented at the British Orthopaedic Resarch Society, London: 2017.

7.3.2 Patent filings

Doyle R, Bartolome L, Boughton O, Jeffers J. Tissue Differentiating Self-Stop Drill Bit, *P257824GB*, 2018.

Doyle R, Ghouse S, Jeffers J. Impactor Device, *P269114GB*, 2019.

7.3.3 Public outreach

Segment of BAFTA award winning BBC show 'Operation Ouch'

https://www.bbc.co.uk/cbbc/watch/operation-ouch-skull-shapes

7.4 Future work

In this thesis current clinical as well as novel impaction techniques were investigated using a newly developed *in-vitro* model. It is hoped that the work presented in this thesis will be of use to audiences including surgeons, engineers and researchers. However these works also present a number of clear research avenues that would improve the understanding of impaction in hip arthroplasty even further. This section details the main topics that should be investigated in future studies.

7.4.1 Cadaveric/*ex-vivo* testing

It is acknowledged throughout this thesis that a key limitation of the work presented is the use of a synthetic bone substitute rather than human tissues. While the reasons for the choice of synthetic materials have been clearly reported, and mitigated to some extent by the use of the rig described in Chapter 3, the most effective *in-vitro* replication of *in-vivo* conditions is the use of cadaveric tissues.

The variability of cadaveric tissue is too great to test multiple independent variables to high degrees of outcome confidence without using a huge number of samples. This is extremely resource heavy and difficult to approach within the constraints applied by the research environment. However each human cadaver has two hips which are closely matched, allowing dual factor experiments to be carried out in a resource effective manner.

Therefore further work could include cadaveric testing to prove the efficacy of one impaction technique over another (Chapters 4 & 5), or prove the advantages of emerging seating techniques versus traditional (Chapter 6). These tests should be conducted in order to support the conclusions of the studies presented in this thesis.

The final, and most representative, proving ground of these ideas is the *in-vivo* surgical environment. With the evidence attained by the pre-clinical testing described in this thesis, plus additional cadaveric testing, ethical approval for a randomized control trial (RCT) could be requested. This could be used to compare the outcomes of implants seated with the technique and impact energies recommended in Chapters

4 and 5, versus implants seated with a surgeon's standard technique. A similar study could be performed to assess novel oscillating seating technologies.

While these studies would represent a significant investment of time and resource such high quality assessment would be the most effective way of validating the conclusions of this thesis.

7.4.2 Strain deterioration mechanism and prevention

The strain deterioration mechanism described during this thesis is potentially important, and warrants further investigation. Firstly, cadaveric testing should be conducted to confirm the presence of the mechanism *in-vivo*. Currently the cause of the deterioration is not fully understood. By conducting a detailed analysis of the forces upon the introducer during seating it may be possible to reduce the deterioration through implant or introducer design.

7.4.3 Effect of impaction variables

7.4.3.1 Effect of poor impaction technique

Much of the testing described is based upon the assumptions of correct technique provided by the impaction rig. The effects of real world imperfections, such as using a poorly chosen interference fit, or off-axis impact strikes, should be investigated and quantified.

7.4.3.2 Effect of varying impaction technique during seating

The studies presented do not consider more than one energy during seating. Surgeons are likely to vary impaction during the seating of an implant, and therefore this must be explored.

7.4.3.3 Effect of introducer type upon seating mechanics

In most impact-based experimental work the stiffness of the colliding material, as well as the masses of the objects being accelerated, has a strong effect upon the resulting impact dynamics.[193] The process of hip impaction can be broadly split into 3 colliding objects: the surgical mallet, the introducer and the hip (acetabulum or femur).

Chapter 3 quantifies the mass and dynamic properties of the hip and provides instruction to greatly improve the representation of the dynamics of impaction in the surgical theatre.[238] Chapters 4 and 5 quantifies the effects of mallet mass and strike conditions upon the important parameters during arthroplasty (strain, implant fixation and polar gap). However the introducer used during all experiments in this thesis was the same, chosen to represent a 'standard' tool, as used in theatre.

Preliminary work, excluded from this thesis but published as conference proceedings,[239] reports the effect of introducer type upon peak impact force delivered to the patient. 'Straight' and 'bent' introducers are both commonly used in surgery (Figure 7.4.1). However each has a different mass and stiffness. It was found that the peak force delivered to the simulated patient with a straight introducer of lower mass and higher stiffness was 150% of the bent introducer value under the same conditions. Similarly, Krull et. al. report the importance of the introducer tip used to assemble modular implants.[37]

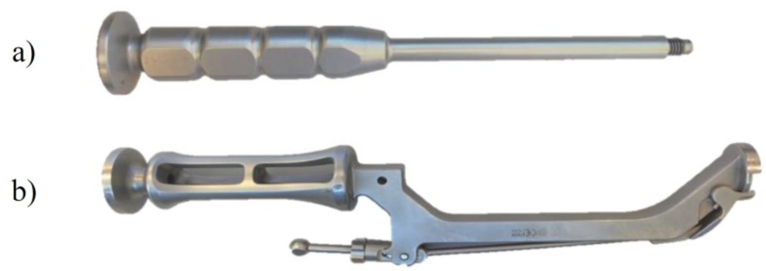

Figure 7.4.1: Two types of surgical introducer commonly used in surgery - a) Straight introducer of higher stiffness and lower mass; b) Bent introducer of lower stiffness and higher mass

Therefore an important avenue of future work would be to investigate the effect of introducer stiffness and weight upon key implant seating parameters. Another key variable to explore would be the effect of different strike surfaces. The testing presented during this thesis was based upon a titanium load cell strike surface and a stainless steel introducer. This has been reported and maintained the same through each study. However strike surface is a key variable in impact dynamics[161] and should also be quantified in relation to implant seating.

The same methods presented in this thesis could be used to conduct this work. Independent variables would be introducer mass, introducer stiffness and strike surface. These would be representative of the range currently seen in THA. Dependent variables would remain bone and implant strain, implant fixation, strikes to seat and polar gap.

7.4.3.4 Effect of implant surface finish

The effect of implant surface finish upon fixation in bone is discussed in Chapter 2. A number of studies report a significant effect of surface morphology upon implant fixation achieved.[83,92,115] A difference in fixation levels was reported even when comparing different commercially available surface treatments.[116] Two main surface finishes available on the majority of commercial implants are plasma sprayed titanium and sintered titanium beads (Figure 7.4.2).

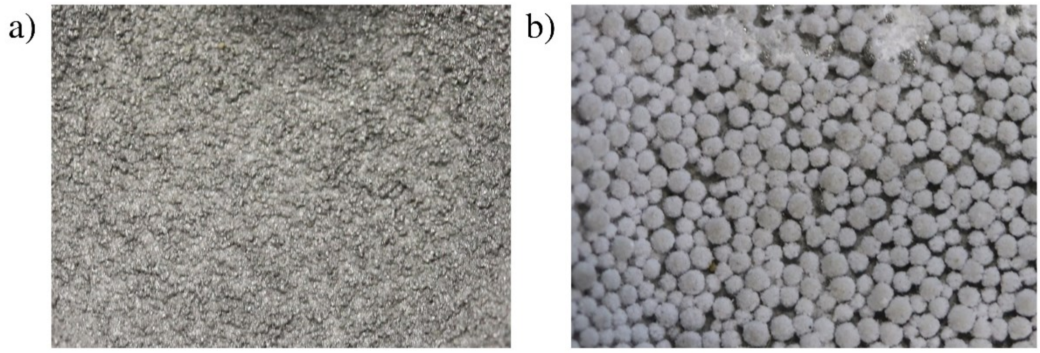

Figure 7.4.2: Commonly available surface finishes for orthopaedic implants: a) Plasma sprayed b) Sintered Bead

The studies presented in this thesis all use the same surface treatment. Designed to model the most popular cup model at time of writing[11] the finish is most similar to a plasma sprayed surface. Therefore it would be poignant to measure and quantify the effects of a sintered beaded surface. This may be particularly important to the outcomes of Chapter 4, where the process of abrasion and damage caused by the rougher plasma sprayed finish may be important to the strain deterioration mechanism.

7.4.4 Optimisation of oscillatory impaction and component seating

Chapter 7 concludes that oscillatory seating shows some promise as a method of seating cementless implants. However there is a clear requirement for more investigation into the efficacy of such devices. More importantly there is no current research published describing the effects of parameters that will almost certainly change the performance of such devices. These include, but are not limited to:

- Device related parameters. Effect upon implant seating of:
    - Frequency of device oscillation
    - Stroke of impactor
    - Weight of impactor
    - Material/connection method/application of impactor
- Surgical technique parameters. Effect upon implant seating of:
    - Force applied to device
    - Insertion pulse duration

Importantly the severity of strain deterioration due to extended periods of oscillation in low density bone have also not been investigated. This is a key area of concern due to the issues reported in Chapter 5.

The testing methods described in Chapter 6 would be suitable to investigate the various aspects of these new devices that are yet to be reported on. The above parameters would serve as independent variables, while the same dependent variables of seating quality (bone and implant strain, implant fixation and polar gap) would be measured.

7.4.5 Impact and seating mechanics of the femur and femoral stem

This body of work has focused upon the effects of impaction on the acetabular cup. However seating of femoral stems remains a problem facing orthopedic surgeons. Similar to the seating of acetabular cups there are competing factors that must be understood and optimized. For example excessive hoop strain in bone due to large impaction forces may lead to fracture of the intramedullary canal.[27,60,68,176,240,241] However if too little stability is achieved through impaction and press-fit, the stem may be liable to subside[45,242,243] or suffer micromotion and lack long-term bone ingrowth.[86,244] Synthetic models of the femur are available and with similar levels of validation as acetabular models.[147,148,151] During the design and validation of a compliant drop rig, as described in Chapter 3, the boundary conditions of the femur were also calculated and reported. Therefore the same set of testing as conducted for the acetabulum, described in Chapters 4-7, could be conducted for the femur. The outputs of these studies would inform the surgeon of the appropriate impaction technique to use to seat a cementless femoral implant, as well as the efficacy of the new wave of oscillating surgical devices.

7.4.6 Taper impact mechanics

As demonstrated in Chapter 2 the magnitude of impact required to assemble Morse tapers is of considerable interest to the orthopedic industry. Issues with the performance of modular implants have been identified and widely reported.[97,245,246] It is believed that if insufficient impact force is applied to the femoral head during assembly of the components the small ridges on the male taper will not deform.[42,247] This allows fluids found in the *in-vivo* environment to access the taper and cause corrosion.[248] This corrosion may release toxic particulates into the surrounding tissues and cause adverse tissue reactions, known as trunnionosis. Often severe, such reactions may lead to revision of the implant (with a reported incident rate of up to 3%[39]). As the force required to seat sits within a lower and upper limit, another novel device that delivers set impaction forces may be appropriate to remove surgeon variability from the equation.

References

1. Murray CJL, Richards MA, Newton JN, et al. 2013. Articles UK health performance: findings of the Global Burden of Disease Study 2010. Lancet 381(9871):997–1020 Available from: http://dx.doi.org/10.1016/S0140-6736(13)60355-4.

2. Arthtis Reaearch UK. 2013. Osteoarthritis in general practice: Data and perspectives. 1-36 p. Available from: https://www.arthritisresearchuk.org/~/media/Files/Policy files/Policy pages files/Osteoarthritis in general practice July 2013 Arthritis Research UK PDF 421 MB.ashx.

3. Blagojevic M, Jinks C, Jeffery A, Jordan KP. 2010. Risk factors for onset of osteoarthritis of the knee in older adults: a systematic review and meta-analysis. Osteoarthr. Cartil. 18(1):24–33 Available from: http://dx.doi.org/10.1016/j.joca.2009.08.010.

4. Butland B, Jebb S, Kopelman P, et al. 2007. Tackling Obesities: Future Choices – Project report. Gov. Off. Sci. Available from: https://assets.publishing.service.gov.uk/government/uploads/system/uploads/attachment_data/file/287937/07-1184x-tackling-obesities-future-choices-report.pdf.

5. Mobasheri A, Batt M. 2016. An update on the pathophysiology of osteoarthritis. Ann. Phys. Rehabiliative Med. 59:333–339.

6. National Institute for Health and Care Excellence: Clinical guideline CG177 Methods. 2014. Osteoarthritis - Care and Management in Adults:(February) Available from: https://www.nice.org.uk/guidance/cg177/resources/osteoarthritis-care-and-management-pdf-35109757272517.

7. Furner SE, Hootman JM, Helmick CG, et al. 2011. Health-Related Quality of Life of US Adults With Arthritis: Analysis of Data From the Behavioral Risk Factor Surveillance System , 2003 , 2005 , and 2007. Arthritis Care Res. (Hoboken). 63(6):788–799.

8. Anandacoomarasamy A, March L. 2010. Current evidence for osteoarthritis treatments. Ther. Adv. Musculoskelet. Diesease 2(1):17–28.

9. Bennell KL, Hunter DJ, Hinman RS. 2012. Management of osteoarthritis of the knee. BMJ 4934(July):1–8.

10. Mandl LA. 2018. Osteoarthritis year in review 2018: clinical. Osteoarthr. Cartil. (In Press):1–6 Available from: https://doi.org/10.1016/j.joca.2018.11.001.

11. National Joint Registry. 2017. 2017 14th Annual Report - National Joint Registry for

England, Wales, Northern Ireland and the Isle of Man.1821(December 2016):1–202 Available from: http://www.njrreports.org.uk/Portals/0/PDFdownloads/NJR 14th Annual Report 2017.pdf.

12. Mellon SJ, Liddle AD, Pandit H. 2013. Maturitas Hip replacement : Landmark surgery in modern medical history. Maturitas 75(3):221–226 Available from: http://dx.doi.org/10.1016/j.maturitas.2013.04.011.

13. Pivec R, Johnson AJ, Mears SC, Mont MA. 2012. Hip arthroplasty. Lancet 380:1768–1777.

14. Yamada H, Yoshihara Y, Henmi O, et al. 2009. Cementless total hip replacement : past , present , and future. J. Orthop. Sci. (14):228–241.

15. Knight SR, Aujla R, Biswas SP. 2011. Total Hip Arthroplasty - over 100 years of operative history. Orthop. Rev. (Pavia). 3(16):2–4.

16. Hannouche D, Hamadouche M, Bizot P, et al. 2005. Ceramics in Total Hip Replacement. Clin. Orthop. Relat. Res. (430):62–71.

17. Vaishya R, Chauhan M, Vaish A. 2013. Bone cement. J. Clin. Orthop. Trauma 4(4):157–163 Available from: http://dx.doi.org/10.1016/j.jcot.2013.11.005.

18. Leidinger W, Hoffmann G, Meierhofer J, Wölfel R. 2002. Reduction of severe cardiac complications during implantation of cemented total hip endoprostheses in femoral neck fractures. Unfallchirurg 105(8):675–679.

19. Donaldson AJ, Thomson HE, Harper NJ, Kenny NW. 2009. Bone cement implantation syndrome. Br. J. Anaesth. 102(1):12–22.

20. Maggs J, Wilson M. 2017. The Relative Merits of Cemented and Uncemented Prostheses in Total Hip Arthroplasty. Indian J. Orthop. 51(4):1–6.

21. Morscher E, Masar Z. 1988. Development and First Experience with an Uncemented Press-Fit Cup. Clin. Orthop. Relat. Res. 232:96–103.

22. Tonino A, Therin M, Doyle C. 1999. Hydroxyapatite-coated femoral stems: Histology and histomorphometry around five components retrieved at post mortem. Bone Joint J. 81–B(No. 1) Available from: https://doi.org/10.1302/0301-620X.81B1.0810148.

23. Mcminn DJW, Snell KIE, Daniel J, et al. 2012. Mortality and implant revision rates of hip arthroplasty in patients with osteoarthritis : registry based cohort. BMJ 3319(June):1–19.

24. Kendal AR, Prieto-alhambra D, Arden NK, et al. 2013. Mortality rates at 10 years after metal-on-metal hip resurfacing compared with total hip replacement in England :

retrospective cohort analysis of hospital. BMJ 6549(November):1–12.

25. Banaszkiewicz P a. 2014. Porous-coated hip replacement. The factors governing bone ingrowth, stress shielding, and clinical results. Class. Pap. Orthop. 69(1):51–55.

26. Pilliar RM, Lee JM, Maniatopoulos C. 1985. Observations on the effect of movement on bone ingrowth into porous-surfaced implants. Clin. Orthop. Relat. Res. 208:108–113.

27. Davidson D. 2008. Intraoperative Periprosthetic Fractures During Total Hip Arthroplasty - Evaluation and Management. J. Bone Jt. Surg. 90(9):2000 Available from: http://jbjs.org/cgi/doi/10.2106/JBJS.H.00331.

28. Spires WP, Cook SD, Kester MA. 1988. Tissue response to porous-coated implants lacking initial bone apposition. J. Arthroplasty 3(4):337–346.

29. Springer BD, Habet N a., Griffin WL, et al. 2012. Deformation of 1-Piece Metal Acetabular Components. J. Arthroplasty 27(1):48–54 Available from: http://dx.doi.org/10.1016/j.arth.2011.03.019.

30. Kim Y. 2017. Acetabular Cup Revision. Hip Pelvis 29(3):155–158.

31. Pulido L, Rachala S, Cabaela M. 2011. Cementless acetabular revision: past, present, and future. Int. Orthop. (35):289–298.

32. Higgins BT, Barlow DR, Heagerty NE, Lin TJ. 2015. Anterior vs . Posterior Approach for Total Hip Arthroplasty , a Systematic Review and Meta-analysis. J. Arthroplasty 30(3):419–434 Available from: http://dx.doi.org/10.1016/j.arth.2014.10.020.

33. Fritsche A, Bialek K, Mittelmeier W, et al. 2008. Experimental investigations of the insertion and deformation behavior of press-fit and threaded acetabular cups for total hip replacement. J. Orthop. Sci. 13(3):240–247 Available from: http://link.springer.com/10.1007/s00776-008-1212-z.

34. Beaule PE, Duff M Le, Campbell P, et al. 2004. Metal-on-Metal Surface Arthroplasty With a Cemented Femoral Component. J. Arthroplasty 19(8):17–22.

35. Schlegel UJ, Rothstock S, Siewe J, et al. 2011. Does Impaction Matter in Hip Resurfacing? A Cadaveric Study. J. Arthroplasty 26(2):296–302 Available from: http://linkinghub.elsevier.com/retrieve/pii/S088354031000210X.

36. Marlowe DE, Parr JE, Michael B. 1997. Modularity of Orthopedic Implants.(STP 1301):117–126.

37. Krull A, Morlock MM, Bishop NE. 2018. Maximizing the fixation strength of modular

components by impaction without tissue damage. Bone Jt. Res. 7(2):196–204.

38. Lundberg HJ, Ha NQ, Hall DJ, et al. 2015. Contact Mechanics and Plastic Deformation at the Local Surface Topography Level After Assembly of Modular Head-Neck Junctions in Modern Total Hip Replacement Devices. ASTM Int. STP1591:59–82.

39. Mistry JB, Chughtai M, Elmallah RK, Diedrich A. 2016. Trunnionosis in total hip arthroplasty : a review. J. Orthop. Traumatol. 17(1):1–6.

40. Rehmer A, Bishop NE, Morlock MM. 2012. How To Assemble a Femoral Head To the Stem Taper of a Modular Hip Prosthesis. J. Biomech. 45:S1 Available from: http://linkinghub.elsevier.com/retrieve/pii/S0021929012703159.

41. Baxmann M, Jauch SY, Schilling C, et al. 2013. The influence of contact conditions and micromotions on the fretting behavior of modular titanium alloy taper connections. Med. Eng. Phys. 35(5):676–683 Available from: http://linkinghub.elsevier.com/retrieve/pii/S1350453312002093.

42. Panagiotidou A, Cobb T, Meswania J, et al. 2018. Effect of impact assembly on the interface deformation and fretting corrosion of modular hip tapers: An in vitro study. J. Orthop. Res. 36(1):405–416.

43. Gie G, Linder L, Ling R, et al. 1993. Impacted cancellous allografts and cement for revision hip arthroplasty. J Bone Jt. Surg 75(B):14–21.

44. Ornstein E, Linder L, Ranstam J, et al. 2009. Femoral impaction bone grafting with the Exeter stem - the Swedish experience: survivorship analysis of 1305 revisions performed between 1989 and 2002. J. Bone Joint Surg. Br. 91(4):441–446.

45. Hostner J, Hultmark P, Karrholm J, et al. 2001. Impaction Technique and Graft Treatment in Revisions of the Femoral Component: Laboratory Studies and Clinical Validation. J. Arthroplasty 16(1).

46. Mazhar Tokgözoğlu a, Aydin M, Atilla B, Caner B. 2000. Scintigraphic evaluation of impaction grafting for total hip arthroplasty revision. Arch. Orthop. Trauma Surg. 120:416–419.

47. Bavadekar a, Cornu O, Godts B, et al. 2001. Stiffness and compactness of morselized grafts during impaction: an in vitro study with human femoral heads. Acta Orthop. Scand. 72(5):470–476.

48. Korda M, Blunn G, Phipps K, et al. 2006. Can mesenchymal stem cells survive under normal impaction force in revision total hip replacements? Tissue Eng. 12(3):625–30

Available from: http://www.ncbi.nlm.nih.gov/pubmed/16579695.

49. Pekkarinen J, Alho a, Lepistö J, et al. 2000. Impaction Bone Grafting in Revision Hip Surgery. A High Incidence of Complications. Br J Bone Jt Surg 82(1):103–107.

50. Stefan R, Timo T, Sylvain S, et al. 2019. Uncemented THA Through the Direct Anterior Approach: Analysis of a Consecutive Series of 275 Hips with a Minimum Follow-up of 10 years. J. Arthroplasty Available from: https://doi.org/10.1016/j.arth.2019.01.062.

51. Sharkey PF, Hozack WJ, Callaghan JJ, et al. 1999. Acetabular fracture associated with cementless acetabular component insertion: a report of 13 cases. J. Arthroplasty 14(4):426–31 Available from: http://www.ncbi.nlm.nih.gov/pubmed/10428222.

52. Streit MR, Haeussler D, Bruckner T. 2016. Early Migration Predicts Aseptic Loosening of Cementless Femoral Stems : A Long-term Study. Clin. Orthop. Relat. Res. 474(7):1697–1706.

53. Sundfeldt M, V Carlsson L, B Johansson C, et al. 2006. Aseptic loosening, not only a question of wear: A review of different theories. Acta Orthop. 77(2):177–197 Available from: http://www.tandfonline.com/doi/full/10.1080/17453670610045902.

54. Peterson BYCA, D M, Allen DGLEW, D M. 1996. Periprosthetie Fracture of the Acetabulum after Total Hip Arthroplasty. J. Bone Jt. Surg. 78–A(8):1206–1213.

55. Chatoo M, Parfitt J, Pearse MF. 1998. Case Report Periprosthetic Acetabular Fracture Associated With Extensive Osteolysis. J. Arthoplasty 13(7):843–845.

56. Farfalli GL, Buttar MA, Piccaluga F. 2007. Femoral Fractures in Revision Hip Surgeries with Impacted Bone Allograft. Clin. Orthop. Relat. Res. 6(462):130–136.

57. Asayama I, Kinsey TL, Mahoney OM. 2006. Two-Year Experience Using a Limited-Incision Direct Lateral Approach in Total Hip Arthroplasty. J. Arthroplasty 21(8):1083–1091.

58. Hartford JM, Knowles SB. 2018. Risk Factors for Perioperative Femoral Fractures : Cementless Femoral Implants and the Direct Anterior Approach Using a Fracture Table. J. Arthroplasty 31(9):2016 Available from: http://dx.doi.org/10.1016/j.arth.2016.02.045.

59. Thien TM, Chatziagorou G, Garellick G, et al. 2014. Periprosthetic Femoral Fracture within Two Years After Total Hip Replacement: Analysis of 437,629 Operations in the Nordic Arthroplasty Register Association Database. J Bone Jt. Surg Am. 96(19):e167 Available from: http://jbjs.org/content/96/19/e167.abstract.

60. Masri B a, Meek RMD, Duncan CP. 2004. Periprosthetic fractures evaluation and

treatment. Clin. Orthop. Relat. Res. (420):80–95.

61. Kim YS, Callaghan J, Ahn P, Brown T. 1995. Fracture of the Acetabulum during Insertion of an Oversized Hemispherical Component. J. Bone Jt. Surg. 77–A.

62. Curtis MJ, Jinnah RH, Wilson VD, Hungerford DS. 1992. The initial stability of uncemented acetabular components. J. Bone Joint Surg. Br. 74(3):372–376.

63. Finlay BJ, Bourne RB, Landsberg RP, Andreae P. 1986. Pelvic Stresses In-Vitro I - Malsizing of Endoprostheses.19(9):703–714.

64. Deligianni DD, Maris A, Missirlis YF. 1994. Stress relaxation behavioue of trabecular bone specimens. J. Biomech. 27(12):1469–1476.

65. Miller A. 1972. Late Fracture of the Acetabulum after Total Hip Replacement. J. Bone Jt. Surg. 54B(4):600–606.

66. Haidukewych GJ, Jacofsky DJ, Hanssen AD, Lewallen DG. 2006. Intraoperative Fractures of the Acetabulum During Primary Total Hip Arthroplasty. J. Bone Jt. Surg. 88–A(9):1952–1956.

67. Hailer NP, Garellick G, Kärrholm J. 2010. Uncemented and cemented primary total hip arthroplasty in the Swedish Hip Arthroplasty Register. Acta Orthop. 81(1):34–41 Available from: http://www.pubmedcentral.nih.gov/articlerender.fcgi?artid=2856202&tool=pmcentrez&rendertype=abstract.

68. Schwarz E, Reinisch G, Brandauer A, et al. 2018. Load transfer and periprosthetic fractures after total hip arthoplasty: Comparison of periprosthetic fractures of femora implanted with cementless distal-load or proximal-load femoral components and measurement of the femoral strain at the time of implant. Clin. Biomech. 54(March):137–142 Available from: https://doi.org/10.1016/j.clinbiomech.2018.03.010.

69. McElfresh EC, Coventry MB. 1974. Femoral and Pelvic Fractures after Total Hip Arthroplasty. J. Bone Jt. Surg. 56(3):483–492.

70. Chitre A, Wynn Jones H, Shah N, Clayson A. 2013. Complications of total hip arthroplasty: Periprosthetic fractures of the acetabulum. Curr. Rev. Musculoskelet. Med. 6(4):357–363.

71. Flannery OM, Britton JR, O'Reilly P, et al. 2010. The threshold force required for femoral impaction grafting in revision hip surgery - A preliminary study in sow femurs. Acta Orthop. 81(3):303–307 Available from:

http://www.tandfonline.com/doi/full/10.3109/17453674.2010.480936.

72. Cummins F, Reilly PO, Flannery O, et al. 2011. Defining the impaction frequency and threshold force required for femoral impaction grafting in revision hip arthroplasty. A human cadaveric mechanical study. Acta Orthop. 82(4):433–7 Available from: http://www.pubmedcentral.nih.gov/articlerender.fcgi?artid=3237033&tool=pmcentrez&rendertype=abstract.

73. Goebel P, Kluess D, Wieding J, et al. 2013. The influence of head diameter and wall thickness on deformations of metallic acetabular press-fit cups and UHMWPE liners : a finite element analysis. J. Orthop. Sci. (18):264–270.

74. Liu F, Chen Z, Gu Y, et al. 2012. Deformation of the Durom Acetabular Component and Its Impact on Tribology in a Cadaveric Model — A Simulator Study. PLoS One 7(10).

75. Pandorf T, Czak R. 2006. Impaction forces and proper seating of ceramic ball heads Poster No . 2256. In: 56th Annual Meeting of the Orthopaedic Research Society. p 2256.

76. Ong KL, Rundell S, Liepins I, et al. 2009. Biomechanical Modeling of Acetabular Component Polyethylene Stresses , Fracture Risk , and Wear Rate following Press-Fit Implantation. J. Orthop. Res. (November):1467–1472.

77. Adler E, Stuchin SA, Kummer FJ. 1992. Stability of Press-fit Acetabular Cups. J. Arthroplasty 7(3):295–301.

78. Markel DC, Hora N, Grimm M. 2002. Press-fit stability of uncemented hemispheric acetabular components: A comparison of three porous coating systems. Int. Orthop. 26(2):72–75.

79. Hsu JT, Chang CH, Huang HL, et al. 2007. The number of screws, bone quality, and friction coefficient affect acetabular cup stability. Med. Eng. Phys. 29(10):1089–1095.

80. Baleani M, Fognani R, Toni A. 2001. Initial Stability of a Cementless Acetabular Cup Design : Experimental Investigation on the Effect of Adding Fins to the Rim of the Cup. Artif. Organs 25(8):664–669.

81. Antoniades G, Smith EJ, Deakin AH, Wearing SC. 2013. Primary stability of two uncemented acetabular components of different geometry : hemispherical or peripherally enhanced? Bone Jt. Res. 2(12):264–269.

82. Crosnier EA, Keogh PS, Miles AW. 2016. The effect of dynamic hip motion on the micromotion of press-fit acetabular cups in six degrees of freedom. Med. Eng. Phys. 38:717–724.

83. Spears IR, Martin P, Schneider E, et al. 2000. Interfacial conditions between a press-fit acetabular cup and bone during daily activities : implications for achieving bone in-growth. J. Biomech. 33:1471–1477.

84. Pilliar RM, Lee JM, Maniatopoulos C. 1986. Observations on the Effect of Movement on Bone Ingrowth into Porous-Surfaced Implants. Clin Orthop Relat Res 208:108–113.

85. Duyck J, Vandamme K, Geris L, et al. 2006. The influence of micro-motion on the tissue differentiation around immediately loaded cylindrical turned titanium implants. Arch. Oral Biol. 51(1):1–9.

86. Jasty M, Bragdon C, Burke D, et al. 1997. In Vivo Skeletal Responses to Porous-Surfaced Implants Subjected to Small Induced Motions. Am J Bone Jt Surg 79(May):707–714.

87. American Joint Replacement Registry. 2017. Fourth AJRR Annual Report on Hip and Knee Arthroplasty Data.:1–71 Available from: http://www.ajrr.net/images/annual_reports/AJRR-2017-Annual-Report---Final.pdf?hsCtaTracking=61a2fedc-0f48-4241-a282-2bca6e4b68ad%7Ce4ed88d8-6b8e-4d0c-9a47-d1c169759e83.

88. Corten K, Au K, Bourne R. 2009. Acetabular Options: notes from the other side. Orthopaedics 32(9) Available from: orthosupersite.com/view.asp?rID=42834.

89. Nivbrant B, Karrholm J, Ingemar O, et al. 1996. Migration of Porous Press-fit Cups in Hip Revision Arthroplasty: A Radiostereometric 2-Year Follow-up Study of 60 Hips. J. Arthroplasty 11(4):390–396.

90. Hothi HS, Busfield JJC, Shelton JC. 2011. Explicit finite element modelling of the impaction of metal press-fit acetabular components. Proc. Inst. Mech. Eng. Part H J. Eng. Med. 225(3):303–314.

91. Kwong LM, Connor DO, Sedlacek RC, et al. 1994. A Quantitative In Vitro Assessment of Fit and Screw Fixation on the Stability of a Cementless Hemispherical Acetabular Component. J. Arthroplasty 9(2).

92. Spears IR, Morlock MM, Martin P, et al. 1999. The influence of friction and interference on the seating of a hemispherical press-fit cup: a finite element investigation. J. Biomech. 32:1183–1189.

93. Kroeber M, Ries MD, Suzuki Y, et al. 2002. Impact biomechanics and pelvic deformation during insertion of press-fit acetabular cups. J. Arthroplasty 17(3):349–354 Available from: http://linkinghub.elsevier.com/retrieve/pii/S0883540302281048.

94. Udomkiat P, Dorr LD, Wan Z. 2002. Cementless hemispheric porous-coated sockets implanted with press-fit technique without screws: Average ten-year follow-up. J. Bone Jt. Surg. - Ser. A 84(7):1195–1200.

95. Nakasone S, Takao M, Nishii T, et al. 2012. Incidence and Natural Course of Initial Polar Gaps in Birmingham Hip Resurfacing Cups. J. Arthroplasty 27(9):1676–1682 Available from: http://dx.doi.org/10.1016/j.arth.2012.02.028.

96. Schmalzried TP, Wessinger SJ, Hill GE, Harris WH. 1994. The Harris-Galante porous acetabular component press-fit without screw fixation. Five-year radiographic analysis of primary cases. J. Arthroplasty 9(3):235–242.

97. American Joint Replacement Registry. 2016. Third AJRR Annual Report on Hip and Knee Arthroplasty Data 2016.

98. Issack PS, Guerin J, Butler A, et al. 2004. Intraoperative Complications of Revision Hip Arthroplasty Using a Porous-Coated , Distally Slotted , Fluted Femoral Stem. Clin. Orthop. Relat. Res. (425):173–176.

99. Matassi F, Carulli C, Civinivi R, Innocenti M. 2013. Joints Cemented versus cementless fixation in total knee arthroplasty. Joints 1(3):121–125.

100. Goodman SB. 1994. The effects of micromotion and particulate materials on tissue differentiation. Bone chamber studies in rabbits. Acta Orthop. Scand. Suppl. 258(258):1–43.

101. Ries M, Pugh J, Au JANC, et al. 1989. Cortical Pelvic Strains with Varying Hemiarthroplasty in-vitro. J. Biomech. 22(7):775–780.

102. Zhang Q, Wang J, Lupton C, et al. 2010. A subject-specific pelvic bone model and its application to cemented acetabular replacements $. J. Biomchanics 43(14):2722–2727 Available from: http://dx.doi.org/10.1016/j.jbiomech.2010.06.023.

103. MacKenzie JR, Callaghan JJ, Pedersen DR, Brown TD. 1994. Areas of contact and extent of gaps with implantation of oversized acetabular components in total hip arthroplasty. Clin. Orthop. Relat. Res. 298(298):127–136.

104. Jin ZM, Meakins S, Morlock MM, et al. 2006. Deformation of press-fitted metallic resurfacing cups . Part 1 : experimental simulation. Proc Inst Mech Eng H 220:299–309.

105. Dold P, Pandorf T, Flohr M, et al. 2016. Acetabular shell deformation as a function of shell stiffness and bone strength. Proc. Inst. Mech. Eng. Part H J. Eng. Med. 230(4):259–264 Available from: http://pih.sagepub.com/lookup/doi/10.1177/0954411916632792.

106. Widmer K-H, Zurfluh B, Morscher EW. 2002. Load transfer and fixation mode of press-fit acetabular sockets. J. Arthroplasty 17(7):926–935 Available from: http://linkinghub.elsevier.com/retrieve/pii/S0883540302000992.

107. Postak PD, Rosca M, Greenwald AS. 2009. Do thin acetabular shells increase the disassociation risk of ceramic liners? J. Bone Jt. Surg. - Ser. A 91(SUPPL. 6):129–133.

108. Yew A, Jin ZM, Donn A, et al. 2006. Deformation of press-fitted metallic resurfacing cups . Part 2 : finite element simulation. Proc. Inst. Mech. Eng. Part H J. Eng. Med. 220:311–319.

109. Hothan A, Huber G, Weiss C, et al. 2011. Deformation characteristics and eigenfrequencies of press-fit acetabular cups. Clin. Biomech. 26(1):46–51 Available from: http://dx.doi.org/10.1016/j.clinbiomech.2010.08.015.

110. Squire M, Griffin WL, Mason JB, et al. 2006. Acetabular Component Deformation with Press-Fit Fixation. J. Arthroplasty 21(6):72–77.

111. Hanaor DAH, Gan Y, Einav I. 2016. Tribology International Static friction at fractal interfaces. Tribiology Int. 93:229–238 Available from: http://dx.doi.org/10.1016/j.triboint.2015.09.016.

112. Kuiper JH, Huiskes R. 1996. Friction and Stem Stiffness Affect Dynamic Interface Motion in Total Hip Replacement. J. Orthop. Res. 1(2):36–43.

113. Damm NB, Morlock MM, Bishop NE. 2015. Friction coefficient and effective interference at the implant-bone interface. J. Biomech. 48(12):3517–3521 Available from: http://dx.doi.org/10.1016/j.jbiomech.2015.07.012.

114. Bishop NE, Höhn JC, Rothstock S, et al. 2014. The influence of bone damage on press-fit mechanics. J. Biomech. 47(6):1472–1478.

115. Le Cann S, Galland A, Rosa B, et al. 2014. Does surface roughness influence the primary stability of acetabular cups ? A numerical and experimental biomechanical evaluation. Med. Eng. Phys. 36(9):1185–1190 Available from: http://dx.doi.org/10.1016/j.medengphy.2014.07.003.

116. Weißmann V, Boss C, Schulze C, et al. 2018. Experimental Characterization of the Primary Stability of Acetabular Press-Fit Cups with Surface Layer. Metals (Basel). 8(10):839.

117. Wetzel R, Simnacher M, Scheller G. 2005. Initial stability of press-fit cups: an in-vitro study. Biomed. Tech. 50:400–403.

118. Smith and Nephew. 2013. Poly and Ceramic - Surgical Technique - R3 (Promotional

Material).

119. Stryker. 2004. Trident- PSL Acetabular System (Surgical Protocol).

120. JRI Orthopaedic. 2009. HAC Coated CSF plus Cup (Surgical Protocol).

121. Morscher E, Bereiter H, Lampart C. 1989. Cementless Press-Fit Cup; Principles, Experimental Data, and Three Year Follow-Up Study. Clin. Orthop. Relat. Res. 249:12–20.

122. Macdonald W, Carlsson L V, Charnley GJ, Jacobsson CM. 1999. Press-fit acetabular cup fixation : principles and testing. Proc. Inst. Mech. Eng. Part H J. Eng. Med. 213:33–39.

123. Kim, Yong Sik; Callaghan, John J.; Ahn, Peter B.; Brown TD. 1995. Fracture of the Acetabulum during insertion of an Oversized Hemispherical Component. J. Bone Jt. Surg. - Am. Vol. 77(A):111–117 Available from: http://ovidsp.tx.ovid.com/sp-3.17.0a/ovidweb.cgi?T=JS&PAGE=fulltext&D=ovft&AN=00004623-199501000-00013&NEWS=N&CSC=Y&CHANNEL=PubMed.

124. Ries MD, Salehi A, Shea J. 1999. Photoelastic analysis of stresses produced by different acetabular cups. Clin. Orthop. Relat. Res. (369):165–174.

125. Bishop NE, Burton A, Maheson M, Morlock MM. 2010. Biomechanics of short hip endoprostheses — The risk of bone failure increases with decreasing implant size. JCLB 25(7):666–674 Available from: http://dx.doi.org/10.1016/j.clinbiomech.2010.04.013.

126. Ridzwan M, Shuib S, Hassan A, et al. 2007. Problem of Stress Shielding and Improvement to the Hip Implant Designs: A Review. J. Med. Sci. 7(3):460–467.

127. Vogel D, Rathay A, Teufel S, et al. 2017. Experimental analysis of insertion torques and forces of threaded and press-fit acetabular cups by means of ex vivo and in vivo measurements. Acta Bioeng. Biomech. 19(3).

128. Bergmann G, Deuretzbacher G, Heller M, et al. 2001. Hip contact forces and gait patterns from routine activities. J. Biomchanics 34:859–871.

129. Brockett C, Williams S, Jin Z, et al. 2006. Friction of Total Hip Replacements With Different Bearings and Loading Conditions. J. Biomed. Mater. Res. Part B Appl. Biomater. :508–515.

130. Wimmer MA, Nassutt R, Sprecher C, et al. 2006. Investigation on stick phenomena in metal-on-metal hip joints after resting periods. Proc Inst Mech Eng H 220(Special Issue Paper):219–227.

131. Tuke MA, Eng HNCM. 2009. The Problem with Large Diameter Metal-on-Metal

Acetabular Cup Inclination. Bull. NYU Hosp. Jt. Dis. 67(2):189–192.

132. Crosnier EA, Keogh PS, Miles AW. 2015. A novel method to assess primary stability of press-fit acetabular cups. J. Eng. Med. 228(11):1126–1134.

133. Ries MD, Harbaugh M, Shea J, Lambert R. 1997. Effect of cementless acetabular cup geometry on strain distribution and press-fit stability. J. Arthroplasty 12(2):207–212.

134. Goossens Q, Leuridan S, Henyš P, et al. 2017. Development of an acoustic measurement protocol to monitor acetabular implant fixation in cementless total hip Arthroplasty : A preliminary study. Med. Eng. Phys. 49:28–38.

135. Tijou A, Rosi G, Hernigou P, et al. 2018. Ex vivo evaluation of cementless acetabular cup stability using impact analyses with a hammer instrumented with strain sensors. Sensors (Switzerland) 18(1).

136. Michel A, Bosc R, Mathieu V, et al. 2014. Monitoring the press-fit insertion of an acetabular cup by impact measurements : Influence of bone abrasion. Jounral Eng. Med. 228(10):1027–1034.

137. Bosc R, Tijou A, Rosi G, et al. 2018. Influence of soft tissue in the assessment of the primary fixation of acetabular cup implants using impact analyses. Clin. Biomech. (In Press) Available from: http://linkinghub.elsevier.com/retrieve/pii/S0268003318302481.

138. Michel A, Nguyen VH, Bosc R, et al. 2017. Finite element model of the impaction of a press-fitted acetabular cup. Med. Biol. Eng. Comput. 55(5):781–791.

139. Clarke SG, Phillips ATM, Bull AMJ. 2012. Validation of FE Micromotions and Strains Around a Press-Fit Cup : Introducing a New Micromotion Measuring Technique. Ann. Biomed. Eng. 40(7):1586–1596.

140. Schulze C, Vogel D, Sander M, Bader R. 2018. Engineering Calibration of crushable foam plasticity models for synthetic bone material for use in finite element analysis of acetabular cup deformation and primary stability. Comput. Methods Biomech. Biomed. Engin. 0(0):1–13 Available from: https://doi.org/10.1080/10255842.2018.1524884.

141. Keavney T. 1998. Cancellous Bone. In: Black J, Hastings G, editors. Handbook of Biomaterial Properties. Springer. p 15–23.

142. Small SR, Berend ME, Howard L a., et al. 2013. Acetabular Cup Stiffness and Implant Orientation Change Acetabular Loading Patterns. J. Arthroplasty 28(2):359–367 Available from: http://dx.doi.org/10.1016/j.arth.2012.05.026.

143. Macdonald W, Carlsson L, Charnley G, et al. 1999. Inaccuracy of Acetabular Reaming Under Surgical Conditions. J. Arthoplasty 14(6):730–737.

144. Brenner E. 2014. Human body preservation - old and new techniques. J. Anat. 224(3):316–344.

145. ASTM. 2014. F1839 - 08: Standard Specification for Rigid Polyurethane Foam for use as a Standard Material for Testing Orthopaedic Devices and Instruments. ASTM B. Stand. 13.01(October):6–11.

146. Sawbones. 2017. Sawbones 4th Generation Femur. [cited 2019 Mar 19] Available from: https://www.sawbones.com/femur-medium-left-4th-generation-composite.html.

147. Cristofolini L, Viceconti M, Cappello A, Toni A. 1996. Mechanical Validation of Whole Bone Composite Femur Models. J. Biomech. 2(4):525–535.

148. Heiner AD, Brown TD. 2001. Structural properties of a new design of composite replicate femurs and tibias. J. Biomech. 34:773–781.

149. ASTM. 2017. Standard Specification and Test Methods for Metallic Medical Bone Screws. PA. 1-22 p. Available from: https://doi.org/10.1520/F0543-17.

150. Mina SRA, Schemitsch H, Zdero R. 2017. Chapter 10 - Biomechanical Testing of the Intact and Surgically Treated Pelvis. In: Experimental Methods in Orthopaedic Biomechanics. Academic Press. p 149–165.

151. Maharaj G, Jamison R. 1993. Intraoperative Impact: Characterization and Laboratory Simulation on Composite Hip prostheses. Compos. Mater. Implant Appl. Hum. Body Charact. Testing, ASTM STP 1178 :98–108 Available from: http://www.astm.org/doiLink.cgi?STP15546S.

152. Szivek J, Thomas M, Benjamin J. 1993. Characterization of a synthetic foam as a model for human cancellous bone. J. Appl. Biomater. 4(3):269–72.

153. Murphy W, Black J, Hastings G. 2016. Handbook of Biomaterial Properties, Second Edi. New York: Springer.

154. Ayers MP, Clift SE, Gheduzzi S. 2014. Morsellised sawbones is an acceptable experimental substitute for the in vitro elastic and viscoelastic mechanical characterisation of morsellised cancellous bone undergoing impaction grafting. Med. Eng. Phys. 36(1):26–31 Available from: http://dx.doi.org/10.1016/j.medengphy.2013.08.005.

155. Meding JB, Ms SRS, Jones ME, et al. 2013. Acetabular Cup Design Influences

Deformational Response in Total Hip Arthroplasty. Clin. Orthop. Relat. Res. (471):403–409.

156. Schmidig G, Patel A, Liepins I, et al. 2010. The Effects of Acetabular Shell Deformation and Liner Thickness on Frictional Torque in Ultrahigh-Molecular- Weight Polyethylene Acetabular Bearings. J. Arthroplasty 25(4):644–653 Available from: http://dx.doi.org/10.1016/j.arth.2009.03.020.

157. Michel A, Bosc R, Vayron R, Haiat G. 2015. In Vitro Evaluation of the Acetabular Cup Primary Stability by Impact Analysis. J. Biomech. Eng. 137(3):031011 Available from: http://biomechanical.asmedigitalcollection.asme.org/article.aspx?doi=10.1115/1.4029505.

158. West C, Fryman JC. 2008. Cadaveric measurement of impact force on total hip arthroplasty surgical instrumentation. Am. Soc. Biomech. 2008, Annu. Conf. Ann Arbor, Michigan, USA. Poster 173.

159. Scholl L, Schmidig G, Faizan a., et al. 2016. Evaluation of surgical impaction technique and how it affects locking strength of the head-stem taper junction. Proc. Inst. Mech. Eng. Part H J. Eng. Med. 230(7):661–667 Available from: http://pih.sagepub.com/lookup/doi/10.1177/0954411916644477.

160. Mathieu V, Michel A, Flouzat Lachaniette CH, et al. 2013. Variation of the impact duration during the in vitro insertion of acetabular cup implants. Med. Eng. Phys. 35(11):1558–1563 Available from: http://dx.doi.org/10.1016/j.medengphy.2013.04.005.

161. Ireland D. 1974. Procedures and Problems Associated with Reliable Control of the Instrumented Impact Test.(ASTM STP563-EB):3–29.

162. Goldsmith W. 2001. Impact, 2nd ed. New York: Dover Publications.

163. Robinovitch SN, McMahon TA, Hayes WC. 1995. Force attenuation in Trochanteric soft tissues during impact from a fall. J. Orthop. Res. 13:956–962.

164. Bouxsein ML, Szulc P, Munoz F, et al. 2007. Contribution of trochanteric soft tissues to fall force estimates, the factor of risk, and prediction of hip fracture risk. J. Bone Miner. Res. 22(6):825–831.

165. Laing AC, Robinovitch SN. 2010. Characterizing the effective stiffness of the pelvis during sideways falls on the hip. J. Biomech. 43:1898–1904.

166. Levine IC, Bhan S, Laing AC. 2013. The effects of body mass index and sex on impact force and effective pelvic stiffness during simulated lateral falls. Clin. Biomech. 28(9–10):1026–1033 Available from: http://dx.doi.org/10.1016/j.clinbiomech.2013.10.002.

167. Robinovitch SN, Hayes WC, McMahon T. 1991. Prediction of femoral impact forces in falls on the hip. J. Biomech. Eng. 113(December 1991):366–374.

168. Bhan S, Levine IC, Laing AC. 2014. Energy absorption during impact on the proximal femur is affected by body mass index and flooring surface. J. Biomech. 47(10):2391–2397 Available from: http://dx.doi.org/10.1016/j.jbiomech.2014.04.026.

169. Etheridge BS, Beason DP, Lopez RR, et al. 2005. Effects of trochanteric soft tissues and bone density on fracture of the female pelvis in experimental side impacts. Ann. Biomed. Eng. 33(2):248–254.

170. Cavanagh PR. 1998. The Penn State Safety Floor : Part II — Reduction of Fall-Related Peak Impact Forces on the Femur. J. Biomech. Eng. 120(August):527–532.

171. Derler S, Spierings a. B, Schmitt KU. 2005. Anatomical hip model for the mechanical testing of hip protectors. Med. Eng. Phys. 27(6):475–485.

172. Robinovitch SN, Hayes WC, McMahon T a. 1997. Predicting the impact response of a nonlinear single-degree-of-freedom shock-absorbing system from the measured step response. J. Biomech. Eng. 119(3):221–227.

173. Kannus P, Parkkari J, Poutala J. 1999. Comparison of force attenuation properties of four different hip protectors under simulated falling conditions in the elderly: An in vitro biomechanical study. Bone 25(2):229–235.

174. Robinovitch SN, Hayes WC, McMahon T a. 1995. Energy-shunting hip padding system attenuates femoral impact force in a simulated fall. J. Biomech. Eng 117(November):409–413.

175. Nambu S, Ewing M, Timmerman L, et al. 2018. Effect Of Assembly Impaction And Cyclic Loading Forces On The Micromotion In The Modular Neck-Stem Interface. In: Orthopaedic Proceedings. London: Bone & Joint Publishing.

176. Kold S, Bechtold JE, Mouzin O, et al. 2005. Importance of pre-clinical testing exemplified by femoral fractures in vitro with new bone preparation technique. Clin. Biomech. 20(1):77–82.

177. Bullock MW, De Gregorio M, Danelson KA, et al. 2018. Quantifying the force transmission through the pelvic joints during total hip arthroplasty: A pilot cadaveric study. Clin. Biomech. 58(May):69–73.

178. Cruce J, Erwin J, Remick K, et al. 2011. Peri-Prostetic Fracture Vibration Testing. In: Sensors, Instrumentation and Special Topics. New York: Springer. p 207–225.

179. Scholl L, Pierre D, Rajaravivarma R, et al. 2018. Effect of the support systems' compliance on total hip modular taper seating stability. Proc. Inst. Mech. Eng. Part H J. Eng. Med. 232(9):862–870.

180. Krull A, Bishop NE, Steffen NM, et al. 2017. Influence of the compliance of a patient's body on the head taper fixation strength of modular hip implants. Clin. Biomech. 46(April):1–5.

181. Fung, Y. C. 1993. Mechanical Properties of Living Tissues, 2nd ed. New York: Springer-Verlag.

182. Korhonen R, Saarakkala S. 2011. Biomechanics and Modeling of Skeletal Soft Tissues. In: Theoretical Biomechanics. IntechOpem. p 113–132.

183. Robinovitch SN, Hayes WC, McMahon TA. 1997. Distribution of contact force during impact to the hip. Ann. Biomed. Eng. 25(3):499–508.

184. Robinovitch SN, Hayes WC, McMahon T a. 1997. Predicting the impact response of a nonlinear single-degree-of-freedom shock-absorbing system from the measured step response. J. Biomech. Eng. 119(3):221–227.

185. Kohan L, Appleyard R, Hogg M, et al. 2005. Impaction Loads During the Insertion Of Hip Resurfacing Components. 53rd Annu. Meet. Orthop. Res. Soc. 36(2):Poster No 1701.

186. Webster J. 1999. The Measurement and Instrumentation and Sensors Handbook. CRC Press and IEEE.

187. Cheresh M, McMichael S. 1987. Instrumented Impact Test Data Interpretation. PA. 9-23 p. Available from: https://doi.org/10.1520/STP19371S.

188. Driscoll D. 1970. Impact Testing of Metals. PA. 1-322 p. Available from: https://doi.org/10.1520/STP466-EB.

189. Gaberson HA. 2011. Shock Data Filtering Consequences. In: Structural Dynamics, Volume 32. New York: Springer. p 961–967 Available from: https://doi.org/10.1007/978-1-4419-9834-7_85.

190. Cain PJ. 1987. Digital Filtering of Impact Data.(ASTM STP936-EB):81–102 Available from: https://doi.org/10.1520/STP19375S.

191. Belingardi G, Vadori R. 2002. Low velocity impact tests of laminate glass-fiber-epoxy matrix composite material plates. J. Impact Eng. 27:213–229.

192. Metz R. 2007. Impact and Drop Testing with ICP force sensors. Sound Vib. (February):18–

20.

193. Brach R. 1991. Mechanical Impact Mechanics. New York: Wiley-Interscience.

194. Tang L, Tennant JK, Forster A, Reddy M. 2016. Acetabular cup seating impact sensing for press-fit acetabular cup fixation. MESA 2016 - 12th IEEE/ASME Int. Conf. Mechatron. Embed. Syst. Appl. - Conf. Proc. :0–5.

195. Schlegel UJ, Knifka J, Röllinghoff M, et al. 2011. Effects of impaction on cement mantle and trabecular bone in hip resurfacing. Arch. Orthop. Trauma Surg. 131(4):459–464 Available from: http://link.springer.com/10.1007/s00402-010-1147-7.

196. Scheller G, Schwarz M, Pfanne D. 1999. Initial Stability of Press-fit Acetabular Cups . In vitro Lever-out Trials. Biomed. Tech. (12):356–359.

197. Souffrant R, Zietz C, Fritsche A, et al. 2012. Advanced material modelling in numerical simulation of primary acetabular press-fit cup stability. Comput. Methods Biomech. Biomed. Engin. 15(8):787–793.

198. Reuters. 2018. BRIEF-Depuy Synthes Signs Definitive Agreement To Acquire Assets Of Medical Enterprises Distribution. [cited 2019 Jan 12] Available from: https://www.google.com/search?q=medical+enterprises+distribution&rlz=1C1GGRV_enGB769GB769&oq=medical+enterprises+distr&aqs=chrome.0.0j69i57j69i60j0.11880j0j7&sourceid=chrome&ie=UTF-8.

199. Medical Enterprises Distrubition LLC. 2017. Medical Enterprises Core Animation - ME1000. [cited 2019 Jan 12] Available from: https://vimeo.com/204199082.

200. Medical Enterprises Distrubition LLC. 2017. Controlled Impaction - ME1000 (Promotional Material). [cited 2019 Jan 12] Available from: https://vimeo.com/204198524.

201. DePuy Synthes. 2018. Application of Energy in Total Hip Arthroplasty (Promotional Material). Available from: https://jnjinstitute.com/online-profed-resources/resources/kincisetm-surgical-automated-system-energy-analysis.

202. DePuy Synthes. 2017. Exclusive Co-Marketing Agreement with Medical Enterprises Distribution, LLC to Further Transform Hip Replacement with New Automated Technology. [cited 2019 Jan 12] Available from: https://www.depuysynthes.com/about/news-press/qs/exclusive-co-marketing-agreement-with-medical-enterprises-distribution-llc-to-further-transform-hip-replacement-with-new-automated-technology--.

203. IMT Medical. 2019. What's great about pneumatic broaching with the Woodpecker

(Promotional Material). [cited 2019 Jan 12] Available from: http://www.imt-medical.com/advantages/.

204. IMT Medical. 2019. The Woodpecker, IMT. [cited 2016 Jun 29] Available from: http://www.imt-medicalusa.com/products/woodpecker-hip-broaching-system.aspx.

205. Bolland B, New A, Madabhushi S, et al. 2007. Vibration-assisted bone-graft compaction in impaction bone grafting of the femur. J. Bone Joint Surg. Br. 89(5):686–92 Available from: http://www.ncbi.nlm.nih.gov/pubmed/17540758.

206. Eroglu S. 2012. The Utility of Woodpecker in Total Hip Arthroplasty. Saudi Med J 33:3–8.

207. Branovacki G, Meininger A, Redondo M, et al. 2010. PERIOPERATIVE COMPLICATIONS IN TOTAL HIP ARTHROPLASTY WHEN USING A PNEUMATIC BROACHING SYSTEM FOR ZWEYMULLER-TYPE, SQUARE-TAPERED HIP STEMS. A PROSPECTIVE REVIEW OF 330 CASES USING STEMS FROM EIGHT DIFFERENT MANUFACTURERS. J Bone Jt. Surg Br Vol. 92B(150) Available from: http://www.bjjprocs.boneandjoint.org.uk/content/92-B/SUPP_I/150.3.short.

208. Hourlier H, Fennema P, H, et al. 2008. Pneumatic broaching may prevent massive stem subsidence in femoral revision hip replacement. Interact. Surgery, Springer 3(2):81–87.

209. Goossens Q, Pastrav LC, Leuridan S, et al. 2018. The use of the Woodpecker Instrument to follow up Implant Insertion in Cementless THA: An In-Vitro Study. Orthop. Proc. 99–B(SUPP 2).

210. Daniel J, Ziaee H, Kamali A, et al. 2012. What are the risks accompanying the reduced wear benefit of low-clearance hip resurfacing? Clin. Orthop. Relat. Res. 470(10):2800–2809.

211. Langdown AJ, Pickard RJ, Hobbs CM, et al. 2007. Incomplete seating of the liner with the Trident acetabular system: A CAUSE FOR CONCERN? J. Bone Jt. Surg. - Br. Vol. 89–B(3):291–295 Available from: http://www.bjj.boneandjoint.org.uk/cgi/doi/10.1302/0301-620X.89B3.18473.

212. Benazzo F, Formagnana M, Bargagliotti M, Perticarini L. 2015. Periprosthetic acetabular fractures. Int. Orthop. 39(10):1959–1963 Available from: http://link.springer.com/10.1007/s00264-015-2971-8.

213. Lindberg-larsen M, Jørgensen CC, Solgaard S, Anne G. 2017. Increased risk of intraoperative and early postoperative periprosthetic femoral fracture with uncemented stems Increased risk of intraoperative and early postoperative peri- prosthetic femoral fracture with uncemented stems 7 , 169 total hip arthroplastie. Acta Orthop. 3674(May):8–

13.

214. Thillemann TM, Pedersen AB, Johnsen SøP, Søballe K. 2008. Inferior outcome after intraoperative femoral fracture in total hip arthroplasty. Acta Orthop. 79(3):327–334 Available from: http://www.tandfonline.com/doi/full/10.1080/17453670710015210.

215. Phipps K, Saksena J, Muirhead-Allwood S, et al. 2006. Evaluation of Femoral Impaction Grafting Forces. Bone Joint J. 88–B(Supp 3):373.

216. Schmidig G, Scholl L, Thakore M, Faizain A. 2013. Evaluation of Variability in Head Impaction Forces Among Multiple Orthopaedic Surgeons. Orthop. Res. Soc. (Poster 1708).

217. Danoff JR, Bobman JT, Cunn G, et al. 2016. Redefining the Acetabular Component Safe Zone for Posterior Approach Total Hip Arthroplasty. J. Arthroplasty 31(2):506–511 Available from: http://dx.doi.org/10.1016/j.arth.2015.09.010.

218. Nassutt R, Mollenhauer I, Klingbeil K, et al. 2006. Die Bedeutung der Setzkraft für die Sicherheit einer Konuskopplung von Hüftstiel und keramischem Prothesenkopf / Relevance of the insertion force for the taper lock reliability of a hip stem and a ceramic femoral head. Biomed. Tech. Eng. 51(2):103–109 Available from: http://www.degruyter.com/view/j/bmte.2006.51.issue-2/bmt.2006.018/bmt.2006.018.xml.

219. Brown JM, Borchard DOKS, Robbins CE, et al. 2017. Management and Prevention of Intraoperative Acetabular Fracture in Primary Total Hip Arthroplasty. Am. J. Orthop. 46(5):232–237.

220. Ries M, Harbaugh M, Shea J, Lambert R. 1997. Effect of cementless acetabular cup geometry on strain distribution and press-fit stability. J. Arthroplasty 12(2):207–212.

221. Sundfeldt M, Carlsson L V., Johansson CB, et al. 2006. Aseptic loosening, not only a question of wear: A review of different theories. Acta Orthop. 77(2):177–197.

222. NJR Editorial Board. 2014. National Joint Registry - England, Wales & Northern Island.

223. Doyle R, Boughton O, Plant D, et al. 2019. An in vitro model of impaction during hip arthroplasty. J. Biomech. 82:220–227 Available from: https://linkinghub.elsevier.com/retrieve/pii/S0021929018308078.

224. Arkel RJ Van, Ghouse S, Milner PE, Jeffers JRT. 2018. Additive Manufactured Push-Fit Implant Fixation With Screw-Strength Pull Out. J. Orthop. Res. (May):1508–1518.

225. Fritsche A, Zietz C, Teufel S, et al. 2011. A851. IN-VITRO AND IN-VIVO INVESTIGATIONS OF THE IMPACTION AND PULL-OUT BEHAVIOR OF METAL-

BACKED ACETABULAR CUPS. In: J Bone Joint Surg Br. p 406.

226. Damm NB, Morlock MM, Bishop NE. 2017. Influence of trabecular bone quality and implantation direction on press-fit mechanics. J. Orthop. Res. 35(2):224–233.

227. Shirazi-Adl A, Dammak M, Zukort DJ. 1994. Fixation pull-out response measurement of bone screws and porous-surfaced posts. J. Biomech. 27(10):1249–1258.

228. Howison S. 2005. Asymptotic Expansions. In: Practical Applied Mathematics - Modelling, Analysis, Approxiamation. Cambridge University Press. p 173–180.

229. Winter W, Karl M. 2014. Basic considerations for determining the amount of press fit in acetabular cup endoprostheses as a function of the elastic bone behavior. Biomed. Tech. 59(5):413–420.

230. Bone MC, Dold P, Flohr M, et al. 2015. The influence of the strength of bone on the deformation of acetabular shells A LABORATORY EXPERIMENT IN CADAVERS. Bone Joint J. 97(4):473–477.

231. Wiznia DH, Joyal G, Schmidig, Gregg Rajaravivarma, Raja Lokesh, Raja Schwartzkopf R, et al. 2019. The Effect of Interposed Tissue and Contamination on the Initial Stability of a Highly Porous Press-Fit Acetabular Cup. J. Orthop. Res. In-press.

232. Springer BD, Fehring TK, Griffin WL, et al. 2009. Why Revision Total Hip Arthroplasty Fails. Clin. Orthop. Relat. Res. 467:166–173.

233. Valle CJ Della, Berger RA, Rosenberg AG, Galante JO. 2004. Cementless Acetabular Reconstruction in Revision Total Hip Arthroplasty. Clin. Orthop. Relat. Res. 420(March):96–100.

234. Perona PG, Lawrence J, Paprosky WG, et al. 1992. Acetabular micromotion as a measure of initial implant stability in primary hip arthroplasty. An in vitro comparison of different methods of initial acetabular component fixation. J. Arthroplasty 7(4):537–547.

235. Doyle R. 2019. Hammer Velocities. Vimeo Available from: https://vimeo.com/327435898.

236. IMT Medical. [date unknown]. The Woodpecker [Promotional Leaflet]. Available from: http://www.imt-medical.com/medi/.

237. Goossens Q, Leuridan S, Pastrav L, et al. 2018. Comparison of Cementless THA Stem Insertion using the Woodpecker vs Hammer Blows by Strain and Vibrational Measurements: an In-Vitro Study. Orthop. Proc. (In Press).

238. Doyle R, Boughton O, Desoutter G, et al. 2018. An In-Vitro Model of Impact during Hip

Arthroplasty. J. Biomech. Under Revi.

239. Doyle R, Boughton O, Desoutter G, et al. 2016. Pre-clinical Impaction Testing in Hip Arthoplasty May Not Represent the Clinical Scenario. In: International Society of Technology in Arthroplasty. Boston: Bone & Joint Publishing. p 2049–4416.

240. Bhattacharyya T. 2007. Mortality After Periprosthetic Fracture of the Femur. J. Bone Jt. Surg. 89(12):2658 Available from: http://jbjs.org/cgi/doi/10.2106/JBJS.F.01538.

241. Dumont GD, Zide JR, Huo MH. 2010. Periprosthetic Femur Fractures : Current Concepts and Management. YSART 21(1):9–13 Available from: http://dx.doi.org/10.1053/j.sart.2009.12.013.

242. Knight JL, Helming C. 2000. Collarless Polished Tapered Impaction Grafting of the Femur During Revision Total Hip Arthroplasty Pitfalls of the Surgical Technique and Follow-Up in 31 Cases. J. Arthroplasty 15(2).

243. Fosse L, Rønningen H, Lund-Larsen J, et al. 2004. Impacted bone stiffness measured during construction of morsellised bone samples. J. Biomech. 37(11):1757–1766 Available from: http://linkinghub.elsevier.com/retrieve/pii/S0021929004000545.

244. Vandamme K, Naert I, Geris L, et al. 2007. The effect of micro-motion on the tissue response around immediately loaded roughened titanium implants in the rabbit. Eur. J. Oral Sci. 115(1):21–29.

245. Morlock M, Bunte D, Guhrs J, Bishop N. 2017. Corrosion of the Head-Stem Taper Junction — Are We on the Verge of an Epidemic? HSS J. (13):42–49 Available from: http://dx.doi.org/10.1007/s11420-016-9526-4.

246. Mali S, Gilbert JL. 2015. Correlating Fretting Corrosion and Micromotions in Modular Tapers: Test Method Development and Assessment. ASTM Spec. Tech. Publ. 1591 Implant Modul. :259–282.

247. Langton DJ, Sidaginamale R, Lord JK, et al. 2012. Taper junction failure in large-diameter metal-on-metal bearings. Bone Joint Res. 1(4):56–63 Available from: http://www.pubmedcentral.nih.gov/articlerender.fcgi?artid=3626207&tool=pmcentrez&rendertype=abstract.

248. Nassif NA, Nawabi DH, Stoner K, et al. 2014. Taper Design Affects Failure of Large-head Metal-on-metal Total Hip Replacements. Clin. Orthop. Relat. Res. 472(2):564–571 Available from: http://link.springer.com/10.1007/s11999-013-3115-3.

Appendix

9.1 MATLAB MSD simulation – Effect of mass, spring and dashpot co-efficient

Note: The same code with different variables was used for mass and damping

```
%% Effect of spring

% Prelim
clear all
close all

% Body
figure('units','normalized','outerposition',[0 0 1 1])

for k = [0.1 1 10 100] % Vary K

m = 1;
b = 0;

sys=tf(1,[m b k]); % Create transfer function

F = 1; % Input force shape
I = 1;

SimTime = 2*pi/(sqrt((0.1)/(m))); % Display for 1 oscillation
SampRate = 100;
t=[0:1/SampRate:SimTime]; % Create time vector

u = zeros(length(t),1); % Create input force trace
u(1:SampRate) = F;

[SimOutput]=lsim(sys,u,t);
hold on

plot(t.',SimOutput)
end

% Format
xlabel('Time (Seconds)','FontSize',22)
set(gca,'FontSize',20,'LineWidth',1.5)
ylabel('Displacement (m)','FontSize',22)
legend('k = 0.1 N/m','k = 1 N/m','k = 10 N/m','k = 100
N/m','Location','NorthEast','FontSize',20)
```

9.2 MATLAB MSD simulation – Effect of loading time

```
%% Effect on energy transfer

% Prelim
clear all
close all

% Body
figure('units','normalized','outerposition',[0 0 1 1])
i=1;

for LoadingPercent = [0.05:0.05:1]

k =1;
m = 1;
b = 0;

sys=tf(1,[m b k]); % Create transfer function

I = 1; % Maintain const. impulse
LoadingPeriod = 6.28*LoadingPercent; % LoadingTime in sec
F = 1/LoadingPeriod; % Calulate F

SimTime = 2*pi/(sqrt((1)/(m))); % Display for 1 oscillation
SampRate = 100;
t=[0:1/SampRate:SimTime]; % Create time vector

u = zeros(length(t),1);
u(1:LoadingPeriod*SampRate) = F; % Create load signal

[SimOutput]=lsim(sys,u,t);

x(i)=max(SimOutput) % Record max displacement

i=i+1;
end

LoadingPercent = [0.05:0.05:1];
plot(LoadingPercent,x.^2,'k'); % ^2 to convert to energy
```

9.3 Load cell details

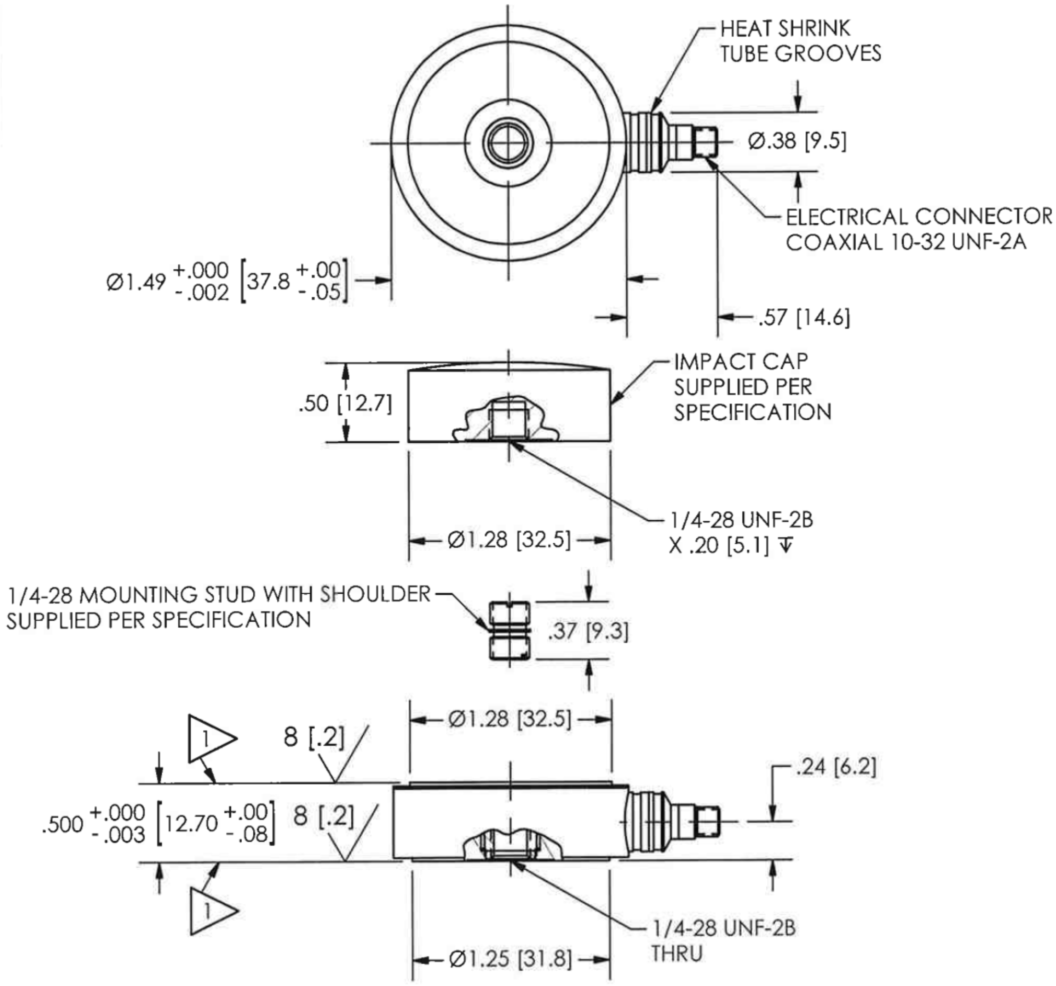

Appendix 9.3.1: Load cell and supplied strike surface drawings (PCB 200C20)

Load cell details

CALIBRATION CERTIFICATE

Model: 200C20
Serial #: 6754
Description: Force Sensor
Type: ICP

Sensitivity*: 0.2515 mV/LBF
0.0565 mV/N

Linearity*: 0.7% FS
Uncertainty:** +/- 1 %

Date: 5/4/2016
By: Fran Coleman, Cal. Tech.
Station: 0-100.000 lb Load Cell (Test Procedure AT501-7)

Temp: 74 deg F [23deg C]
Humidity: 53 %

Cert #: 607731

Bias: 10.13 VDC

* Zero based, least-squares straight line.
** Measurement uncertainty represented using a coverage factor of k=2 which provides a level of confidence of approximately 95 %.

Condition of Unit:
As Found: Not applicable
As Left: In tolerance, new unit

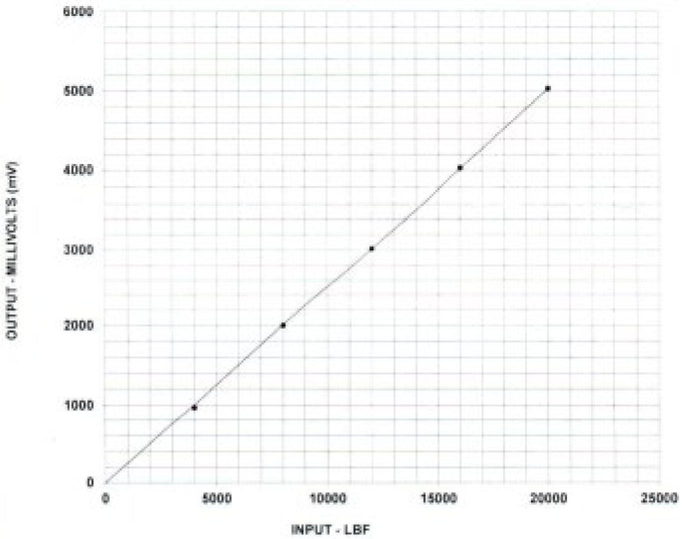

TEST DATA

INPUT (LBF)	OUTPUT (mV)
4000	972
8000	2002
12000	3019
16000	4031
20000	5034

Notes:
1 Station # 26
2 Calibration is traceable to NIST and is accredited to ISO 17025 and ANSI/NCSL Z540.3.
3 NIST traceability through PCB control # KE051.
4 This certificate may not be reproduced, except in full, without written approval from PCB Piezotronics, Inc.

ACCREDITED
CALIBRATION CERT #1862.01

PCB PIEZOTRONICS
Tel: 716-684-0001 Fax: 716-684-0987 Email: sales@pcb.com
3425 Walden Avenue, Depew NY 14043

ISO 9001 CERTIFIED

Page 1 of 1

Appendix 9.3.2: Load cell calibration certificate (PCB 200C20)

Model Number 200C20	ICP® FORCE SENSOR	Revision: F ECN #: 30055

Performance	ENGLISH	SI	
Sensitivity(± 15 %)	0.25 mV/lb	56.2 mV/kN	
Measurement Range(Compression)	20,000 lb	88.96 kN	
Maximum Static Force(Compression)	30,000 lb	133.44 kN	
Broadband Resolution(1 to 10,000 Hz)	0.30 lb-rms	1.3 N-rms	[2]
Low Frequency Response(-5 %)	0.0003 Hz	0.0003 Hz	[3]
Upper Frequency Limit	40 kHz	40 kHz	[4]
Non-Linearity	≤1 % FS	≤1 % FS	[5]
Environmental			
Temperature Range	-65 to +250 °F	-54 to +121 °C	
Temperature Coefficient of Sensitivity	≤0.08 %/°F	≤0.144 %/°C	
Electrical			
Discharge Time Constant(at room temp)	≥2000 sec	≥2000 sec	
Excitation Voltage	20 to 30 VDC	20 to 30 VDC	[1]
Constant Current Excitation	2 to 20 mA	2 to 20 mA	
Output Impedance	≤100 ohm	≤100 ohm	
Output Bias Voltage	8 to 14 VDC	8 to 14 VDC	
Spectral Noise(1 Hz)	0.039 lb/√Hz	0.17 N/√Hz	[2]
Spectral Noise(10 Hz)	0.012 lb/√Hz	0.054 N/√Hz	[2]
Spectral Noise(100 Hz)	0.0034 lb/√Hz	0.015 N/√Hz	[2]
Spectral Noise(1 kHz)	0.00088 lb/√Hz	0.0039 N/√Hz	[2]
Output Polarity(Compression)	Positive	Positive	
Physical			
Stiffness	63 lb/µin	11 kN/µm	[2]
Size (Diameter x Height)	1.5 in x 0.5 in	38.1 mm x 12.7 mm	
Weight	3.1 oz	88 gm	
Housing Material	Stainless Steel	Stainless Steel	
Sealing	Hermetic	Hermetic	
Electrical Connector	10-32 Coaxial Jack	10-32 Coaxial Jack	
Electrical Connection Position	Side	Side	
Mounting Thread	1/4-28 Female	Not Applicable	

CE [6]

All specifications are at room temperature unless otherwise specified.
In the interest of constant product improvement, we reserve the right to change specifications without notice.

ICP® is a registered trademark of PCB Group, Inc.

OPTIONAL VERSIONS

Optional versions have identical specifications and accessories as listed for the standard model except where noted below. More than one option may be used.

N - Negative Output Polarity		
Output Polarity(Compression)	Negative	Negative
W - Water Resistant Cable		
Electrical Connector	Sealed Cable	Sealed Cable
Electrical Connection Position	Side	Side

NOTES:
[1] Minimum 25 VDC required for maximum output voltage.
[2] Typical.
[3] Calculated from discharge time constant.
[4] Estimated using rigid body dynamics calculations.
[5] Zero-based, least-squares, straight line method.
[6] See PCB Declaration of Conformance PS023 for details.

SUPPLIED ACCESSORIES:
Model 080A81 Thread Locker (1)
Model 081A06 Mounting stud, 1/4-28 to 1/4-28 x .37 in. long, BeCu, no shoulder (1)
Model 081B20 Mounting Stud, with shoulder (1/4-28 to 1/4-28) (1)
Model 084B23 Impact cap, convex (for Model 200C20) (1)
Model M081A61 Mounting Stud 1/4-28 to M6 X 1 (1)

Entered: BS	Engineer: BH	Sales: RNM	Approved: EB	Spec Number:
Date: 2/10/09	Date: 2/4/09	Date: 2/4/09	Date: 2/9/09	5889

PCB PIEZOTRONICS
FORCE / TORQUE DIVISION
3425 Walden Avenue, Depew, NY 14043

Phone: 716-684-0001
Fax: 716-684-8877
E-Mail: force@pcb.com

Appendix 9.3.3: Load cell specification (PCB 200C20) including stiffness and max acquisition frequency

9.4 Figure licensing

Appendix 9.3.1: Licensing agreements for the reproduction of images not created by the author of this thesis

Order Date	**Article Title**	**Publication**	**Figure**	**Type of use**	**Order Status**	**License Number**
Mar 31, 2019	Periprosthetic Fracture of the Acetabulum after Total Hip Arthroplasty	Journal of Bone and Joint Surgery	1c	Reuse in a thesis/dissertation	Completed	4559361128070
Mar 31, 2019	Load transfer and fixation mode of press-fit acetabular sockets	Journal of Arthroplasty	6	Reuse in a thesis/dissertation	Completed	4559420642011
Mar 31, 2019	Impact biomechanics and pelvic deformation during insertion of press-fit acetabular cups	Journal of Arthroplasty	4, 5	Reuse in a thesis/dissertation	Completed	4559470066946
Mar 31, 2019	Does surface roughness influence the primary stability of acetabular cups? A numerical and experimental biomechanical evaluation	Journal of Arthroplasty	4	Reuse in a thesis/dissertation	Completed	4559491097169
Apr 1, 2019	Press-fit stability of uncemented hemispheric acetabular components: a comparison of three porous coating systems	International Orthopaedics	2	Reuse in a thesis/dissertation	Completed	4560130345927
Apr 1, 2019	Experimental investigations of the insertion and deformation behavior of press-fit and threaded acetabular cups for total hip replacement	Journal of Orthopaedic Science	2	Reuse in a thesis/dissertation	Completed	4560150028787
Apr 1, 2019	Finite element model of the impaction of a press-fitted acetabular cup	Medical & Biological Engineering & Computing	6	Reuse in a thesis/dissertation	Completed	4560160010131
Apr 1, 2019	Photoelastic Analysis of Stresses Produced by Different Acetabular Cups	Clinical Orthopaedics and Related Research	3, 5	Reuse in a thesis/dissertation	Completed	4560160369653
Apr 1, 2019	Incidence and Natural Course of Initial Polar Gaps in Birmingham Hip Resurfacing Cups	The Journal of Arthroplasty	5A	Reuse in a thesis/dissertation	Completed	4560201322669
Apr 1, 2019	Chapter 10 - Biomechanical Testing of the Intact and Surgically Treated Pelvis	Experimental Methods in Orthopaedic Biomechanics	4	Reuse in a thesis/dissertation	Completed	4560221501515

All images not cited here are either licensed under the creative-commons attribution license (CC-BY-NC 4.0) or were produced by the author

9.5 Ethical approval

Imperial College Healthcare Tissue Bank
Department of Surgery and Cancer
Charing Cross Hospital
Fulham Palace Road
London W6 8RF
Tel: 0203 311 7173
Email: tissuebank@imperial.ac.uk

ICHTB HTA licence: 12275
REC Wales approval: 17/WA/0161

Dr Jonathan Jeffers
Mechanical Engineering Department
Imperial College London
South Kensington Campus
London
SW7 2AZ

22nd December 2017

Dear Dr Jeffers

Re: Tissue Bank application number; R15022-4A

Project title; Physiological load transfer in hip and knee replacement

I am pleased to confirm that the Imperial College Healthcare Tissue Bank Review Committee has received and approved the following amendment for the above mentioned project;

Amendment 4A

- Title of project now includes 'and knee'.
- Knee specimens added (bought from Science Care Inc, United States of America) for research into bi-compartmental arthroplasty configurations compared to total knee replacement.
- The project will support a research degree (MD Research).

In order to satisfy HTA tracking requirements, would you please ensure the samples you use are reported to the tissue bank via the online database and sub-collection, along with any publications you produce, that should contain the acknowledgment wording as per the signed MTA.

Yours sincerely,

Professor Gerry Thomas
DI, HTA Research Licence.

Appendix 9.5.1: Ethical approval for cadaveric experiments

9.6 DIC testing

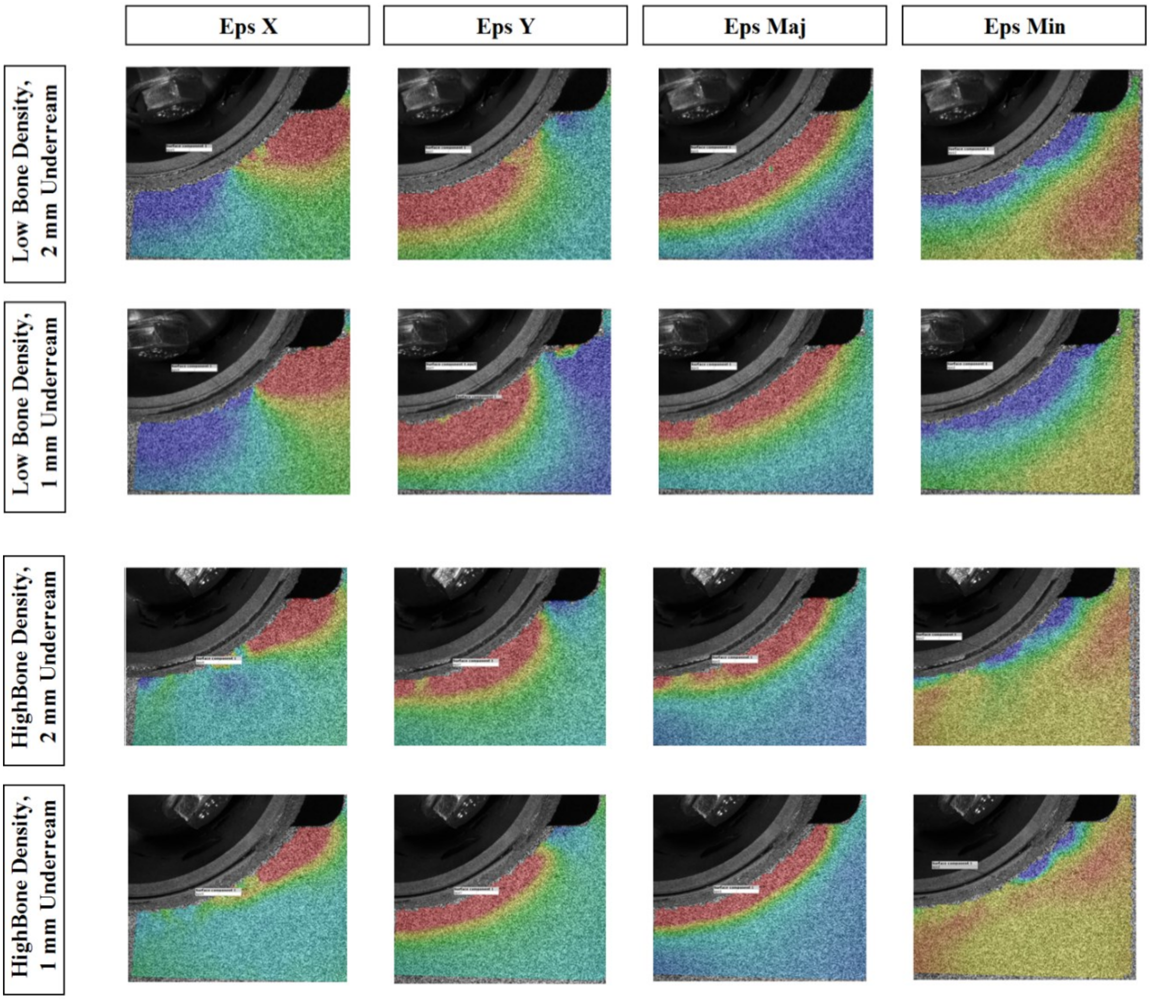

Appendix 9.6.1: Strain field during implant insertion in synthetic bone model

9.7 Traditional impact strikes: Raw data

9.7.1 Specification labels

Appendix 9.7.1: Description of specification labels and associated impact parameters

			Impact Parameters		
Specification	**Bone Density (PCF)**	**Cup Size (mm)**	**Mass (kg)**	**Velocity (m/s)**	**Energy (J)**
1	15	55	0.6	1.5	0.68
2			1.2	1.5	1.35
3			1.8	1.5	2.03
4			0.6	2.75	2.27
5			1.2	2.75	4.54
6			1.8	2.75	6.81
7			0.6	4	4.80
8			1.2	4	9.60
9			1.8	4	14.40
10	30	54	0.6	1.5	0.68
11			1.2	1.5	1.35
12			1.8	1.5	2.03
13			0.6	2.75	2.27
14			1.2	2.75	4.54
15			1.8	2.75	6.81
16			0.6	4	4.80
17			1.2	4	9.60
18			1.8	4	14.40

9.7.2 Impact parameters

Appendix 9.7.2: Peak strike force (mean with standard deviation) for each impact specification

Peak Strike Force (N)

		Spec								
	Strike	**1**	**2**	**3**	**4**	**5**	**6**	**7**	**8**	**9**
Avg	1	3762	4904	4830	7109	8732	10513	10241	14363	17056
	2	3904	5055	5470	7335	8846	10748	10720	14294	19055
	3	3935	5106	5751	7125	8933	11798	10903	14136	19336
	4	3910	5160	5778	7215	9036	12722	11058	13906	19659
	5	3919	5150	5730	7078	9001	13041	10917	13791	20232
	6	3911	5138	5920	7152	8795	13159	10415	13735	19498
	7	3935	5397	6065	7106	8750	13519	10272	14551	19882
	8	3908	5194	6271	7180	8677	13465	11149	14587	20065
	9	3899	5111	6410	7118	8861	13348	10926	14340	19867
	10	3910	5141	6274	7142	9022	13700	11035	14437	20529
Std	1	299	270	838	689	505	823	368	2092	892
	2	437	463	445	643	546	729	936	2063	1040
	3	400	384	437	418	475	750	356	1876	541
	4	420	409	424	697	565	742	487	2000	614
	5	362	347	417	557	671	674	348	2006	1601
	6	379	354	255	630	912	836	643	2003	1242
	7	485	228	269	488	850	789	248	1855	1151
	8	486	428	621	533	938	1009	402	1861	755
	9	449	425	644	629	757	997	548	2400	804
	10	545	392	863	737	592	1236	682	2334	1689

		Spec								
	Strike	**10**	**11**	**12**	**13**	**14**	**15**	**16**	**17**	**18**
Avg	1	4163	5493	7237	7570	9407	13369	11698	14592	17880
	2	4266	5596	7572	7670	9289	14179	11738	14899	19273
	3	4226	5797	7634	7772	9342	14104	11558	14757	20233
	4	4224	5676	7628	7678	9368	15259	11735	14605	20908
	5	4234	5649	7705	7795	9380	15621	11606	15202	21080
	6	4161	5690	7718	7786	9314	15722	11680	15077	21227
	7	4218	5687	7716	7739	9364	15748	11691	15543	21216
	8	4223	5689	7739	7812	9309	15896	11578	15329	21211
	9	4242	5715	7809	7870	9199	15904	11671	15156	21226
	10	4228	5618	7812	7684	9302	15959	11603	15074	21267
Std	1	414	221	824	323	365	426	344	1013	938
	2	449	298	580	239	411	867	265	1071	915
	3	431	368	484	101	460	981	533	1096	1091
	4	405	270	424	236	421	1095	174	1214	635
	5	499	387	490	37	354	1120	316	1388	519
	6	426	238	452	161	327	1105	174	1364	585
	7	413	266	441	296	377	1055	218	1531	576
	8	455	263	461	140	414	1243	396	1602	643
	9	397	267	400	79	434	1121	194	1481	704
	10	418	239	475	294	438	1141	438	1391	624

Appendix 9.7.3: Impulse (mean with standard deviation) for each impact specification

Impulse (Ns)

		Spec								
	Strike	**1**	**2**	**3**	**4**	**5**	**6**	**7**	**8**	**9**
Avg	1	0.76	1.81	2.39	1.52	3.39	4.56	2.19	5.16	7.75
	2	0.91	2.08	3.08	1.60	3.68	6.15	2.15	5.93	8.74
	3	0.91	2.16	3.30	1.65	4.13	6.46	2.40	5.94	8.78
	4	0.95	2.19	3.53	1.70	4.26	6.46	2.47	6.06	8.65
	5	0.94	2.28	3.72	1.72	4.32	6.45	2.49	5.97	8.52
	6	0.97	2.35	3.79	1.77	4.23	6.49	2.46	6.00	8.62
	7	0.96	2.42	3.81	1.77	4.20	6.49	2.45	6.02	8.72
	8	0.98	2.38	3.73	1.77	4.04	6.45	2.36	6.03	8.80
	9	0.97	2.41	3.77	1.78	4.32	6.45	2.49	6.00	8.69
	10	0.99	2.43	3.78	1.79	4.31	6.51	2.33	5.90	8.65
Std	1	0.21	0.20	0.27	0.17	0.08	0.28	0.14	0.40	0.28
	2	0.14	0.18	0.08	0.13	0.14	0.19	0.17	0.29	0.53
	3	0.12	0.10	0.19	0.09	0.23	0.16	0.13	0.16	0.50
	4	0.12	0.14	0.13	0.08	0.14	0.15	0.16	0.19	0.84
	5	0.12	0.12	0.11	0.06	0.12	0.20	0.12	0.18	0.74
	6	0.11	0.12	0.13	0.06	0.38	0.13	0.15	0.21	0.45
	7	0.11	0.12	0.12	0.06	0.49	0.12	0.11	0.15	0.39
	8	0.10	0.11	0.15	0.06	0.90	0.16	0.20	0.81	0.45
	9	0.10	0.12	0.11	0.06	0.23	0.13	0.09	0.18	0.34
	10	0.11	0.11	0.07	0.05	0.23	0.09	0.21	0.10	0.23

		Spec								
	Strike	**10**	**11**	**12**	**13**	**14**	**15**	**16**	**17**	**18**
Avg	1	0.88	1.84	2.59	1.47	3.52	4.82	2.25	5.46	7.43
	2	0.90	1.95	2.97	1.48	3.57	5.95	2.18	5.85	8.93
	3	0.96	2.11	3.18	1.69	3.96	6.30	2.69	6.32	9.41
	4	0.97	2.14	3.33	1.72	4.02	6.43	2.74	6.34	9.43
	5	1.03	2.21	3.47	1.79	4.24	6.43	2.77	6.43	9.48
	6	1.03	2.30	3.59	1.82	4.27	6.38	2.78	6.43	9.49
	7	1.04	2.36	3.66	1.87	4.31	6.39	2.79	6.34	9.48
	8	1.05	2.37	3.68	1.88	4.30	6.42	2.77	6.44	9.51
	9	1.08	2.44	3.70	1.89	4.36	6.36	2.79	6.43	9.56
	10	1.07	2.39	3.69	1.90	4.29	6.39	2.79	6.44	9.56
Std	1	0.16	0.26	0.23	0.30	0.19	0.36	0.26	0.39	0.43
	2	0.08	0.16	0.19	0.25	0.36	0.16	0.18	0.43	0.49
	3	0.08	0.24	0.21	0.27	0.29	0.24	0.31	0.38	0.50
	4	0.12	0.27	0.23	0.30	0.16	0.30	0.12	0.52	0.51
	5	0.12	0.28	0.19	0.30	0.18	0.35	0.17	0.47	0.39
	6	0.08	0.25	0.20	0.33	0.16	0.36	0.21	0.45	0.39
	7	0.09	0.23	0.17	0.28	0.14	0.37	0.21	0.46	0.40
	8	0.11	0.24	0.18	0.31	0.14	0.36	0.19	0.45	0.45
	9	0.10	0.22	0.17	0.28	0.23	0.34	0.19	0.43	0.37
	10	0.09	0.27	0.17	0.29	0.11	0.31	0.20	0.43	0.36

Appendix 9.7.4: Velocity (mean with standard deviation) for each impact specification

		Velocity (m/s)								
		Spec								
	Strike	1	2	3	4	5	6	7	8	9
Avg	1	1.58	1.55	1.51	2.82	2.81	2.76	4.01	4.02	4.04
	2	1.58	1.55	1.52	2.81	2.82	2.76	4.02	4.03	4.05
	3	1.57	1.55	1.56	2.80	2.81	2.77	3.94	4.04	4.04
	4	1.57	1.56	1.55	2.78	2.81	2.77	4.04	4.03	4.04
	5	1.58	1.56	1.54	2.77	2.81	2.76	4.02	4.02	4.04
	6	1.57	1.57	1.55	2.79	2.80	2.78	4.03	4.03	4.04
	7	1.57	1.57	1.55	2.80	2.80	2.77	4.00	4.03	4.05
	8	1.57	1.57	1.55	2.78	2.80	2.79	4.01	4.05	4.05
	9	1.57	1.56	1.55	2.78	2.80	2.76	4.05	4.03	4.04
	10	1.56	1.56	1.53	2.78	2.81	2.78	4.00	3.99	4.05
Std	1	0.03	0.03	0.03	0.07	0.04	0.04	0.08	0.04	0.03
	2	0.03	0.04	0.03	0.06	0.04	0.03	0.08	0.05	0.03
	3	0.02	0.03	0.01	0.03	0.01	0.01	0.16	0.02	0.02
	4	0.02	0.01	0.01	0.03	0.01	0.03	0.09	0.04	0.03
	5	0.02	0.01	0.02	0.02	0.01	0.02	0.10	0.03	0.03
	6	0.02	0.02	0.02	0.01	0.01	0.02	0.10	0.05	0.01
	7	0.02	0.01	0.01	0.02	0.01	0.01	0.09	0.03	0.02
	8	0.03	0.02	0.02	0.03	0.01	0.02	0.07	0.04	0.03
	9	0.02	0.01	0.01	0.02	0.01	0.03	0.12	0.04	0.03
	10	0.01	0.02	0.02	0.01	0.01	0.02	0.07	0.06	0.03

		Spec								
	Strike	10	11	12	13	14	15	16	17	18
Avg	1	1.56	1.53	1.51	2.73	2.78	2.76	4.01	4.00	3.97
	2	1.57	1.52	1.51	2.75	2.77	2.76	4.05	4.00	4.00
	3	1.56	1.54	1.51	2.74	2.77	2.75	4.01	4.00	4.00
	4	1.56	1.54	1.52	2.75	2.78	2.75	4.02	4.01	3.99
	5	1.56	1.52	1.52	2.74	2.77	2.76	3.99	4.00	3.98
	6	1.56	1.54	1.52	2.76	2.77	2.76	4.00	4.02	3.98
	7	1.56	1.54	1.52	2.75	2.77	2.75	4.00	4.01	3.99
	8	1.56	1.54	1.52	2.75	2.77	2.75	3.99	4.01	3.98
	9	1.55	1.53	1.53	2.76	2.78	2.76	4.00	4.00	3.99
	10	1.56	1.53	1.52	2.76	2.77	2.76	4.00	4.00	3.98
Std	1	0.06	0.02	0.04	0.05	0.04	0.04	0.07	0.02	0.07
	2	0.02	0.02	0.04	0.02	0.03	0.03	0.07	0.02	0.07
	3	0.03	0.02	0.03	0.03	0.03	0.02	0.07	0.02	0.06
	4	0.02	0.03	0.02	0.02	0.04	0.03	0.05	0.02	0.07
	5	0.03	0.03	0.02	0.03	0.04	0.01	0.05	0.03	0.08
	6	0.03	0.02	0.03	0.02	0.03	0.01	0.02	0.03	0.06
	7	0.03	0.02	0.02	0.03	0.04	0.01	0.04	0.02	0.07
	8	0.02	0.02	0.02	0.03	0.04	0.01	0.03	0.01	0.06
	9	0.03	0.00	0.02	0.02	0.03	0.02	0.04	0.01	0.06
	10	0.03	0.02	0.00	0.02	0.04	0.01	0.04	0.03	0.07

9.7.3 Strains

Appendix 9.7.5: Peak tensile bone strain (mean with standard deviation) for each impact specification

Peak Tensile Bone Strain (με)

	Strike	**Spec 1**	**2**	**3**	**4**	**5**	**6**	**7**	**8**	**9**
Avg	1	188.2	268.2	355.3	347.2	370.2	422.9	373.1	551.3	475.7
	2	210.9	307.3	448.8	349.7	418.0	456.7	409.2	642.4	601.2
	3	241.7	354.3	500.1	443.8	518.6	535.3	571.7	537.0	499.1
	4	249.1	359.4	517.3	463.4	504.8	549.8	544.5	481.6	390.4
	5	256.7	381.2	518.8	446.4	507.0	471.5	448.2	426.5	272.3
	6	272.4	396.1	497.9	442.1	485.1	400.2	415.3	390.1	202.1
	7	238.4	400.7	492.8	425.1	467.6	369.4	366.9	377.9	109.9
	8	237.3	397.8	498.7	411.0	440.0	335.5	335.8	299.8	62.0
	9	239.4	397.3	507.4	406.2	378.0	301.9	289.2	268.9	42.6
	10	229.7	394.0	516.0	394.5	359.6	273.4	264.7	247.7	25.9
Std	1	9.5	25.7	20.7	29.6	31.1	88.2	61.5	49.7	71.0
	2	7.7	38.0	75.7	28.5	52.6	125.9	132.9	75.2	155.8
	3	12.2	23.1	78.2	46.8	80.0	139.7	32.3	59.6	66.8
	4	36.9	16.2	60.5	44.6	88.1	156.6	30.3	91.1	53.7
	5	16.7	38.1	67.0	37.4	84.4	134.9	117.7	113.7	57.4
	6	21.3	46.7	75.3	38.3	79.5	111.7	104.3	141.4	63.3
	7	37.9	40.6	88.8	42.5	68.7	115.2	113.0	203.0	45.9
	8	26.1	32.8	103.2	37.1	68.5	107.7	103.5	147.3	52.5
	9	22.5	33.2	105.7	35.8	56.8	100.8	88.3	125.9	43.7
	10	18.1	39.5	111.2	47.0	71.8	99.1	92.0	138.0	58.3

	Strike	**Spec 10**	**11**	**12**	**13**	**14**	**15**	**16**	**17**	**18**
Avg	1	195.6	298.7	325.1	300.9	397.0	501.9	403.5	502.8	552.9
	2	263.1	321.2	461.8	328.0	630.0	494.2	513.6	479.3	517.1
	3	299.7	405.6	519.3	408.1	726.8	499.0	538.5	420.1	472.7
	4	308.4	428.1	535.5	425.9	641.8	488.0	532.7	389.6	460.2
	5	318.4	440.8	532.6	423.9	585.4	480.3	501.5	378.6	430.3
	6	321.0	450.9	527.8	437.9	564.3	476.1	469.1	370.6	406.5
	7	320.7	453.4	508.8	427.5	550.8	471.4	450.4	369.9	422.8
	8	329.5	451.2	491.5	400.7	537.8	425.6	436.6	358.1	401.1
	9	325.4	440.6	480.3	390.9	529.6	461.4	430.1	351.6	393.4
	10	317.4	424.3	472.7	377.1	521.8	456.0	423.9	348.7	400.4
Std	1	46.9	27.2	42.6	38.4	73.4	33.6	72.5	91.3	43.8
	2	69.4	28.6	43.4	87.1	93.2	89.3	99.0	135.5	155.8
	3	89.1	26.1	55.8	119.8	89.6	116.5	99.2	147.6	152.8
	4	106.5	44.8	57.2	129.4	48.4	120.5	96.6	137.5	145.5
	5	110.3	53.9	63.4	146.0	54.4	119.0	77.7	135.7	125.6
	6	113.9	60.3	74.1	146.5	58.5	118.1	77.1	134.9	114.4
	7	111.4	71.0	72.2	146.0	62.9	116.7	77.9	136.2	113.1
	8	112.3	78.7	69.4	145.3	65.3	68.3	76.2	131.5	109.4
	9	112.2	81.4	67.1	140.4	65.5	115.3	77.0	129.2	109.8
	10	116.6	79.0	64.6	135.7	66.3	114.1	75.3	128.5	116.2

Appendix 9.7.6: Post-strike tensile bone strain (mean with standard deviation) for each impact specification

Post-strike Tensile Bone Strain (με)

	Strike	Spec 1	2	3	4	5	6	7	8	9
Avg	1	106.5	179.7	228.0	214.7	215.3	261.4	220.7	292.1	233.1
	2	138.1	198.6	290.7	255.7	267.1	266.6	252.1	228.7	128.7
	3	159.2	229.8	331.5	250.9	252.0	218.3	205.8	64.1	0.0
	4	150.6	241.3	315.8	223.8	207.6	164.8	130.8	19.6	0.0
	5	149.3	239.2	299.5	201.7	166.5	113.8	68.2	7.2	0.0
	6	115.2	222.0	276.9	182.6	136.9	63.7	65.4	0.0	0.0
	7	99.3	214.9	250.0	165.3	114.5	69.9	0.0	0.0	0.0
	8	92.4	202.4	226.1	152.9	96.1	0.0	0.0	0.0	0.0
	9	81.8	194.2	210.1	139.2	69.5	0.0	0.0	0.0	0.0
	10	78.1	183.6	196.4	133.1	53.3	0.0	0.0	0.0	0.0
Std	1	18.7	29.5	41.4	10.3	25.1	62.2	32.1	35.5	83.3
	2	10.7	39.1	48.7	28.3	32.2	73.8	51.2	77.4	118.6
	3	18.7	33.3	49.6	32.3	37.3	74.6	26.6	140.9	41.1
	4	17.2	7.8	55.6	26.0	35.3	61.5	117.3	112.2	36.9
	5	28.7	28.5	65.2	20.2	39.8	79.0	61.4	105.3	43.2
	6	12.9	34.7	61.0	23.2	54.3	93.4	68.6	97.5	46.9
	7	38.3	36.9	54.7	20.1	72.7	59.3	19.0	91.1	51.1
	8	21.7	35.6	50.4	25.7	82.4	62.1	85.8	86.4	51.6
	9	24.7	40.6	48.4	26.8	88.3	46.0	58.0	81.9	52.6
	10	25.6	42.9	48.7	27.2	82.4	38.9	76.0	76.7	51.9

	Strike	Spec 10	11	12	13	14	15	16	17	18
Avg	1	138.7	217.0	264.5	187.1	286.6	366.0	269.0	356.6	360.2
	2	200.4	265.3	374.9	258.9	440.4	399.9	372.8	362.7	342.4
	3	215.7	307.4	411.2	267.6	496.1	375.6	420.8	337.0	296.8
	4	222.2	315.9	439.6	305.1	479.9	351.1	429.7	310.5	274.2
	5	232.8	326.3	446.7	321.3	442.0	335.8	415.0	299.2	254.3
	6	233.8	342.4	437.0	334.5	418.3	324.7	391.6	290.5	240.0
	7	231.3	341.0	415.0	325.4	401.3	315.6	377.2	282.2	234.5
	8	232.2	339.3	398.7	314.1	387.9	315.1	366.9	276.5	220.7
	9	228.8	347.8	386.2	299.9	377.3	302.1	359.5	270.6	208.8
	10	224.4	309.7	376.2	286.3	369.3	298.9	350.3	265.0	195.3
Std	1	35.5	27.2	42.6	38.4	73.4	33.6	75.3	74.8	40.2
	2	56.2	28.6	43.4	87.1	93.2	89.3	83.4	122.8	100.2
	3	79.2	26.1	55.8	119.8	89.6	116.5	89.8	135.6	108.5
	4	94.7	44.8	57.2	129.4	48.4	120.5	92.6	127.3	109.0
	5	98.2	53.9	63.4	146.0	54.4	119.0	79.7	125.1	112.2
	6	107.6	60.3	74.1	146.5	58.5	118.1	81.4	124.1	115.0
	7	105.9	71.0	72.2	146.0	62.9	116.7	81.4	124.0	111.4
	8	106.1	78.7	69.4	145.3	65.3	68.3	80.9	120.7	119.6
	9	102.1	82.0	67.1	140.4	65.5	115.3	81.1	119.1	126.1
	10	106.1	79.0	64.6	135.7	66.3	114.1	79.8	117.9	132.5

Appendix 9.7.7: Peak compressive bone strain (mean with standard deviation) for each impact specification

Peak Compressive Bone Strain (με)

	Spec									
	Strike	**1**	**2**	**3**	**4**	**5**	**6**	**7**	**8**	**9**
Avg	1	-138.0	-79.1	-123.7	-60.5	-157.0	-201.7	-248.0	-260.0	-444.9
	2	-181.5	-94.7	-179.5	-118.6	-209.0	-362.9	-276.2	-424.2	-639.0
	3	-201.5	-125.7	-225.3	-178.4	-312.7	-483.0	-366.6	-513.5	-722.7
	4	-221.8	-156.3	-303.8	-188.2	-371.6	-530.0	-374.3	-544.2	-728.0
	5	-227.1	-180.8	-351.2	-191.0	-420.5	-526.1	-410.7	-566.2	-778.2
	6	-246.7	-200.9	-401.0	-214.3	-440.1	-511.2	-422.6	-592.2	-862.2
	7	-223.2	-213.1	-446.2	-227.6	-450.4	-511.3	-446.1	-602.2	-949.6
	8	-199.1	-228.2	-484.2	-248.5	-448.3	-529.3	-465.1	-630.4	-997.9
	9	-206.6	-240.6	-505.2	-262.6	-452.9	-532.8	-483.0	-639.9	-1017.5
	10	-206.8	-257.9	-519.0	-265.7	-458.3	-559.4	-475.9	-662.0	-1049.7
Std	1	145.5	44.2	25.6	35.3	80.8	69.4	165.7	49.4	60.5
	2	158.3	65.2	38.7	50.2	88.2	90.7	121.6	56.5	77.0
	3	164.1	83.9	27.4	38.3	104.0	153.8	97.3	74.7	36.0
	4	173.3	69.9	39.5	49.2	102.0	175.7	60.0	89.0	96.4
	5	175.4	70.7	46.0	55.1	89.6	148.7	74.0	83.0	107.2
	6	175.2	80.8	30.8	46.3	91.2	158.4	94.7	63.9	132.0
	7	117.3	96.6	47.2	51.1	89.7	131.4	73.3	52.4	135.2
	8	51.0	93.8	51.7	53.2	94.2	147.0	75.2	39.6	133.7
	9	47.3	89.6	52.1	55.3	94.0	146.0	62.7	37.6	133.3
	10	57.9	97.1	55.2	55.0	98.0	147.8	68.4	44.1	115.6

	Spec									
	Strike	**10**	**11**	**12**	**13**	**14**	**15**	**16**	**17**	**18**
Avg	1	-6.1	-10.7	-3.6	-10.2	-85.7	-11.0	-1.5	-2.9	-66.5
	2	-1.5	5.3	53.6	0.9	-28.1	11.5	97.8	-37.7	-217.5
	3	-10.7	11.1	45.0	-6.8	-14.0	-92.3	68.9	-217.6	-340.1
	4	-5.9	6.4	38.3	-8.4	-59.7	-168.8	41.0	-259.3	-355.8
	5	-5.7	-0.1	17.5	-12.8	-123.1	-177.6	6.4	-279.3	-373.5
	6	-7.1	-0.2	-19.7	-24.7	-149.6	-184.9	-9.4	-284.7	-384.0
	7	-10.6	-5.5	-56.7	-32.0	-168.1	-189.5	-17.1	-277.3	-388.8
	8	-6.9	-23.2	-71.7	-46.9	-180.9	-200.9	-24.3	-293.7	-390.0
	9	-4.0	-32.7	-84.3	-55.6	-189.5	-199.0	-32.7	-296.6	-401.6
	10	-16.6	-59.3	-94.3	-61.1	-198.5	-202.1	-40.3	-299.9	-402.6
Std	1	2.6	4.6	0.7	3.6	76.2	2.2	0.1	3.4	61.2
	2	29.6	24.8	38.5	44.0	110.4	76.6	54.1	70.1	68.9
	3	53.1	48.5	54.8	80.9	112.6	102.7	51.6	77.7	67.9
	4	72.0	64.2	54.9	97.3	87.2	107.4	62.3	76.9	79.3
	5	74.2	74.9	52.7	112.1	75.9	104.4	55.5	74.4	86.7
	6	76.8	83.4	53.6	115.0	81.5	100.7	63.7	72.0	94.9
	7	75.5	92.2	55.6	116.9	84.6	96.5	65.1	106.7	103.3
	8	77.0	97.3	50.6	122.0	86.5	77.0	65.4	69.0	105.9
	9	79.0	88.7	48.4	117.9	87.8	114.6	64.7	66.1	111.5
	10	82.6	90.4	45.5	114.7	89.7	90.4	65.1	64.6	115.8

Appendix 9.7.8: Post-strike compressive cup strain (mean with standard deviation) for each impact specification

		Post-strike Compressive Cup Strain (με)								
		Spec								
	Strike	**1**	**2**	**3**	**4**	**5**	**6**	**7**	**8**	**9**
Avg	1	-11.5	-20.3	-31.1	-25.6	-34.0	-63.8	-40.6	-70.6	-82.0
	2	-18.6	-28.9	-43.4	-45.5	-63.3	-89.4	-64.2	-50.8	-24.8
	3	-20.5	-40.0	-57.9	-49.2	-64.2	-64.3	-48.2	-21.2	2.0
	4	-21.7	-47.6	-62.4	-47.3	-56.0	-51.5	-40.7	-14.1	3.7
	5	-22.2	-50.5	-61.6	-47.6	-47.4	-33.4	-23.8	-13.5	2.5
	6	-20.8	-50.2	-58.8	-45.6	-41.0	-24.7	-25.5	-11.2	1.6
	7	-20.9	-47.8	-56.5	-42.3	-34.7	-18.8	-6.0	-10.3	0.9
	8	-21.4	-49.4	-54.3	-40.6	-27.8	-5.7	-13.4	-9.8	0.7
	9	-20.9	-48.0	-52.6	-38.4	-23.3	-5.7	-1.8	-8.9	0.1
	10	-20.9	-47.1	-51.8	-36.4	-15.9	1.4	-1.2	-7.4	-0.3
Std	1	3.1	3.4	1.3	2.7	8.6	8.4	4.7	10.8	8.5
	2	2.0	7.2	3.0	5.7	12.7	12.9	5.0	22.0	30.0
	3	2.0	10.8	8.3	6.9	7.1	22.4	12.0	32.3	7.9
	4	2.4	7.8	9.0	7.2	8.7	18.7	9.9	29.8	4.2
	5	3.1	6.9	9.7	7.5	10.8	20.8	17.9	27.3	3.9
	6	2.8	7.5	8.6	6.9	12.2	17.4	12.2	25.2	4.0
	7	3.4	6.0	7.6	6.3	14.2	10.9	13.8	22.7	3.9
	8	4.1	8.2	6.9	6.2	14.6	9.6	9.1	20.5	3.7
	9	4.3	8.3	6.2	6.2	15.6	6.6	8.0	19.1	2.8
	10	4.1	8.6	5.8	6.0	12.2	5.1	4.1	16.3	3.4

		Spec								
	Strike	**10**	**11**	**12**	**13**	**14**	**15**	**16**	**17**	**18**
Avg	1	-21.4	-32.3	-65.4	-37.1	-74.7	-134.2	-57.6	-151.3	-183.6
	2	-37.0	-63.1	-111.5	-65.6	-132.3	-193.4	-114.3	-194.9	-186.4
	3	-42.0	-74.7	-141.1	-80.7	-152.5	-180.3	-146.7	-183.2	-173.7
	4	-46.5	-89.7	-164.6	-98.9	-158.6	-171.9	-155.6	-176.9	-167.2
	5	-51.1	-102.8	-177.7	-111.5	-150.8	-168.8	-153.4	-174.3	-162.9
	6	-53.9	-112.8	-175.1	-119.2	-147.4	-166.4	-147.9	-171.0	-159.6
	7	-56.2	-118.8	-168.0	-120.9	-144.8	-164.6	-144.9	-169.2	-154.2
	8	-57.4	-122.4	-164.0	-120.5	-143.1	-163.3	-143.1	-167.5	-150.3
	9	-57.9	-120.0	-161.6	-118.2	-141.6	-161.8	-141.5	-167.7	-147.7
	10	-57.4	-115.5	-159.8	-115.6	-140.3	-160.4	-140.3	-166.1	-144.7
Std	1	4.6	8.4	4.3	3.4	10.2	17.8	13.3	21.0	6.3
	2	7.9	16.4	9.4	16.4	14.2	29.2	25.2	18.8	8.0
	3	11.3	17.5	10.2	24.3	22.7	30.5	31.2	18.9	11.6
	4	12.6	21.5	8.5	21.7	24.3	28.9	32.2	18.8	17.3
	5	13.0	24.0	6.0	22.7	23.4	28.3	29.2	18.7	22.7
	6	13.4	25.9	5.5	21.1	22.5	28.3	30.0	18.4	25.2
	7	13.8	26.6	4.8	19.3	21.7	28.0	29.6	18.1	32.5
	8	14.4	27.1	4.7	17.8	21.1	27.7	29.6	18.0	36.7
	9	15.1	53.7	4.8	17.9	20.8	27.0	29.2	17.6	40.3
	10	15.3	26.2	5.0	17.7	20.5	26.9	28.9	17.4	43.4

9.7.4 Pushout fixation

Appendix 9.7.9: Pushout fixation values (mean with standard deviation): a) For 10 strikes in low density bone b) For optimum number of strikes in low density bone c) For optimum number of strikes in high density bone

Pushout Force (N)

a)	10 Strikes								
Spec	1	2	3	4	5	6	7	8	9
Strikes	10	10	10	10	10	10	10	10	10
Avg	123.2	247.8	362.3	171.6	127.4	90.0	45.1	59.7	48.5
Std	11.7	16.2	18.4	19.2	48.4	18.8	13.6	14.0	6.1

b)	Optimum Strikes								
Spec	1	2	3	4	5	6	7	8	9
Strikes	10	10	6	7	4	2	3	2	2
Avg	123.2	247.8	442.5	289.2	355.6	495.6	367.8	442.2	630.0
Std	11.7	16.2	38.0	46.2	76.9	21.6	9.6	79.2	65.3

c)	Optimum Strikes								
Spec	10	11	12	13	14	15	16	17	18
Strikes	7	7	5	8	4	3	4	3	2
Avg	256.3	598.7	787.4	605.4	982.0	1066.2	786.3	1120.0	1233.5
Std	33.9	21.0	58.4	40.3	68.8	69.6	48.4	22.7	34.9

9.7.5 Cup seating

Appendix 9.7.10: Polar gap (mean with standard deviation) for each impact specification

Polar Gap (mm)

		Spec								
	Strike	**1**	**2**	**3**	**4**	**5**	**6**	**7**	**8**	**9**
Avg	0	-6.34	-7.67	-6.55	-7.32	-7.40	-6.95	-6.83	-6.63	-6.34
	1	-5.05	-5.32	-3.48	-4.69	-3.22	-2.04	-3.12	-1.53	-0.72
	2	-4.55	-4.29	-2.43	-3.51	-1.61	-0.80	-1.80	-1.11	-0.59
	3	-4.19	-3.56	-1.71	-2.86	-1.08	-0.79	-1.57	-1.25	-0.54
	4	-3.87	-2.97	-1.30	-2.45	-0.97	-0.78	-1.52	-1.12	-0.38
	5	-3.66	-2.57	-1.11	-2.14	-0.96	-0.82	-1.71	-0.90	-0.23
	6	-3.50	-2.33	-1.00	-1.91	-0.95	-0.87	-1.51	-0.67	-0.16
	7	-3.29	-2.10	-0.95	-1.77	-0.94	-0.77	-1.82	-0.48	-0.25
	8	-3.14	-1.97	-0.91	-1.69	-0.95	-0.88	-1.50	-0.41	-0.19
	9	-3.01	-1.84	-0.87	-1.64	-0.91	-0.71	-1.50	-0.36	-0.07
	10	-2.89	-1.74	-0.84	-1.58	-0.88	-0.71	-1.33	-0.33	-0.14
Std	0	0.62	0.97	0.49	1.12	0.52	0.46	0.25	0.39	0.19
	1	0.33	0.77	0.58	1.10	0.51	0.62	0.18	0.11	0.30
	2	0.36	0.70	0.38	1.12	0.38	0.40	0.29	0.47	0.27
	3	0.31	0.64	0.25	1.01	0.25	0.37	0.16	0.51	0.35
	4	0.32	0.63	0.14	0.82	0.25	0.32	0.11	0.15	0.11
	5	0.33	0.59	0.11	0.58	0.29	0.28	0.19	0.21	0.13
	6	0.32	0.49	0.11	0.34	0.33	0.36	0.22	0.27	0.15
	7	0.20	0.42	0.11	0.23	0.34	0.17	0.22	0.19	0.11
	8	0.16	0.35	0.11	0.15	0.32	0.20	0.23	0.32	0.13
	9	0.15	0.27	0.13	0.11	0.31	0.13	0.11	0.24	0.10
	10	0.12	0.22	0.12	0.05	0.23	0.13	0.17	0.11	0.10

		Spec								
	Strike	**10**	**11**	**12**	**13**	**14**	**15**	**16**	**17**	**18**
Avg	0	-5.67	-5.35	-5.39	-6.38	-5.98	-6.04	-5.74	-5.28	-5.61
	1	-4.27	-3.38	-2.42	-3.84	-2.15	-1.22	-2.51	-1.01	-0.60
	2	-3.62	-2.51	-1.56	-2.79	-1.04	-0.38	-1.32	-0.33	-0.17
	3	-3.26	-2.06	-1.03	-2.09	-0.67	-0.27	-0.71	-0.19	-0.17
	4	-3.03	-1.67	-0.68	-1.62	-0.47	-0.27	-0.51	-0.20	-0.16
	5	-2.84	-1.43	-0.45	-1.31	-0.46	-0.23	-0.41	-0.23	-0.14
	6	-2.69	-1.21	-0.41	-1.17	-0.43	-0.24	-0.40	-0.18	-0.11
	7	-2.57	-1.07	-0.41	-1.06	-0.39	-0.27	-0.43	-0.27	-0.16
	8	-2.48	-0.97	-0.34	-0.92	-0.38	-0.28	-0.44	-0.26	-0.10
	9	-2.39	-0.94	-0.38	-0.90	-0.34	-0.26	-0.44	-0.27	-0.11
	10	-2.35	-0.91	-0.40	-0.86	-0.33	-0.26	-0.42	-0.21	-0.11
Std	0	0.58	1.40	0.53	1.33	0.69	0.55	0.49	0.18	0.31
	1	0.59	0.29	0.42	1.12	0.71	0.29	0.27	0.22	0.35
	2	0.56	0.16	0.36	0.90	0.44	0.16	0.29	0.06	0.20
	3	0.49	0.09	0.34	0.61	0.36	0.13	0.24	0.04	0.12
	4	0.46	0.07	0.36	0.38	0.27	0.12	0.22	0.08	0.11
	5	0.40	0.15	0.28	0.28	0.23	0.13	0.19	0.06	0.11
	6	0.38	0.20	0.27	0.24	0.18	0.10	0.17	0.09	0.08
	7	0.32	0.17	0.27	0.14	0.19	0.10	0.16	0.05	0.05
	8	0.27	0.17	0.24	0.12	0.11	0.08	0.15	0.05	0.09
	9	0.26	0.21	0.23	0.13	0.11	0.08	0.08	0.04	0.09
	10	0.28	0.21	0.22	0.08	0.04	0.03	0.08	0.05	0.03

9.8 Traditional impact strike: Data fitting

9.8.1 Goodness of fit graphs

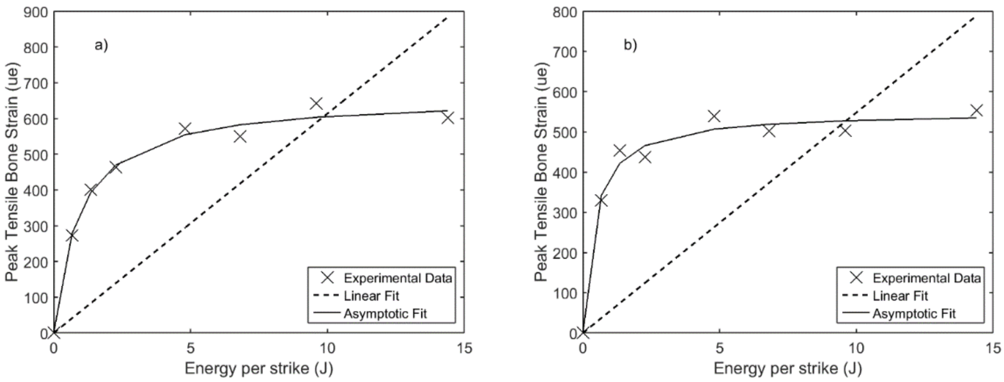

Appendix 9.8.1: Goodness of fit of linear and asymptotic fit to peak tensile bone strain vs energy per strike in a) Low density bone b) High density bone

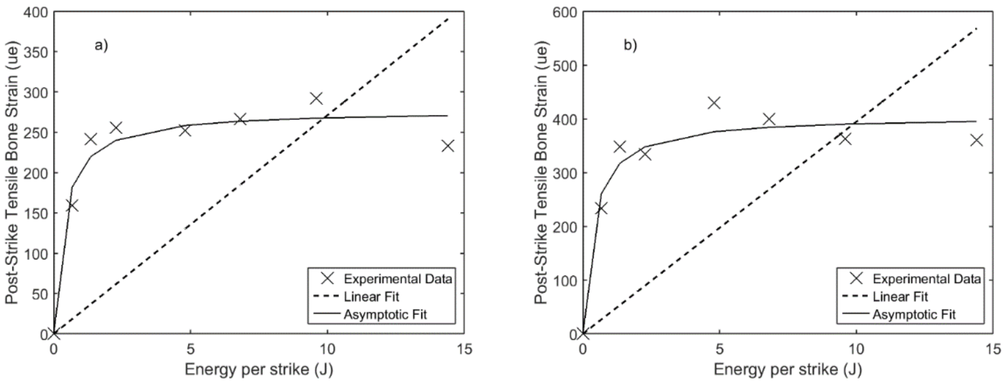

Appendix 9.8.2: Goodness of fit of linear and asymptotic fit to post-strike tensile bone strain vs energy per strike in a) Low density bone b) High density bone

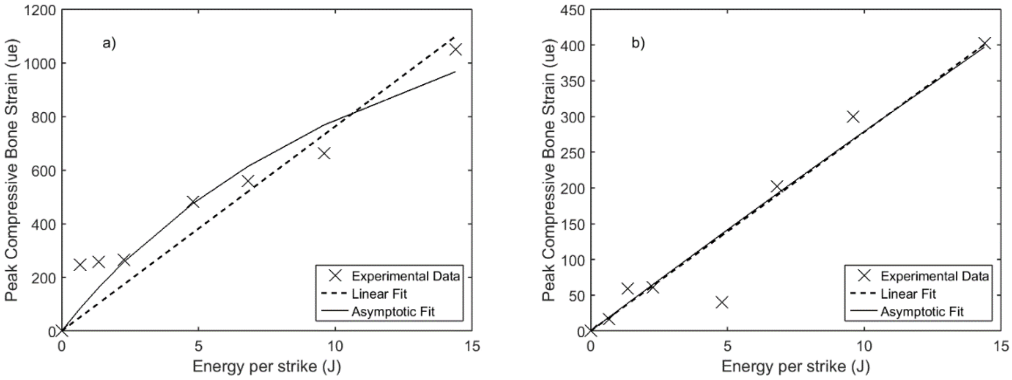

Appendix 9.8.3: *Goodness of fit of linear and asymptotic fit to peak compressive bone strain vs energy per strike in a) low density bone b) high density bone*

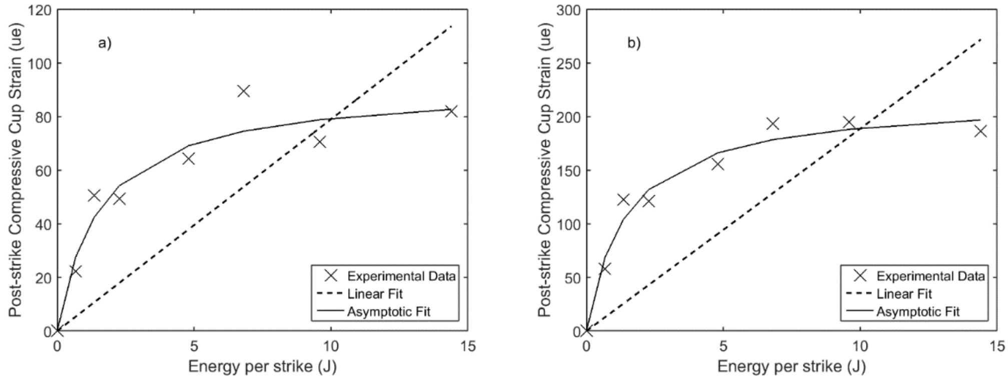

Appendix 9.8.4: *Goodness of fit of linear and asymptotic fit to post-strike compressive cup strain vs energy per strike in a) Low density bone b) High density bone*

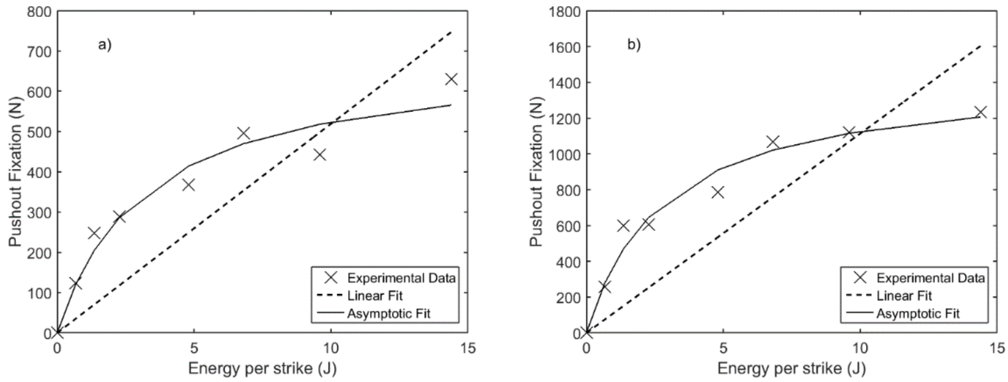

Appendix 9.8.5: *Goodness of fit of linear and asymptotic fit to pushout fixation vs energy per strike in a) Low density bone b) High density bone*

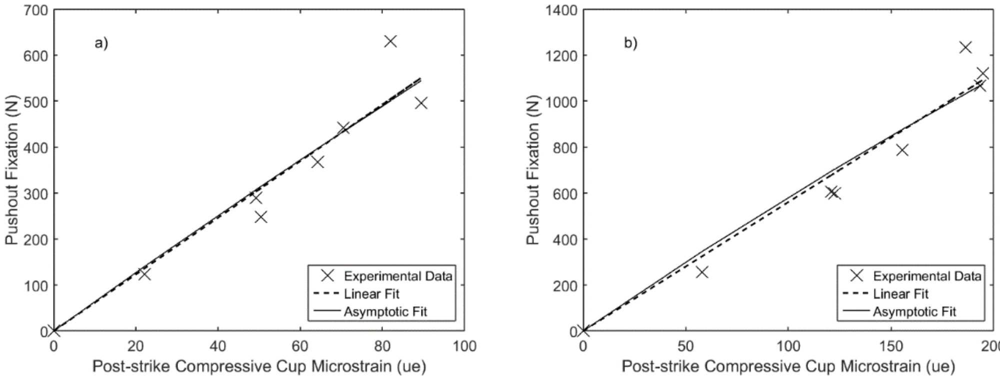

Appendix 9.8.6: *Goodness of fit of linear and asymptotic fit to pushout fixation vs post-Strike compressive cup strain in a) Low density bone b) High density bone*

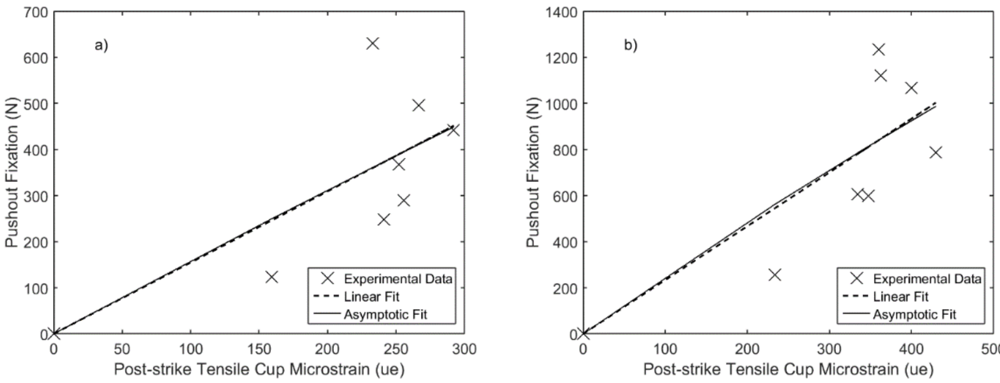

Appendix 9.8.7: *Goodness of fit of linear and asymptotic fit to pushout fixation vs post-strike tensile bone strain in a) Low density bone b) High density bone*

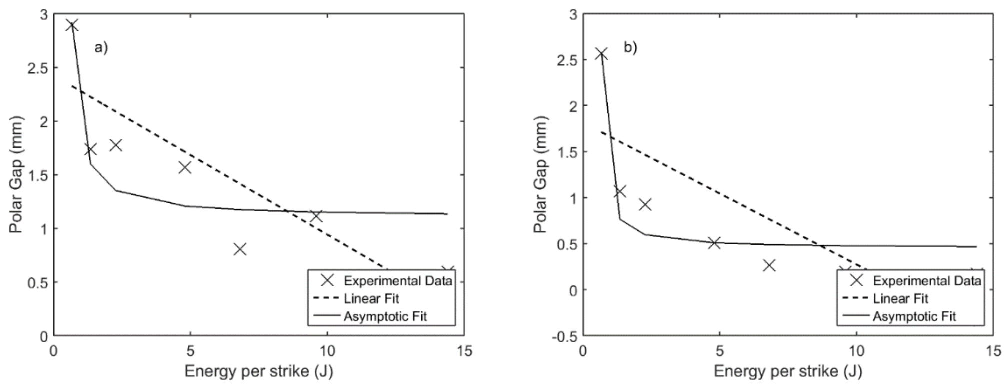

Appendix 9.8.8: *Goodness of fit of linear and asymptotic fit to polar gap vs energy per strike in a) Low density bone b) High density bone*

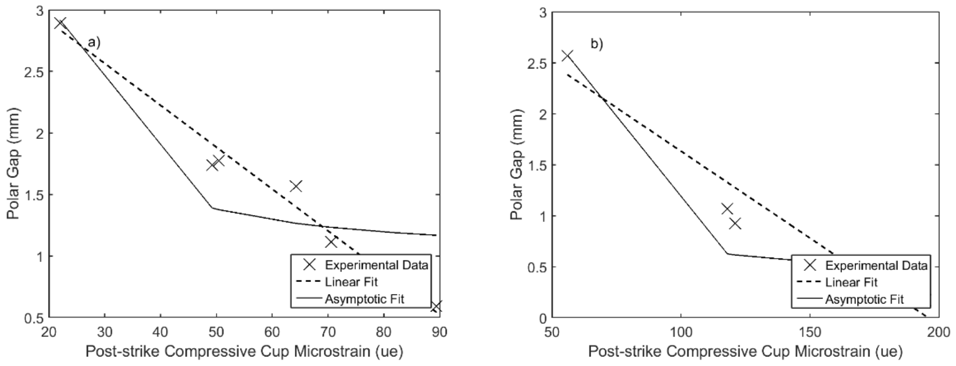

Appendix 9.8.9: Goodness of fit of linear and asymptotic fit to polar gap vs post-strike compressive cup strain in a) Low density bone b) High density bone

9.9 Traditional impact strikes: Statistics

9.9.1 Analysis of variance (ANOVA)

Appendix 9.9.1: Analysis of variance – Assumptions and interactions for peak tensile bone strain in: a) Low density bone b) High density bone

a) Peak Tensile Bone Strains - Low Density Bone (15 PCF)

	Impact Velocity	Low Velocity			Medium Velocity			High Velocity		
	Impact Mass	**Low**	**Med**	**High**	**Low**	**Med**	**High**	**Low**	**Med**	**High**
Assumptions	Outliers	0								
	Normality (Shapiro Wilk) > 0.05 passes	0.583	0.136	0.536	0.119	0.722	0.672	0.114	0.220	0.054
	Velocity*Mass sphericity (Mauchlys) > 0.05 passes	0.265								
Interactions	Two way interaction (< 0.05 is significant)	0.007								
	Within-subject effects (is there a relationship between dependant and mass at different velocity levels? < 0.05 is significant)	0			0.530			0.210		
	Within-subject effects (is there a relationship between dependant and mass at different velocity levels? < 0.05 is significant)				0.002					
						0.207				
							0.084			

b) Peak Tensile Bone Strains - High Density Bone (30 PCF)

	Impact Velocity	Low Velocity			Medium Velocity			High Velocity		
	Impact Mass	**Low**	**Med**	**High**	**Low**	**Med**	**High**	**Low**	**Med**	**High**
Assumptions	Outliers	0								
	Normality (Shapiro Wilk) > 0.05 passes	0.876	0.458	0.231	0.367	0.819	0.624	0.782	0.498	0.201
	Velocity*Mass sphericity (Mauchlys) > 0.05 passes	0.432								
Interactions	Two way interaction (< 0.05 is significant)	0.420								
	Within-subject effects (is there a relationship between dependant and mass at different velocity levels? < 0.05 is significant)	0.03			0.164			0.322		
	Within-subject effects (is there a relationship between dependant and mass at different velocity levels? < 0.05 is significant)				0.121					
						0.117				
							0.239			

Appendix 9.9.2: Analysis of variance – Assumptions and interactions for post-strike strain deterioration: a) Low density bone b) High density bone

a) Post-strike Strain Deterioration - Low Density Bone (15 PCF)

	Impact Velocity	Low Velocity			Medium Velocity			High Velocity		
	Impact Mass	Low	Med	High	Low	Med	High	Low	Med	High
Assumptions	Outliers	0								
	Normality (Shapiro Wilk) > 0.05 passes	0.117	0.507	0.362	0.209	0.108	0.805	0.657	0.328	0.913
	Velocity*Mass sphericity (Mauchlys) > 0.05 passes	0.365								
Interactions	Two way interaction (< 0.05 is significant)	0								
	Within-subject effects (is there a relationship between dependant and mass at different velocity levels? < 0.05 is significant)	0.070			0			0		
	Within-subject effects (is there a relationship between dependant and mass at different velocity levels? < 0.05 is significant)				0					
						0				
							0			

b) Post-strike Strain Deterioration - High Density Bone (30 PCF)

	Impact Velocity	Low Velocity			Medium Velocity			High Velocity		
	Impact Mass	Low	Med	High	Low	Med	High	Low	Med	High
Assumptions	Outliers	0								
	Normality (Shapiro Wilk) > 0.05 passes	0.410	0.884	0.530	0.539	0.191	0.173	0.575	0.765	0.489
	Velocity*Mass sphericity (Mauchlys) > 0.05 passes	0.014								
Interactions	Two way interaction (< 0.05 is significant)	0.238								
	Within-subject effects (is there a relationship between dependant and mass at different velocity levels? < 0.05 is significant)	0			0.364			0.356		
	Within-subject effects (is there a relationship between dependant and mass at different velocity levels? < 0.05 is significant)				0.810					
						0.167				
							0.302			

*Lower bound epsilon is < 0.25 therefore Greenhouse-geisser correction is used according to: Maxwell & Delaney (2004)

Appendix 9.9.3: Analysis of variance – Assumptions and interactions for polar gap: a) Low density bone b) High density bone

a) Polar Gap - Low Density Bone (15 PCF)

	Impact Velocity	Low Velocity			Medium Velocity			High Velocity		
	Impact Mass	**Low**	**Med**	**High**	**Low**	**Med**	**High**	**Low**	**Med**	**High**
Assumptions	Outliers	0								
	Normality (Shapiro Wilk) > 0.05 passes	0.438	0.845	0.163	0.404	0.916	0.040	0.762	0.407	0.552
	Velocity*Mass sphericity (Mauchlys) > 0.05 passes	0.443								
Interactions	Two way interaction (< 0.05 is significant)	0								
	Within-subject effects (is there a relationship between dependant and mass at different velocity levels? < 0.05 is significant)	0			0			0.03		
	Within-subject effects (is there a relationship between dependant and mass at different velocity levels? < 0.05 is significant)				0					
						0.03				
							0.037			

b) Polar Gap - High Density Bone (30 PCF)

	Impact Velocity	Low Velocity			Medium Velocity			High Velocity		
	Impact Mass	**Low**	**Med**	**High**	**Low**	**Med**	**High**	**Low**	**Med**	**High**
Assumptions	Outliers	0								
	Normality (Shapiro Wilk) > 0.05 passes	0.435	0.789	0.451	0.940	0.312	0.285	0.131	0.918	0.468
	Velocity*Mass sphericity (Mauchlys) > 0.05 passes	0.022								
Interactions	Two way interaction (< 0.05 is significant)	0.238								
	Within-subject effects (is there a relationship between dependant and mass at different velocity levels? < 0.05 is significant)	0			0.01			0.006		
	Within-subject effects (is there a relationship between dependant and mass at different velocity levels? < 0.05 is significant)				0					
						0.006				
							0.293			

*Lower bound epsilon is <0.25 therefore Greenhouse-geisser correction is used according to: Maxwell & Delaney (2004)

9.9.2 Post-hoc T-Tests

Appendix 9.9.4: Post-Hoc T-Tests – Difference, significance and confidence in peak tensile bone strain, velocity – mass comparison in a) Low density bone b) High density bone

a) Peak Tensile Bone Strain (με), Low Density Bone Strain (15 PCF)

	Velocity (m/s)	Mass (kg)		Mean Difference (Col1 - Col2)	Std Err	Significance ($p < 0.05$)	Confidence	
T-Tests - (Velocity - Mass)	1.5	0.6	1.2	-82.112*	12.5	***0.00***	-121.3	-42.9
			1.8	-158.519*	22.5	***0.00***	-228.9	-88.1
		1.2	0.6	82.112*	12.5	***0.00***	42.9	121.3
			1.8	-76.408	26.9	0.075	-160.6	7.8
		1.8	0.6	158.519*	22.5	***0.00***	88.1	228.9
			1.2	76.408	26.9	0.075	-7.8	160.6
	2.75	0.6	1.2	-41.330	27.9	0.548	-128.7	46.1
			1.8	-23.305	47.7	1.000	-172.4	125.8
		1.2	0.6	41.330	27.9	0.548	-46.1	128.7
			1.8	18.026	28.7	1.000	-71.8	107.9
		1.8	0.6	23.305	47.7	1.000	-125.8	172.4
			1.2	-18.026	28.7	1.000	-107.9	71.8
	4	0.6	1.2	-48.796	29.7	0.435	-141.8	44.2
			1.8	19.061125	37.9	1.000	-99.4	137.6
		1.2	0.6	48.796	29.7	0.435	-44.2	141.8
			1.8	67.857	43.4	0.485	-67.8	203.5
		1.8	0.6	-19.061125	37.9	1.000	-137.6	99.4
			1.2	-67.857	43.4	0.485	-203.5	67.8

b) Peak Tensile Bone Strain (με), High Density Bone Strain (30 PCF)

	Velocity (m/s)	Mass (kg)		Mean Difference (Col1 - Col2)	Std Err	Significance ($p < 0.05$)	Confidence	
T-Tests - (Velocity - Mass)	1.5	0.6	1.2	-74.0039125	48.2	0.505	-224.6	76.6
			1.8	-172.931*	22.8	***0.00***	-244.4	-101.5
		1.2	0.6	74.0039125	48.2	0.505	-76.6	224.6
			1.8	-98.927	44.1	0.179	-236.8	38.9
		1.8	0.6	172.931*	22.8	***0.00***	101.5	244.4
			1.2	98.927	44.1	0.179	-38.9	236.8
	2.75	0.6	1.2	-177.125	94.1	0.306	-471.5	117.2
			1.8	-88.940	85.9	1.000	-357.5	179.6
		1.2	0.6	177.125	94.1	0.306	-117.2	471.5
			1.8	88.185	81.1	0.939	-165.5	341.8
		1.8	0.6	88.940	85.9	1.000	-179.6	357.5
			1.2	-88.185	81.1	0.939	-341.8	165.5
	4	0.6	1.2	76.411	75.5	1.000	-159.8	312.6
			1.8	93.9497875	43.6	0.205	-42.5	230.4
		1.2	0.6	-76.411	75.5	1.000	-312.6	159.8
			1.8	17.539	67.6	1.000	-193.9	229.0
		1.8	0.6	-93.9497875	43.6	0.205	-230.4	42.5
			1.2	-17.539	67.6	1.000	-229.0	193.9

Appendix 9.9.5: Post-Hoc T-Tests – Difference, significance and confidence in peak tensile bone strain, mass - Velocity comparison in a) Low density bone b) High density bone

a) Peak Tensile Bone Strain (με), Low Density Bone Strain (15 PCF)

	Mass (kg)	Velocity (m/s)		Mean Difference (Col1 - Col2)	Std Err	Significance ($p < 0.05$)	Confidence	
T-Tests - (Mass Velocity)	0.6	1.5	2.75	-64.630*	15.8	***0.01***	-114.1	-15.1
			4	-92.938*	17.3	***0.00***	-147.0	-38.8
		2.75	1.5	64.630*	15.8	***0.01***	15.1	114.1
			4	-28.308	27.6	1.000	-114.8	58.1
		4	1.5	92.938*	17.3	***0.00***	38.8	147.0
			2.75	28.308	27.6	1.000	-58.1	114.8
	1.2	1.5	2.75	-23.849	20.6	0.853	-88.2	40.5
			4	-59.623	37.6	0.471	-177.3	58.1
		2.75	1.5	23.849	20.6	0.853	-40.5	88.2
			4	-35.774	35.0	1.000	-145.1	73.5
		4	1.5	59.623	37.6	0.471	-58.1	177.3
			2.75	35.774	35.0	1.000	-73.5	145.1
	1.8	1.5	2.75	70.585	35.7	0.265	-41.0	182.2
			4	84.642*	26.7	***0.05***	1.2	168.0
		2.75	1.5	-70.585	35.7	0.265	-182.2	41.0
			4	14.058	46.6	1.000	-131.5	159.7
		4	1.5	-84.642*	26.7	***0.05***	-168.0	-1.2
			2.75	-14.058	46.6	1.000	-159.7	131.5

b) Peak Tensile Bone Strain (με), High Density Bone Strain (30 PCF)

	Mass (kg)	Velocity (m/s)		Mean Difference (Col1 - Col2)	Std Err	Significance ($p < 0.05$)	Confidence	
T-Tests - (Mass Velocity)	0.6	1.5	2.75	-45.1446125	88.7	1.000	-322.6	232.3
			4	-167.346*	48.8	***0.03***	-320.1	-14.6
		2.75	1.5	45.1446125	88.7	1.000	-232.3	322.6
			4	-122.202	89.2	0.639	-401.1	156.7
		4	1.5	167.346*	48.8	***0.03***	14.6	320.1
			2.75	122.202	89.2	0.639	-156.7	401.1
	1.2	1.5	2.75	-148.266	66.2	0.180	-355.2	58.6
			4	-16.931	59.4	1.000	-202.6	168.7
		2.75	1.5	148.266	66.2	0.180	-58.6	355.2
			4	131.335	88.4	0.543	-145.3	407.9
		4	1.5	16.931	59.4	1.000	-168.7	202.6
			2.75	-131.335	88.4	0.543	-407.9	145.3
	1.8	1.5	2.75	38.846	58.6	1.000	-144.3	222.0
			4	99.5345375	32.8	0.057	-2.9	202.0
		2.75	1.5	-38.846	58.6	1.000	-222.0	144.3
			4	60.688	70.8	1.000	-160.8	282.2
		4	1.5	-99.5345375	32.8	0.057	-202.0	2.9
			2.75	-60.688	70.8	1.000	-282.2	160.8

Appendix 9.9.6: Post-Hoc T-Tests – Difference, significance and confidence in post-strike strain gradient, velocity – mass comparison in a) Low density bone b) High density bone

a) Post-strike Strain Gradient (με/strike), Low Density Bone Strain (15 PCF)

T-Tests - (Velocity - Mass)

Velocity (m/s)	Mass (kg)		Mean Difference (Col1 - Col2)	Std Err	Significance ($p < 0.05$)	Confidence	
1.5	0.6	1.2	1.900626116	3.3	1.000	-8.4	12.2
		1.8	-4.975764063	2.6	0.303	-13.2	3.3
	1.2	0.6	-1.900626116	3.3	1.000	-12.2	8.4
		1.8	-6.876	2.4	0.068	-14.3	0.5
	1.8	0.6	5.0	2.6	0.303	-3.3	13.2
		1.2	6.876	2.4	0.068	-0.5	14.3
2.75	0.6	1.2	-15.931*	3.6	***0.01***	-27.2	-4.6
		1.8	-28.959*	5.7	***0.00***	-46.9	-11.0
	1.2	0.6	15.931*	3.6	***0.01***	4.6	27.2
		1.8	-13.028	6.6	0.265	-33.6	7.6
	1.8	0.6	28.959*	5.7	***0.00***	11.0	46.9
		1.2	13.028	6.6	0.265	-7.6	33.6
4	0.6	1.2	8.979	5.5	0.434	-8.1	26.1
		1.8	-42.869*	10.6	***0.01***	-76.1	-9.7
	1.2	0.6	-8.979	5.5	0.434	-26.1	8.1
		1.8	-51.849*	11.7	***0.01***	-88.4	-15.3
	1.8	0.6	42.869*	10.6	***0.01***	9.7	76.1
		1.2	51.849*	11.7	***0.01***	15.3	88.4

b) Post-strike Strain Gradient (με/strike), High Density Bone Strain (30 PCF)

T-Tests - (Velocity - Mass)

Velocity (m/s)	Mass (kg)		Mean Difference (Col1 - Col2)	Std Err	Significance ($p < 0.05$)	Confidence	
1.5	0.6	1.2	-8.238*	1.1	***0.00***	-11.7	-4.8
		1.8	-9.975*	1.6	***0.00***	-15.1	-4.8
	1.2	0.6	8.238*	1.1	***0.00***	4.8	11.7
		1.8	-1.737	1.9	1.000	-7.7	4.3
	1.8	0.6	9.975*	1.6	***0.00***	4.8	15.1
		1.2	1.737	1.9	1.000	-4.3	7.7
2.75	0.6	1.2	-4.759	4.8	1.000	-19.8	10.3
		1.8	-0.801	3.8	1.000	-12.5	10.9
	1.2	0.6	4.759	4.8	1.000	-10.3	19.8
		1.8	3.958	1.6	0.140	-1.2	9.1
	1.8	0.6	0.801	3.8	1.000	-10.9	12.5
		1.2	-3.958	1.6	0.140	-9.1	1.2
4	0.6	1.2	1.749	4.5	1.000	-12.2	15.7
		1.8	-5.685550178	6.5	1.000	-25.9	14.6
	1.2	0.6	-1.749	4.5	1.000	-15.7	12.2
		1.8	-7.434	4.7	0.465	-22.0	7.2
	1.8	0.6	5.685550178	6.5	1.000	-14.6	25.9
		1.2	7.434	4.7	0.465	-7.2	22.0

Appendix 9.9.7: Post-Hoc T-Tests – Difference, significance and confidence in post-strike strain gradient, mass - velocity comparison in a) Low density bone b) High density bone

a) Post-strike Strain Gradient (με/strike), Low Density Bone Strain (15 PCF)

	Mass (kg)	Velocity (m/s)		Mean Difference (Col1 - Col2)	Std Err	Significance ($p < 0.05$)	Confidence	
T-Tests - (Mass Velocity)	0.6	1.5	2.75	0.063583855	2.4	1.000	-7.5	7.7
			4	-41.698*	2.3	***0.00***	-48.8	-34.6
		2.75	1.5	-0.063583855	2.4	1.000	-7.7	7.5
			4	-41.762*	2.6	***0.00***	-50.0	-33.6
		4	1.5	41.698*	2.3	***0.00***	34.6	48.8
			2.75	41.762*	2.6	***0.00***	33.6	50.0
	1.2	1.5	2.75	-17.768*	4.4	***0.02***	-31.7	-3.9
			4	-34.620*	5.0	***0.00***	-50.1	-19.1
		2.75	1.5	17.768*	4.4	***0.02***	3.9	31.7
			4	-16.852	5.9	0.073	-35.3	1.6
		4	1.5	34.620*	5.0	***0.00***	19.1	50.1
			2.75	16.852	5.9	0.073	-1.6	35.3
	1.8	1.5	2.75	-23.919*	4.6	***0.00***	-38.4	-9.4
			4	-79.592*	10.9	***0.00***	-113.8	-45.4
		2.75	1.5	23.919*	4.6	***0.00***	9.4	38.4
			4	-55.673*	10.3	***0.00***	-88.0	-23.3
		4	1.5	79.592*	10.9	***0.00***	45.4	113.8
			2.75	55.673*	10.3	***0.00***	23.3	88.0

b) Post-strike Strain Gradient (με/strike), High Density Bone Strain (30 PCF)

	Mass (kg)	Velocity (m/s)		Mean Difference (Col1 - Col2)	Std Err	Significance ($p < 0.05$)	Confidence	
T-Tests - (Mass Velocity)	0.6	1.5	2.75	-9.319*	2.4	***0.02***	-16.9	-1.7
			4	-10.63055857	4.3	0.125	-24.0	2.7
		2.75	1.5	9.319*	2.4	***0.02***	1.7	16.9
			4	-1.312	5.5	1.000	-18.4	15.8
		4	1.5	10.6	4.3	0.125	-2.7	24.0
			2.75	1.312	5.5	1.000	-15.8	18.4
	1.2	1.5	2.75	-5.840	2.8	0.235	-14.7	3.0
			4	-0.644	2.7	1.000	-9.1	7.8
		2.75	1.5	5.840	2.8	0.235	-3.0	14.7
			4	5.196	3.7	0.611	-6.4	16.8
		4	1.5	0.644	2.7	1.000	-7.8	9.1
			2.75	-5.196	3.7	0.611	-16.8	6.4
	1.8	1.5	2.75	-0.145	2.3	1.000	-7.3	7.0
			4	-6.340705833	4.6	0.631	-20.7	8.0
		2.75	1.5	0.145	2.3	1.000	-7.0	7.3
			4	-6.196	6.0	1.000	-24.9	12.5
		4	1.5	6.340705833	4.6	0.631	-8.0	20.7
			2.75	6.196	6.0	1.000	-12.5	24.9

Appendix 9.9.8: Post-Hoc T-Tests – Difference, significance and confidence in polar gap, velocity – mass comparison in a) Low density bone b) High density bone

a) Polar gap (mm), Low Density Bone Strain (15 PCF)

T-Tests - (Velocity - Mass)	Velocity (m/s)	Mass (kg)		Mean Difference (Col1 - Col2)	Std Err	Significance ($p < 0.05$)	Confidence	
	1.5	0.6	1.2	-1.156*	0.1	***0.00***	-1.5	-0.8
			1.8	-1.889*	0.0	***0.00***	-2.0	-1.8
		1.2	0.6	1.156*	0.1	***0.00***	0.8	1.5
			1.8	-.733*	0.1	***0.00***	-1.1	-0.4
		1.8	0.6	1.889*	0.0	***0.00***	1.8	2.0
			1.2	.733*	0.1	***0.00***	0.4	1.1
	2.75	0.6	1.2	-.803*	0.1	***0.01***	-1.2	-0.4
			1.8	-.970*	0.1	***0.01***	-1.5	-0.4
		1.2	0.6	.803*	0.1	***0.01***	0.4	1.2
			1.8	-0.167	0.2	1.000	-1.0	0.6
		1.8	0.6	.970*	0.1	***0.01***	0.4	1.5
			1.2	0.167	0.2	1.000	-0.6	1.0
	4	0.6	1.2	-0.453	0.2	0.380	-1.4	0.5
			1.8	-.973*	0.1	***0.01***	-1.5	-0.5
		1.2	0.6	0.453	0.2	0.380	-0.5	1.4
			1.8	-0.520	0.2	0.175	-1.3	0.3
		1.8	0.6	.973*	0.1	***0.01***	0.5	1.5
			1.2	0.520	0.2	0.175	-0.3	1.3

b) Polar Gap (mm), High Density Bone Strain (30 PCF)

T-Tests - (Velocity - Mass)	Velocity (m/s)	Mass (kg)		Mean Difference (Col1 - Col2)	Std Err	Significance ($p < 0.05$)	Confidence	
	1.5	0.6	1.2	-1.500*	0.2	***0.01***	-2.3	-0.7
			1.8	-2.123*	0.2	***0.00***	-3.1	-1.1
		1.2	0.6	1.500*	0.2	***0.01***	0.7	2.3
			1.8	-.622*	0.1	***0.00***	-0.9	-0.4
		1.8	0.6	2.123*	0.2	***0.00***	1.1	3.1
			1.2	.622*	0.1	***0.00***	0.4	0.9
	2.75	0.6	1.2	-0.455	0.2	0.135	-1.1	0.2
			1.8	-.657*	0.1	***0.00***	-1.0	-0.4
		1.2	0.6	0.455	0.2	0.135	-0.2	1.1
			1.8	-0.202	0.1	0.660	-0.8	0.3
		1.8	0.6	.657*	0.1	***0.00***	0.4	1.0
			1.2	0.202	0.1	0.660	-0.3	0.8
	4	0.6	1.2	-0.314	0.1	0.060	-0.6	0.0
			1.8	-.335*	0.1	***0.01***	-0.6	-0.1
		1.2	0.6	0.314	0.1	0.060	0.0	0.6
			1.8	-0.021	0.1	1.000	-0.3	0.3
		1.8	0.6	.335*	0.1	***0.01***	0.1	0.6
			1.2	0.021	0.1	1.000	-0.3	0.3

Appendix 9.9.9: Post-Hoc T-Tests – Difference, significance and confidence in polar gap, mass - velocity comparison in a) Low density bone b) High density bone

a) Polar gap (mm), Low Density Bone Strain (15 PCF)

T-Tests - (Mass Velocity)	Mass (kg)	Velocity (m/s)		Mean Difference (Col1 - Col2)	Std Err	Significance ($p < 0.05$)	Confidence	
	0.6	1.5	2.75	-1.120*	0.1	***0.00***	-1.5	-0.7
			4	-1.328*	0.1	***0.00***	-1.6	-1.1
		2.75	1.5	1.120*	0.1	***0.00***	0.7	1.5
			4	-0.209	0.1	0.236	-0.6	0.1
		4	1.5	1.328*	0.1	***0.00***	1.1	1.6
			2.75	0.209	0.1	0.236	-0.1	0.6
	1.2	1.5	2.75	-.767*	0.1	***0.01***	-1.2	-0.3
			4	-0.625	0.2	0.138	-1.5	0.2
		2.75	1.5	.767*	0.1	***0.01***	0.3	1.2
			4	0.142	0.1	0.928	-0.3	0.6
		4	1.5	0.625	0.2	0.138	-0.2	1.5
			2.75	-0.142	0.1	0.928	-0.6	0.3
	1.8	1.5	2.75	-0.201	0.2	0.787	-0.8	0.4
			4	-.412*	0.1	***0.01***	-0.7	-0.1
		2.75	1.5	0.201	0.2	0.787	-0.4	0.8
			4	-0.212	0.1	0.650	-0.8	0.4
		4	1.5	.412*	0.1	***0.01***	0.1	0.7
			2.75	0.212	0.1	0.650	-0.4	0.8

b) Polar gap (mm), High Density Bone Strain (30 PCF)

T-Tests - (Mass Velocity)	Mass (kg)	Velocity (m/s)		Mean Difference (Col1 - Col2)	Std Err	Significance ($p < 0.05$)	Confidence	
	0.6	1.5	2.75	-1.646*	0.2	***0.00***	-2.3	-1.0
			4	-2.062*	0.1	***0.00***	-2.4	-1.7
		2.75	1.5	1.646*	0.2	***0.00***	1.0	2.3
			4	-0.417	0.1	0.140	-1.0	0.2
		4	1.5	2.062*	0.1	***0.00***	1.7	2.4
			2.75	0.417	0.1	0.140	-0.2	1.0
	1.2	1.5	2.75	-0.600	0.2	0.087	-1.3	0.1
			4	-.876*	0.1	***0.00***	-1.2	-0.5
		2.75	1.5	0.600	0.2	0.087	-0.1	1.3
			4	-0.276	0.1	0.237	-0.7	0.2
		4	1.5	.876*	0.1	***0.00***	0.5	1.2
			2.75	0.276	0.1	0.237	-0.2	0.7
	1.8	1.5	2.75	-0.180	0.2	0.925	-0.8	0.4
			4	-0.2748	0.2	0.777	-1.1	0.6
		2.75	1.5	0.180	0.2	0.925	-0.4	0.8
			4	-0.095	0.1	1.000	-0.5	0.3
		4	1.5	0.2748	0.2	0.777	-0.6	1.1
			2.75	0.095	0.1	1.000	-0.3	0.5

9.10 Novel impaction technique: Raw data

9.10.1 Specification labels

Appendix 9.10.1: Description of specification labels and associated impaction parameters

Specification	Bone Density (PCF)	Cup Size (mm)	Axial Force (N)
1			40
2	30	55	60
3			80

9.10.2 Strains

Appendix 9.10.2: Peak tensile bone strain (mean with standard deviation) for each impact specification

		Peak Tensile Bone Strain (με)		
		Spec		
	Pulse Time (s)	1	2	3
Avg	0.5	188.5	419.9	448.9
	1	202.0	333.4	363.0
	1.5	205.7	299.6	316.6
	2	204.2	272.7	301.8
	2.5	202.3	252.4	289.4
	3	202.7	246.2	281.1
	3.5	193.8	235.0	278.1
	4	194.8	222.6	267.1
Std	0.5	0.2	62.1	46.2
	1	32.6	16.5	30.7
	1.5	38.9	40.9	21.3
	2	35.3	27.9	15.4
	2.5	30.1	18.6	16.2
	3	30.1	20.1	12.7
	3.5	28.7	17.5	17.5
	4	31.7	17.5	13.9

Appendix 9.10.3: Post-strike tensile bone strain (mean with standard deviation) for each impact specification

		Post-strike Tensile Bone Strain (με) Spec		
	Pulse Time (s)	1	2	3
Avg	0.5	63.2	143.8	142.3
	1	72.7	119.8	134.8
	1.5	76.9	111.5	124.9
	2	84.5	102.6	116.9
	2.5	81.6	93.4	111.9
	3	82.4	81.6	105.7
	3.5	75.4	79.0	104.0
	4	74.8	65.8	99.6
Std	0.5	26.7	13.6	13.6
	1	40.1	16.0	13.2
	1.5	36.1	20.4	18.2
	2	34.5	21.4	24.6
	2.5	31.5	23.0	27.5
	3	31.2	25.5	27.8
	3.5	36.1	27.5	26.7
	4	33.0	17.2	28.0

Appendix 9.10.4: Peak compressive bone strain (mean with standard deviation) for each impact specification

		Peak Compressive Bone Strain (με) Spec		
	Pulse Time (s)	1	2	3
Avg	0.5	-55.0	-81.7	-115.3
	1	-61.4	-103.7	-137.6
	1.5	-59.9	-120.1	-151.2
	2	-56.8	-132.9	-172.1
	2.5	-62.8	-153.0	-192.4
	3	-69.5	-167.9	-206.1
	3.5	-73.0	-178.2	-232.0
	4	-83.7	-185.5	-244.2
Std	0.5	30.4	33.8	41.2
	1	40.5	43.4	61.8
	1.5	42.1	51.8	56.2
	2	34.0	45.2	45.6
	2.5	38.8	47.9	47.2
	3	42.1	50.6	48.2
	3.5	35.1	56.2	47.9
	4	39.1	51.5	51.2

Appendix 9.10.5: Post-strike compressive cup strain (mean with standard deviation) for each impact specification

		Post-strike Compressive Cup Strain (με)		
		Spec		
	Pulse Time (s)	**1**	**2**	**3**
Avg	0.5	-26.1	-68.3	-68.8
	1	-32.2	-68.7	-70.5
	1.5	-34.2	-68.9	-72.2
	2	-38.1	-68.8	-76.9
	2.5	-34.7	-68.5	-70.5
	3	-38.3	-69.5	-76.4
	3.5	-41.8	-69.1	-73.4
	4	-41.2	-67.7	-72.5
Std	0.5	4.8	4.9	10.8
	1	8.8	4.0	8.3
	1.5	9.1	3.4	8.8
	2	9.2	3.2	13.7
	2.5	7.3	3.5	13.1
	3	9.9	3.7	13.0
	3.5	9.2	3.5	14.0
	4	8.5	3.3	12.4

9.10.3 Pushout fixation

Appendix 9.10.6: Pushout fixation values (mean with standard deviation): a) For full 4s pulse b) For optimum (0.5 s) pulse

	Pushout Force (N)		
a)	**Full Pulse**		
Spec	1	2	3
Pulse Time (s)	0.5	0.5	0.5
Avg	107.3	245.0	323.6
Std	42.3	59.4	91.3

b)	**Optimum Pulse**		
Spec	1	2	3
Pulse Time (s)	0.5	0.5	0.5
Avg	154.5	435.0	506.8
Std	24.5	13.8	81.0

9.10.4 Cup seating

Appendix 9.10.7: Polar gap (mean with standard deviation) for each impact specification

		Polar Gap (mm)		
		Spec		
	Pulse Time (s)	1	2	3
Avg	0	4.79	4.72	4.77
	0.5	2.74	1.16	1.18
	1	2.46	0.95	0.98
	1.5	2.27	0.84	0.83
	2	2.13	0.76	0.70
	2.5	2.02	0.70	0.63
	3	1.91	0.66	0.56
	3.5	1.83	0.61	0.51
	4	1.75	0.58	0.47
Std	0	0.23	0.18	0.23
	0.5	0.32	0.24	0.17
	1	0.33	0.19	0.10
	1.5	0.31	0.18	0.09
	2	0.30	0.16	0.11
	2.5	0.29	0.16	0.11
	3	0.27	0.15	0.13
	3.5	0.27	0.15	0.13
	4	0.26	0.14	0.14

9.11 Novel impaction technique: Statistics

Appendix 9.11.1: T-Tests – Traditional vs oscillatory seating

Traditional Seating vs	0.5 s Pulse (Optimum) Oscillatory Seating P-Value			4 s Pulse Oscillatory Seating P-Value		
Axial Force	**Low**	**Medium**	**High**	**Low**	**Medium**	**High**
Peak Tensile Bone Strain	0.001	0.000	0.370	0.003	0.000	0.370
Post-Strike Bone Tensile Strain	0.000	0.000	0.000	0.001	0.000	0.000
Peak Compressive Bone Strain	0.282	0.762	0.025	0.064	0.029	0.727
Post-Strike Cup Compressive Strain	0.000	0.000	0.000	0.002	0.000	0.000
Pushout Fixation	0.002	0.000	0.000	0.001	0.000	0.000
Polar Gap	0.297	0.003	0.000	0.006	0.441	0.050